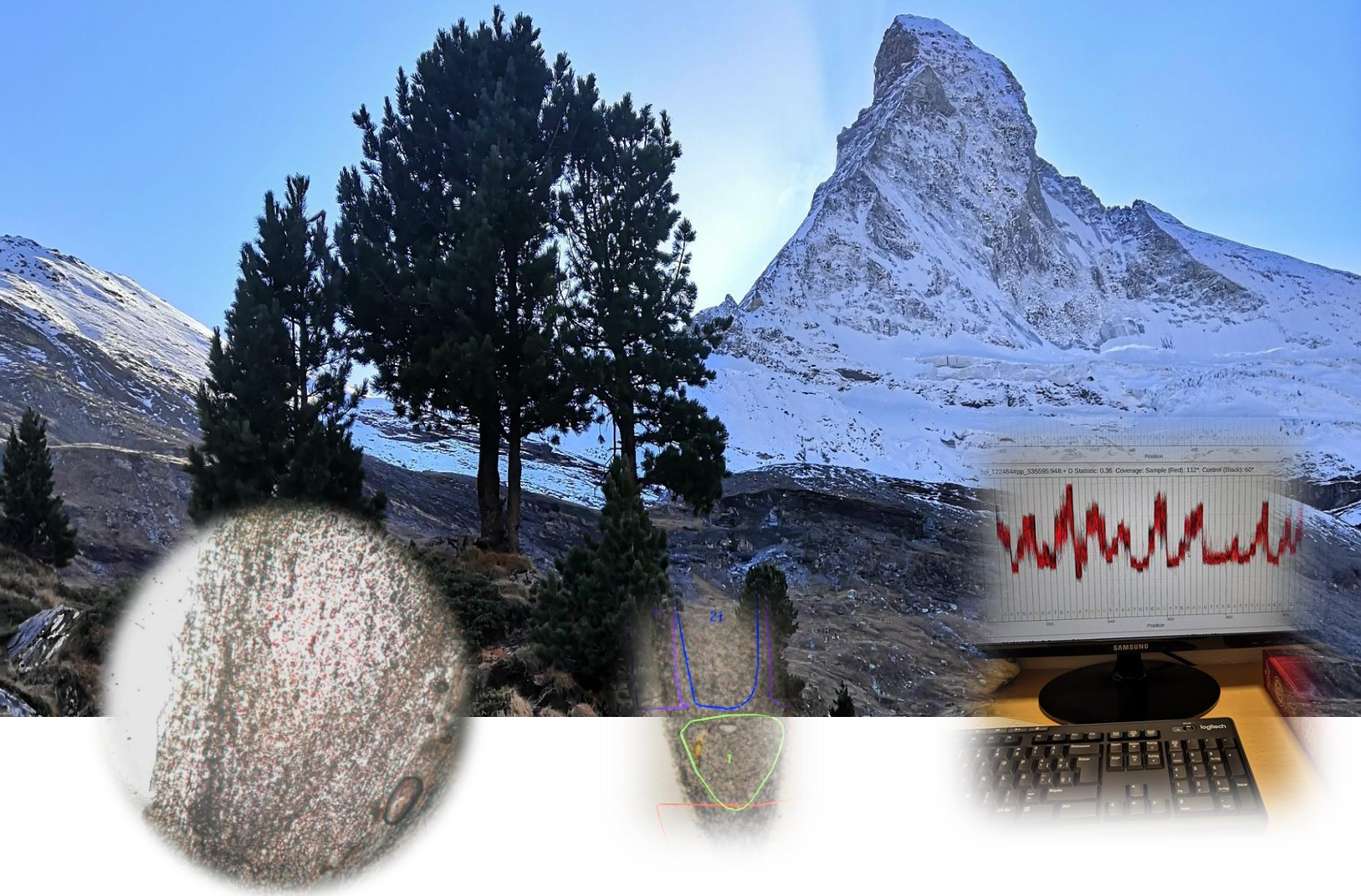


TESIS DOCTORAL

Programa de Doctorado en Biología Celular y Molecular



Importancia de la nutrición nitrogenada en plantas: genómica funcional de la respuesta a la nutrición con amonio en raíces de pino

Francisco Ortigosa Peña

Marzo 2021

Director : Rafael A. Cañas Pendón

Facultad de Ciencias, Universidad de Málaga
Departamento de Biología Molecular y Bioquímica



UNIVERSIDAD DE MÁLAGA



UNIVERSIDAD
DE MÁLAGA

DEPARTAMENTO DE BIOLOGÍA MOLECULAR Y
BIOQUÍMICA FACULTAD DE CIENCIAS

TESIS DOCTORAL

Programa de Doctorado en Biología Celular y Molecular

Importancia de la nutrición
nitrogenada en plantas: genómica
funcional de la respuesta a la
nutrición con amonio en raíces de
pino


Francisco Ortigosa Peña
2021





UNIVERSIDAD
DE MÁLAGA

AUTOR: Francisco Ortigosa Peña

 <https://orcid.org/0000-0002-7517-7594>

EDITA: Publicaciones y Divulgación Científica. Universidad de Málaga



Esta obra está bajo una licencia de Creative Commons Reconocimiento-NoComercial-SinObraDerivada 4.0 Internacional:

<http://creativecommons.org/licenses/by-nc-nd/4.0/legalcode>

Cualquier parte de esta obra se puede reproducir sin autorización pero con el reconocimiento y atribución de los autores.

No se puede hacer uso comercial de la obra y no se puede alterar, transformar o hacer obras derivadas.

Esta Tesis Doctoral está depositada en el Repositorio Institucional de la Universidad de Málaga (RIUMA): riuma.uma.es





UNIVERSIDAD
DE MÁLAGA



DECLARACIÓN DE AUTORÍA Y ORIGINALIDAD DE LA TESIS PRESENTADA PARA OBTENER EL TÍTULO DE DOCTOR

D./Dña FRANCISCO ORTIGOSA PEÑA

Estudiante del programa de doctorado BIOLOGÍA CELULAR Y MOLECULAR de la Universidad de Málaga, autor/a de la tesis, presentada para la obtención del título de doctor por la Universidad de Málaga, titulada: IMPORTANCIA DE LA NUTRICIÓN NITROGENADA EN PLANTAS: GENÓMICA FUNCIONAL DE LA RESPUESTA A LA NUTRICIÓN CON AMONIO EN RAÍCES DE PINO

Realizada bajo la tutorización de RAFAEL ANTONIO CAÑAS PENDÓN y dirección de RAFAEL ANTONIO CAÑAS PENDÓN (si tuviera varios directores deberá hacer constar el nombre de todos)

DECLARO QUE:

La tesis presentada es una obra original que no infringe los derechos de propiedad intelectual ni los derechos de propiedad industrial u otros, conforme al ordenamiento jurídico vigente (Real Decreto Legislativo 1/1996, de 12 de abril, por el que se aprueba el texto refundido de la Ley de Propiedad Intelectual, regularizando, aclarando y armonizando las disposiciones legales vigentes sobre la materia), modificado por la Ley 2/2019, de 1 de marzo.

Igualmente asumo, ante a la Universidad de Málaga y ante cualquier otra instancia, la responsabilidad que pudiera derivarse en caso de plagio de contenidos en la tesis presentada, conforme al ordenamiento jurídico vigente.

En Málaga, a 16 de FEBRERO de 2021

Fdo.:






UNIVERSIDAD
DE MÁLAGA



UNIVERSIDAD
DE MÁLAGA

AUTOR: *Francisco Ortigosa Peña (FO)*

 <https://orcid.org/0000-0002-7517-7594>

EDITA: Publicaciones y Divulgación Científica. Universidad de Málaga.

Cualquier parte de esta obra se puede reproducir sin autorización pero con el reconocimiento y atribución de los autores.

No se puede hacer uso comercial de la obra y no se puede alterar, transformar o hacer obras derivadas.

Esta Tesis Doctoral está depositada en el Repositorio Institucional de la Universidad de Málaga (RIUMA): riuma.uma.es

Este trabajo de Tesis Doctoral ha sido financiado por el Ministerio Español de Economía y Competitividad, número de proyecto BIO2015-73512-JIN MINECO/AEI/FEDER, UE, BIO2015-69285-R y RTI2018-094041-B-I00. FO ha sido parcialmente financiado por una beca de la Universidad de Málaga (Programa Operativo de Empleo Juvenil vía SNJG, UMAJI11, FEDER, FSE, Junta de Andalucía).





UNIVERSIDAD
DE MÁLAGA



UNIVERSIDAD
DE MÁLAGA

El *Dr. Rafael Antonio Cañas Pendón*, Profesor Titular del Departamento de Biología Molecular y Bioquímica de la Facultad de Ciencias de la Universidad de Málaga

CERTIFICA:

Que Don *Francisco Ortigosa Peña*, Graduado en Biología, ha realizado en el Departamento de Biología Molecular y Bioquímica de la Facultad de Ciencias de la Universidad de Málaga y bajo su dirección el trabajo de investigación recogido en la presente memoria de Tesis Doctoral bajo el título:

Importancia de la nutrición nitrogenada en plantas: genómica funcional de la respuesta a la nutrición con amonio en raíces de pino

Tras la revisión de la presente Memoria se ha estimado oportuna su presentación ante la Comisión de Evaluación correspondiente, por lo que autorizamos su exposición y defensa para optar al grado de Doctor en Biología.

Y para que así conste, en cumplimiento de las disposiciones legales vigentes, firmamos el presente certificado en Málaga, a 16 de febrero de 2021.

Dr. Rafael Antonio Cañas Pendón



UNIVERSIDAD
DE MÁLAGA

*A mi familia.
Por los que están.
Por los que se fueron.*



UNIVERSIDAD
DE MÁLAGA

En este punto solamente pretendo realizar un poco de introspección. En primer lugar, me gustaría agradecer a los catedráticos Francisco Cánovas y Concepción Ávila por la oportunidad que me brindaron al incluirme en su grupo de investigación. Todavía recuerdo aquel momento en la salida de clase en la que Paco me propuso hacer el Máster que finalmente derivaría en lo que a día de hoy es esta Tesis Doctoral. Ciertamente es que en ese momento no tenía claro la dirección que tomaría mi vida profesional puesto que nunca me he guiado por un camino preestablecido. Sin embargo, no tengo ningún tipo de duda de que fue una buena decisión puesto que el hoy es consecuencia del ayer. Así de simple.

También recuerdo la primera vez que me presentaron al hoy profesor titular Rafael Cañas. ¿Quién hubiera dicho que llegaríamos a este punto? Fue durante la tesina de Máster cuando me di cuenta de la enorme valía de este investigador. Del afán y del tesón. Del gusto de hacer lo que hace. En cuanto a ello, fue y es una inspiración. No obstante, ha sido durante el transcurso de este trabajo de Tesis Doctoral cuando he podido realmente apreciarle más a nivel personal. Solamente tengo buenas palabras para él. Ambos hemos pasado momentos complicados a lo largo de este tiempo. Siempre ha sido un gran apoyo. Ha sido jefe y mentor. Siempre he pensado que un jefe es un jefe, no un compañero, no un igual. En cambio, llegados a este punto puedo decir que es y será constantemente algo más, mucho más. Cañas, ahora puedo decir si me lo permites, que te considero un amigo. Gracias.

Me gustaría también agradecer al resto de compañeros con los que he coincidido en el grupo a lo largo de este tiempo. De todos he aprendido algo. En particular, querría resaltar las figuras de José Miguel Valderrama, César Lobato y Alberto Urbano. Al fin y al cabo, es con quienes he pasado más tiempo. Habéis estado ahí al filo del cañón y eso es de agradecer. Para nosotros se quedan los sábados en el laboratorio tomando café con puntas P5000 o las comidas en los buffet. No sé qué os deparará el futuro, pero seguid así. Llegará un momento en el que cada uno tome su camino, pero sabemos que siempre podremos contar los unos con los otros. Gracias y mil veces gracias porque es por todos vosotros por lo que hoy sigo haciendo lo que hago, por lo que procuro mejorar y avanzar.

Ahora tú, Zaira. Mi compañera de viaje, mi mejor amiga, juntos dos piezas de un mismo puzzle. Tú has sido un pilar muy importante. Para mí eres un espejo en el que

reflejarme. Gracias por mostrarme el verdadero significado de la constancia y de la disciplina, del trabajo y del esfuerzo. Por enseñarme que la mitad de dos no es uno mismo. Este momento es de ambos.

Index

Resumen General en Español.....	1
Introduction.....	17
1. Importance of forest stands	19
2. Conifers and maritime pine as model organism.....	21
3. Nitrogen as a plant nutrient	28
3.1. Ammonium absorption in plants.....	29
3.2. Regulation of the incorporation of ammonium.....	35
3.3. Ammonium assimilation and nitrogen metabolism.....	37
3.4. Ammonium transcriptomic response and regulation.....	41
4. Epitranscriptomics and its importance in plants.	46
5. Questions related to the state of art:.....	47
Objectives.....	49
Chapter 1	53
Introduction	55
Results	57
Discussion	62
Conclusions	67
Chapter 2	69
Introduction	71
Results	75
Discussion	89
Conclusions	95
Chapter 3	97
Introduction	99
Results	103
Discussion	119
Conclusions	131
Chapter 4	133

Introduction.....	135
Results.....	139
Discussion.....	155
Conclusions.....	165
General Discussion.....	169
Conclusions.....	179
Material and Methods	183
Appendix 1	215
Appendix 2	231
References.....	253

Abbreviations

AAT: Aspartate aminotransferase

ACD: Asymmetric cell division

AMT: Ammonium transporter

AS: Asparagine synthetase

ASPG: Asparaginase

ATP: Adenosine triphosphate

bp: Base pairs

BSA: Bovine serum albumin

C: Carbon

CDS: Coding sequence

CH₄N₂O: Urea

CK: Cytokinin

CO₂: Carbon dioxide

cDNA: Complementary DNA

DEG: Differentially expressed gene

DNA: Deoxyribonucleic acid

DRS: Direct RNA Sequencing

DW: Dry weight

ET: Ethylene

FCBA: *Institut Technologique Forêt Cellulose Bois-construction Ameublement*

FW: Fresh weight

GABA: γ -aminobutyric acid

Gbp: Giga base pairs (1,000,000,000 bp)

GDH: Glutamate dehydrogenase

GS: Glutamine synthetase

GOGAT: Glutamate synthase

¹H-NMR: Proton nuclear magnetic resonance

hm⁵C: 5-hydroxymethylcytosine

HATS: High affinity transport systems

HGT: Horizontal gene transfer
IAA: Auxin
LATS: Low affinity transport systems
LCM: Laser capture microdissection
LR: Lateral root
MeRIP-seq: Methylated RNA immunoprecipitation sequencing
mM: Millimolar
Mbp: Million base pairs (1,000,000)
miR: Micro-RNA
mRNA: Messenger RNA
mya: Million years ago
Mitogen-Activated Protein Kinase: MAPK
m¹A: N¹-methyladenosine
m⁵C: 5-methylcytosine
m⁶A: N⁶-methyladenosine
m⁷G: N⁷-methylguanosine
N: Nitrogen
NADH: Nicotinamide adenine dinucleotide
NADPH: Reduced nicotinamide adenine dinucleotide phosphate
NH₄⁺: Ammonium
NH₄NO₃: Ammonium nitrate
NO₃⁻: Nitrate
NiR: Nitrite reductase
NR: Nitrate reductase
NRT3: Nitrate transport regulators
NUE: Nitrogen use efficiency
NUpE: Nitrogen uptake efficiency
NUtE: Nitrogen utilization efficiency
ONT: Oxford Nanopore Technology
P: P-value

PAT: Polar auxin transport
PCR: Polymerase chain reaction
PEARs: PHLOEM EARLY DOFs
Pp: *Pinus pinaster*
PR: Principal root
ppm: Parts per million
QC: Quiescent center
RNA-seq: RNA sequencing
RNA: Ribonucleic acid
RC: Root cap
RDC: Root developmental cortex
RM: Root meristem
RDV: Root developmental vascular zone
ROS: Reactive oxygen species
RSA: Root system architecture
RT-qPCR: Reverse transcription quantitative PCR
SCN: Stem cell niche
SE: Standard error
SEA: Singular Enrichment Analysis
SEs: Sieve-elements
TCA cycle: Tricarboxylic acid cycle
TF: Transcription factor
UTR: Untranslated region
VGT: Vertical gene transmission



UNIVERSIDAD
DE MÁLAGA

Resumen General en Español



Los organismos vegetales constituyen el soporte principal para la vida terrestre pluricelular (Gough, 2011). Para un correcto crecimiento y desarrollo vegetal, el nitrógeno (N) se erige como un nutriente esencial ya que forma parte de las principales moléculas biológicas tales como los ácidos nucleicos, las proteínas, las clorofilas o las fitohormonas. Para las plantas, la biodisponibilidad de N en los suelos naturales constituye un factor limitante para su crecimiento y desarrollo (Rennenberg *et al.*, 2009 y 2010). Dada la gran importancia del N para las plantas, durante el siglo XX se desarrolló el proceso de Haber-Bosch para la producción de fertilizantes nitrogenados a partir del dinitrógeno atmosférico. Así, durante décadas en los sistemas agrícolas y forestales se ha promovido el uso de fertilizantes. El uso de estos fertilizantes nitrogenados ha permitido un importante incremento de la productividad agrícola durante el siglo XX, siendo uno de los principales factores en la conocida como Revolución Verde, que ha permitido alimentar a una población mundial creciente. Sin embargo, el uso extensivo de los fertilizantes puede causar importantes problemas ambientales como la contaminación de aguas subterráneas y acuíferos, la eutrofización de las reservas de agua, tanto naturales como artificiales, y/o la contaminación atmosférica mediante la emisión de gases de efecto invernadero. Todo ello puede plantear serios problemas en términos económicos, sociales y sanitarios. Por ello, el estudio de la absorción de N y su uso por parte de las plantas se ha convertido en un factor clave a través del cual obtener herramientas biotecnológicas que permitan mitigar los efectos adversos derivados de las prácticas agrícolas extensivas, con las que se consiguen satisfacer las enormes y crecientes necesidades de una población en continuo auge. Además, ello constituye un aspecto fundamental, más si cabe, en el ámbito de la silvicultura puesto que la obtención de materia prima derivada de especies arbóreas forestales es un proceso que se alarga en el tiempo pudiendo durar varios años. Por todas estas razones, la nutrición y el metabolismo nitrogenado se han convertido en un tópico esencial en el campo de la investigación y que debe ser debidamente incluido dentro de la educación científica.

En los suelos naturales, las principales formas de N inorgánico aprovechable por las plantas son el amonio (NH_4^+) y el nitrato (NO_3^-). La incorporación de NH_4^+ por parte del aparato radicular de las plantas es llevada a cabo principalmente mediante el transporte selectivo de este ion. Las proteínas encargadas de este transporte se

denominan transportadores de NH_4^+ (*ammonium transporter*, AMT) y pertenecen a la superfamilia AMT / MEP / Rh, la cual está presente en todos los seres vivos (Winkler, 2006). En el linaje vegetal, los transportadores de amonio se encuentran divididos en dos subfamilias denominadas AMT1 y AMT2 (von Wittgenstein *et al.*, 2014), las cuales se diferencian entre sí principalmente por su historia evolutiva y estructura génica (McDonald *et al.*, 2010 and 2012; von Wittgenstein *et al.*, 2014; Castro-Rodríguez *et al.*, 2016). A través de aproximaciones fisiológicas y bioquímicas ha sido posible caracterizar funcionalmente integrantes de ambas subfamilias de proteínas AMTs, describiéndose la existencia de transportadores de alta (*high affinity transport systems*, HATS) y baja afinidad (*low affinity transport systems*, LATS) tanto en especies herbáceas como arbóreas (Loqué *et al.*, 2006; Castro-Rodríguez *et al.*, 2016). A su vez, una vez que se ha incorporado el N, su asimilación es llevada a cabo principalmente a través del ciclo formado por las enzimas glutamina sintetasa (EC 6.3.1.2, GS) y glutamato sintasa (EC 1.4.1.14, NADH-GOGAT / EC 1.4.7.1, Fd-GOGAT) (Hirel y Krapp, 2020). Este ciclo efectúa la amidación de glutamato consumiendo NH_4^+ y ATP, por lo que la principal forma asimilable de N es el NH_4^+ . Este NH_4^+ puede proceder de la incorporación directa por el tejido radicular, por la reducción del NO_3^- o derivado de procesos biológicos como la fotorrespiración el catabolismo de aminoácidos, entre otros (Hirel y Lea, 2001).

En contrapartida a la gran importancia del NH_4^+ como punto central del metabolismo del N, múltiples plantas de alto interés agronómico tales como el aguacate o el tomate presentan una alta sensibilidad a la presencia de este ion pudiendo verse comprometido la tasa de crecimiento y desarrollo de estos cultivos (Lobit *et al.*, 2007; Xun *et al.*, 2020). Cuando el NH_4^+ está presente en concentraciones del rango milimolar (mM) a menudo causa toxicidad y efectos fenotípicos adversos. En general, esto da como resultado un detrimento del crecimiento de la planta (tanto en brotes como en raíces), una disminución en la relación raíz/brote y cambios en la arquitectura sistémica radicular (RSA), entre otros (Esteban *et al.*, 2016). Estos efectos morfológicos se han relacionado con la alteración del equilibrio iónico, cambios en el pH extracelular e intracelular, la inhibición de la respiración radicular, el aumento del estrés oxidativo, la alta demanda y coste energético para mantener el equilibrio del NH_4^+ citosólico, la

alteración del equilibrio hormonal y los cambios en la arquitectura del sistema radicular (“*root system architecture*”, RSA) con el de las raíces laterales y la inhibición del crecimiento de la raíz principal (Esteban *et al.*, 2016; Liu y von Wirén, 2017).

En los últimos años, varios trabajos han demostrado que el NH_4^+ puede desencadenar múltiples respuestas tanto a nivel fisiológico como a nivel morfológico. La respuesta y los mecanismos moleculares desencadenados por el NH_4^+ y su vínculo con los efectos fenotípicos de la raíz siguen sin estar claros. Hasta la fecha, la RSA inducida por el NH_4^+ ligada a la inhibición del alargamiento de las raíces principales ha relacionado con dos factores independientes: a la alteración de la N-glicosilación de proteínas y a elevados niveles de especies reactivas de oxígeno (“*reactive oxygen species*”, ROS) (Liu y von Wirén, 2017). Sin embargo, los efectos del NH_4^+ sobre las raíces de las coníferas y la respuesta de la raíz inducida por el NH_4^+ no están bien descritos. Diversos estudios transcriptómicos realizados en diferentes organismos vegetales y en diferentes momentos temporales muestran un mayor impacto por parte NO_3^- que del NH_4^+ en el corto plazo (<8 horas), mientras que la respuesta inducida por el NH_4^+ sobre la expresión diferencial de genes aumenta conforme lo hace el tiempo de exposición a este nutriente (Patterson *et al.*, 2010, Canales *et al.*, 2010; Sun *et al.*, 2017; Yang *et al.*, 2018). Asimismo, la presencia de NH_4^+ desencadena un profundo efecto en la expresión de genes relacionados con diversos procesos biológicos, entre los que destacan las respuestas al estrés biótico / abiótico, la biosíntesis de metabolitos secundarios, el metabolismo de carbohidratos y aminoácidos, así como genes relacionados con diversas vías hormonales (ácido abscísico / ABA, etileno y auxina) (Patterson *et al.*, 2010; Yang *et al.*, 2015; Sun *et al.*, 2017; Yang *et al.*, 2018). Asimismo, se ha descrito que los efectos y respuestas desencadenadas por la presencia de N pueden deberse a que el amonio puede comportarse a modo de señal (Liu y von Wirén, 2017).

Sin embargo, la proporción de estos elementos (NH_4^+ y NO_3^-) en el suelo es muy variable y depende principalmente de procesos metabólicos llevados a cabo por microorganismos, así como de la influencia del entorno sobre los mismos. Por ello, los suelos con un pH bajo, es decir suelos ácidos, y con una tasa de aireación limitada muestran mayores tasas de amonificación que de nitrificación, como es el caso de humedales, selvas, sabanas o bosques templados húmedos. Por ejemplo, en

los suelos de los bosques boreales y húmedos el NH_4^+ es la forma predominante de N (con una concentración media de 2 mM) (Bijlsma *et al.*, 2000). En estas últimas zonas las coníferas son el grupo vegetal predominante, las cuales están clasificadas dentro del grupo de las gimnospermas (Farjon, 2018). Las gimnospermas (*Gymnospermae*) son plantas vasculares y espermatofitas que aparecieron en la Tierra hace más de 350 millones de años. A través de estudios paleobotánicos y moleculares, se estima que la divergencia entre las plantas gimnospermas y las plantas angiospermas se puede remontar al Carbonífero, hace alrededor de 300 millones de años (Clarke *et al.*, 2011; Crisp y Cook, 2011; Magallón *et al.*, 2013). Las gimnospermas representan cuatro de los cinco principales linajes de plantas con semillas: cícadas (*Cycadophyta*), ginkgos (*Ginkgophyta*), gnetofitas (*Gnetophyta*) y coníferas (*Coniferophyta*) (Crisp y Cook, 2011), que se han dividido en cuatro subclases (*Cycadidae*, *Ginkgoideae*, *Gnetidae* y *Pinidae*) (Magallón *et al.*, 2013). De estos cuatro grupos, las coníferas constituyen el grupo más numeroso presentando alrededor de unas 615 especies y que ocupan más del 11% de la superficie del planeta. Las coníferas tienen una serie de características que hacen que su estudio sea muy complicado: como el gran tamaño de los individuos, los largos ciclos vitales, la acumulación de compuestos secundarios o el gran tamaño de sus genomas, estimados entre 18-35 Gbp lo que es más de 6 y 150 veces el tamaño del genoma humano y el de *Arabidopsis* respectivamente (Cañas *et al.*, 2019). Sin embargo, con el surgimiento y democratización tanto de la biología molecular como de las ciencias ómicas, ha sido posible incrementar la información disponible sobre estas especies y mantener la puerta abierta a los intereses industriales. Por lo general las coníferas presentan una alta tolerancia a la nutrición amoniacal, aspecto que no es así para buena parte de las plantas de interés agronómico. Una de las principales coníferas usadas como modelo de estudio es *Pinus pinaster* Ait., también conocido como pino marítimo. El pino marítimo es una especie autóctona de la región Mediterránea y que ocupa más de 4 millones de hectáreas en el continente europeo. El pino marítimo es un árbol de hoja perenne que presenta un amplio espectro ecológico, estando presente en catorce de los veinte fitoclimas descritos en la Península Ibérica (Allué Andrade, 1990), siendo también predominante en suelos pobres de naturaleza silíceo y / o arenosa (Viñas *et al.*, 2016). Sin embargo, esta especie también se puede encontrar en suelos calcáreos y crece bien en suelos compuestos de peridotita, una roca ígnea plutónica que es tóxica para la mayoría de

las plantas (Farjon, 2018), siendo un gran ejemplo las formaciones arbóreas de pino marítimo de Sierra Bermeja (Málaga) (Cañas *et al.*, 2015b). A su vez, las condiciones ambientales donde se suele encontrar al pino marítimo (clima templado) favorecen el proceso nitrificación, al menos durante las estaciones cálidas. Es destacable mencionar que el pino marítimo también presenta una enorme plasticidad fisiológica y morfológica, mostrando grandes niveles de diferenciación entre poblaciones en diferentes ambientes (Aranda *et al.*, 2010). Por todo ello, la distribución en España del pino marítimo se ha visto incrementada a través de su uso en labores de reforestación y en la estabilización de suelos (Seoane *et al.*, 2007).

Por otro lado, buena parte de la biomasa vegetal en el planeta se encuentra en forma de masas forestales. Los bosques ocupan alrededor del 30% de la superficie de la Tierra y además sirven como fuente de recursos materiales, alimentos, medicinas y combustible. Por tanto, las masas forestales intervienen activamente en el desarrollo socioeconómico de muchas zonas rurales. Además de los intereses “más inmediatos” del ser humano, las masas forestales protegen el suelo de la erosión, albergan más del 75% de la biodiversidad terrestre del mundo y también juegan un papel importante en la captación de dióxido de carbono (CO₂). El beneficio es aún más importante si se considera que la mayoría de las personas que dependen en primera o última instancia de los bosques tienen escaso poder económico (Agrawal *et al.*, 2013). Además, las masas forestales sirven para mejorar la capacidad de producción agrícola (Foli *et al.*, 2014) puesto que los bosques influyen en el ciclo hidrológico (Ellison *et al.*, 2017) al proporcionar materia orgánica (Kimble *et al.*, 2007) y compost a agricultura (Sinu *et al.*, 2012) y siendo fundamentales para los procesos de polinización (Roubik, 1995).

Por estos motivos y junto con el surgimiento y la democratización tanto de la biología molecular como de las ciencias ómicas, ha sido posible incrementar la información disponible sobre esta especie, lo que ha permitido a su vez mantener la puerta abierta a los intereses industriales. El pino marítimo ha sido utilizado como planta modelo forestal en el grupo de investigación de Biología Molecular y Biotecnología de la Universidad de Málaga desde los inicios de los años 90 (Cánovas *et al.*, 1991). El trabajo de este equipo junto con el de otros grupos de investigación europeos ha permitido desarrollar importantes recursos genómicos

como un transcriptoma de referencia (Canales *et al.* 2014), un atlas de la expresión génica en los diferentes tejidos de las plántulas de pino (Cañas *et al.* 2017) o un borrador de su genoma (Sterck *et al.* en preparación). Además, se han desarrollado diferentes herramientas biotecnológicas que son esenciales para la investigación actual en biología vegetal como la plataforma de transformación genética del FCBA (*Institut Technologique Forêt Cellulose Bois-construction Ameublement*, Champs-sur-Marne, France) (El-Azaz *et al.* 2020). Sin embargo, una adecuada caracterización nutricional y fisiológica del pino marítimo en respuesta a las principales formas de N inorgánico en el suelo y la caracterización de la preferencia por parte de esta especie forestal por una forma de N, así como los procesos involucrados en esta preferencia y una profunda caracterización de la expresión génica por parte de esta conífera a la nutrición nitrogenada eran tareas pendientes.

De este modo, para suplir las carencias sobre la nutrición nitrogenada y en particular sobre la respuesta amonio por parte del pino marítimo inicialmente se han propuesto los siguientes objetivos:

1. Desarrollo de una experiencia práctica de laboratorio para demostrar la importancia de la nutrición nitrogenada en las plantas.
2. Estudiar la respuesta diferencial en términos fisiológicos y metabólicos de plántulas de pino marítimo a la nutrición amoniacal y nítrica.
3. Determinar la dinámica transcriptómica en respuesta a la nutrición amoniacal en el ápice radicular de plántulas de pino marítimo.
4. Caracterizar la respuesta a corto plazo provocada por la nutrición amoniacal en las raíces de pino marítimo utilizando enfoques multi-ómicos.

Con el propósito de ilustrar la importancia de la nutrición nitrogenada y para reforzar el conocimiento teórico impartido durante las clases (Objetivo 1), en esta Tesis se presenta un nuevo protocolo práctico de laboratorio para estudiantes (Capítulo 1). Para ello, se han utilizado plantas de tomate *cherry* (*Solanum lycopersicum* var. *cerasiforme*), ya que presentan un rápido crecimiento y desarrollo, así como una buena acumulación diferencial de biomasa en relación a la nutrición nitrogenada, lo que *a priori* son resultados sencillos de obtener y muy ilustrativos acerca de la importancia del N para las plantas. Además, la modularidad

de la experiencia práctica permite que se pueda adaptar a los alumnos de los diferentes niveles del sistema educativo. En el ámbito universitario la práctica permite que los estudiantes puedan comprobar empíricamente lo tratado en las clases teóricas aplicando técnicas provenientes de diferentes disciplinas y con diferente grado de dificultad. Además, mediante el uso de aproximaciones bioquímicas clásicas y moleculares ampliamente asentadas en los laboratorios de biología molecular de plantas, se han estudiado importantes marcadores fisiológicos y moleculares tales como el contenido de proteínas solubles y clorofilas o la expresión de genes relevantes en el metabolismo del N, así como la actividad enzimática de proteínas clave en la nutrición nitrogenada (Capítulo 1). Tanto la actividad glutamina sintetasa como la expresión génica de los cinco genes codificantes de glutamina sintetasa en tomate han sido utilizados como marcadores moleculares del estatus nitrogenado de las plantas. El uso de RT-qPCR durante el desarrollo de la práctica de laboratorio permite identificar qué genes contribuyen principalmente en la respuesta a la nutrición nitrogenada y por tanto al incremento de la actividad enzimática. Los resultados del Capítulo 1 han sido publicados en un artículo científico en la revista *Biochemistry and Molecular Biology Education* indexada en el JCR (Ortigosa *et al.*, 2019 *Biochem. Mol. Biol. Edu.* 47: 450-458).

Con el propósito de dar respuesta al segundo objetivo, en el Capítulo 2 se muestran los resultados a nivel fisiológico y metabólico en respuesta a la nutrición con diferentes formas y proporciones de N. Las plántulas de pino marítimo se cultivaron a medio-largo plazo en un invernadero con cinco soluciones que contenían diferentes proporciones de NO_3^- y NH_4^+ . El estatus nitrogenado fue caracterizado analizando su biomasa y diferentes marcadores bioquímicos y moleculares, así como su perfil metabólico mediante $^1\text{H-NMR}$. Las plántulas tratadas con NH_4^+ exhibieron una mayor acumulación de biomasa que las plántulas tratadas con NO_3^- . Este efecto se debió principalmente a un mayor aumento de la biomasa de las raíces tratadas con NH_4^+ que parece ligado a un mayor desarrollo de este órgano. Esto podría tener una utilidad futura para procesos de reforestación puesto que un desarrollo adecuado de las raíces es un factor muy importante para establecimiento de las plántulas de las coníferas (Davis y Jacobs, 2005; Gruffman *et al.*, 2012). Por otra parte, fue posible determinar que el NO_3^- se acumulaba principalmente en el tallo, mientras que se observaron mayores cantidades de NH_4^+ en las raíces. A su

vez, las acículas de las plántulas regadas con NH_4^+ tenían mayores contenidos de N y aminoácidos, pero menores niveles de diferentes actividades enzimáticas relacionadas con el metabolismo del N. Estudiando los cambios en los perfiles metabólicos, se han encontrado mayores cantidades de azúcares solubles y L-arginina en las raíces de plántulas tratadas con NH_4^+ . En cambio, se observó una acumulación de L-asparagina en las raíces de las plántulas alimentadas con NO_3^- . Por ello, los perfiles de metabolitos observados en las raíces sugieren problemas con la asimilación de carbono y N en plántulas tratadas con NO_3^- . Además, a través de experimentos con moléculas nitrogenadas marcadas con ^{15}N se pudo confirmar que las tasas de incorporación de NH_4^+ y NO_3^- eran diferentes para el pino marítimo. Se encontró que las plántulas exhiben una mayor preferencia por el NH_4^+ que por el NO_3^- y estando el proceso de absorción de N altamente limitado y regulado a partir de los primeros minutos desde su suministro. Así se ha podido observar que el NH_4^+ es incorporado de una forma más eficiente que el NO_3^- por parte de las raíces del pino marítimo, el efecto final es que el índice de absorción de nitrógeno (NUpE) es mayor cuando la nutrición nitrogenada de las plántulas es principalmente con NH_4^+ . Los resultados del Capítulo 2 han sido publicados en un artículo científico en la revista *Plants* indexada en el JCR (Ortigosa *et al.*, 2020 *Plants* 9: 481).

Utilizando pino marítimo como planta modelo, puesto que exhibe una alta preferencia y tolerancia por este macronutriente y utilizando la técnica de captura por microdissección láser (“*laser capture microdissection*”, LCM), se ha estudiado la respuesta transcriptómica local inducida por el NH_4^+ en los ápices de las raíces (Objetivo 3). Este constituye el primer trabajo que utiliza LCM para estudiar los procesos relacionados con la respuesta a la presencia de NH_4^+ en los ápices de las raíces de las plantas. Comprobado el estado metabólico de las plántulas y el tipo de respuesta observado a los tiempos en los que se desarrollaron los experimentos, se pudo comprobar que la respuesta al NH_4^+ que se observó estaba principalmente ligada a su efecto como molécula señalizadora o efectora más que a su efecto nutricional. Los resultados obtenidos muestran que el NH_4^+ afecta la expresión de múltiples factores de transcripción (FTs) y transcritos relacionados con procesos hormonales, que probablemente pueden estar involucrados en el desarrollo y mantenimiento del meristemo radicular en pino marítimo. Para muchos transcritos,

este trabajo constituye la primera vez que se ha descrito su conexión con el metabolismo del N, destacando por ejemplo los factores de transcripción *PpSHR* o *PpSHOOT-GRAVITROPISM*. Además, se ha podido determinar la existencia de nuevos transcritos no identificados previamente en el transcriptoma de pino marítimo tales como *PpNAC38*, *PpDOF11* o *PpDOF12* (Capítulo 3). Asimismo, nuestros resultados también sugieren que el NH_4^+ podría causar una alteración en el transporte de auxinas (IAAs), al menos en la zona de la punta de la raíz, pudiendo dar lugar a acumulaciones de esta fitohormona en la región cortical lo que podrían ser parte de la explicación molecular del fenotipo radicular ligado a la nutrición amoniacal (inhibición del crecimiento de la raíz principal y aumento del número de raíces laterales).

Esto se relaciona con el proceso de elongación radicular en el que intervienen tres procesos biológicos interconectados entre sí: la división celular, la expansión celular y la diferenciación celular (Wang y Ruan, 2013; Youssef *et al.*, 2018). Las IAAs juegan un papel destacado en los dos primeros procesos (Wang y Ruan, 2013). Las IAA se pueden sintetizar en el meristema de la raíz (“*root meristem*”, RM) y transportar hacia las regiones adyacentes aguas arriba a través de transportadores específicos, como son la proteína AUXIN RESPONSE 1 (AUX1) y las proteínas PINFORMED 1-7 (PIN1-7) (Grunewald y Friml, 2010). Nuestros datos sugieren nuevos mecanismos moleculares que podrían afectar al RSA inducido por NH_4^+ en pino marítimo mediante la interconexión entre el papel de diversos factores de transcripción y de fitohormonas (Capítulo 3). Localizándose estos aspectos en las zonas radiculares denominadas como caliptra (“*root cap*”, RC) y el putativo meristema radicular (“*root meristem*”, RM), donde nuestros datos sugieren que se ubica la verdadera posición del meristema radicular de las coníferas. Por otro lado, en las secciones relativas a la zona cortical (“*root developmental cortex*”, RDC) se observó una importante inducción de la expresión de genes relacionados con la respuesta defensiva. Estos resultados han puesto de manifiesto una especialización y coordinación de la respuesta génica frente a la presencia de NH_4^+ por parte de las diferentes regiones tisulares estudiadas.

También, mediante una aproximación meramente holística y con el objetivo de estudiar la respuesta sistémica de la raíz del pino marítimo y los procesos de regulación inducidos por la presencia de NH_4^+ se ha realizado un abordaje multi-

ómico (Objetivo 4). Algunas de las aproximaciones realizadas constituyen la primera descripción de su aplicación en cuanto al metabolismo del N en plantas. Destacando la aplicación de la secuenciación directa del ARN y los estudios de epitranscriptómica general utilizando la tecnología de Oxford Nanopore (ONT) o centrados en el papel de la N⁶-metiladenosina (m⁶A) mediante MeRIP-seq (Capítulo 4). Es importante mencionar que la plataforma de ONT es capaz de secuenciar moléculas individuales de ARN conforme estas atraviesan una plataforma de nanoporos permitiendo secuenciar ARN de manera directa, sin necesidad reacciones enzimáticas de síntesis de elongación de la hebra de ADN (Garalde *et al.*, 2018). De este modo es posible obtener una visión más realista de la expresión génica, puesto que se evita la aparición de sesgos debidos a las reacciones de PCR utilizadas en la obtención de librerías en los protocolos de secuenciación de segunda generación (“*next generation sequencing*”, NGS), tales como la reducción de la complejidad de la librería de ADN complementario (ADNc), la distorsión en la abundancia relativa de ADNc, la pérdida de algunos tipos de ARN o las modificaciones químicas de las bases nitrogenadas. Hasta la fecha, se han identificado más de 160 modificaciones diferentes en el ARN (Shen *et al.*, 2019). A partir de ellos, se han identificado modificaciones del epitranscriptoma de ARNm de *Arabidopsis thaliana* m⁷G, m⁶A, m¹A, m⁵C, hm⁵C y de uridilación (Shen *et al.*, 2019). De entre estas modificaciones químicas del ARN, la m⁶A es la más abundante en los ARN mensajeros (ARNm). En múltiples estudios se ha descrito que la modificación química m⁶A interviene en importantes procesos celulares relacionados con el metabolismo del ARN, como la estabilidad del ARNm (Luo *et al.*, 2014; Shen *et al.*, 2016; Wei *et al.*, 2018) o la eficiencia traduccional (Luo *et al.*, 2014). Además, se ha descrito que una correcta deposición de m⁶A es esencial durante el desarrollo del embrión de *Arabidopsis* (Vespa *et al.*, 2004; Zhong *et al.*, 2008; Růžicka *et al.*, 2017), estando esto acorde a lo ya descrito en otros organismos eucariotas (Wang *et al.*, 2014; Geula *et al.*, 2015).

Utilizando estas tecnologías, nuestros resultados han puesto de manifiesto que en las raíces de pino marítimo el NH₄⁺ desencadena cambios en la expresión génica de transcritos importantes en el metabolismo del carbono y del nitrógeno, al igual que de genes relacionados con procesos defensivos, de genes relacionados con el estrés oxidativo y con la vía de señalización del etileno (ET) en pino marítimo. Además,

se ha descrito que la ET es una importante fitohormona reguladora en respuesta al exceso de NH_4^+ , activando la vía de transducción de señales MAPK (Sun *et al.*, 2017). Estas evidencias sugieren que la marca m^6A interviene en procesos biológicos fundamentales y subyace a los programas de desarrollo básicos en eucariotas (Fray y Simpson, 2015; Vandivier y Gregory, 2018; Shen *et al.*, 2019). Además, también se ha descrito que la m^6A interviene en la regulación de la respuesta al estrés biótico y abiótico en plantas (Martínez-Pérez *et al.*, 2017; Anderson *et al.*, 2018), en la maduración de frutos (Zhou *et al.*, 2019), en el proceso de transición de la floración (Duan *et al.*, 2017), en la morfogénesis foliar (Arribas-Hernández *et al.*, 2018), en el desarrollo de tricomas (Vespa *et al.*, 2004; Bodi *et al.*, 2012) y en el desarrollo de los meristemos de los brotes apicales (Shen *et al.*, 2016).

Mediante la aplicación de estudios epitranscriptómicos diferenciales de la N^6 -metiladenosina (m^6A) los resultados sugieren que la deposición diferencial de m^6A podría desempeñar un importante papel regulador en la ruta de transducción de señales vía MAPK. Constituyendo la primera descripción de este tipo de aproximación en lo concerniente al metabolismo nitrogenado y, en particular, en la respuesta a la presencia de NH_4^+ . A su vez, la localización de las modificaciones m^6A diferencialmente identificadas en los transcritos reveló que estas modificaciones químicas se encontraban principalmente en la región 3'-no codificante (“3-untranslated región”, 3'-UTR), presentando una secuencia consenso $\text{RR}\underline{\text{A}}\text{CH}$ (R = A / G; H = A / U / C; siendo la $\underline{\text{A}}$ una m^6A). Además, los resultados epitranscriptómicos generales obtenidos utilizando la tecnología Oxford Nanopore Technology (ONT) sugirieron que la modificación química diferencial en el ARNm está involucrada en la regulación de la expresión génica y el proceso de traducción. Este trabajo constituye un avance importante en la nutrición nitrogenada del pino marítimo puesto que pone de manifiesto puntos clave sobre cómo las plantas responden a un estímulo y propone posibles razones por las que esta respuesta puede diferir entre diferentes sistemas biológicos, más allá del diseño experimental en sí (Capítulo 4). Otro importante punto de regulación de la expresión génica lo constituyen los micro-ARN. Los micro-ARN (miR) en plantas son secuencias de ARN con una longitud entre 19-24 nucleótidos que intervienen en la regulación de la expresión génica mediante la degradación o comprometiendo

la traducción de sus dianas de ARNm (Jones-Rhoades *et al.*, 2006; Vakilian, 2020). Debido a la importancia de este tipo de ARN, los aspectos reguladores por parte de los miR han sido estudiados en respuesta a la presencia de NH_4^+ . De este modo, ha sido posible identificar un posible nuevo miR regulado por la presencia de NH_4^+ . Realizando una identificación de sus posibles dianas en nuestro transcriptoma de referencia se observó que una posible acción puede ser la de regular la expresión la *glutamina sintetasa 1b* (*PpGS1b*). Teniendo en cuenta el conocimiento actual, esto representa la primera evidencia de este tipo de regulación postranscripcional para transcritos de glutamina sintetasa (GS) (Thomsen *et al.*, 2014) (Capítulo 4).

En base a los datos presentados y discutidos en este trabajo de Tesis Doctoral se establecen las siguientes conclusiones:

1. La práctica de laboratorio acerca de la nutrición nitrogenada de las plantas diseñada y ejecutada en este trabajo permite a los estudiantes universitarios y de posgrado desarrollar habilidades técnicas y científicas interdisciplinarias, desde la agronomía y fisiología vegetal hasta la bioquímica y la biología molecular.
2. El amonio y el nitrato son fuentes alternativas de N inorgánico para la nutrición del pino marítimo. En las raíces, el amonio se incorpora de manera más eficiente que el nitrato siendo el principal órgano involucrado en la acumulación de un exceso de amonio mientras que el tallo es el principal órgano involucrado en la acumulación de exceso de nitrato.
3. La nutrición con amonio promueve un mayor aumento de la biomasa de la raíz del pino marítimo que la nutrición con nitrato. El estatus nitrogenado de las acículas fue mayor en la nutrición con amonio que en la nutrición nítrica.
4. Los datos del presente trabajo apoyan que el amonio actúa como molécula señal en la etapa de desarrollo estudiada del pino marítimo.
5. La aplicación de la captura por microdissección láser seguida de secuenciación NGS (*Next Generation Sequencing*) permitió identificar nuevos transcritos no incluidos en bases de datos transcriptómicas preexistentes en pino marítimo, como *PpNAC38*, *PpDOF11* o *PpDOF12*.

6. El amonio influye, de manera directa o indirecta, en la expresión génica de factores de transcripción probablemente involucrados en la arquitectura radicular, como *PpSHR* o *PpSHOOT-GRAVITROPISM*.
7. El amonio provoca cambios en la expresión génica de transcritos ligados al metabolismo y transporte de fitohormonas importantes en la arquitectura radicular (auxinas, citoquininas y etileno).
8. Los cambios en el transcriptoma, epitranscriptoma y proteoma observados y su integración reveló un papel regulador del amonio en diferentes vías como el metabolismo del carbono y el nitrógeno, en la respuesta defensiva, en la vía de señalización mediada por etileno y en la composición proteica de los ribosomas.

De este modo, el trabajo realizado en *Pinus pinaster* Ait. permite ampliar considerablemente el conocimiento de los diferentes procesos que atañen a la nutrición nitrogenada de esta planta. A su vez los resultados de este trabajo se asientan como importantes precedentes para futuras líneas de investigación, abarcando aspectos tan amplios como los mecanismos moleculares que subyacen a la compartimentalización de las diferentes formas de nitrógeno inorgánico, al fenotipo radicular o a la respuesta defensiva en coníferas, pasando por el estudio de los procesos moleculares afectados por la presencia de modificaciones químicas en el ARN y sus efectos tanto a nivel fisiológico como morfológico o la verificación de la actividad reguladora de miR en pino y su posible utilización en ámbitos silvícolas con la que lograr una mejora en la gestión sostenible de las masas forestales.



Introduction



1. Importance of forest stands

Forests occupy around 30% of the Earth's surface (Figure I.1), serving as a source of raw materials, food, drugs and fuel. Thus, they intervene in the socioeconomic development of many rural areas. In addition to the “more immediate” interests of the human being, forest masses protect the soil from erosion, host more than 75% of the world's terrestrial biodiversity and play an important role sequestering carbon dioxide (CO₂). CO₂ is one of the main greenhouse gases related to the increase in terrestrial temperature, commonly known as global warming (FAO, 2018), and plays an important role during ocean acidification (Osborne *et al.*, 2020; Verspagen, 2020). Since the beginning of the Industrial Revolution (18th century) and as a consequence of the alteration of the carbon cycle largely due to anthropogenic alterations, the concentration of carbon dioxide (CO₂) in the air has increased from 278 to 400 ppm (Le Quéré *et al.*, 2017). Only three agents (oceans, soil and forests) naturally intervene as carbon sinks. It is estimated that around 50% of anthropogenic CO₂ is absorbed by the oceans and forests. Translated into numerical data and to the role of the forests, yields an amount close to 2 giga-tons (2000 million tons) of CO₂ absorbed per year.

During the world summit that led to the Paris Agreement (2015), the Intergovernmental Panel on Climate Change highlighted that effective forest management could strengthen resilience to natural disasters related to climate, which highlighted as necessary for reducing the risk of natural catastrophes and a concomitant reduction of greenhouse gas emissions relative to deforestation and forest degradation (UNFCCC, 2015).

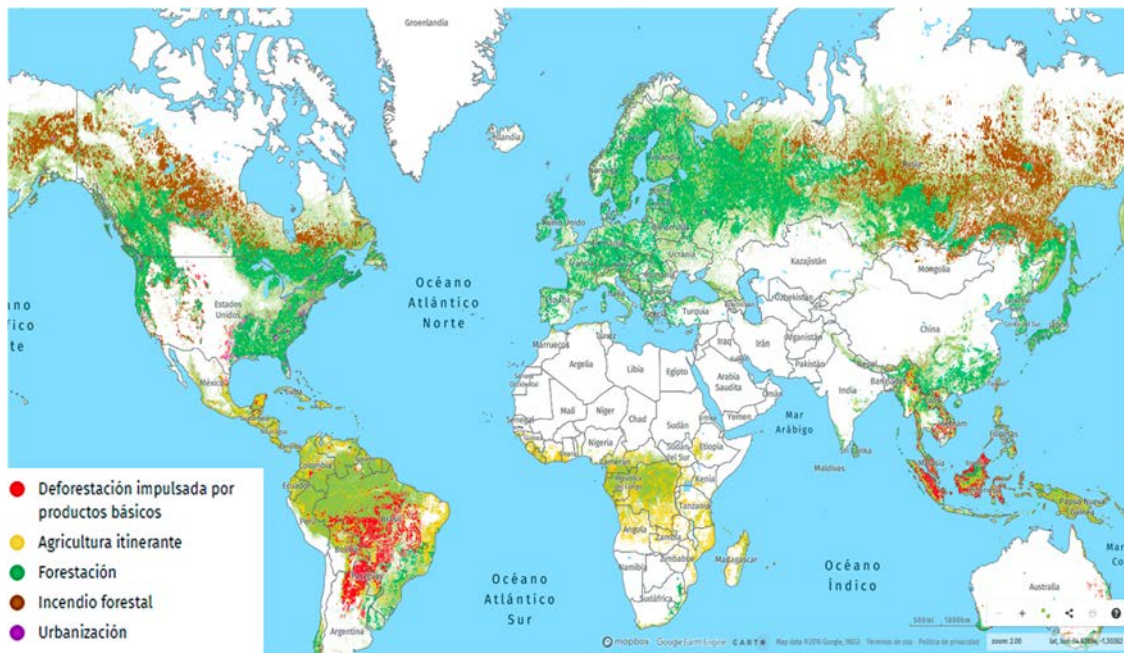


Figure I.1. Situation of the main forest stands in 2019. Image from globalforestwatch.org.

Taking into account that the forecasts provided by the United Nations foresee an increase in the world population to 8,500 million people in 2030 and close to 10,000 million people in 2050 (UN Report, 2019), it is essential to highlight that forest formations provide food products, energy source and raw materials to the human being (FAO, 2018). The benefit is even more important if it is considered that most of the people who depend in first or last instance on the forests have poor economic power (Agrawal *et al.*, 2013). Additionally, forest stands serve to the improvement of capacity of agricultural production (Foli *et al.*, 2014) because forests influence the hydrological cycle (Ellison *et al.*, 2017) by providing organic matter (Kimble *et al.*, 2007) and compost to agriculture (Sinu *et al.*, 2012) and being fundamental for pollination processes (Roubik, 1995).

In addition, the continuing concern of the governments and the general population about climate change and the growth in greenhouse gas emissions have led several countries to introduce new policies to mitigate global warming. In this area, it is necessary to highlight that forests generate a supply of renewable energy, estimated at 40% worldwide in the form of wood fuel. This equates to the energy provided by hydroelectric, wind and solar platforms (FAO, 2018). Although, this type of energy is considered as “renewable” it is referred to the fact that it has a net zero carbon

emission rate. This assertion is widely said because of the balance of the amount of carbon emitted with an equivalent amount offset or sequestered, which is achieved during the growth of forest stands (Bright and Strømman, 2009; Zhang *et al.*, 2010). However, this concept is currently a controversial issue. It is true as long as in the long term the conditions are not altered, so in the short term it is not fully fulfilled due to the CO₂ and other greenhouse gases are emitted directly to the atmosphere when forest biomass is used as an energy source and the development of the next generation of trees takes decades (Vanhala *et al.*, 2013).

Therefore, forest masses are a very important object of study including their different aspects: the set of elements that make them up, the relationships established between them, the relationship of these factors with the growth rate and renewal of forests, as well as the study of its behavior and response, both molecular and physiological to different environmental conditions and types of stress, as well as the genetic component at all its levels. All of it becomes a *sine qua non* condition to implement efficient sustainable management with which to obtain the greatest benefits that these plant extensions can provide to human beings.

2. Conifers and maritime pine as model organism

Gymnosperms (*Gymnospermae*) are cormophytic and spermatophytic vascular plants that appeared on Earth more than 350 million years ago (mya). Through paleobotanical and molecular studies, it is estimated that the divergence between gymnosperms and angiosperms can be dated back to the Carboniferous (~ 300 mya) (Clarke *et al.*, 2011; Crisp and Cook, 2011; Magallón *et al.*, 2013), but it was not until the Permian (~ 290 mya) when the great expansion of this group of plants took place, contributing very notably to coal reserves during the Mesozoic (~ 150 mya) (Rothwell *et al.*, 2012) (Figure I.2). Currently, this ancient and widespread plant lineage comprises around 1.000 different species (Wang and Ran, 2014). Gymnosperms represent four of the five major seed plant lineages: cycacads (*Cycadophyta*), ginkgos (*Ginkgophyta*), gnetophytes (*Gnetophyta*), and conifers (*Coniferophyta*) (Crisp and Cook, 2011), which have been divided into four subclasses (*Cycadidae* , *Ginkgoideae*, *Gnetidae* and *Pinidae*) (Magallón *et al.*, 2013).

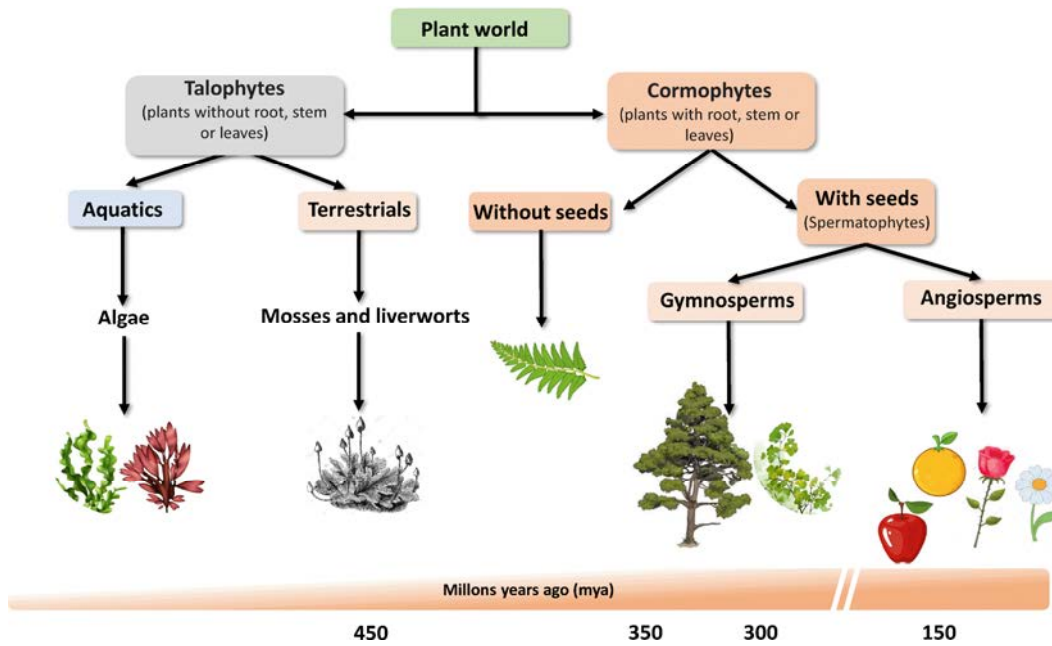


Figure I.2. Classification of the plant world. The graduated bar at the bottom of the image corresponds to a time scale of appearance of the different groups of plants (time scale in millions of years of the appearance of the different plant groups counting from the present days).

Within gymnosperm plants, conifers constitute the most numerous and representative group from an economic and ecological point of view, presenting around 615 species and a wide distribution throughout the world (Farjon, 2018). Conifers form vast vegetation extensions mainly in the Northern Hemisphere (Figure I.3). For example, they are the main members of the forests of North America and Eurasia. However, the extensions occupied by this group of vascular plants are quite smaller in the Southern Hemisphere. This results in a certain paradox because it is in these regions where the greatest diversity of coniferous species is found (Farjon, 2018) (Figure I.3).

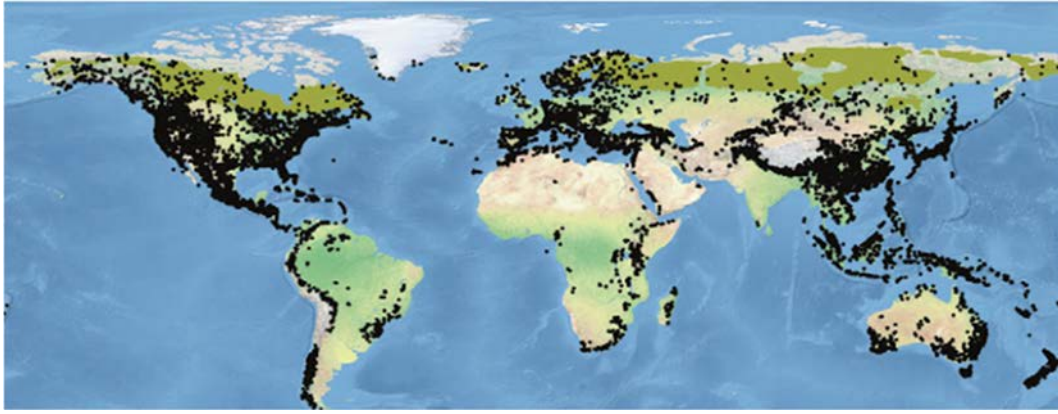


Figure I.3. Ecological distribution of conifers. Image from Farjon, A., & Filer, D. (2013) (Farjon, 2013).

The distribution of conifers shows great versatility in terms of adaptation, since species located both at sea level (*Pinus pinaster*) (Burban and Petit, 2003) and even in the Himalayas (*Eastern Himalayan Sub-Alpine Conifer Forests, World Wildlife Fund; Soharn et al., 2017; Farjon, 2018*) are observed. However, it is possible to observe a certain trend in their distribution since conifers are mainly present in sub-optimal climates and / or soils for the growth of most plant species (mainly belonging to the group of angiosperms) which exhibits the adaptation process that conifers have developed throughout their evolutionary history (Farjon, 2018). One of the causes that can explain this process and, therefore, the distribution they present is the symbiotic interactions established between the roots of conifers and fungi. These interactions usually form ectomycorrhizal systems that increase the capacity for uptake of water and nutrients up to ten thousand times (Taylor and Alexander, 2005; Högberg *et al.*, 2010; Glassman *et al.*, 2015; Farjon, 2018). Considering the long evolutionary trajectory of conifers compared to angiosperms, it is feasible to think that the development and improvement of these symbiotic relationships have been preserved due to the appearance and subsequent dominance of angiosperms (Farjon, 2018). From an economic point of view, conifers are the largest contributors of raw material to the wood industries (Cooper, 2003), assuming higher yields due to better growth and more predictable wood shapes and sizes compared to angiosperms (Farjon, 2018). The second most important use in economic terms is its use as an ornamental plant, which initially arose during the 19th century. During this time, seeds of different types of conifers from various sources were used to decorate gardens and parks. Currently the interest of the

Introduction

ornamental plants industry towards conifers lies in obtaining individuals with a smaller size which has encouraged investment, as is indicated by companies such as Conifer Holdings Inc (<https://www.cnfrh.com/>).

With the emergence and democratization of both molecular biology and omics sciences it has been possible to increase the information available on these species and keep the door open to industrial interests. It is true that the approach from a molecular and omics view of the different species of conifers presents important limitations such as the large size of adult individuals or their long-life cycles (Cañas *et al.*, 2019). These characteristics mean that in many cases the studies focus on young seedlings. However, this issue should not necessarily be considered as a handicap, since the most vulnerable stage of woody plants is the seedling phase (Losso *et al.*, 2019). Therefore, this kind of approximation is essential to obtain achievements that can be transferred to economic areas. As an added difficulty, trees in general, present a large quantity of secondary metabolites such as phenolic compounds or lignin among others, which can restrict the quality and / or quantity of nucleic acid (DNA and RNA) and protein purifications (Chaffey, 2002). On the other hand, they have unique characteristics within vascular plants that make them of great interest such as their high genetic variability (Hamrick *et al.*, 1992), their longevity and survival, the deposition of wood or their adaptation to seasonality. However, in the case of conifers, the size of the genome is an added difficulty that makes genomic approaches difficult. This is because these plants have megagenomes of an estimated size between 18-35 Gbp (Mackay *et al.*, 2012; Pellicer and Leitch, 2019) which is more than 6 and 150 times the size of the human genome and that of *Arabidopsis*, respectively. The high size of the genome is largely due to several factors such as the high number of repetitive sequences that they present, being estimated around 40-50% of the total size of the coniferous genome (Nystedt *et al.*, 2013; Neale *et al.*, 2014; Wegrzyn *et al.*, 2014; Cañas *et al.*, 2017). Another factor to consider is the abundance of pseudogenes that is around 2-5% of the genome size (Nystedt *et al.*, 2013; Neale *et al.*, 2014).

<i>Arabidopsis</i>		Conifers
20-25 cm	Size	0.03-100 m
Herbaceous	Plant type	Woody
2483	Articles in 2020	91
135 Mbp	Genome size	4-36 Gbp
High quality and fidelity	Genome assembly	Fragmented
Annual (6 weeks)	Life cycle	Perennial (several years)
≈ 300.000	Mutants lines	-
Floral dipping	Transformation methods	Somatic embryogenesis

Figure I.4. Comparison between the characteristics of *Arabidopsis* and conifers. * Number of articles in August 2020. The article number search was carried out using the “Web of Science” search engine using “*Arabidopsis thaliana*” and “Conifer” as keywords. Image adapted from Cañas *et al.* (2019).

Despite the difficulties that conifers present as model plants (Figure I.4), thanks to second and third sequencing techniques generation, multiple omics data have been published and are now available (Gion *et al.*, 2005; Hall *et al.*, 2011; Nystedt *et al.*, 2013; Canales *et al.*, 2014; Zimin *et al.*, 2014; Cañas *et al.*, 2015a; Warren *et al.*, 2015; Stevens *et al.*, 2016; Neale *et al.*, 2017; Zimin *et al.*, 2017; Kang *et al.*, 2019) (Table I.1).

Table I.1. Different approach examples to achieve genomic and transcriptomic study in conifers. The strategy used is specified in parentheses.

SPECIE	APPROXIMATION	REFERENCES
<i>Picea glauca</i>	Genomic (shotgun), transcriptomic (RNA-Seq)	Biol et al., 2013; Raherison et al., 2015
<i>Picea abies</i>	Genomic (shotgun)	Nystedt et al., 2013
<i>Pinus taeda</i>	Genomic (shotgun)	Neale et al., 2014; Zimin et al., 2014; Zimin et al., 2017
<i>Pinus densiflora</i>	Genomic (Oxford Nanopore Technology), transcriptomic (RNA-Seq)	Kang et al., 2019, Liu et al., 2015
<i>Pinus pinaster</i>	Genecapture, Transcriptome assembly, RNA-Seq, Single-cell RNA-Seq	Seoane-Zonjic et al., 2016; Canales et al., 2014; Cañas et al., 2015a ; Cañas et al., 2017
<i>Pinus halepensis</i>	Transcriptomic (RNA-Seq)	Fox et al., 2018
<i>Pinus lambertiana</i>	Genomic (shotgun)	Stevens et al., 2016

Pinus pinaster Aiton, commonly known as maritime pine, is a tall tree (20-40 meters high) and relatively thick (30-45 centimeters in diameter). Its distribution covers mainly the western Mediterranean European region (Portugal, Spain, South of France and Italy) occupying more than 4 million hectares on the European continent and also presenting forest formations in North Africa, mainly in Morocco and Algeria (Critchfield and Little, 1966) (Figure I5A). Maritime pine is a species that presents an extensive ecological spectrum, being present in fourteen of the twenty phytoclimates described in the Iberian Peninsula (Allué Andrade, 1990) and also being predominant in poor soils of a siliceous and / or sandy nature (Viñas et al., 2016). However, it can also be found in calcareous soils and grows well in soils composed of peridotite, a plutonic igneous rock that is toxic to most plants, as occurs in Sierra Bermeja (Málaga) (Cañas et al., 2015b; Farjon, 2018).



Figure I.5. Map of Mediterranean (A) (<http://www.euforgen.org/>) and world (B) (<https://www.cabi.org/>) distribution of *Pinus pinaster*.

The great versatility of the maritime pine provides tools that facilitate its adaptation to different environmental conditions (Cañas *et al.*, 2015b), presenting a great capacity to adapt to dry and poor soils (Picon *et al.*, 1996). It is notable to mention that maritime pine also has as an enormous physiological and morphological plasticity, showing great levels of differentiation between populations in different environments (Aranda *et al.*, 2010). For all this, the distribution in Spain of maritime pine has been increased through its use in reforestation tasks and in soil stabilization (Seoane *et al.*, 2007). Additionally, and as a consequence of its higher growth rate compared to the rest of the conifers and its great versatility as a source of products derived from wood this species has been introduced in regions where it is not native such as South Africa, New Zealand or Australia (Butcher, 2007) (Figure I.5B). In this sense, in economic terms, maritime pine feeds various industries nation-wide with raw material. It is true that because of the global economic crisis of 2008 there was a notable decrease in the consumption of raw

materials from *Pinus pinaster*, mainly related to wood (carpentry, construction, and the like). This has contributed to the fact that industrial interests have changed in recent years, redirecting interest in maritime pine towards obtaining cellulose pulp for the manufacture of paper and the collection of biomass and pellets for the energy industry (Fundación HAZI Fundazioa, 2019). As a result of its enormous ecological and economic interest, multiple projects have been carried out in all scientific fields that have led to the obtaining of powerful molecular tools with which to obtain a better and deeper understanding of the biology of *Pinus pinaster*. Some examples are the construction of a reference transcriptome (Canales *et al.*, 2014), the adaptation of a protocol for the cDNA synthesis and amplification (CRA+) (Cañas *et al.*, 2014) or an atlas of the gene expression of the different tissues from the *Pinus pinaster* seedlings (Cañas *et al.*, 2017). Within the business field, the creation of the FCBA Technological Institute (Institut Technologique Forêt Cellulose Bois-construction Ameublement) (<https://www.fcba.fr/>) stands out in 2007, which has developed a platform for transforming trees of industrial interest such as maritime pine.

3. Nitrogen as a plant nutrient

Nitrogen (N) constitutes an essential macronutrient for all living beings, forming part of the main biomolecules such as nucleic acids, proteins, amino acids, chlorophylls and (phyto)-hormones, among others (Miller and Cramer, 2005). For decades, it has been known that both nitrogen and carbon are important elements for the proper plant growth and development (Näsholm *et al.*, 1998; Chapter 1). Various estimates made in the greatest interest crops (maize, wheat, rice, and soybeans) reveal that to obtain 1Kg of net matter, between 20-50 g of N absorbed by the roots is required (Robertson and Vitousek, 2009). For plants the availability of nitrogen in the natural soils constitutes a limiting factor (Rennenberg *et al.*, 2009 and 2010). Thus, for decades in agriculture and forestry systems the use of fertilizers has been promoted. This has led to improve the production of food and raw materials (Good *et al.*, 2004). However, the excess of N from agricultural production systems entails important ecological problems, affecting the quality of soils, water and air by causing an increase in leaching from soils to drainage water, being able to experience the release of nitrous oxide and reactive N species towards the troposphere. These events result in the eutrophication of waterways and

favoring the acidification of soils (Robertson and Vitousek, 2009; Guo *et al.*, 2010; Xu *et al.*, 2012). For this reason, the study of N uptake and use in plants is established as a key factor through which to obtain biotechnological tools that allow mitigating the adverse effects derived from the extensive agricultural productions in order to provide the increasing population needs. Furthermore, it is a fundamental aspect for forestry since to obtain the raw material derived from forest tree species can take years.

In general, most plants have a marked sensitivity to ammonium (NH_4^+), whose exposure can affect the growth and development rate of great agronomic interest crops such as avocado or tomato, among others (Lobit *et al.*, 2007; Xun *et al.*, 2020). Conifers in their natural environment show a marked preference / tolerance for NH_4^+ over NO_3^- (Kronzucker *et al.*, 1997). This could probably be due to the presence in these forest areas of processes that interfere with soil nitrification such as a high presence of phenolic compounds (Vitousek *et al.*, 1982), low temperatures, lower rate of soil aeration or microbial decomposition of biomass (Schimel and Bennet, 2004). Related to *Pinus pinaster*, this preference of ammonium over nitrate was known (Warren and Adams, 2002) and has recently been corroborated at inert substrate (Chapter 2).

3.1. Ammonium absorption in plants

The transport of ammonium into the cell is carried out, mainly and selectively, through a group of transmembrane proteins known as ammonium transporters that belong to the *AMT / MEP / Rh* gene family, present in all living beings lineages (Winkler, 2006).

In plants, ammonium transporters are divided into two subfamilies: AMT1 and AMT2. AMT proteins have 10-12 transmembrane domains (TM) (Von Wittgenstein *et al.*, 2014, Castro-Rodríguez *et al.*, 2016). On the one hand, evolutionary studies on these proteins have shown that the AMT1 subfamily forms a monophyletic group in eukaryotes (McDonald *et al.*, 2010 and 2012) and its acquisition by land plants could be originated through vertical gene transmission (VGT) events (McDonald *et al.*, 2010 and 2012; Von Wittgenstein *et al.*, 2014). On the other hand, the AMT2 subfamily is related to fungal proteins (MEP). It has been shown that the appearance of the AMT2 subfamily in plants is due to successive

Introduction

horizontal gene transfer (HGT) processes (Von Wittgenstein *et al.*, 2014; McDonald *et al.*, 2010 and 2012). The appearance in terrestrial plant organisms of these two subfamilies of ammonium transporters followed two different evolutionary paths (Figure I.6), an aspect that is also reflected in the fairly conserved intron-exon gene structure in the AMT2 members. While the AMT1 subfamily does not usually present introns (Yuan *et al.*, 2007; Castro-Rodríguez *et al.*, 2016; 2017).

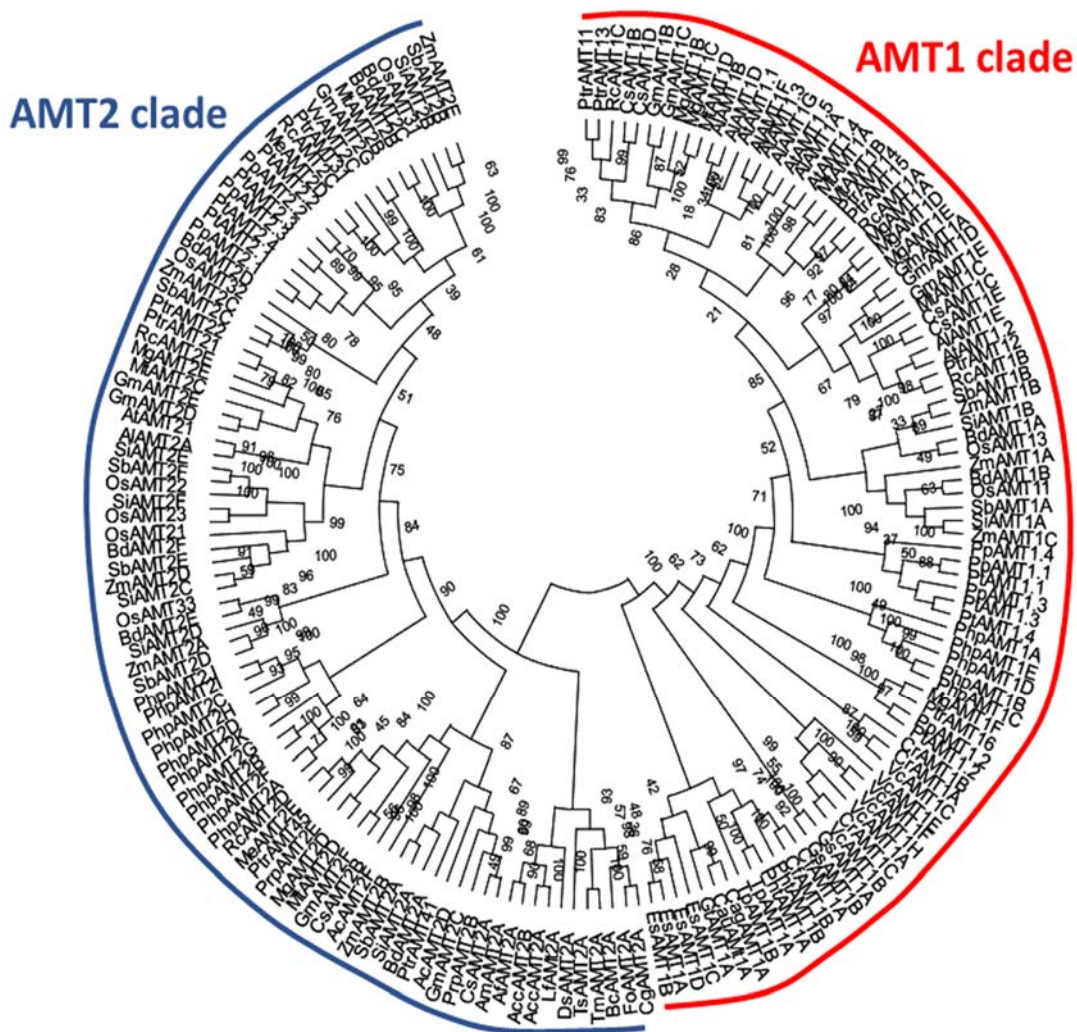


Figure I.6. Phylogenetic tree of ammonium transporter proteins (AMT) in the plant lineage. (MegaX, Muscle alignment, tree made using NJ algorithm with bootstrap value = 1000). The protein sequences were obtained from Congenie, GenBank and McDonald *et al.*, 2010; 2012. Abbreviations: Acc, *Acidithiobacillus caldus*; Af, *Acidithiobacillus ferrooxidans*; Al, *Arabidopsis lyrata*; Am, *Acidiphilium*

multivorum; At, *Arabidopsis thaliana*; Bc, *Baudoinia compniacensis*; Bd, *Brachypodium distachyon*; Cag, *Chloroflexus aggregans*; Cf, *Cylindrotheca fusiformis*; Cg, *Cladonia grayi*; Cs, *Cucumis sativus*; Cr, *Chlamydomonas reinhardtii*; Ds, *Dacryopinax spathularia*; Es, *Ectocarpus siliculosus*; Fo, *Fusarium oxysporum*; Gm, *Glycine max*; Gs, *Galdieria sulphuraria*; Gt, *Guillardia theta*; Lf, *Leptospirillum ferriphilum*; Mg, *Mimulus guttatus*; Mt, *Medicago truncatula*; Os, *Oryza sativa*; Php, *Physcomitrella patens*; Pht, *Phaeodactylum tricornutum*; Pp, *Pinus pinaster*; Prp, *Prunus pérsica*; Pt, *Pinus taeda*; Ptr, *Populus trichocarpa*; Rc, *Ricinus communis*; Sb, *Sorghum bicolor*; Si, *Setaria itálica*; Tm, *Talaromyces marneffeii*; Tp, *Thalassiosira pseudonana*; Vc, *Volvox carteri*; Zm, *Zea mays*.

The plant AMT1 subfamily proteins are very well conserved and present a similar three-dimensional structure, homo / heterotrimers that generate a central pore through which the transport itself takes place (Neuhäuser *et al.*, 2014). The structure of these proteins from different organisms has been studied by protein crystallization and X-ray diffraction (Zhen *et al.*, 2004; Andrade *et al.*, 2005; Lupo *et al.*, 2007; Gruswitz *et al.*, 2010) presenting in all cases three main characteristics. A binding site for ammonium, a "phenylalanine gate" (Phe) and a motif for two histidines (His). Several studies in bacteria seem to indicate that for transport into the cell, ammonium must be deprotonated in its electro-neutral form. Once it reaches the cytoplasmic section of the pore, it undergoes re-protonation due to the intracellular pH (Bostick *et al.*, 2007; Lin *et al.*, 2009; Neuhäuser *et al.*, 2014). This mechanistic has been postulated for plants due to the binding sites are quite conserved (Neuhäuser *et al.*, 2009) (Figure I.7). Through crystallographic studied of the structures of AMT / Rh proteins, it has been described that the pore is occluded by two Phe residues which act as a "gate" (Neuhäuser *et al.*, 2014), intervening in recruiting and stabilizing ammonium through cationic interactions (Khademi *et al.*, 2004; Yang *et al.*, 2007; Ganz *et al.*, 2019). The twin histidines motif intervenes in the affinity for ammonium and its selectivity against ions with similar structural characteristics such as potassium (K⁺) (Ganz *et al.*, 2020).

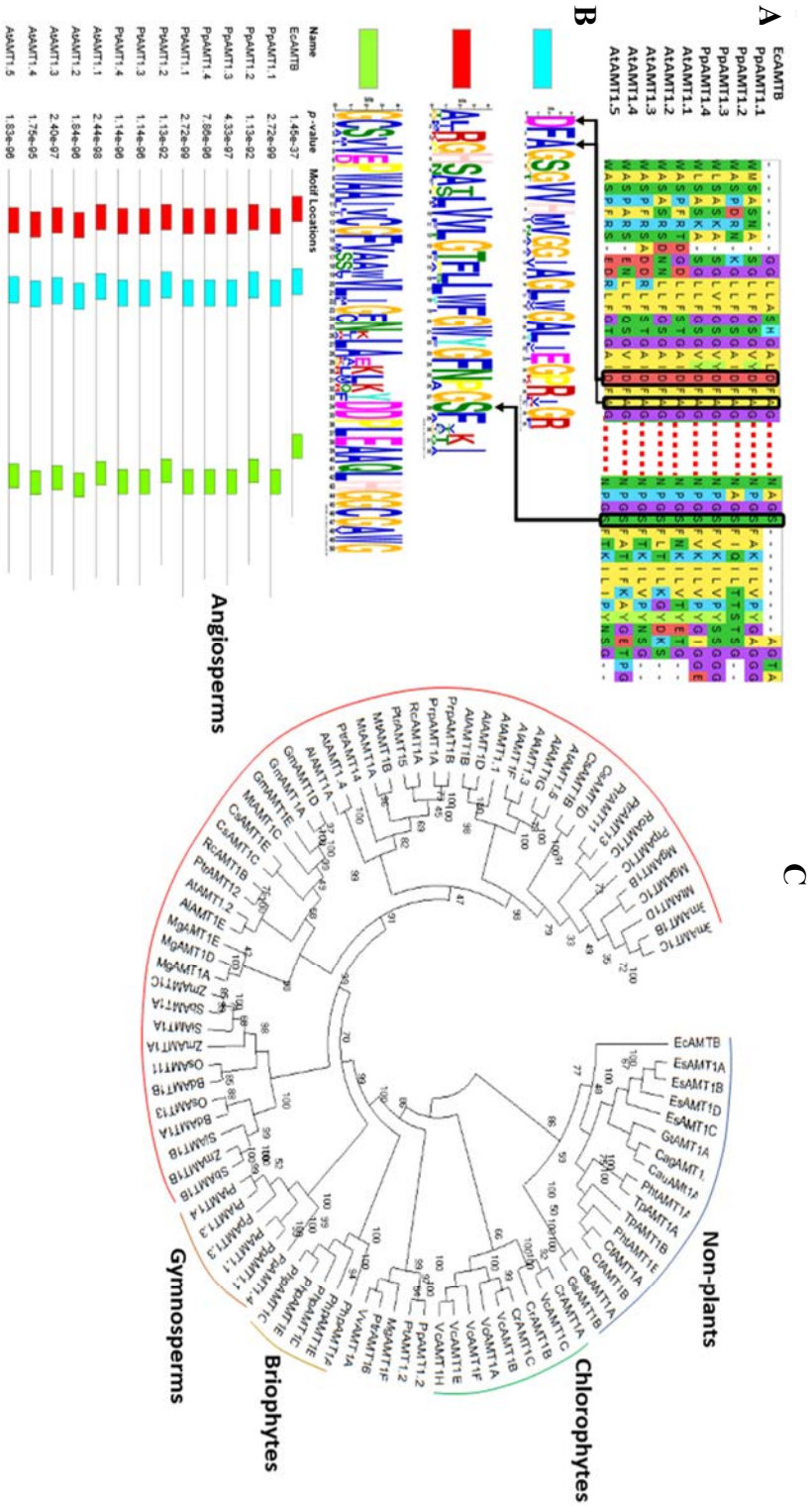


Figure 1.7. A) Alignment of ammonium transporters (AMT) of *Escherichia coli* (Ec), *Pinus pinaster* (Pp) and *Arabidopsis thaliana* (At). B) Common motifs in AMTs. In A and B the residues involved in ammonium binding are highlighted. C) Phylogenetic tree of the AMT1 subfamily in different lineages of living beings (Megax, alignment by Muscle, tree made using the NJ algorithm with a bootstrap value = 1000). The protein sequences were obtained from Congenie, GenBank and McDonald *et al.*, 2010 and 2012.

Several biochemical and physiological studies have demonstrated the presence of high affinity transport systems (HATS) and low affinity transport systems (LATS) for ammonium in the roots of vascular plants (Loqué *et al.*, 2006; Castro-Rodríguez *et al.*, 2016). The HATS constitute a saturable system that operates at micromolar concentrations (μM) of NH_4^+ and is regulated based on the external concentration of this nutrient. On the other hand, LATS systems come into action at concentrations in the millimolar (mM) range (Castro-Rodríguez *et al.*, 2016). Different ammonium transporters have been functionally characterized as HATS and LATS in both woody and non-woody plants (Castro-Rodríguez *et al.*, 2017). Thus, it has been described that in *Pinus pinaster* PpAMT1.1-1.3 and PpAMT2.3 act as HATS while PpAMT2.1 acts as LATS (Castro-Rodríguez *et al.*, 2016). In *Populus tremula* \times *alba* PtAMT1.2 and PtAMT1.6 constitute a high affinity transport systems, while PtAMT1.1, PtAMT1.5, PtAMT2.1, PtAMT2.2 and PtAMT4.5 are low affinity transporters (Couturier *et al.*, 2007). In non-woody plants, they have been described as HATS BnAMT1.2, LjAMT1.1-1.3, PbAMT1.3, OsAMT1.1 and OsAMT1.2 and AtAMT1.1-1.5 and AtAMT2 in *Brassica napu*, *Lotus japonicus*, *Pyrus betulaefolia*, *Oryza sativa* and *Arabidopsis thaliana*, respectively (Pearson *et al.*, 2002; Kumar *et al.*, 2003; Sonoda *et al.*, 2003; D'Apuzzo *et al.*, 2004; Yuan *et al.*, 2009; Von Wittgenstein *et al.*, 2014; Li *et al.*, 2016). The belonging of these transporters to one or another AMT subfamily is not an exclusive determinant of their characteristic as transporters (HATS or LATS), which could support the evolutionary theory of ammonium transporters over plant kingdom.

In addition, it has been possible to characterize the importance in the incorporation of NH_4^+ in *Arabidopsis* roots of the six different AMTs present in its genome (*AtAMT1.1*, *AtAMT1.2*, *AtAMT1.3*, *AtAMT1.4*, *AtAMT1.5* and *AtAMT2*) (Xiaoxue *et al.*, 2016). So, it is estimated that under nitrogen limiting conditions, between 60-70% of the incorporation rate of this ion is due to the activity of the isoforms *AtAMT1.1* and *AtAMT1.3* (Loqué *et al.*, 2006). Giehl *et al.* (2017) demonstrated that *AtAMT2* is mainly involved in ammonium translocation from the root zone towards the aerial part of the plant. At the same time, other studies in different plant species that present more than one isoform of the AMT2 subfamily relate their biological function to the establishment of interactions with mycorrhizae (Guether

Introduction

et al., 2009; Breuillin-Sessoms *et al.*, 2015). In conifers, determining the relevance of each ammonium transporter has not been possible for now. It is partly due to the great difficulty involved in obtaining mutant lines and transgenic organisms as mentioned above. In contrast, the tissue location of the ammonium transporters has been characterized in *Pinus pinaster* (Castro-Rodríguez *et al.*, 2016). It is observed that PpAMTs are related to the tissue location described in *Arabidopsis* (Yuan *et al.*, 2007). The AMT1 subfamily presents a more external root location in both angiosperms and gymnosperms, located in the cortical and epidermal area (Yuan *et al.*, 2007; Castro-Rodríguez *et al.*, 2016). In contrast, the AMT2 subfamily exhibits a more internal root location, being located around the pericycle and the vascular cylinder (Yuan *et al.*, 2007; Castro-Rodríguez *et al.*, 2016).

In addition to the incorporation of NH_4^+ through these specific proteins, there are other alternative and/or complementary routes for the incorporation of this element. These are integrated by non-specific transport systems that include potassium transporters/channels (AKT, HAK) (Miller and Cramer, 2005; Hoopen *et al.*, 2010), non-selective cation channels (NSCC) (Hoopen *et al.*, 2010) and aquaporins (AQP) (Jahn *et al.*, 2004) (Figure I8). In this way, plants present numerous tools that allow them to ensure a continuous supply of this compound that supplies their nutritional needs.

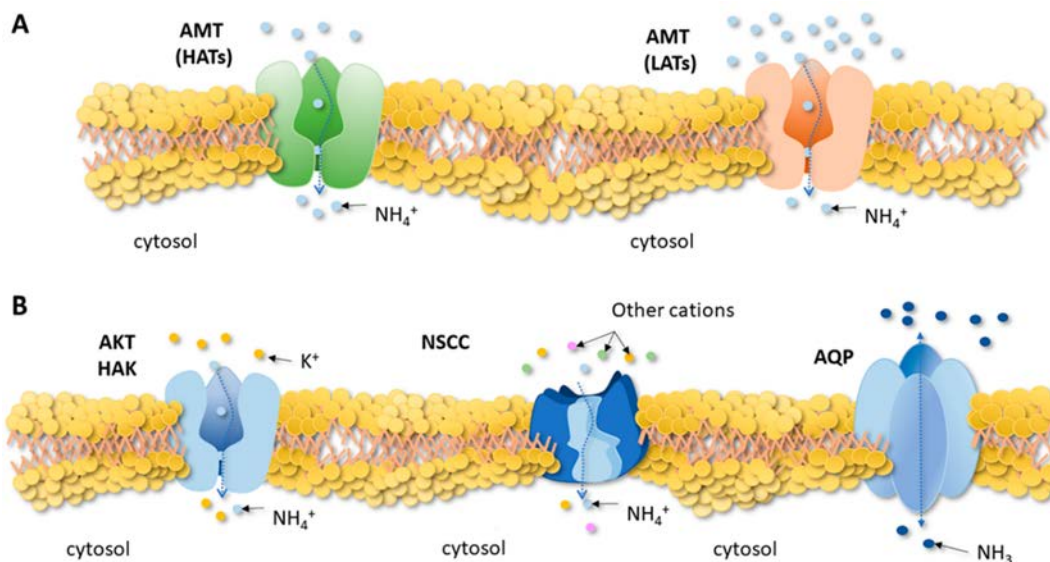


Figure I.8. Pathways of incorporation of ammonium (NH_4^+) in a plant cell. A) Specific transport of ammonium by high affinity (HAT) and low affinity (LAT) ammonium transporter (AMT). B) Non-specific transport by potassium transporters

/ channels (AKT, HAK), non-selective cation channels (NSCC) and / or aquaporins (AQP).

3.2. Regulation of the incorporation of ammonium

There are multiple mechanisms that regulate both the expression and the activity of ammonium transporters. The intracellular concentration of this ion constitutes a key regulation point due to its inherent toxicity acting as a negative feedback loop. Therefore, when the fluctuation of the intracellular concentration exceeds a certain threshold, it is common for this excess of NH_4^+ to become compartmentalized, mainly in the vacuoles (Zhou *et al.*, 2015). This helps, on the one hand, to reduce the negative or toxic effect that a high concentration of NH_4^+ in the cytoplasm can cause and in turn favors the osmotic balance, facilitating the absorption of water (Zhou *et al.*, 2015). Components of this response linked to the increased endogenous NH_4^+ levels are the AtTIP2.1, AtTIP2.3 (tonoplast intrinsic protein, TIP) and AtCAP1 ($[\text{Ca}_2^+]$ cyt-associated protein kinase) proteins described in *Arabidopsis thaliana*. The expression of these transcripts is induced in the presence of nitrogen and through heterologous assays in yeast it has been described the ability of AtTIP2.1 and AtTIP2.3 to transport methylammonium (an NH_4^+ analog) into the vacuole (Loqué *et al.*, 2005; Bai *et al.*, 2014a) contributing to the maintenance of its homeostasis. In addition, it has been shown the role of CAP1 as a modulator of cytosolic NH_4^+ levels, playing a key role with the growth of root hairs. This aspect is regulated by NH_4^+ homeostasis through the modulation of cytoplasmic Ca^{2+} gradients (Bai *et al.*, 2014a and 2014b). Although the function of CAP1 has been studied in the root system, it is likely that it also intervenes in the maintenance of cytosolic levels of NH_4^+ in the rest of the plant tissues (Bai *et al.*, 2014a).

Regarding the expression regulation of the coding genes for AMTs, it responds to multiple factors, such as endogenous glutamine levels (Rawat *et al.*, 1997). In addition, Gazzarrini *et al.* (1999) showed that the *AtAMT1.3* exhibits light-dependent expression patterns whose maximum expression values occur towards the end of the photoperiod. Presumably this phenomenon was observed because to procure an efficiently NH_4^+ assimilation it is required an appropriate flow of carbon

Introduction

skeletons. The end of the day is the moment in which plants normally present higher carbohydrates levels (Kerr *et al.*, 1985).

The regulation of the incorporation of NH_4^+ also presents its effect from a post-translational plane. Phospho-proteomic approaches have identified phosphorylated residues in the C-terminal cytosolic region (CTR) of AtAMT1.1, specifically in a conserved threonine residue 460 (Thr, T460) (Nüsche *et al.*, 2004; Yuan *et al.*, 2013; Menz *et al.*, 2016). Punctual mutation in this residue leads to the inactivation of the complex formed by AMTs (Loqué *et al.*, 2007). This process is triggered in a specific way when a high supply of ammonium is supplied (Lanquar *et al.*, 2009; Beier *et al.*, 2018). This line of regulation is carried out by the AtCIPK23-AtCBL1 kinase protein complex (Straub *et al.*, 2017) (Figure I.9).

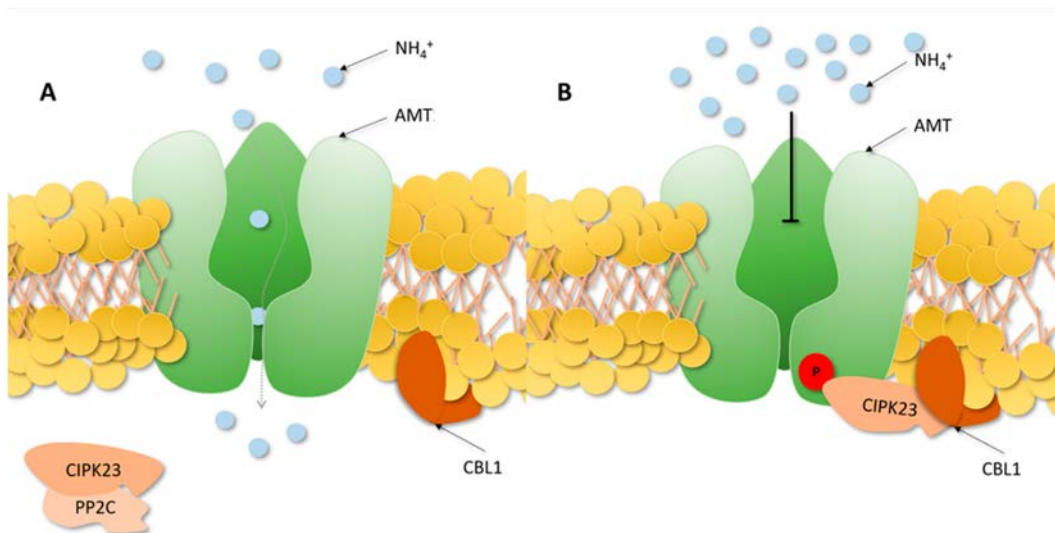


Figure I.9. Regulation model of the ammonium (NH_4^+) incorporation process. A) CIPK23 is found to interact with PP2C in the low cytosol when the extracellular ammonium concentration is low / moderate and / or the intracellular ammonium demand is high. The ammonium transporter (AMT1) is dephosphorylated and active. B) CIPK23 phosphorylates the ammonium transporter (AMT1) causing its inactivation under conditions of high extracellular ammonium concentration and / or when the intracellular ammonium demand is low.

This allosteric regulation mechanism seems to be conserved throughout evolution, thus constituting a baseline regulatory line (Loqué *et al.*, 2009). Additionally, CTR is critical for the formation of homo/heterotrimers between the AtAMT1.1 and

AtAMT1.3 isoforms acting as a trans-activator of the allosteric regulation of the activity of these transporters (Yuan *et al.*, 2013). Regulation by phosphorylation of AMTs is a very dynamic process that can take place at various Thr residues of the CTR. This alternative phosphorylation promotes an adaptation of the NH_4^+ transport activity against the signal generated by different types of nitrogen (Beier *et al.*, 2018). This ensure an ideal incorporation of this ion in response to the characteristics of the environment. At this point, it is worth highlighting the effect of the nitrate described on the incorporation of ammonium in the roots. Trials using ^{13}N and microelectrodes techniques have described that the co-provision of nitrate accelerates the incorporation of ammonium in roots of *Oryza sativa*, *Brassica napus* and *Populus popularis* (Kronzucker *et al.*, 1999; Babourina *et al.*, 2007; Luo *et al.*, 2013). Recently it has been shown that the addition of NO_3^- intervenes in the dephosphorylation cycle of several residues of the non-conserved C-terminal cytosolic domain of the *Arabidopsis* transporter AMT1.3, intervening in the regulation of ammonium incorporation (Wu *et al.*, 2019).

The incorporation of nutrients into cell interior (in this case, NH_4^+) constitutes a highly and finely regulated process with very diverse strategies that end up leading to the ability to provide great flexibility in its response and thus be able to coordinate the following stages of the process of nutrition according to the requirements.

3.3. Ammonium assimilation and nitrogen metabolism

The main forms of nitrogen present in soils are NH_4^+ and nitrate NO_3^- . As regards NO_3^- , once it has been incorporated into the cell it is reduced in the cytosol to nitrite (NO_2^-) by the enzyme nitrate reductase (EC 1.7.1.1, NR) consuming NADH. Nitrite is transported into plastids where it is reduced to NH_4^+ via nitrite reductase (EC 1.7.2.1, NiR) using six molecules of reduced ferredoxin. This process involves a high energy expenditure that is contributed mainly by the energy derived directly from photosynthesis in chloroplasts or indirectly by the action of the enzyme ferredoxin-NADP(+) reductase in amyloplasts using NADPH obtained from photosynthates transported from the apical zone to the root zone (Buchanan, 2015; Hirel and Krapp, 2020).

Introduction

For its part, NH_4^+ can come directly from the transport from the soil into the plant, from the reduction of nitrate, as well as being a derivative of cellular processes such as photorespiration, the use of nitrogen transport forms, the metabolism of phenylpropanoids or the amino acid catabolism (Hirel and Lea, 2001). Regardless of the NH_4^+ origin, it is mainly assimilated through the cycle formed by the enzymes glutamine synthetase (EC 6.3.1.2, GS) and glutamate synthase (EC 1.4.1.14, NADH-GOGAT / EC 1.4.7.1, Fd-GOGAT) (Figure I.10) (Hirel and Krapp, 2020). GS produces glutamine by the amidation of glutamate consuming NH_4^+ and an ATP molecule during the enzymatic reaction. Glutamine serves as a substrate for the GOGAT enzyme which transfers the amido group to 2-oxoglutarate using reducing power to generate two glutamate molecules. One of the glutamate molecules is used to re-fuel the cycle, while the other constitutes the net product of the cycle. The reducing power used by GOGAT can come from NADH or from ferredoxin (Fd) depending on the enzyme isoform and its tissular / organ localization. Fd-GOGAT is present mainly in photosynthetic tissues, while NADH-GOGAT is more localized in non-photosynthetic tissues (Suzuki and Knaff, 2005)) (Figure I.10).

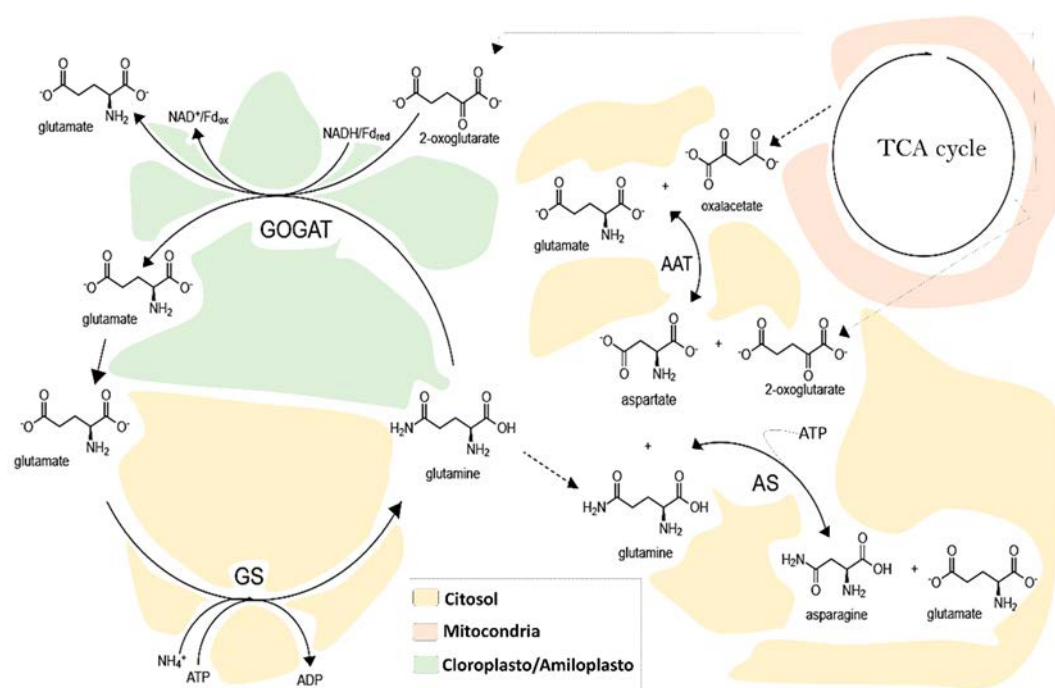


Figure I.10. Scheme of the glutamine synthetase / glutamate synthase (GS / GOGAT) cycle and the biosynthesis of aspartate and asparagine. GS: glutamine synthetase, GOGAT: glutamate synthase, AAT: aspartate aminotransferase, AS: asparagine synthetase, TCA cycle: tricarboxylic acid cycle.

In turn, GSs form little subfamilies in plants producing proteins with different physiological roles, and tissular and subcellular localizations. In angiosperms and in ginkgo, there are several genes encoding cytosolic isoforms of *GS*, called *GS1* and, generally, a gene encoding a chloroplastid isoform called *GS2* (Bernard and Habash, 2009). *GS2*, together with *Fd-GOGAT*, intervenes in the assimilation of ammonium from the reduction of nitrate in the leaves and of that released during the photorespiration (Miflin and Habash, 2002), while *GS1* acts mainly with *NADH-GOGAT* in the assimilation of nitrogen incorporated into the root tissues and in the re-assimilation processes derived from the catabolism of nitrogenated molecules (Miller and Cramer, 2005; Cánovas *et al.*, 2007).

In the rest of gymnosperms except ginkgo, there are two isoforms of *GS1*: *GS1a* and *GS1b*. (Cánovas *et al.*, 2007). In studies carried out in pine, the expression profiles of *GS1a* are correlated with the development of chloroplasts, they are influenced by light and in turn an overlap of the expression with *Fd-GOGAT* is observed (García-Gutiérrez *et al.*, 1998; Suárez *et al.*, 2002). Therefore, as Cantón *et al.* (1998) pointed out, the physiological function of *GS1a* coincides with the function of *GS2* in angiosperms. In contrast, *GS1b* expression patterns are predominantly localized in the vascular zone of roots and hypocotyls (Ávila *et al.*, 2001), suggesting that *GS1b*, in addition to intervening in the primary assimilation of nitrogen from the environment, can also act in the translocation of nitrogen from the roots to the rest of the plant (Ávila *et al.*, 2001). However, it has recently been found a third gene, called *GS1c*, in the *Pinus* and *Picea* genera, possibly the product of a recent gene duplication of *GS1b* whose function has not been fully clarified. Based on its expression patterns, this enzyme appears to be related to meristematic activity and early development phases (Valderrama-Martín *et al.*, in preparation).

Following the production of glutamine and glutamate during the primary assimilation of NH_4^+ through the *GS / GOGAT* cycle, nitrogen can be incorporated into other amino acids through successive reactions mainly carried out by aminotransferases. The enzyme aspartate aminotransferase (EC 2.6.1.1, AAT) catalyzes the reversible amination of oxaloacetate with glutamate, generating 2-oxoglutarate and aspartate. Aspartate in turn can serve as a precursor for asparagine synthesis through asparagine synthetase activity (EC 6.3.5.4, AS). AS uses the

Introduction

aspartate generated by AAT to obtain asparagine, thus, through the energy provided by the hydrolysis of ATP, transfers the amido group of a glutamine to the aspartate, obtaining glutamate and asparagine (Figure I.10). AS, like GS1b, has a cytosolic location and its expression patterns locate it in vascular areas which reinforces the idea that these enzymes contribute to nitrogen transport in the plant (Cañas *et al.*, 2006). Glutamate dehydrogenase (GDH, EC 1.4.1.2) catalyzes the reversible deamination of glutamate producing 2-oxoglutarate (Dubois *et al.*, 2003). Considering its *in vitro* amination activity, the GDH was initially thought to be the main source of glutamate synthesis in plants (Hirel and Krapp, 2020). However, several studies have shown that the main role of GDH is to obtain 2-oxoglutarate when C becomes limited (Fontaine *et al.*, 2012; Tercé-Laforgue *et al.*, 2013). Another observation that supports this evidence regarding the role of GDH is that intracellular levels of sugars influence the expression of GDH. In this way, it has been observed that under conditions of high availability of sugars, the expression of GDH is inhibited (Masclaux-Daubresse *et al.*, 2002). This means that when a plant is subjected to the presence of NH_4^+ , an increase in both the expression levels and the activity of GDH is observed (Abiko *et al.*, 2005; Sun *et al.*, 2020a), being another example of the important interconnection between nitrogen metabolism and carbon metabolism.

These enzymatic reactions in which organic acids such as carbon skeletons intervene are an example of the high degree of interconnection between both metabolisms (carbon and nitrogen), necessary for a correct assimilation of nitrogen. In fact, the expression of the AS (asparagine synthetase) depends on the C/N balance. Several works have shown that the addition of sugars in *Arabidopsis* plants adapted to a dark condition and in glucose-deprived maize (*Zea mays*) roots inhibits the expression of genes coding for AS (Lam *et al.*, 1994, Chevalier *et al.*, 1996). In *Phaseolus vulgaris*, the induction and repression of the expression of these genes has been described under dark and light conditions, respectively (Silvente *et al.*, 2008). In turn, several studies and reviews have shown that the C/N balance is altered in the presence of NH_4^+ in concentrations of the millimolar (mM) range (Ariz *et al.*, 2013; Esteban *et al.*, 2016; Liu and von Wirén, 2017). In pea (*Pisum sativum*), the induction of the expression of the ASI isoform has been described, as well as a high content of asparagine (Asn) in the leaf tissue when exposed to high

concentrations of NH_4^+ and in low intensity light conditions (Ariz *et al.*, 2013), which supports the role of carbon limitation in the regulation of the expression of AS. It is another example of the importance of the C/N ratio in the regulation of the AS. Thus, these evidences have led to the demonstration that both light and sugars, and the C/N ratio through amino acid levels constitute regulatory factors that intervenes in the control of expression de la AS (Lam *et al.*, 1998; Silvente *et al.*, 2008; Ariz *et al.*, 2013; Curtis *et al.*, 2018).

3.4. Ammonium transcriptomic response and regulation.

The transcriptomic response to NH_4^+ nutrition has been studied in multiple plant species both in herbaceous such as *Arabidopsis* (Patterson *et al.*, 2010), *Oryza* (Sun *et al.*, 2017), *Camellia* (Li *et al.*, 2017; Yang *et al.*, 2018) or *Brassica* (Tang *et al.*, 2019) as in woody ones such as *Pinus* (Canales *et al.*, 2010) or *Populus* (Poovaiah *et al.*, 2019). The comparison between the number of differentially expressed genes (DEGs) and the signaling pathways that make up them in the presence of different concentrations and forms of nitrogen varies among themselves (Patterson *et al.*, 2010; Poovaiah *et al.*, 2019; Tang *et al.*, 2019). Transcriptomic studies carried out at different times show a greater impact by nitrate in the short term (<8 hours), while the response induced by NH_4^+ on the differential expression of transcripts increases with the exposure time to this nutrient (Patterson *et al.*, 2010, Canales *et al.*, 2010; Sun *et al.*, 2017; Yang *et al.*, 2018).

The presence of NH_4^+ triggers a differential expression of transcripts involved in various processes such as: responses to biotic / abiotic stresses, biosynthesis of secondary metabolites, carbohydrate and amino acid metabolisms, as well as hormonal pathways (abscisic acid/ABA, ethylene and auxin) (Patterson *et al.*, 2010; Yang *et al.*, 2015; Sun *et al.*, 2017; Yang *et al.*, 2018). To some extent, the response to abiotic stress induced by ammonium may be due to an acidification of the apoplast in roots. This is important because in *Arabidopsis* between 20% and 40% of the genes that respond to NH_4^+ are over-expressed when the external pH is acidic (Liu and von Wirèn, 2017) (Figure I.11). However, thanks to the use of the glutamine synthetase inhibitor methionine sulfoximine (MSX) it has been possible to separate a subset of genes induced by NH_4^+ and that do not respond to extracellular pH (Patterson *et al.*, 2010). An example of this are the transcription

Introduction

factors *AtWRKY33* (*AT2G38470*), *AtWRKY40* (*AT1G80840*), *AtWRKY53* (*AT4G23810*) and *AtWRKY70* (*AT3G56400*) (Patterson, 2010), which have been shown to be involved in the regulation of defensive response in plants (Pandey and Somssich, 2009).

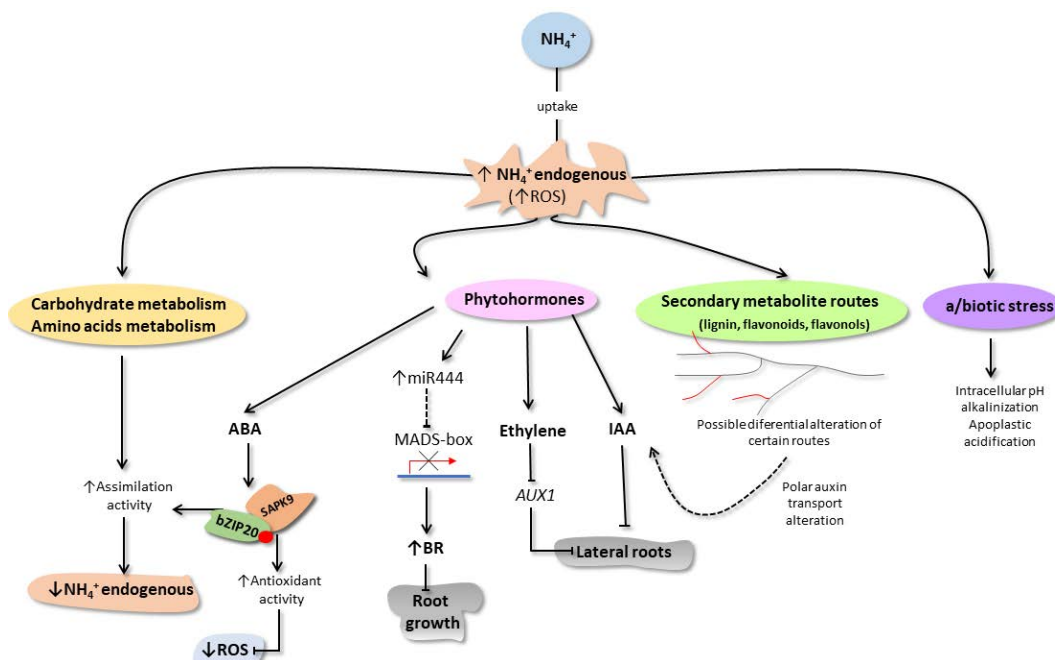


Figure I.11. Scheme of the processes involved in the transcriptional response to the presence of ammonium (NH_4^+) in plants.

On the other hand, the biosynthesis of secondary metabolites constitutes a nitrogen sink as in the case of phenolic compounds (coumarins, lignin, lignans, anthocyanins or flavonols, among others) whose biosynthesis begins from the aromatic amino acid phenylalanine (Phe) and many of which are related to defense processes (Taiz, 2015) (Figure I.12). The exposure of *Camellia sinensis* (Yang *et al.*, 2018) and interestingly also of *Populus* (Poovaiah *et al.*, 2019) to different nitrogen sources (NH_4^+ , NO_3^- or NH_4NO_3) induces the expression of transcripts related to the synthesis of metabolites secondary, this response being much greater in the presence of NH_4^+ . For example, in *Populus* a positive correlation is observed between the DEGs involved in these pathways and the presence of lignin. These results are in agreement with other previous studies carried out in tea where it is suggested that the different forms of nitrogen could regulate the biosynthesis of secondary metabolites by activating or deactivating genes of different pathways (Ruan *et al.*, 2007; Li *et al.*, 2015; Li and Silva, 2018) (Figure I.11).

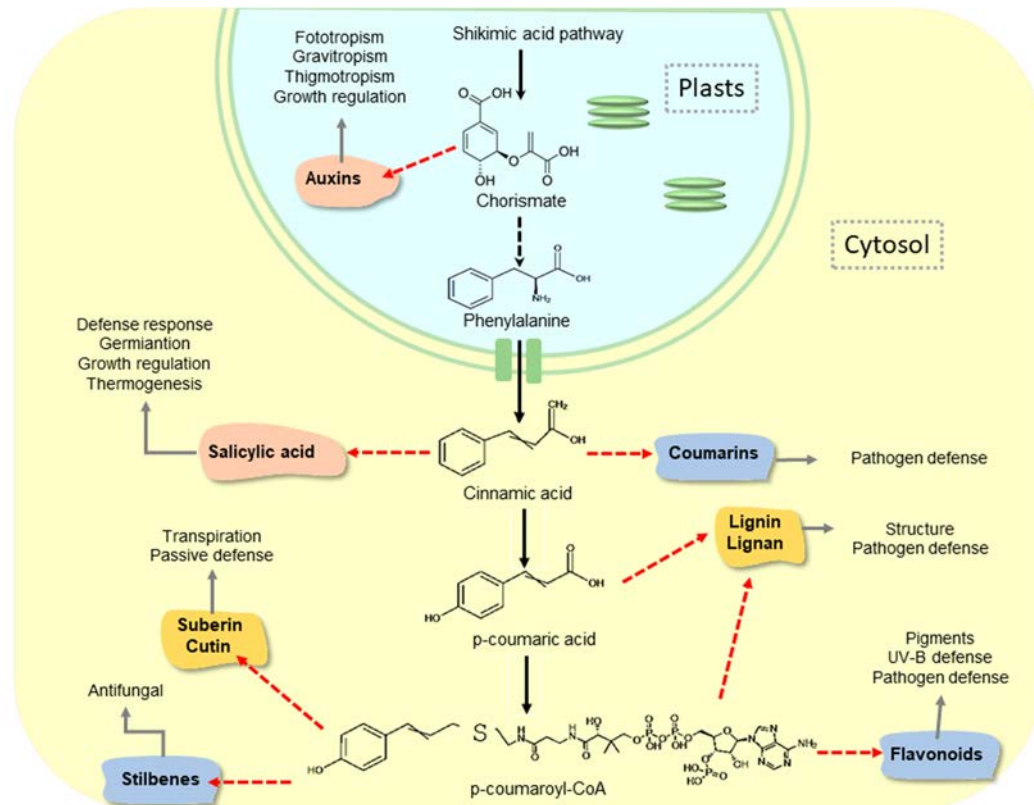


Figure I.12. Scheme of the biosynthesis of the main secondary metabolites derived from the amino acid phenylalanine and their biological function.

In transcriptomic studies in roots and in the aerial apex, comparing the response to the absence/excessive presence of NH_4^+ against an optimal control condition for rice growth, they have shown that the lack of nitrogen causes a decrease in the expression of transcripts related to carbohydrate and amino acid metabolisms (Yang *et al.*, 2015). This suggests that in this case NH_4^+ is a limiting factor that can regulate the expression of the enzyme *glutamine synthetase* (*GS*) in roots (Yang *et al.*, 2015). The decrease in endogenous glutamine levels can constitute a signal in the apex to decrease carbon skeletons production in photosynthetically active tissues and thus be able to coordinate the carbohydrate metabolism with amino acid metabolism. Paradoxically, when the external NH_4^+ concentration is high, the response exhibited by roots follows the same dynamics previously mentioned in the roots. However, the opposite occurs in apex (Yang *et al.*, 2015), which seems to indicate that when faced with excessive NH_4^+ conditions, it would initially be incorporated and assimilated by roots. When the assimilatory capacity of the roots is exceeded, the NH_4^+ excess could be sent to the apex. This would cause an increase in this ion in the aerial zone, which could explain the observed transcriptional response in order

to modulate and redirect this excess towards its assimilation and obtaining of amino acids (Yang *et al.*, 2015) (Figure I.11). The same response has been observed in *Pinus pinaster* (Canales *et al.*, 2010). In this case, changes in the expression of *PpAS*, *PpAAT* and *PpASPG* reinforce the idea that nitrogen derived from an excessive extracellular concentration of NH_4^+ causes the accumulation of amino acids in a transient way. Considering that *AS* and *ASPG* present a temporally coordinated expression (Cañas *et al.*, 2007), it could imply that one of the factors that intervene in the increase in tolerance to the presence of NH_4^+ is the relationship between biosynthesis glutamine/asparagine (Canales *et al.*, 2010) although it is necessary to continue to study this hypothesis in depth.

Likewise, the relationship between NH_4^+ and different phytohormones has also been analyzed. The apex of rice seedlings experiences an increase in the expression of auxin response genes, as well as genes involved in the synthesis of flavonoids (Sun *et al.*, 2017). Some flavonoids alter auxin transport (Brown *et al.*, 2001; Peer and Murphy, 2007; Yin *et al.*, 2014). This could be related to the suppression of lateral root formation when NH_4^+ is administered in the apical zone (SSA, shoot-supplied ammonium), that could lead a decrease in the response in roots to auxin as a result of the alteration of the long-distance polar transport process from the apices to the roots (Li *et al.*, 2011). In the presence of NH_4^+ , the aerial and root tissues of *Arabidopsis* and *Oryza*, respectively, undergo overexpression of genes involved in ethylene and ABA (abscisic acid) biosynthesis (Li *et al.*, 2014; Sun *et al.*, 2017). This possible increase in endogenous levels of ethylene in the aerial section induced by SSA could repress the expression of the *AUX1* transporter, contributing to the reduction of the polar transport of auxins from the aerial part to the root zone and avoiding or decreasing the formation of lateral roots (Li *et al.*, 2014) (Figure I.11).

However, in roots the physiological function of ABA seems to be related to an increase in NH_4^+ tolerance, at least in rice (Sun *et al.*, 2020a). The increase in endogenous levels of ABA caused by the presence of NH_4^+ acts at two levels: 1) Increasing the activity of key enzymes in the NH_4^+ assimilation process such as GS, GOGAT and GDH (Sun *et al.*, 2020a), which had already been observed for GDH2 in *Arabidopsis* and *Brassica* in the presence of NH_4^+ (Patterson *et al.*, 2010; Ristova *et al.*, 2016; Tang *et al.*, 2019). 2) Reducing cell damage due to the presence of

reactive oxygen species (ROS) by regulating antioxidant activities, such as ascorbate peroxidase (APX), catalase (CAT) or superoxide dismutase (SOD) (Sun *et al.*, 2020a). Typically, these types of responses are regulated by transcription factors. In the work of Sun *et al.* (2020b), it is described that the expression of *OsbZIP20* is induced under NH_4^+ presence. *OsbZIP20* interacts with the protein kinase *OsSAPK9*. This kinase phosphorylates *OsbZIP20*, transactivating it. Therefore, this study shows that the *OsbZIP20*-*OsSAPK9* interaction intervenes in the regulation induced by the increased endogenous ABA levels, promoting the assimilation of NH_4^+ and antioxidative processes. In this way, it is observed how there are several transcription factors (TF) that have been related to the coordination of the response of many genes involved in the absorption and metabolism of NH_4^+ in different species (Kumar *et al.*, 2009; Patterson *et al.*., 2010; Xuan *et al.*, 2013; Chiasson *et al.*, 2014; Wu *et al.*, 2017; Gao *et al.*, 2020; Sun *et al.*, 2020a and 2020b).

At present, little is known about the regulatory effect of small RNAs (sRNAs) and their relationship with the NH_4^+ nutrition process compared to nitrate nutrition (Vidal *et al.*, 2010; Zhao *et al.*, 2011; Zhao *et al.*, 2013; Li *et al.*, 2016). Despite this, by means of miRNA-seq, several miRNAs have been discovered that present interesting targets within the process of regulation of NH_4^+ nutrition. An example of this is *OsmiR159*, whose expression responds to the presence of nitrogen and targets transcription factors related to the gibberellin pathway (Li *et al.*, 2016). Another example is *OsmiRNA160*, whose expression is higher in the presence of NH_4^+ compared to the presence of NO_3^- , although its function in rice has not been fully clarified. In *Arabidopsis*, *miR160* has been shown to promote the formation of lateral roots by inhibiting the expression of the auxin response factor *ARF16* (Wang *et al.*, 2005). Because of that *AtmiR160* has been proposed to play certain regulatory role in root system remodeling described under limiting nitrogen conditions (Liang *et al.*, 2012). *OsBRD1* is a key gene in the biosynthesis of brassinosteroids (BRs). It has recently been observed in rice that the expression of *OsmiR444* is induced under NH_4^+ nutrition and several MADS-box-like transcription factors have been identified as targets for this miRNA. These FTs can bind to the *OsBRD1* promoter through the *CArG* motif close to the start codon. This results in the repression of this gene (Jiao *et al.*, 2020). Furthermore, through double hybrid (Y2H) approach

in yeast it has been observed that, at least in this system, these MADS-boxes interact with each other, so their biological function could be mediated through the formation of homo/heteromeric protein complexes (Jiao *et al.*, 2020). In *OsMADS57* overexpressing rice seedlings, a hyposensitivity response to NH_4^+ and a decrease in BRs content is observed, while in *OsmiR444* overexpressing plants the opposite response is observed. Thus, it is shown that NH_4^+ activates the *OsmiR444-OsBRD1* regulatory pathway that leads to an increase in BR synthesis whose phenotypic effect results in the inhibition of root growth (Jiao *et al.*, 2020) (Figure I.11).

4. Epitranscriptomics and its importance in plants.

In order to fully understand the gene response and its regulation, it is essential to understand all aspects of RNA metabolism. For this reason, in recent years a new discipline / field of study called epitranscriptomics has appeared. Epitranscriptomics is defined as a field within molecular biology that includes the study of chemical modifications present in the transcriptome, from which different aspects are covered such as the study of how these chemical modifications are generated or the study of the cellular processes that are regulated by them, among others (Peer *et al.*, 2017). Until now, the knowledge about this new level of information located between the transcriptome and the proteome is limited although in continuous emergence especially in aspects related to human pathological processes (Bohnsack and Sloan, 2018; Lian *et al.*, 2018). This could be paradoxical because the existence of chemical modifications in RNA has been known since the 1950s with the discovery of pseudouridine (Ψ) (Grosjean, 2005). Both in animals and in plants, one of the main chemical modifications present in messenger RNA (mRNA) is N^6 -methyladenosine (m^6A) (Fray and Simpson, 2015). Regarding plant research, the study of the epitranscriptome is even more limited and the publications are mainly focused on the model plant *Arabidopsis thaliana*, partly thanks to the possibility of obtaining mutant lines in the proteins managing the epitranscriptomics modifications (*writers*, RNA-methyltransferases; *erasers*, RNA-demethylases; and *readers*) (Vandivier and Gregory, 2018).

Several works have used knockout or knockdown mutant lines of different editing enzymes (*writers*) of the methylome complex, demonstrating the importance of

m⁶A in the embryonic development of *Arabidopsis* (Zhong *et al.*, 2008; Růžička *et al.*, 2017). In turn, it has also been described that a deficiency in m⁶A levels affects plant fitness causing less growth in height and loss of apical dominance, as well as an abnormal root development and changes in root architecture (Bodi *et al.*, 2012; Růžička *et al.*, 2017). Similarly, the intracellular regulatory role of eraser enzymes has been inferred showing that they intervene in important aspects of mRNA metabolism. For example, a greater susceptibility to viral infections has been demonstrated due to the absence of the eraser enzyme *AtALKBH9B* (*AT2G17970*). This evidence describes that m⁶A can intervene in the plant-pathogen interaction (Martínez-Pérez *et al.*, 2017). Furthermore, it has been described that *eraser* proteins can influence the silencing / degradation of certain mRNAs (Arribas-Hernández *et al.*, 2018). Other studies have shown that reader proteins can increase mRNA stability of certain transcripts (Wei *et al.*, 2018) and, also can intervene as mediators in the polyadenylation process of the mRNA 3'-UTR end (Wei *et al.*, 2018).

However, the relationship between the epitranscriptome and regulatory aspects responsible for the transcriptomic response related to other processes, such as nutrition, is still an enigma that has yet to be clarified.

5. Questions related to the state of art:

Based on the great importance of N for plants both at an academic level and as an object of study, the following questions are raised:

- How to teach in a didactic and applied way the importance of nitrogen nutrition in plants?
- Since *Pinus pinaster* Ait. is an important conifer present in the Western Mediterranean, is ammonium the preferred inorganic form of nitrogen for maritime pine and what are the differences that underlie ammonium and nitrate nutrition?
- Since the ammonium in the environment is incorporated through the root system, what effect does it have on gene expression in the presence of ammonium? Is the response at the complete root similar to the response at the root tip?

Introduction

- Based on the great importance of chemical RNA modification regulating all aspects of RNA processes, is there any link between the regulatory role of epitranscriptomics and ammonium nutrition?

Objectives



The general aim of this Doctoral Thesis work is to deepen the knowledge of key aspects of nitrogen nutrition in plants, a research line developed by the research group Molecular Biology and Biotechnology at the Universidad de Malaga. Most part of the experimental work is addressed to explore the molecular mechanisms involved in the regulation of nitrogen acquisition and metabolism and how this essential nutrient can influence the growth and development of maritime pine (*Pinus pinaster* Ait.), a conifer of great ecological and economic importance.

The following objectives were initially proposed:

1. Development of a practical laboratory experience to demonstrate the importance of nitrogen nutrition in plants.
2. To study the differential response in physiological and metabolic terms of maritime pine seedlings to ammonium and nitrate nutrition.
3. To determine the transcriptomic dynamics in response to ammonium nutrition in the root apex of maritime pine seedlings.
4. To characterize the short-time response triggered by ammonium nutrition in maritime pine roots using multi-omic approaches.



Chapter 1

Understanding plant nitrogen nutrition through a laboratory experiment

Francisco Ortigosa, José Miguel Valderrama-Martín, Concepción Ávila, Francisco M. Cánovas, Rafael A. Cañas (2019).

Published in Biochemistry and Molecular Biology Education journal, 47: 450-458.



Introduction

A balanced nitrogen (N) nutrition is essential for plant growth and development, with nitrogen availability being the principal limiting factor. Since plants are the main autotrophs that sustain the pluricellular terrestrial life, and crops are the fundamental source of food for humanity, plant nitrogen nutrition is of paramount importance in biology and agronomy. The knowledge that soil fertilization is a requirement to improve crop yield led to the Green Revolution occurred during the twentieth century, which promoted higher crop yields to cope with the uncontrolled increase in the world population (Pingali, 2012). However, the massive use of nitrogen fertilizers in agriculture has led to a strong increase in the production costs and many environmental problems, such as eutrophication (Good and Beatty, 2011).

Considering this outlook, plant nutrition is a highly important task in the biological sciences, which students must know and understand. Universities have developed programs for teaching plant N nutrition, including practical approaches, which have been focused on particular aspects, e.g. the role of nitrate reductase (Pike *et al.*, 2002; or long tests to determine crop yield under different nutritional conditions (Voogt and Poorter, 1996).

Glutamine synthetase (GS, EC 6.3.1.2) is the enzyme that incorporates inorganic N into organic molecules and synthesizes glutamine from ammonium and glutamate using an ATP molecule (Figure 1.1). In plants, there are plastidic isoforms (GS2), which are usually coded by one nuclear gene, and several cytosolic isoforms (GS1), which are coded by a small gene family (Bernard and Habash, 2009). The gene expression of some of these genes is regulated by the N availability and by different physiological processes with N reallocation. Usually, the gene expression and GS activity levels are adequate markers to determine the N status of a plant, correlating well with other parameters such as biomass accumulation, nitrogen-use efficiency (NUE) and chlorophyll content (Martin *et al.*, 2006; Cañas *et al.*, 2009; 2017) .

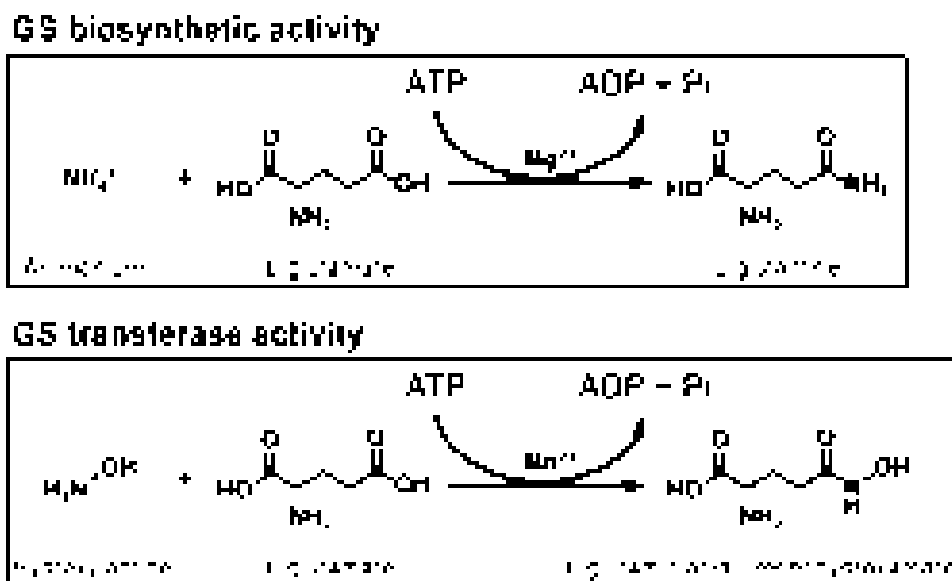


Figure 1.1. Schematic representation of the glutamine synthetase activities. Biosynthetic activity occurs in the plant cells. Transferase activity is an alternative assay that uses hydroxylamine as the substrate and produces L-glutamic acid γ -monohydroxamate as the product, which can form a colored conjugated with the Fe contained in the GS-STOP solution that is used in the enzymatic assay.

In the present work, a new laboratory experiment for teaching plant N nutrition is proposed. The aim is to follow the N status of tomato plants growth in different nutritional conditions (low N and optimal N supply) with such markers as chlorophyll content, biomass, GS activity and gene expression levels. The expected results are the decrease in the levels of these markers for the plants growth under low N conditions.

The practical training is designed to optimize the working time in a semester or even during the term of a quarter. The plant growth until harvesting will take two months, and the primary markers of the plant N status can be analyzed in two consecutive laboratory sessions. Additionally, the experience can be modified depending on the educational level by reducing the most complicated approaches, such as reverse transcription quantitative polymerase chain reaction (RT-qPCR), or by including new objectives and methods and adding more laboratory tests according to plant development and growth. The results can be used to elaborate a scientific report by the students for training not only in the analysis and interpretation of results but also in scientific communication skills.

Results

Technical and scientific results

Important differences in plant growth in response to the N nutrition level can be observed, finding that N⁺ plants were taller and had a higher number of whorls (Figure 2.1A). In this occasion, the tomatoes have been grown with a relatively low fertilization to reveal the differences in biomass accumulation (Figure 2.1B) being the final amount of N supplied to N⁺ plants was 0.045 g and to N⁻ plants 0.006 g. The accumulation of biomass in N⁺ plants was significantly higher than in N⁻ plants, mainly in the shoots, where there was nearly a ten-fold difference. However, the NUE was significantly higher when it was determined in the whole plants and roots; meanwhile, no differences were found in the shoots. These NUE results are in line with the modification of the root:shoot ratio between N⁺ (R:S = 0.09) and N⁻ plants (R:S = 0.18).

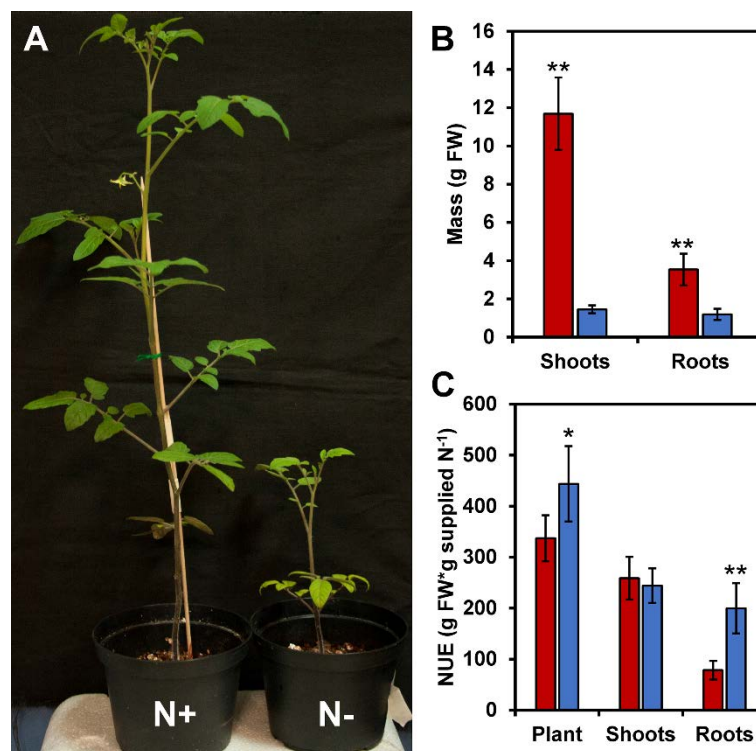


Figure 2.1. Visual aspect, biomass accumulation and NUE comparison. **A.** The visual aspect of the tomato plants cultured under different N regimes is presented. N⁺ corresponds to plants cultured under normal N supply. N⁻ corresponds to plants cultured under low N supply. **B.** Biomass accumulation with respect to the fresh weight of the tomato plants in g. **C.** NUE index of the entire plants and parts of the

tomato plants. Red bars correspond to plants cultured under normal N supply (N+). Blue bars correspond to plants cultured under low N supply (N-). Values are the mean \pm SD of four independent plant samples. Significant differences between N regimes via Student's t test are indicated in the graph (* for $P \leq 0.05$; ** for $P \leq 0.01$).

Two good markers to evaluate the N status of plants are the contents of soluble proteins and chlorophyll (Marschner, 2012). In our results, both variables were significantly higher in N+ plants (Figure 1.3).

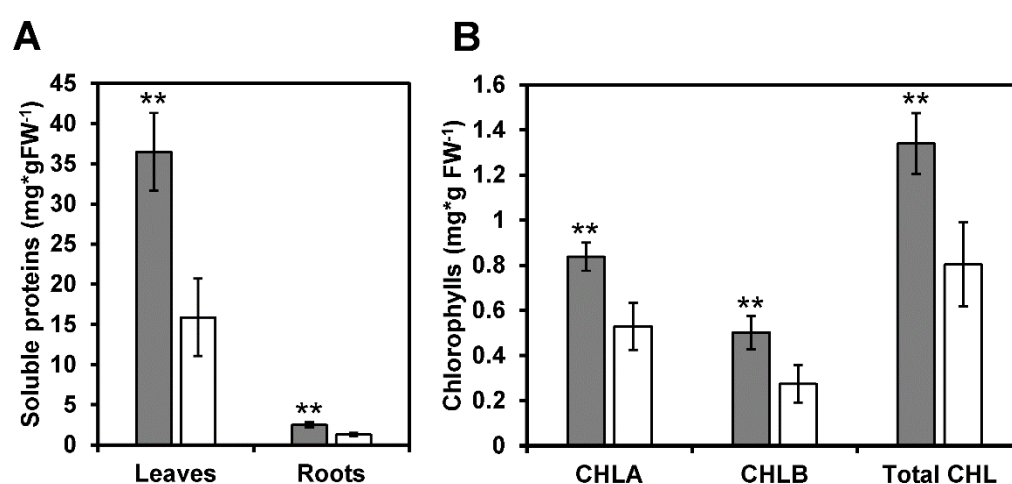


Figure 1.3. Soluble protein and chlorophyll contents. **A.** Soluble protein accumulation in the leaves and roots of tomato plants cultured under different N regimes. **B.** Chlorophyll A (CHLA), chlorophyll B (CHLB) and total chlorophyll (Total CHL) content in leaves. Gray bars correspond to plants cultured under normal N supply. White bars correspond to plants cultured under low N supply. Values are the mean \pm SD of four independent plant samples. Significant differences between N regimes via Student's t test are indicated in the graph (* for $P \leq 0.05$; ** for $P \leq 0.01$).

However, in the present experience using tomato plants, there are no significant differences, only minor changes, such as the absence of some proteins lower than 37 kDa in the N- roots compared with that in N+ roots (Figure 1.4A). However, a western blotting allowed to identify the size of the different GS polypeptides and their distributions in different plant organs or tissues; the higher band signal corresponded to the plastid GS2, while the lower band signal belonged to the

cytosolic GSs (GS1 family) (Figure 1.4B). These results related to N metabolism presents the well-known profile of GS peptides, in which high amounts of GS2 are detected in leaves and not in roots, while GS1 peptides are present in both tissues with lower levels in leaves than in roots

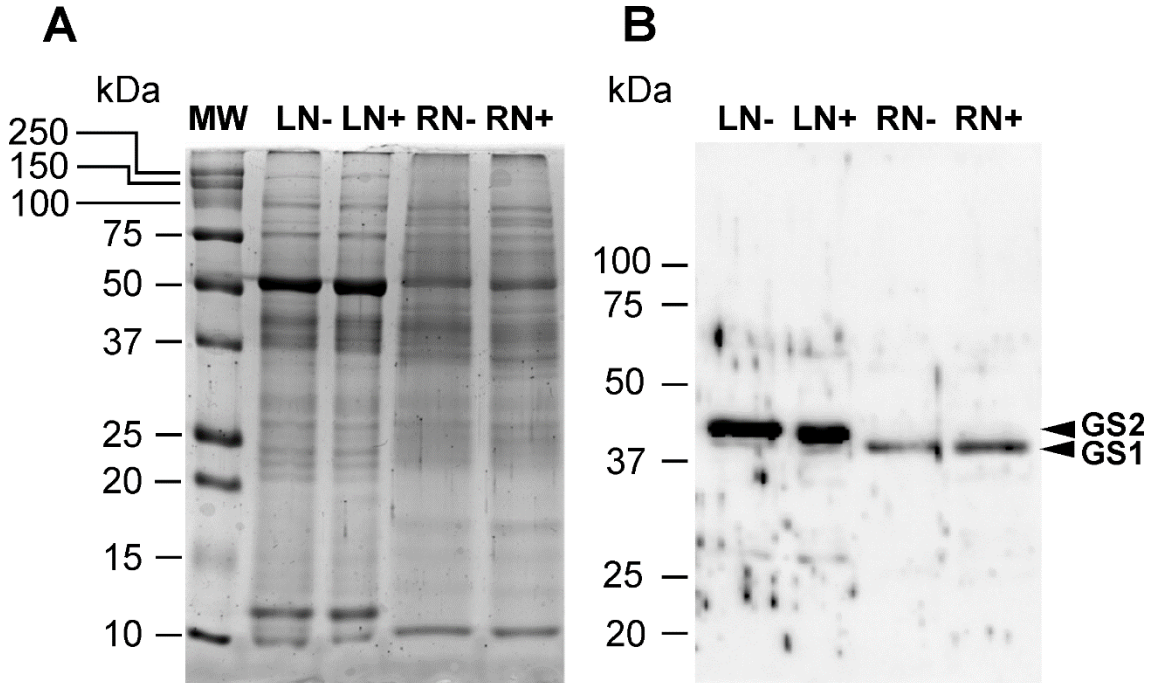


Figure 1.4. Protein profile and glutamine synthetase immunodetection. **A.** SDS-PAGE gel stained with Coomassie blue indicating the protein profiles of the leaf and root samples from tomato plants cultured under different N regimes. **B.** Immunodetection of glutamine synthetase polypeptides from tomato plants cultured under different N regimes. The detection was made using antiserum against pine GS1 (Cantón *et al.*, 1996). Lanes: molecular-weight size marker (MW), leaves under low N nutrition (LN-), leaves under optimal N nutrition (LN+), roots under low N nutrition (RN-) and roots under optimal N nutrition (RN+). The amount of proteins loaded in each lane was 20 μ g.

Enzymatic activity determination results clearly showed that the GS activity level per fresh weight of sample was higher in plants under optimal N supply than in plants under limited or low N supply (Figure 1.5A).

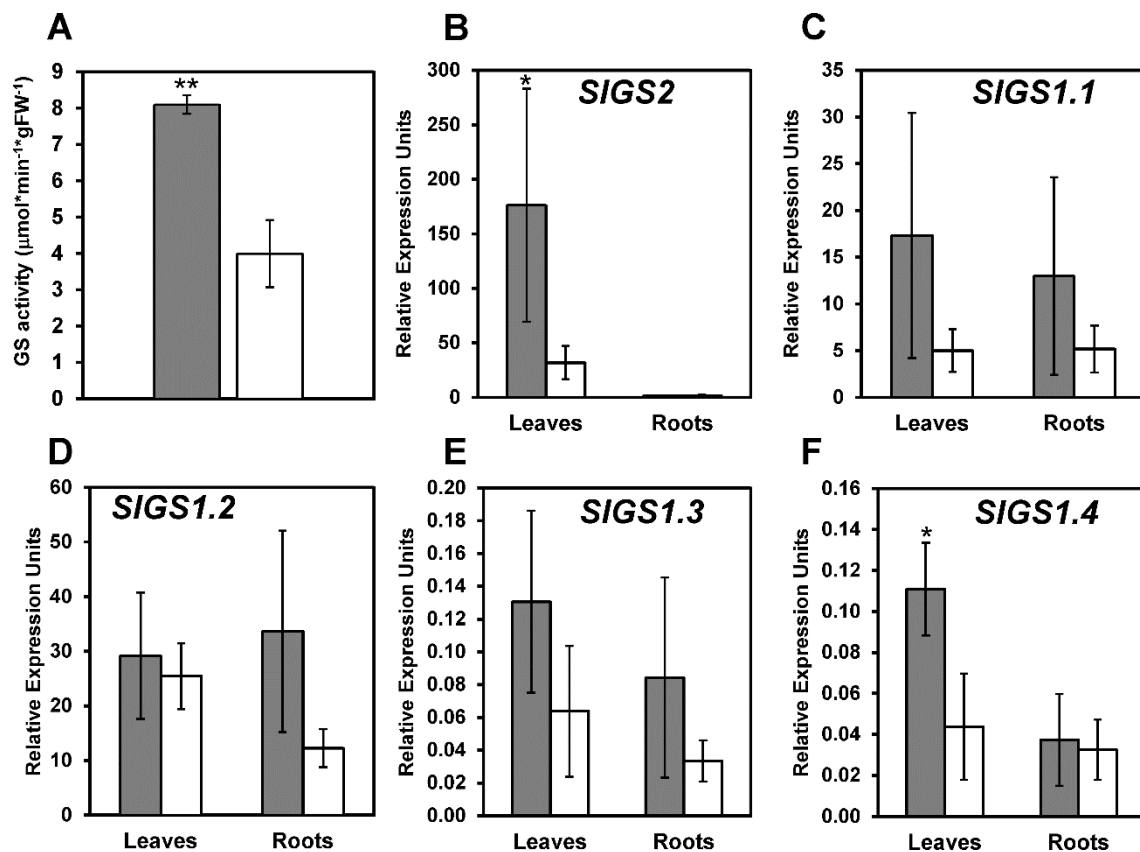


Figure 1.5. Glutamine synthetase enzyme activity and gene expression. **A.** Glutamine synthetase activity with respect to fresh weight of leaves. Panels **B** to **F.** Gene expression of the individual genes of the GS family in tomato; *SIGS2*, *SIGS1.1*, *SIGS1.2*, *SIGS1.3* and *SIGS1.4*, respectively. Gray bars correspond to plants cultured under normal N supply. White bars correspond to plants cultured under low N supply. Values are the mean \pm SD of four independent plant samples. Significant differences between N regimes via Student's t test are indicated in the graph (* for $P \leq 0.05$; ** for $P \leq 0.01$).

One key step during RNA extraction is the genomic DNA elimination (Figure 1.6). Although this can modify the RT-qPCR outcome, we did not find any relevant interference maintaining the expected results, especially for the *SIGS2* gene (Figure 1.5 B-F). However, the one-step RT-qPCR protocol that we have selected to reduce the practice time introduces some deviation in the biological replicates, reducing the statistically significant results to *SIGS2* and *SIGS1.4* transcripts in the leaves.

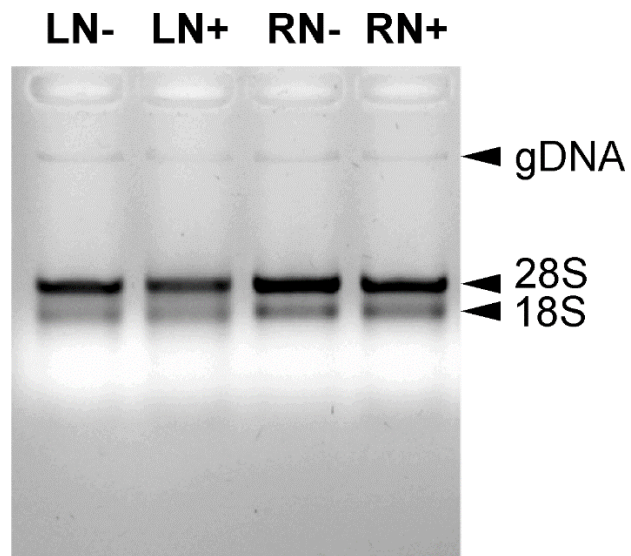


Figure 1.6. Total RNA profile of leaves and roots from the tomato plants cultured under different N regimes. Lanes: leaves under low N nutrition (LN-), leaves under optimal N nutrition (LN+), roots under low N nutrition (RN-) and roots under optimal N nutrition (RN+). The amount of total RNA loaded in each lane was 1 μ g.

Discussion

Technical and scientific results

The cherry tomato variety (*Solanum lycopersicum* var. *cerasiforme*) has been selected for this practical experience due to its small size and rapid growth. First, it is possible to obtain plants with differential growth in response to N nutrition in only two months and with enough plant material to develop the different physiological, biochemical and molecular measures required in the experience. However, the presented practical training can be performed with different plant species, preferably with crop species, such as maize. In fact, similar laboratory practices (mainly in Plant Physiology) are conducted in universities all over the world, and usually, plant growth is maintained until harvesting of the fruit (Voogt and Poorter, 1996). Although we have used leaves and roots, this variety of tomato can produce fruits very fast, in three-four months. An alternative to our proposal would be the analysis of the tomato fruit yield for the calculation of NUE (tomato fruit g per N supplied g).

However, this practice under low N nutrition can result in plants with a very low biomass accumulation. Sometimes this results in insufficient plant biomass to be harvested for the analyses. Alternatively, the nutrient solution can be applied once a week to increase biomass and, at the same time, maintain good differential appearance (Figure 2.1). The NUE results obtained are as expected when analyzing plants of the same variety/line under different nutritional conditions (Figure 2.1). Furthermore, these results are in line with the modification of the root:shoot ratio between N⁺ and N⁻ plants, showing the clear effect of N starvation on the root development with respect to the aerial part of the plant (Marschner, 2012). The changes observed at soluble protein and chlorophyll content are interesting since both parameters are indicative of the metabolic flow of N from Gln/Glu to the remaining amino acids (to produce proteins) and to other N compounds (chlorophylls) (Buchanan et al., 2015). In addition to these measures and with more time for a practical program, it would be possible to measure other N status markers such as the total and/or individual contents of free amino acids and nitrate and ammonium levels. These additional measurements can facilitate a complete picture of the N metabolism in the plants under both nutritional regimes.

In some circumstances, protein profiles can be markers of the N status of the sample (Llebrés *et al.*, 2018). Because of that, soluble protein quantification is a good N

status marker. For users unfamiliar with laboratory work, protein quantification using the Bradford assay (Bradford, 1976) may cause wasted time during the practical class.

However, the time taken for the protein quantification can be reduced if a previously calculated equation for the BSA standard curve is available. However, it is more instructive for the students to simultaneously obtain the BSA standard curves. On one hand, the evaluation of the protein profiles is a useful practice for undergraduate students because they perform SDS-PAGE separation; however, it does not contribute to the relevant data for teaching of N nutrition of plants (Figure 1.4A). On the other hand, utilizing the appropriate antibodies and samples, this method is a useful technique that includes SDS-PAGE and demonstrated the basic principles of N metabolism in plants (Figure 1.4B). Anti-GS antibodies for plants are available commercially (e.g. ABIN2559393 from antibodies-online.com); however, their price can increase the cost of the laboratory activity. Thus, these techniques can be optional in the present proposal because they are time consuming, and they need of specific and sometimes expensive probes such as antibodies.

GS is one of the best markers of plant N status and the key enzyme in inorganic N assimilation and recycling (Cañas *et al.*, 2017). GS activity can be determined through different methods. The GS activity determination protocol proposed in the present manuscript is a robust and highly sensitive enzymatic assay (Cánovas *et al.*, 1984). With adequate facilities, this procedure can be conducted in educational levels lower than the university level. However, the monitor and students must be careful regarding hydroxylamine toxicity and with ATP degradation with excess temperature (it must be maintained on ice until use). It must be indicated that GS activity in tomato is easy to measure in the leaves but not possible in the roots under our experimental conditions. This is due to the presence of an inhibitory protein in this organ (Gallardo *et al.*, 1992). A possible alternative to measure the GS activity in roots is to perform gel filtration chromatography to separate the GS protein from its inhibitor. Nevertheless, this would need considerable time to complete the entire procedure.

Total RNA extraction is time-consuming and, as with chlorophyll determination, needs two days to be completed (Supplemental Figure 1.1). At this point, this procedure is recommended for university students due to its complexity and dangerousness. The total RNA extraction is a complex method that uses toxic

compounds and requires a careful work by the students. Alternatively, it is possible to perform total RNA extractions with a commercial kit, which reduces the time spent. In the present work, the procedure has been simplified for the experience to reduce the manipulation time, reducing the risk of RNA degradation. Therefore, the elimination of genomic DNA has been eliminated from the protocol, resulting in a slight genomic contamination of the samples (Figure 1.6).

The UVette® cuvettes are a good alternative to measure the nucleic acid amount on a spectrophotometer. Alternatively, it is possible to use a Nanodrop (Thermo, MA, USA), which is faster; however, the use of conventional spectrophotometers is more didactical since the students must calculate the total RNA concentration from the absorbance values.

Similar to total RNA extraction, RT-qPCR requires specialized facilities and instruments that are not available to all educational levels. Depending on the student level (undergraduate or postgraduate) the gene-expression calculation from the raw RT-qPCR data can be performed either by the students or by the instructor. During the one-step RT-qPCR protocol total RNA was added to each plate well; thus, the normalization of the reverse-transcriptase reaction with the reference gene is useless. This means that the results can be normalized with respect to the total RNA amount used for each RT-qPCR reaction. Nonetheless, the use of a reference gene can be maintained in the practice since it demonstrates to the students the regular procedure used in research. In this case, the GS gene primers used for RT-qPCR were designed including an intron in the possible amplicon to favor the amplification of amplicons from mRNA but not from genomic DNA contamination. The RT-qPCR amplicons for all the primer pairs were sequenced and corresponded to the right genes. Using the appropriate primers, the expression of other N metabolism genes as nitrate reductase or nitrate transporters could also be analyzed. Although a one-step RT-qPCR is used, it is possible to conduct a separate reverse-transcription and then a qPCR. However, this is more time consuming and can introduce more error to the results.

Educational implications

Context

The present practical training has been developed in the frame of a “Biochemistry of Plant Nutrition” course for students belonging to the 4th level of Biochemistry

Degree. The objective was to integrate theoretical knowledge with the practical experience, putting together the growth chamber and the laboratory. The number of students for a practical session was 16 distributed in 8 working groups. The students used a practical handout for the laboratory exercises (Anexo 1.1), including a time schedule for plant nutrient supply and watering (Supplemental Figure 1.1). Each team measured and analyzed all the proposed markers from a harvested plant. Finally, all the data generated by the teams were shared among them to complete the experimental dataset. Each student had to write a practical report based on the entire set of data obtained in the laboratory.

Educational level

The practical experience has been tested with university students since some of the technical methods proposed require advanced skills. However, the character of the proposal is such that the excision of certain parts (e.g. total RNA extraction and RT-qPCR) allows the implementation of the experience in educational levels lower than the university level, evidently in adequate contexts and with the specific facilities. The tomato culture under different nutritional conditions can be grown easily even in primary schools with not many requirements. However, the practice was intended for university students with the novelty of including the RT-qPCR technique for teaching plant N nutrition in a Biochemistry Degree.

Assessment of Student Learning

The present practice aims to facilitate the understanding of plant N nutrition biochemistry by the students of biological sciences at different levels, integrating theoretical knowledge with practical results. One of the strengths is the variety of disciplines related to their methods and results: plant physiology, biochemistry and molecular biology. The students can approach to the subject from different perspectives using their methods and verifying in an empirical manner the correlation between the different types of nutritional markers. The final report is a way to integrate and think about the concepts involved in the plant N nutrition biochemistry. The lab report was evaluated using a specific rubric (Appendix 1.2). The laboratory work of each student during the exercise was assessed in part using personal appreciations. However, due to the subjectivity of this procedure, the main approach to evaluate the students learning was through the lab report and exams. This included a small questionnaire to assess the learning experience of the students and their concerns regarding this lab experiment (Appendix 1.3). In general, the

results are very positive in improving the written scientific communication skills of the students and their conceptual knowledge regarding plant nitrogen nutrition and metabolism.

Representative Student Comments

Thanks to the questionnaire we can include some comments from the students who have participated in the experience. These comments will be considered to improve the lab exercise in the future:

“In general, I found it a very interesting experience. The only thing to change would be to better explain how the data obtained by qPCR is treated. Another aspect to change would be the moment in which the practices are carried out (we made them close to the exams, they would take more advantage in a less overwhelmed moment, but it is an aspect that does not only depend on professor).”

“I have found the lab exercise very good and useful. The fact of grown tomato plants in different nutritional conditions by ourselves to later use them to perform the experiments seems great, unlike the most laboratory exercises of the college career in which they give you the sample without knowing where it comes from. In addition, we had the great opportunity to perform a real-time PCR for the first time throughout the career. Excellent lab experience that should serve as an example for the others.”

“It seems to me a very interesting experience that had never been done during the grade (not like others that repeat the same procedures over and over again). In addition to showing us a new techniques for the future, precisely that now I am being quite useful.”

“I really liked the lab exercise and it seemed to me new regarding what we had done in the college career. There was some organizational problem, but I do not think it was relevant, something can always fail.”

Conclusions

The present proposal is intended to be an instrument for teaching a fundamental biological problem with implications regarding the environment and human feed. The teaching lab is used to support the theoretical concepts with real data obtained by the students in a nutritional experiment managed by themselves. In our experience, the students have better understood of the nitrogen metabolism of plants due to this laboratory exercise.

Acknowledgments

This work was supported by the *Departamento de Biología Molecular y Bioquímica de la Universidad de Málaga*; and Spanish *Ministerio de Economía y Competitividad* Grants [BIO2015-69285-R and BIO2015-73512-JIN; MINECO/AEI/FEDER, UE]. JMVM was supported by a grant from the Universidad de Málaga (Ayudas para la iniciación a la investigación. Plan Propio de Investigación, N° 201800200000776). FO was supported by a grant from the Universidad de Málaga (Programa Operativo de Empleo Juvenil vía SNJG, UMAJI11, FEDER, FSE, Junta de Andalucía).

Conflict of interest

No potential conflict of interest was reported by the authors.

Supplemental figure

Days	Sowing (D0)	D7	D14	D21	D28	D35	D42	D49	D56	D63	D70	D77	D84	D91	D98-D101
Water	100 mL	80 mL					80 mL		80 mL		80 mL		80 mL		Harvest and lab practice
Hoagland 1/4			40 mL	40 mL	40 mL										
Complete Hoagland						80 mL		80 mL		80 mL		80 mL		80 mL	
Low N Hoagland						80 mL		80 mL		80 mL		80 mL		80 mL	

Days	D98	D99	D100	D101
Plant weighing				
Plant material frozen				
Protein extraction				
Protein Quantification				
SDS-PAGE				
Western blotting				
Chlorophyll meas.				
RNA extraction				
RNA quantification				
RT-qPCR				

Supplemental Figure 1.1. Time schedule including plant irrigation and the main laboratory techniques or objectives. Light blue squares correspond to actions applied for all the samples. Red squares correspond to the group of plants treated with optimal N amount. Orange squares correspond to the group of plants treated with low N amount.

Chapter 2

Inorganic Nitrogen Form Determines Nutrient Allocation and Metabolic Responses in Maritime Pine Seedlings

Francisco Ortigosa, José Miguel Valderrama-Martín, José Alberto Urbano-Gámez, María Luisa García-Martín, Concepción Ávila, Francisco M. Cánovas, Rafael A. Cañas (2020).

Published in *Plants*, 9:481.



Introduction

Nitrogen (N) is an essential element for life because it is a main constituent of biomolecules such as nucleic acids, proteins, chlorophylls, and hormones (Buchanan, 2015). For plants, N is the main limiting nutrient due to the high amount that is needed to maintain sustained growth and its low availability in soil (Marschner, 2012). Although molecular dinitrogen is highly abundant in the atmosphere, it is not directly available to plants because it can only be assimilated by plant species in symbiosis with diazotrophic bacteria (Marschner, 2012). In the soil, there are different organic and inorganic forms of N that can be incorporated by plants. Nevertheless, the amount and proportions of these N molecules change depending on the climate and soil conditions as well as biological competition such as the decrease of soil nitrification caused by secondary metabolites from plant root exudates that inhibit the growth of nitrifying microorganisms (Moreau *et al.*, 2019). The main forms of inorganic N that are available to plants in soil are ammonium and nitrate (Britto and Kronzucker, 2013). Their relative abundances in the soil have an important relationship because of the nitrification performed by microorganisms in the rhizosphere (Wendeborn, 2020). Ammonium is the initial substrate of the nitrification process, which is carried out under aerobic conditions and depends on temperature and pH (Norton and Ouyang, 2019). Overall, plants tolerate or prefer different inorganic N forms depending on the soil in which they are grown. Most crops are adapted to temperate climates, so they grow well with N in the form of nitrate. Due to the economic importance of this fact, nitrate plant nutrition has been widely studied and is quite well understood (Xu *et al.*, 2012; Li H *et al.*, 2017; Iqbal *et al.*, 2020). The strong dependence of crop yield on N supply causes large amounts of N fertilizers to be applied to agricultural soils. This is economically and environmentally costly because it increases production costs and promotes environmental problems (Li H *et al.*, 2017). However, plants that are adapted to soils with low nitrification rates, such as rice or conifers, prefer or tolerate ammonium nutrition (Britto and Kronzucker, 2002).

The assimilation of N into organic molecules always requires that N be in the form of ammonium. Thus, nitrate is reduced by nitrate reductase (NR, EC 1.7.1.1) using reduced nicotinamide adenine dinucleotide (NADH) and producing nitrite in the cytosol. Nitrite is toxic and quickly reduced in plastids by nitrite reductase (NiR, EC 1.7.2.1) using six molecules of reduced ferredoxin to produce ammonium.

Nitrate reduction is a highly energy-consuming process that, depending on the plant species, takes place in the shoots or in the roots. The energy for the process comes from photosynthesis and is mainly expended in the NiR reaction. NiR employs ferredoxin that is directly reduced by the photosynthetic electron transport chain in photosynthetic tissues or is indirectly reduced by NADPH (reduced nicotinamide adenine dinucleotide phosphate): ferredoxin oxidoreductase (EC 1.18.1.2) in the amyloplasts of non-photosynthetic tissues using NADPH obtained from the photoassimilates that are transported from shoots to roots (Buchanan, 2015). Ammonium is assimilated by the glutamine synthetase (GS, EC 6.3.1.2) /glutamate synthase (GOGAT, NADH-dependent EC 1.4.1.14; ferredoxin-dependent EC 1.4.7.1) cycle. GS produces glutamine from glutamate and ammonium expending one molecule of adenosine triphosphate (ATP). Glutamine is used by GOGAT with 2-oxoglutarate to produce two molecules of glutamate using the reduction power of NADH or ferredoxin depending on the enzyme isoform. One glutamate molecule feeds the cycle and the other is the net product of the cycle. Fd-GOGAT is mainly expressed in photosynthetic tissues, while NADH-GOGAT is more highly expressed in non-photosynthetic tissues (Suzuki and Knaff, 2005). In angiosperms and ginkgo, there is usually one gene encoding GS localized in the chloroplasts, GS2, and several genes encoding cytosolic isoforms, called GS1 (Bernard and Habash, 2009). GS2 and Fd-GOGAT act in the photosynthetic tissues and have important roles in the re-assimilation of ammonium released during photorespiration and the assimilation of ammonium from nitrate reduction (Mifflin and Habash, 2002). GS1 and NADH-GOGAT manage the assimilation of N in roots and the reallocation of N in different metabolic and physiological processes such as senescence, fruit filling or stress responses (Cánovas *et al.*, 2007; Bernard and Habash, 2009; Thomsen *et al.*, 2014). All N compounds in plants are derived from the glutamine and glutamate produced in this cycle mainly through aminotransferase reactions (Buchanan, 2015).

Nitrate can be stored in plant vacuoles until its use without causing problems (Granstedt and Huffaker, 1982). Nitrate is preferentially accumulated in different organs depending on the species and is remobilized from vacuoles to be reduced under adequate light conditions when photosynthesis is active because nitrate reduction is coupled to photosynthetic energy production (Liu XY *et al.*, 2014). However, excessive amounts of ammonium are toxic for most plant species even

if large amounts of ammonium can be stored in the vacuoles (Wood *et al.*, 2006). Among the symptoms caused by ammonium excess there are chlorosis, growth suppression, yield depression, declines in cations such as potassium, calcium, and magnesium, increases in amino acids, and decreases in dicarboxylic acids such as malic acid, etc. (Britto and Kronzucker, 2002).

Conifers are trees with long lifespans and life cycles, most of which have perennial leaves. Conifers cover vast areas of planet Earth. This confers extraordinary ecological importance to these plants because their forests are widely extended ecosystems, mainly located in the Northern Hemisphere (Farjon, 2010). Additionally, they represent a remarkable source of raw materials, such as wood or resin, for human use. Sustainable forest management is essential for obtaining adequate yields of these biomaterials while also conserving these ecosystems. As for all other plants, N is essential for conifer growth (Cañas *et al.*, 2016). Most conifers prefer ammonium as the main inorganic N form for their growth (Britto and Kronzucker, 2002; Warren and Adams, 2002; Boczulak *et al.*, 2014). This preference could be linked to the photorespiration process. It has been observed that pine saplings fed with nitrate as their sole N source grew slowly under high atmospheric CO₂ concentrations and showed low photorespiration rates under normal or low atmospheric CO₂ concentrations (Bloom *et al.*, 2012). Interestingly, conifers have no GS2; rather, they have a cytosolic isoform, GS1a, in their photosynthetic tissues that has roles similar to those of GS2, including re-assimilation of ammonium released from photorespiration (Cantón *et al.*, 2005; Cánovas *et al.*, 2007).

Maritime pine (*Pinus pinaster* Ait.) is a conifer tree from the southwestern Mediterranean region with great environmental and economic importance in France, Portugal, and Spain. However, it is also cultured and utilized in other regions. In some cases, it has become an invasive species, particularly in South Africa (Gaertner *et al.*, 2009). This species grows better with ammonium than with nitrate nutrition (Cañas *et al.*, 2016). Despite its high phenotypic plasticity and high tolerance to abiotic stresses (Aranda *et al.*, 2010; Gaspar *et al.*, 2013), this tree is adapted to live in temperate regions where conditions favor soil nitrification, at least during the warm seasons. Additionally, maritime pine has a complete set of transporters related to nitrate transport, including at least 40 members of the Nitrate Transporter 1/Peptide Transporter family (NPF) and 2 members of the Nitrate Transporter 2

Chapter 2. Introduction

family (NRT2), and an expanded family of nitrate transport regulators,6 NRT3 (Castro-Rodríguez *et al.*, 2017). The characterization of the response to inorganic nitrogen nutrition is of paramount importance to understand the development of plants, including trees, which have long life cycles. The aim of the present work is to determine the metabolic changes that the inorganic N form, nitrate or ammonium, causes in maritime pine seedlings. The main goals are to determine the differences in the incorporation rates of two inorganic nitrogen forms (nitrate/ammonium) and to analyze the effects that both nitrogen forms have on the growth and metabolism of pine seedlings, providing information that may serve as a precedent for future works on nitrogen nutrition in maritime pine and conifers.

Results

Biomass accumulation and seedling N content in response to ammonium and nitrate supply

The main goal of the present work was to evaluate the effect of the inorganic N form on maritime pine seedlings. Five different nutritional conditions were tested (Figure 2.1), all with a total N concentration of 8 mM but with different proportions of ammonium and nitrate (8/0 mM; 6/2 mM; 4/4 mM; 2/6 mM; and 0/8 mM, respectively). The first and most obvious effect of the different N sources was the differential biomass accumulation among seedlings (Figure 2.1 a,b). Biomass decreased with the increase in nitrate content in the supplied solution, which was statistically significant in the case of seedlings fed with 8 mM nitrate. However, this effect was mainly caused by the root biomass where there were significant differences among seedlings. No differences among treatments were found in needle and stem biomass. This caused the root:shoot ratios to be significant higher in the seedlings supplied with more ammonium (Figure 2.1 c). The water content was clearly higher in the roots than in the rest of the organs (Figure 2.1 d). There were some differences in the water content between treatments in stem and roots with a slight tendency of a lower water content in the seedlings supplied only with nitrate.

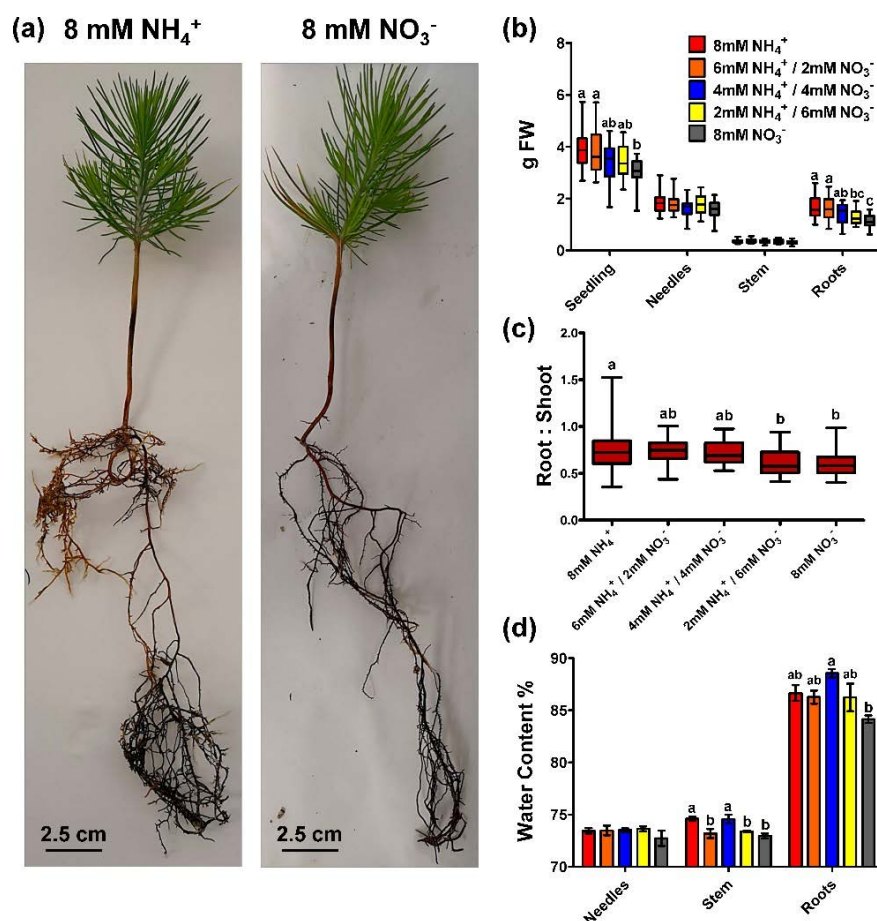


Figure 2.1. Biomass accumulation, root:shoot ratio, and water content in the different organs (needles, stem, and roots) of pine seedlings of 1-month old under the nutrient treatments. **(a)** Photographs of two seedlings after treatment with 8 mM ammonium and 8 mM nitrate; **(b)** Biomass accumulation in the whole seedling and the different organs (needles, stem, and roots); **(c)** Root:shoot ratio; **(d)** Water content. Red columns correspond to 8 mM NH₄⁺ supply; orange columns correspond to 6 mM NH₄⁺/2 mM NO₃⁻ supply; blue columns correspond to 4 mM NH₄⁺/4 mM NO₃⁻ supply; yellow columns correspond to 2 mM NH₄⁺/6 mM NO₃⁻ supply; grey columns correspond to 8 mM NO₃⁻ supply. Significant differences were determined with a one-way ANOVA for each organ or entire seedling. Letters above the columns show significant differences based on a Newman-Keuls post-hoc test ($p < 0.05$). Boxplots show minimum, maximum, and median values with $n = 6$ for biomass and root:shoot ratio. Error bars show SE with $n = 3$. FW corresponds to fresh weight.

Ammonium mainly accumulated in the roots of the pine seedlings (Figure 2.2a). There were significant differences between ammonium-fed and nitrate-fed seedlings in every organ; these differences were most evident in the roots where there was 3 times more ammonium in the seedlings fed only ammonium than in those fed only nitrate. When the ammonium and nitrate contents were compared, the ammonium levels were higher in almost every case except in the stems of plants supplied with more nitrate (Figure 2.2 a,b). The differences were more evident in the roots where the ammonium content was between 30–10 $\mu\text{mol g}^{-1}$ dry weight (DW) and the nitrate content was approximately 1–2 $\mu\text{mol g}^{-1}$ DW. There were no significant differences in the nitrate content among treatments, although there was a tendency for seedlings supplied with higher amounts of nitrate to accumulate nitrate in their stems (Figure 2.2b). However, there was an evident partitioning of nitrate accumulation between organs, with nitrate accumulation being higher in stems than in roots (nearly four times higher) and not being detected in needles. The form of inorganic N did not have an evident effect on the N content in the different organs (Figure 2.2c). The only significant differences were that the N content in the needles was higher in the seedlings supplied with higher amounts of ammonium (Figure 2.2c). In the rest of the organs, no significant differences were observed, though the N content was generally lower in the seedlings fed only nitrate. The patterns above resulted in significant differences in the carbon:nitrogen (C:N) ratios in the needles, which were higher in the seedlings supplied with more nitrate. There were no significant differences in the C:N ratios in the rest of the organs, although the ratio was slightly higher in the seedlings fed only nitrate (Figure 2.2d). This is because there were no significant differences in the carbon (C) content among the seedlings. The nitrogen use efficiency (NUE) reflects differences among treatments in N uptake (Figure 2.2i) but not in N utilization (Figure 2.2h). The nitrogen utilization efficiency (NUtE) was slightly higher in seedlings supplied with more nitrate, while the nitrogen uptake efficiency (NUpE) tended to be higher in seedlings fed with more ammonium, with significant differences from the seedlings only supplied with nitrate.

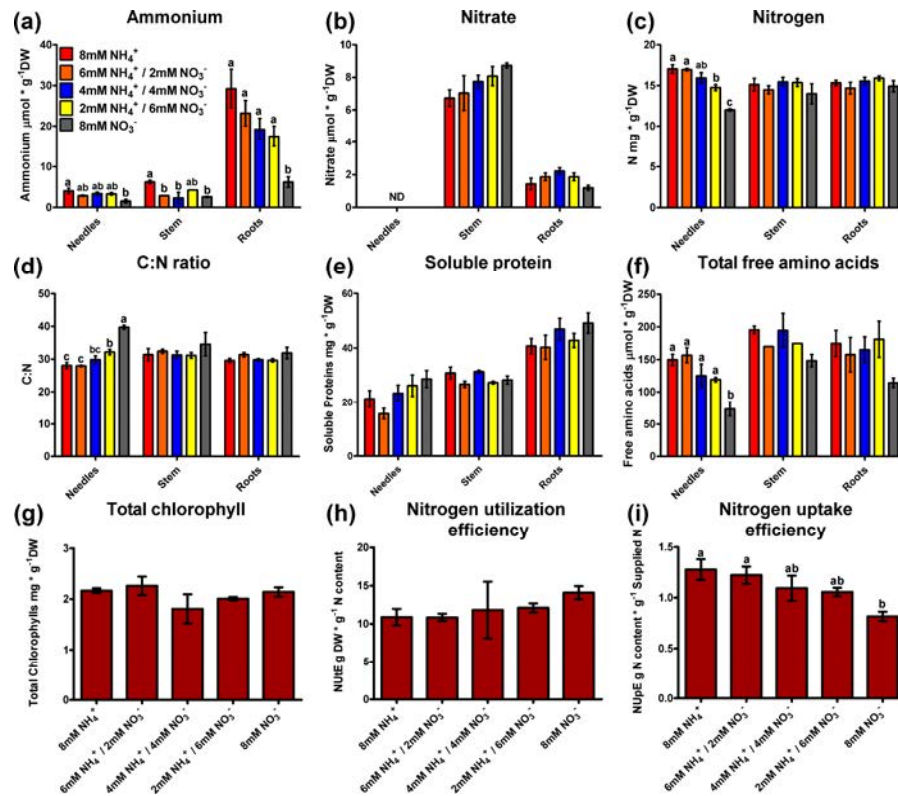


Figure 2.2. Profiles of plant N status markers in different organs (needles, stem, and roots) of pine seedlings under the nutrient treatments. (a) Ammonium content; (b) Nitrate content; (c) N content; (d) C:N ratio; (e) Soluble protein content; (f) Total free amino acid content; (g) Total chlorophyll content in pine seedling needles; (h) Nitrogen utilization efficiency (NUtE) in the seedlings under the different treatments; (i) Nitrogen uptake efficiency (NUpE) in the seedlings under the different treatments. Red columns correspond to 8 mM NH_4^+ supply; orange columns correspond to 6 mM NH_4^+ /2 mM NO_3^- supply; blue columns correspond to 4 mM NH_4^+ /4 mM NO_3^- supply; yellow columns correspond to 2 mM NH_4^+ /6 mM NO_3^- supply; grey columns correspond to 8 mM NO_3^- supply. Significant differences were determined with a one-way ANOVA for each organ or entire seedling. Letters above the columns show significant differences based on a Newman-Keuls post-hoc test ($P < 0.05$). Error bars show SE with $n = 3$.

Additionally, different indicators of the N status that are usually considered N sinks were measured. Soluble proteins and total chlorophylls are two good markers of the N content (Marschner, 2012). In the present work, there were no significant differences in these two parameters among the nutrient treatments (Figure 2.2 g,e).

However, soluble proteins tended to accumulate more in needle and root samples from seedlings fed with higher amounts of nitrate (Figure 2.2 e). An additional analyzed N marker was the free amino acid content (Figure 2.2 f). In the needles, significantly lower levels of amino acids were detected when the plants were supplied only with nitrate than when the plants were grown under the other conditions. No significant differences were observed in the amino acid levels of the stems and roots among the different treatments, although there was a tendency for plants supplied only with nitrate to accumulate lower levels of amino acids.

¹⁵N-labeled ammonium and nitrate uptake

Considering the results for NUpE, the N uptake was analyzed with ¹⁵N-labeled ammonium and nitrate (Figure 2.3). One-month-old seedlings were fed with 7.5 mM of ¹⁵N-labeled ammonium or nitrate. The N incorporation was determined through the measurement of the ¹⁵N content in the different organs. As expected, ¹⁵N accumulation was much higher in the roots than in the other organs (Figure 2.3 a–c). In every organ, the ¹⁵N incorporation during the first 30 min was higher in nitrate-fed seedlings than in ammonium-fed seedlings. From the first hour, there was an inversion of this trend, with higher ¹⁵N incorporation in the ammonium seedlings. This was due to an increase in ¹⁵N accumulation from 30 min to 2 h, although the amount in stems and roots was stable from 2 h to the end of the experiment in the ammonium-fed seedlings, and the ¹⁵N content stabilized in seedlings fed with nitrate (Figure 2.3 a–c, g). This was statistically significant in roots and in whole seedlings, although the profiles were similar for every organ. The ¹⁵N incorporation rate was very high for the first 15 min in nitrate-fed seedlings, followed by an extreme decrease in the ¹⁵N incorporation until the end of the experiment (Figure 2.3 h). For the ammonium condition, the incorporation rate increased from 15 min to one hour, maintaining its value until 2 h and decreasing to minimum levels at the end of the assay (Figure 2.3 h). The distribution of ¹⁵N was analyzed using the percentage of ¹⁵N in each organ with respect to the total ¹⁵N in the seedlings (Figure 2.3 d–f). In the needles and stems, the percentages of ¹⁵N were higher in nitrate seedlings than in ammonium seedlings from 15 and 30 min to the

final point, although the difference was only significant in needles. However, these percentages were inverse in the roots, being higher in ammonium-fed seedlings than in nitrate-fed seedlings at every time point.

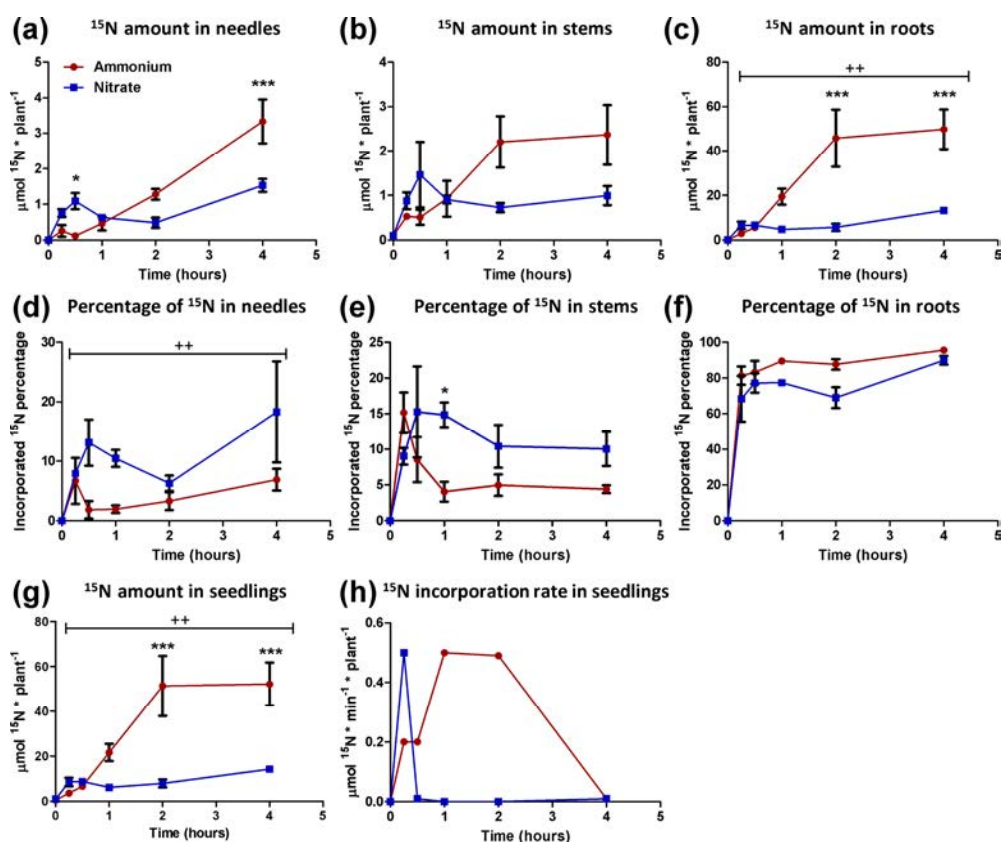


Figure 2.3. ^{15}N incorporation in different organs (needles, stem, and roots) of pine seedlings under the two nutrient treatments. The red line corresponds to 7.5 mM ^{15}N -labeled ammonium. The blue line corresponds to 7.5 mM ^{15}N -labeled nitrate. ^{15}N amount in needles (a); stems (b); roots (c); and the whole seedling (g). Percentage of ^{15}N contained in needles (d); stems (e); and roots (f) with respect to the amount in the whole seedling. ^{15}N Incorporation rate in the seedling (h). Differences between treatments were determined with a two-way ANOVA. Significant differences are indicated with crosses (++ at $p < 0.01$). Differences between treatments in each individual time point were determined with a Bonferroni post-hoc test. Significant differences are indicated with asterisks on top of the columns: * at $P < 0.05$; ** at $P < 0.01$, *** at $P < 0.001$. Error bars show SE with $n = 3$.

Enzyme activity and gene expression profiles

Some of the enzymatic activities and the expression levels of genes coding for the

main actors in N metabolism were measured in the present work (Figure 2.4). GS activity was higher in needles than in stems and roots (by 2–3 times) (Figure 2.4a). In needles, GS activity was significantly higher only in the nitrate-fed seedlings and tended to increase with the nitrate supply. The opposite effect was observed in the stem, with a significant decrease in GS activity in the 8 mM nitrate treatment and tendency to decrease with the nitrate supply. The different treatments did not have a clear effect on glutamate dehydrogenase (GDH) activity, although in the stems, there were significant differences (Figure 2.4b). The GDH activity increased from the top to the bottom of the seedlings. There was a slight and not statistically significant increase in GDH activity in the needles in parallel to the increase in the nitrate supply. Alanine and aspartate aminotransferase (AspAT and AlaAT, respectively) activities increased from the needles to the roots and were, in general, significantly higher under the conditions with more nitrate, except for the AspAT activity in the roots where no significant differences were observed (Figure 2.4c,d).

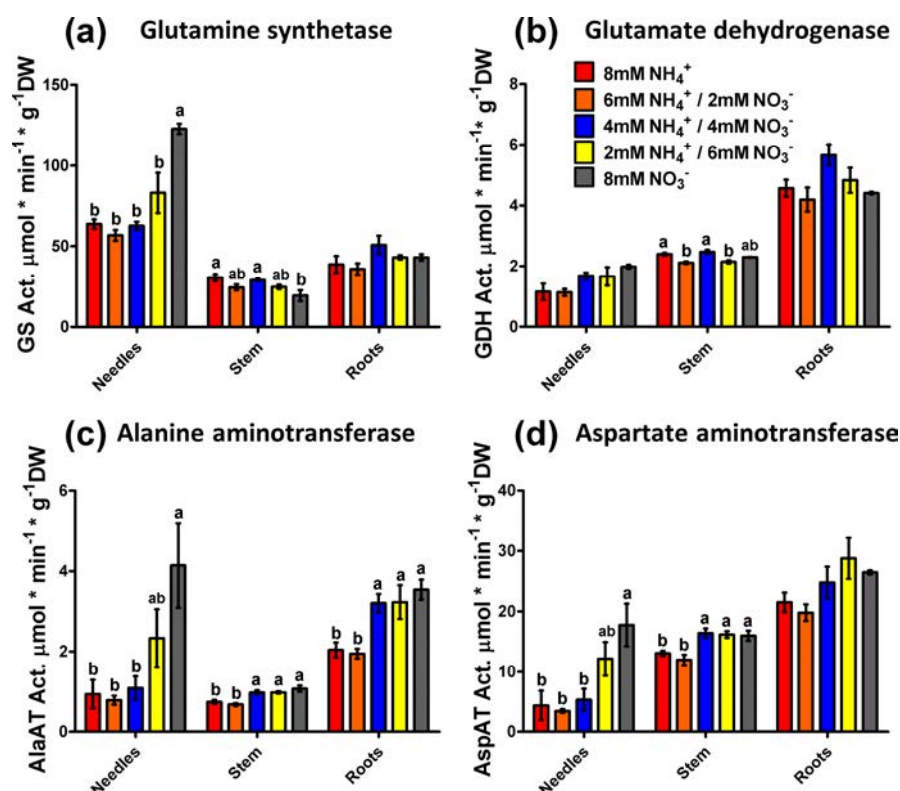


Figure 2.4. Enzyme activity in the different organs (needles, stem, and roots) of pine seedlings under the nutrient treatments. **(a)** Glutamine synthetase (GS, EC 6.3.1.2) activity; **(b)** Glutamate dehydrogenase (GDH, EC 1.4.1.3) activity; **(c)** Alanine aminotransferase (AlaAT, EC 2.6.1.2) activity; **(d)** Aspartate aminotransferase (AspAT, EC 2.6.1.1) activity. Red columns correspond to 8 mM NH₄⁺ supply;

orange columns correspond to 6 mM NH_4^+ /2 mM NO_3^- supply; blue columns correspond to 4 mM NH_4^+ /4 mM NO_3^- supply; yellow columns correspond to 2 mM NH_4^+ /6 mM NO_3^- supply; grey columns correspond to 8 mM NO_3^- supply. Significant differences were determined with a one-way ANOVA for each organ or entire seedling. Letters above the columns show significant differences based on a Newman-Keuls post-hoc test ($P < 0.05$). Error bars show SE with $n = 3$.

The expression of the gene encoding nitrate reductase (*PpNR*) was mainly observed in the needles and roots and was very low in the stems (Figure 2.5 a). In roots, *PpNR* expression was significantly lower in plants under 8 mM nitrate supply, with the highest expression in the roots of seedlings under 8 mM ammonium. The expression profile of the gene encoding nitrite reductase (*PpNiR*) was similar to that of *PpNR*, with two exceptions; the expression in needles was low in comparison to that in roots, and the differences in the roots between treatments were not significant, although the profile was the same as that for *PpNR* expression (Figure 2.5b). The expression of both *GS* genes, *PpGS1a* and *PpGS1b*, had no significant differences among treatments (Figure 2.5 c,d).

PpGS1a was mainly expressed in the needles, while *PpGS1b* was expressed in all the organs, especially in the roots, where the levels were twice those in the needles and stems. The expression profile of the gene encoding ferredoxin-dependent glutamate synthase (*PpFd-GOGAT*) was similar to that of *PpGS1a*; it was expressed mainly in the needles and showed only a slight tendency to decrease in seedlings supplied with nitrate (Figure 2.5 e). However, the transcript levels for the NADH-dependent enzyme (*PpNADH-GOGAT*) among organs were similar to those observed for *PpGS1b*, with higher levels in the roots than in the other organs (Figure 2.5f). Additionally, the expression of *PpNADH-GOGAT* in the stems changed significantly among the treatments; the highest expression was observed in the seedlings with 6 mM ammonium/2 mM nitrate. Lower expression was observed in the seedlings with 8 mM ammonium and 8 mM nitrate with a tendency to diminish its expression with the increase in the nitrate supply. Furthermore, the expression levels of genes encoding enzymes involved in the first use of assimilated N in the form of glutamate were analyzed, i.e., aspartate aminotransferase (*PpAspAT*), alanine aminotransferase (*PpAlaAT*), and glyoxylate-glutamate aminotransferase (*PpGGT*). For all three pine *PpAspAT* genes, there was no clear expression profile related to the

nutritional treatments, although in most of the cases, the expression level in 8 mM ammonium-fed seedlings was the lowest (Figure 2.5 g–i). Only *PpAspAT1* expression in the roots exhibited some significant differences, being higher in the 8 mM nitrate treatment than in the 6 mM ammonium/2 mM nitrate and 2 mM ammonium/6 mM nitrate treatments. *PpAspAT1* encodes a cytosolic protein, and the expression levels among organs were similar. However, the product of *PpAspAT2* has a predicted mitochondrial location, while that of *PpAspAT3* has a putative chloroplastic location. *PpAspAT2* was most highly expressed in roots (Figure 2.5 h), and *PpAspAT3* was most highly expressed in needles (Figure 5i). *PpAlaAT1*, which produces a mitochondrial localized protein, had a moderate expression that was higher in the roots (Figure 2.5 j). Nevertheless, *PpAlaAT2* expression was extremely low and almost residual (Figure 2.5k). As expected, the expression of the *PpGGT* gene was very high in the needles and did not show significant differences among treatments despite its lower expression in the 8 mM ammonium and 8 mM nitrate seedlings in comparison to that for the rest of the conditions, especially in the 6 mM ammonium/2 mM nitrate treatment (Figure 2.5 l).

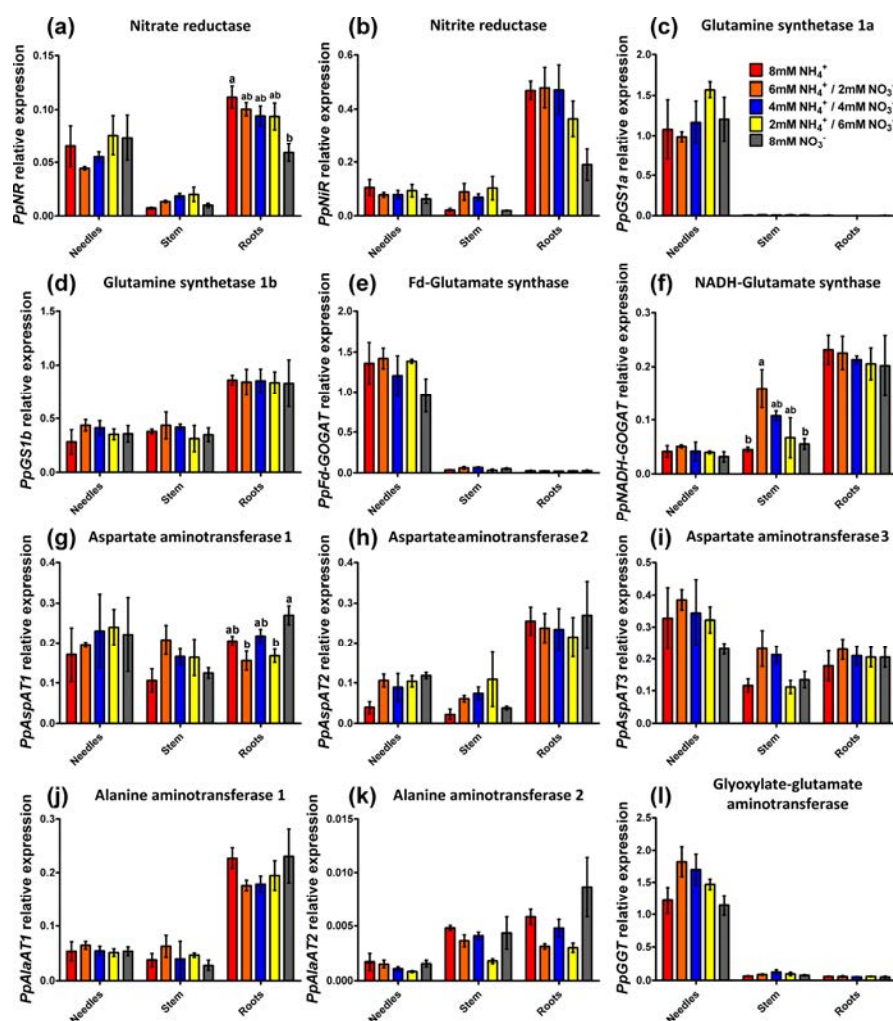


Figure 2.5. Gene expression profiles in the different organs (needles, stem, and roots) of pine seedlings under the nutrient treatments. (a) Nitrate reductase (*PpNR*); (b) Nitrite reductase (*PpNiR*); (c) Glutamine synthetase 1a (*PpGS1a*); (d) Glutamine synthetase 1b (*PpGS1b*); (e) Ferredoxin dependent glutamate synthase (*PpFd-GOGAT*); (f) NADH-dependent glutamate synthase (*PpNADH-GOGAT*); (g) Aspartate aminotransferase 1 (*PpAspAT1*); (h) Aspartate aminotransferase 2 (*PpAspAT2*); (i) Aspartate aminotransferase 3 (*PpAspAT3*); (j) Alanine aminotransferase 1 (*PpAlaAT1*); (k) Alanine aminotransferase 2 (*PpAlaAT2*); (l) Glyoxylate-glutamate aminotransferase (*PpGGT*). Red columns correspond to 8 mM NH₄⁺ supply; orange columns correspond to 6 mM NH₄⁺ / 2 mM NO₃⁻ supply; blue columns correspond to 4 mM NH₄⁺ / 4 mM NO₃⁻ supply; yellow columns correspond to 2 mM NH₄⁺ / 6 mM NO₃⁻ supply; grey columns correspond to 8 mM NO₃⁻ supply. Significant differences were determined with a one-way ANOVA for each organ or entire seedling. Letters above the columns show significant

differences based on a Newman-Keuls post-hoc test ($p < 0.05$). Error bars show SE with $n = 3$.

Metabolite profiling

The observed changes in the N status, enzyme activities, and gene expression should be reflected in equivalent changes in the metabolome. Due to this hypothesis, moderate profiling of polar metabolites was performed using proton nuclear magnetic resonance ($^1\text{H-NMR}$). In the end, 69 metabolites were determined, including different sugars, amino acids, and some secondary metabolites. The results are presented in Table S2.1. As expected, a heatmap analysis of the metabolite profile shows that samples are grouped by organ (Figure 2.6).

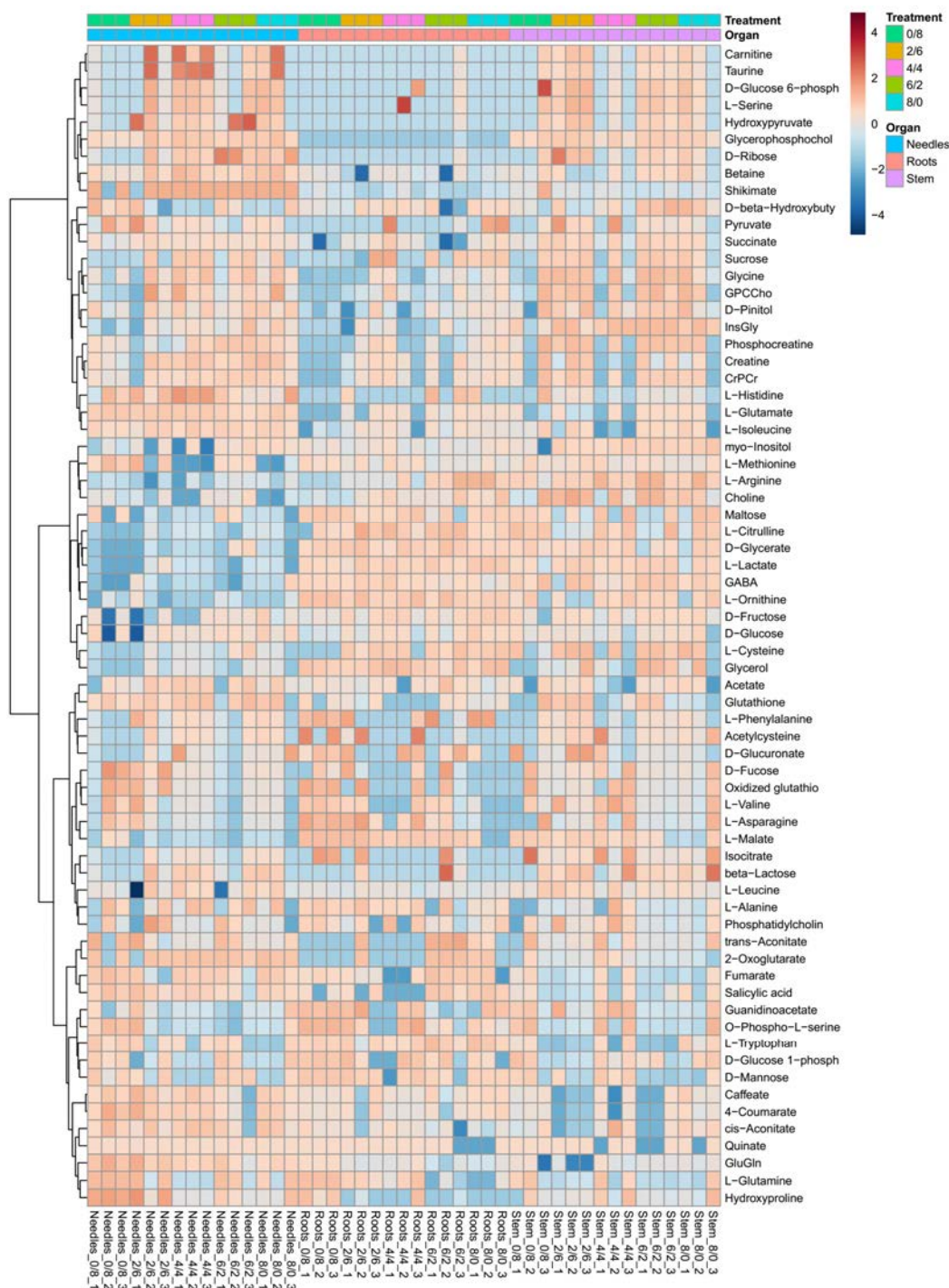


Figure 2.6. Heatmap of the metabolite profile data.

L-arginine was the main metabolite affected by the nutritional treatments in a global ANOVA (Figure 2.7).

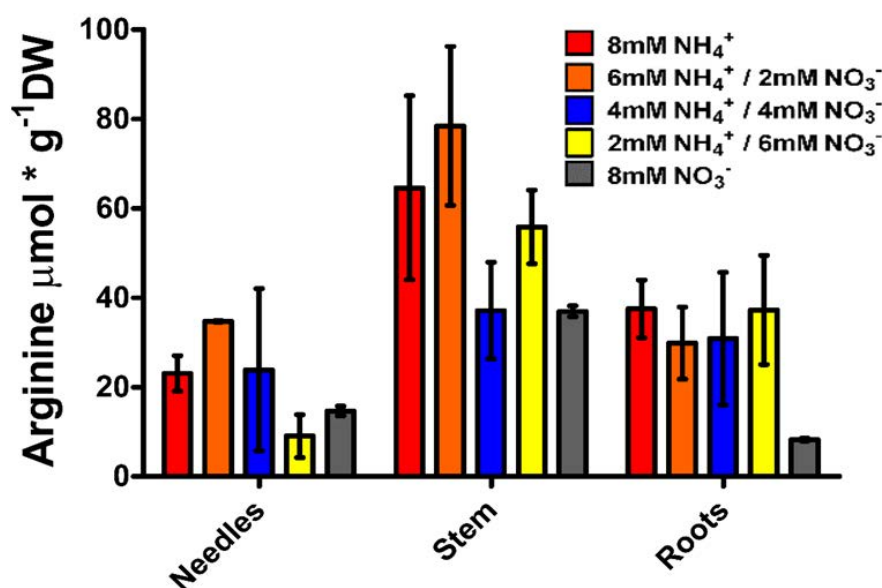


Figure 2.7. L-Arginine amounts in different organs of maritime pine seedling under long term N supply.

When the extreme treatments (8 mM NH₄⁺ and 8 mM NO₃⁻) were analyzed in each organ in an independent manner, significant differences (25 metabolites) between treatments were found in the roots (Table S2.1 and Figure 2.8). Notably, some of the main carbohydrates in pines such as sucrose, D-fructose, D-glucose, and D-pinitol were present at higher levels in ammonium-fed seedlings than in nitrate-fed plants. The same effect was found for several amino acids such as L-glutamate, L-arginine, L-cysteine, and glycine. However, O-phospho-L-serine, L-valine, L-ornithine, L-glutamine, and L-asparagine were present in higher amounts in the roots of nitrate-fed seedlings. D-mannose, 4-coumarate, and oxidized glutathione contents were also higher in roots of nitrate-fed seedlings.

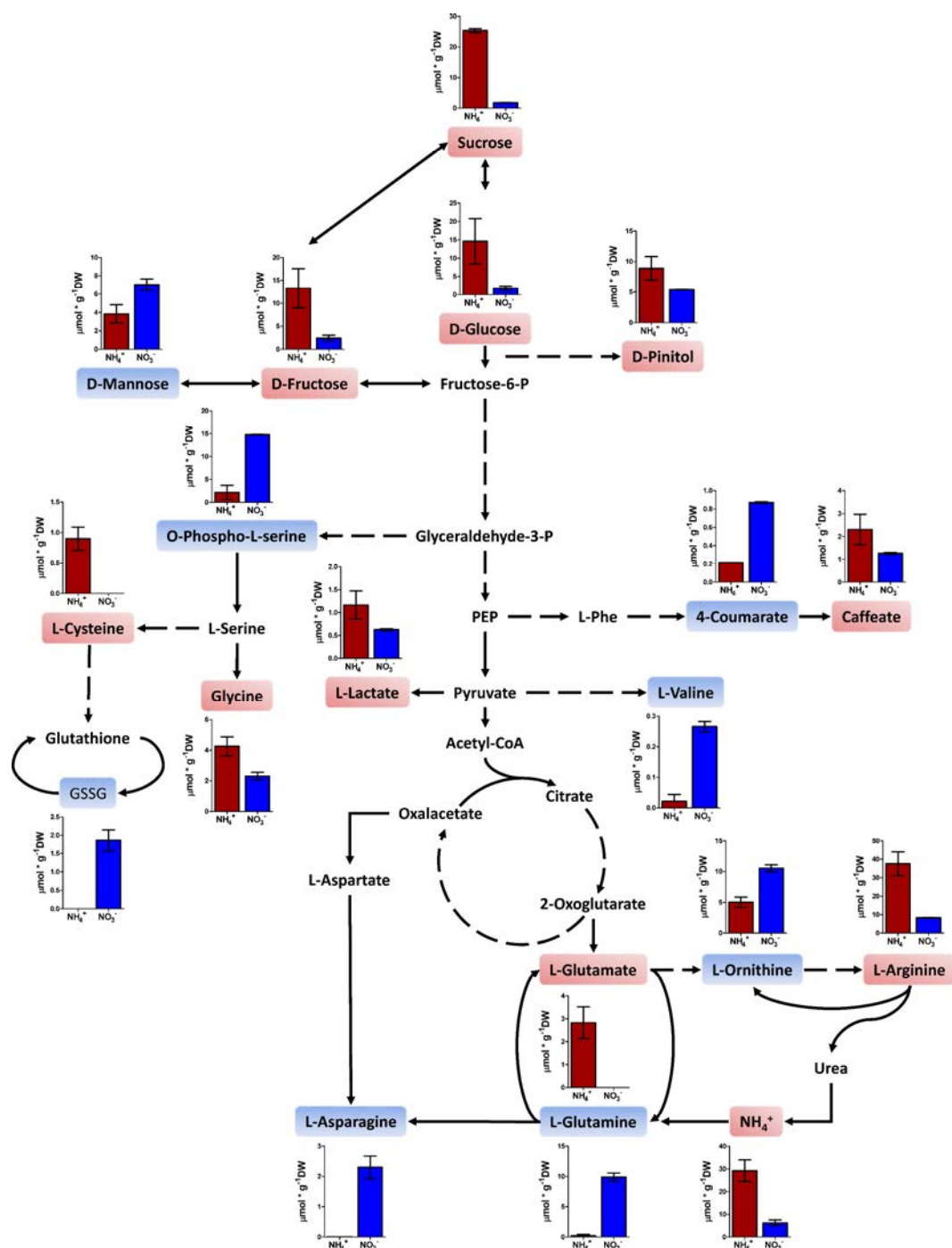


Figure 2.8. Main significant metabolites in the roots of seedlings fed 8 mM ammonium or 8 mM nitrate. Red columns correspond to 8 mM NH_4^+ supply; blue columns correspond to 8 mM NO_3^- supply. Metabolites highlighted in red were significantly more accumulated in the roots of seedlings fed 8 mM ammonium. Metabolites highlighted in blue were significantly more accumulated in the roots of seedlings fed 8 mM nitrate. GSSG: Oxidized glutathione; PEP: Phosphoenolpyruvate; L-Phe: L-Phenylalanine. Significant differences were determined with a *t*-test (FDR < 0.05). Error bars show SE with *n* = 3.

Discussion

The preference of conifers for different inorganic N forms has been previously discussed in different works (Warren and Adams, 2002; Boczulak *et al.*, 2014; Koyama and Kielland, 2019). Depending on the species habitat, including climatic and soil conditions, conifers show preferences for the uptake and utilization of ammonium or nitrate (Boczulak *et al.*, 2014). Most of the conifers are tolerant to ammonium (Kronzucker *et al.*, 1996; Cañas *et al.*, 2016). In the case of *P. pinaster*, its growth is higher with ammonium than with nitrate (Warren and Adams, 2002), although it is a conifer species with extensive families of nitrate transporters (NPF and NRT2) and transport regulators (NRT3) (Castro-Rodríguez *et al.*, 2017) and also lives in the Western Mediterranean region where climate conditions can promote high nitrification rates in the soil. In this context, the goal of the present work was to identify the main changes caused at the metabolic level by ammonium or nitrate supply in maritime pine seedlings.

The results included in this study considerably expand the knowledge of N nutrition in maritime pine provided by previous reports. The seedlings with a higher ammonium supply grew better (Figure 2.1), but the whole plants also accumulated more N through higher N uptake efficiency (NUpE) (Figure 2.2). In fact, the ¹⁵N labeling experiment supported this observation; the ammonium uptake in seedlings was higher, and there was a high incorporation rate (at the μmolar level) during most part of the experiment (Figure 2.3). Interestingly, the differential biomass accumulation took place mainly in the roots, causing an increase in the root:shoot ratio in ammonium-fed seedlings. The application of high amounts of ammonium usually inhibits root growth and decreases the root:shoot ratio in plants (Britto and Kronzucker, 2002). In maritime pine seedlings, it seems that root growth increases following ammonium application, or at least, the growth inhibition is lower than that in seedlings fed with nitrate (Figure 2.1). In conifers, the root growth and the root:shoot ratio vary depending on the N source, which can include organic compounds such as L-arginine, which favors root development and a high root:shoot ratio (Gruffman *et al.*, 2012). In fact, this is considered a good trait for the field establishment of conifer seedlings (Davis and Jacobs, 2005; Gruffman *et al.*, 2012). Thus, the above results support the preference of maritime pine for ammonium as an inorganic N form over nitrate and suggest that the ammonium preference

promotes beneficial root development. In this context, roots were the only organ with significant differences in metabolite content among treatments in the present study (Figure 2.8, Table S2.1).

This is significant considering that roots seem to be the organ where primary N assimilation occurs in pine (Figure 2.5), despite the resolution of the analytical procedure being only in the mM range (400 MHz NMR spectrometer). The N content clearly increased in the seedlings supplied with ammonium that had higher N uptake efficiency (NUpE) (Figure 2.2). However, changes in the N content occurred mainly in the needles. Considering the N partitioning, the free amino acid content seems to be the main factor responsible for this effect, with slight participation from the ammonium content (Figure 2.2). The metabolite profile in roots also suggests that ammonium-fed plants had a better N status (Figure 2.8, Table S2.1). Certain amino acids are good markers of a healthy N status, such as L-glutamate, L-cysteine, and L-arginine. L-glutamate is the net product of the GS/GOGAT cycle, which is the pathway mainly responsible for N assimilation (Miflin and Habash, 2002). L-cysteine is the final product in the sulfur assimilation pathway, but its biosynthesis depends on the availability of assimilated N (Koprivova and Kopriva, 2014). Furthermore, L-cysteine acts as a precursor for antioxidants and defense compounds (Álvarez *et al.*, 2012) and is related to the transcriptional response of ammonium nutrition in plants that have a greater tolerance for ammonium (Sun *et al.*, 2017). L-arginine is synthesized from L-glutamate and is an amino acid with an important role as an N reserve in pine. This amino acid is very abundant in storage proteins and is an important sink for assimilated N surplus (Cañas *et al.*, 2016; Llebrés *et al.*, 2018). Additionally, the metabolite profile in the roots indicates that the availability of C for metabolic processes was reduced in nitrate-fed seedlings (Figure 2.8, Table S2.1). The levels of the main soluble sugars, such as sucrose, D-fructose, and D-glucose, were extremely low in nitrate-fed seedlings in comparison to those in ammonium-fed seedlings. In fact, some C sinks such as D-pinitol or caffeic acid were also more accumulated in the ammonium-feed seedlings. This correlates well with the accumulation of L-asparagine, L-glutamine, and L-ornithine in the nitrate-fed plants. L-asparagine is an amino acid that is synthesized from L-glutamine and L-aspartate and is employed as a temporal N reserve when C is depleted (Gaufichon and Rothstein, 2016). Similarly, the accumulation of L-ornithine could suggest the active catabolism of L-arginine to

mobilize the stored N and produce L-glutamate (Cañas *et al.*, 2008). Interestingly, in the roots of the ammonium-fed seedlings, a greater amount of choline (4 times) was observed than in the roots of nitrate-fed plants (Table S2.1).

Choline is the precursor of glycinebetaine in most living organisms and it is well known to play a role in osmotic stress (Chen and Murata, 2011), which could be related to ammonium levels since a higher water content was observed in the ammonium-fed seedlings compared to nitrate-fed plants (Figure 2.1d). Furthermore, glycinebetaine plays a role in oxidative stress responses by enhancing antioxidative responses (Sakamoto *et al.*, 1998; Chen and Murata, 2011) which could be linked to the transcriptomic response to ammonium (Patterson *et al.*, 2010). Interestingly, the main accumulation of nitrate and ammonium was not in needles. This suggests that the changes in N content in the needles were related to metabolic processes associated with N management (assimilation and recycling). Additionally, the partitioning of ammonium and nitrate within the seedlings was different. The seedlings accumulated the most ammonium in the roots, avoiding major increases in its concentration in aerial organs. In plants, primary ammonium assimilation generally occurs in the roots (Hachiya and Sakakibara, 2017). Pine plants may subtly regulate and buffer the ammonium content in their organs via primary assimilation in the roots and the accumulation of the ammonium excess in the same organ, probably in the vacuoles (Wood *et al.*, 2006; Bai *et al.*, 2014). This regulatory mechanism can prevent problems derived from the high levels of ammonium released during photorespiration in the photosynthetic tissues or during lignification that occurs mainly in the stem (Cánovas *et al.*, 2007). Additionally, free ammonium levels were higher in seedlings fed ammonium, mainly in the roots. However, the differences in nitrate content between the different treatments were not very large (not statistically significant), and the levels of nitrate accumulation were several times lower than the ammonium accumulation in the same organs. This fact and the total N content of the seedlings suggest that ammonium uptake is less restricted than nitrate uptake in maritime pine. The nitrate incorporation rate was only higher than the ammonium incorporation rate during the first 15 min, suggesting precise regulation by nitrate transporters (Figure 2.3). This low nitrate uptake rate has also been observed in white spruce, and the authors proposed that nitrate uptake systems are atrophied in plants that prefer ammonium (Kronzucker *et al.*, 1997; Britto and Kronzucker, 2013). However, maritime pine possesses a

complete set of nitrate transporters and even an expanded gene family that encodes nitrate transport regulators (NRT3). In this context, it is tempting to speculate that maritime pine senses nitrate to be a toxic molecule.

Although it is well known that plants prefer to accumulate nitrate over ammonium, which can produce cellular toxicity in several ways (Britto and Kronzucker, 2002; Hachiya and Sakakibara, 2017), pine is able to store more ammonium than nitrate at similar supply levels. Curiously, excess nitrate is mainly stored in the stem, an organ with a less important N assimilatory role than needles and roots, as suggested by the *PpNR* and *PpNiR* expression levels (Figure 2.5). This observation, along with the observed content of L-arginine in the stem (Figure S2.2) and the accumulation of L-asparagine in the seedling hypocotyl during the post-germination phase (Cañas *et al.*, 2006; 2008), suggests that the pine stem has a role as a store of N that accumulates not only vegetative storage proteins (VSPs) in the bark (Li G and Coleman, 2019), but also free metabolites such as nitrate, L-arginine or L-asparagine. It is known that trees are able to transiently accumulate N in free amino acids (Rennenberg *et al.*, 2010); in the future, it will be interesting to analyze the role of adult pine stems in the storage of N through the accumulation of small metabolites such as nitrate or free amino acids.

Interestingly, nitrate did not accumulate in the needles (Figure 2.2), and the activity of enzymes involved in basal N metabolism increased in the needles with the nitrate supply (Figure 2.4). These results suggest a limited ability for nitrate assimilation in maritime pine, which may be related to the photorespiration pathway. Conifers lack a chloroplastic GS isoform (GS2) that is involved in the photoassimilation of nitrate and the reassimilation of ammonium released during photorespiration in angiosperm plants (Cánovas *et al.*, 2007). This could explain the increase in GS activity in the needles of nitrate-fed seedlings (Figure 2.4). In fact, a strong relationship between nitrate assimilation and photorespiration in pine has been observed in *Pinus taeda* saplings, which grew better with nitrate under low CO₂ concentrations than under elevated CO₂ concentrations; in contrast, CO₂ concentration had no effect in the growth rate of ammonium-fed saplings (Bloom *et al.*, 2012). However, it seems that needle metabolism is influenced by the form of available inorganic N. In this context, these effects appear to be regulated through the allocation of the inorganic N forms to the different organs and through their assimilation in the roots, as indicated by the expression levels of *PpNR* and

PpNiR genes (Figure 2.5). Despite the expression of these genes, the ^{15}N incorporation assay indicated that nitrate was relatively better transported from roots to stem and needles than ammonium (Figure 2.3d–f), at least when the nitrate incorporation rate was high. It is possible that nitrate assimilation into the needles negatively affects photosynthetic/photorespiration metabolism, inducing a negative feedback with nitrate transport in the roots. Nitrate uptake inhibition has been previously observed in different plants when enough nitrate is assimilated, but not in such a drastic manner (Tischner, 2000).

Another interesting finding is the lack of correlation between enzyme activity (GS, AspAT, and AlaAT) and the expression of the genes coding for the enzymes that catalyze these reactions (Figures 2.3 and 2.4). These findings suggest that the response to the N form must be regulated through a post-transcriptional (translational or post-translational) mechanism. This could involve changes in translation or in the proteolysis rates. A second mechanism has been proposed for the GS enzyme in mammals, wherein the increase in glutamine levels drives ubiquitination and proteasome degradation of the protein (Nguyen *et al.*, 2016; Nguyen *et al.*, 2017). In plants, ubiquitination-dependent proteolysis also plays a role in N metabolism during plant adaptation to N starvation (Park *et al.*, 2018; Peng *et al.*, 2018).

Conclusions

The results of the present work demonstrate that ammonium and nitrate nutrients behave differently from each other in pine, although their assimilation into organic molecules occurs through the same pathway, the GS/GOGAT cycle. Their chemical characteristics and the reduction of nitrate to ammonium before its assimilation are crucial differences that affect plant metabolism and growth. Ammonium promotes better root growth than nitrate, which could be used to increase the performance during the field establishment of conifer seedlings. Additionally, other differences were found in the photosynthetic organs, where nitrate induced important changes correlated with the decreased growth of pine seedlings. A differential accumulation of nitrate and ammonium occurred in the pine organs and buffered the individual effects induced by each molecule. The role of pine stems in the storage of N compounds, such as nitrate and L-asparagine, and the interaction between photosynthetic metabolism and nitrate will require further research efforts in the near future.

Supplemental materials:

All the supplemental materials are provided in the folder Chapter 2 – Supplemental Material, accessible through this link:

https://drive.google.com/drive/folders/10V_JjI5sHapuV-zaPZFSrb-LBiS2fNPd?usp=sharing

Table S2.1. Metabolite profile results. (Pendrive)



Chapter 3

Ammonium affects a transcriptional network related to root development in maritime pine roots

Francisco Ortigosa, César Lobato-Fernández, Concepción Ávila, Francisco M. Cánovas, Rafael A. Cañas.



Introduction

Nitrogen (N) is an essential macronutrient for all living organisms, because is a constituent of different biomolecules such as nucleic acids, proteins, amino acids, porphyrins and hormones, among others (Miller and Cramer, 2005). This nutrient is necessary for the correct growth and development of plants which are able to assimilate N from different kind of sources, including organic (peptides, amino acids and urea) and inorganic (nitrate, nitrite and ammonium) forms (Näsholm *et al.*, 1998, Hachiya and Sakakibara, 2017, Ortigosa *et al.*, 2019). Together with nitrate (NO_3^-), ammonium (NH_4^+) is one of the main forms of inorganic N available for plants, changing their relative proportions in soils depending on biological and climate conditions (Bijlsma *et al.*, 2000). NH_4^+ uptake can be carried out by specific and non-specific mechanisms (Hachiya and Sakakibara, 2017). Specific NH_4^+ uptake is performed by members of the ammonium transporter family (AMT) (McDonald and Ward, 2016). It has been extensively described that NH_4^+ at millimolar (mM) levels usually causes toxicity in most plants (Esteban *et al.*, 2016). Among the effects caused by an excessive NH_4^+ supply it should be mentioned plant growth decrease, leaf chlorosis, root/shoot ratio decrease, loss of root gravitropism and changes in the root system architecture (RSA) (Esteban *et al.*, 2016). Related to changes in RSA, it is commonly observed the inhibition of root elongation and an enhancing lateral root formation (Liu and von Wirén, 2017). In the process of root elongation, three interconnected biological processes intervene: cell division, cell expansion and cell differentiation (Wang and Ruan, 2013; Youssef *et al.*, 2018). Auxins (IAAs) play a prominent role in the first two processes (Wang and Ruan, 2013). IAAs can be synthesized in the root meristem (RM) and transported towards upstream adjacent regions through specific transporters, such as AUXIN RESPONSE 1 (AUX1) and PINFORMED 1-7 (PIN1-7) (Grunewald and Friml, 2010). Auxin induces the expression of PLETHORA 1-4 (PLT1-4) transcription factors (TFs) in the RM, which are responsible of cell proliferation maintenance (Galinha *et al.*, 2007). Other TFs have been described to play key roles on the stem cell niche (SCN) and the quiescent center (QC) maintenance to produce all tissues derived to form a mature root, such as *SHORT-ROOT* (*SHR*, *AT4G37650*) and *SCARECROW* (*SCR*, *AT3G54220*) (Sablowski, 2011). *SHR* expression is localized in a zone of the stele that constitutes the central part of the root and stem (Miyashima *et al.*, 2011; Kim *et al.*, 2020). When *SHR* transcripts are translated,

SHR proteins move into the adjacent cells (pericycle cells, endodermis, QC and phloem pole) to activate the expression of *SCR* (Helariutta *et al.*, 2000; Nakajima *et al.*, 2000; Sena *et al.*, 2004; Cui *et al.*, 2007). Recently, Kim *et al.* (2020) described that SHR plays key roles in the phloem development, controlling the asymmetric cell division process (ACD) for the sieve-elements (SEs) development by the regulation of *NARSI* and *SND2* NAC-type transcription factors. This fact is relevant because these cell types constitute the phloem (Greb, 2020), as it is the main means of auxin transport (Chapman and Estelle, 2009). Among the auxin roles in roots under the presence of NH_4^+ have been described to influence the inhibition of root growth, root agravitropic response and lateral root (LR) branching (Cao *et al.*, 1993; Liu *et al.*, 2013; Araya *et al.*, 2016). However, Liu *et al.* (2013) showed that NH_4^+ does not affect the auxin content at the QC, where the maximum level of this phytohormone in roots is localized (Zhou *et al.*, 2010). In *Arabidopsis*, root growth inhibition in response to NH_4^+ represses root cell production by decreasing the meristem size, and the number of dividing cells without altering the cell division rate (Liu *et al.*, 2013). Furthermore, NH_4^+ also decreases the number of root cap cells (Liu *et al.*, 2013). In this sense, several transcription factors have been described to play key roles in root cap development, such as *BEARSKIN* (*BRN*) and *SOMBREIRO* (*SMB*) (Bennett *et al.*, 2010 and 2014; Kamiya *et al.*, 2016). However, the transcriptional pathway regulating NH_4^+ -root cap development have not been deciphered in deep so far.

On the other hand, it has been described that NH_4^+ inhibits the gravitropic response by downregulating the expression of *AUX1* and *PIN2*, which are two pivotal auxin transporters (Liu *et al.*, 2013). LR branching is enhanced by NH_4^+ supply (Araya *et al.*, 2016). Comparing the *AtAMT1.1* and *AtAMT1.3* complemented quadruple AMT knock-out lines (*qko*), only *AtAMT1.3* was able to restore the LR branching phenotype induced by NH_4^+ (Lima *et al.*, 2010), suggesting that the NH_4^+ -induced LR branching process signaling events are dependent of *AtAMT1.3* (Lima *et al.*, 2010). Besides, auxin have been suggested to be involved in this signaling event due to the *PIN2* repression observed under NH_4^+ supply (Liu *et al.*, 2013; Zou *et al.*, 2013). These evidences constitute additional aspects of the described importance of auxin in orchestrating root system configuration in response to a

stress / stimulus. However, the transcriptional regulatory mechanisms that control this response remain unclear.

Together with auxins, cytokinins (CKs) have been previously established to be important in root plant-growth and vascular development (Kamada-Nobusada *et al.*, 2013; Miyashima *et al.*, 2019; Mao *et al.*, 2020). Cytokinin biosynthesis and activity in plants are closely related to N availability (Takei *et al.*, 2004; Kamada-Nobusada *et al.*, 2013). In the roots of rice, NH_4^+ nutrition leads to the accumulation of different CKs and CKs-derived compounds (Kamada-Nobusada *et al.*, 2013). It is described that during Arabidopsis active growth, the content of CKs increased first in the vascular system, reflecting CKs transport from roots to shoots (Shtratnikova *et al.*, 2015). Recently, it has been reported that CK signaling in the early protophloem-sieve-element (ePSE) cell files of Arabidopsis root procambial tissue promotes the expression of several *DOF* transcription factors (Miyashima *et al.*, 2019). Together with the auxin responsive dependent HD-ZIP III proteins, they comprise a transcriptional network that integrates spatial information of the hormonal domains and *miRNA* gradients, which are essential for root vascular development (Miyashima *et al.*, 2019).

Conifers are long life cycle organisms covering large areas in the northern hemisphere with high ecologic and socioeconomic importance (Farjon *et al.*, 2018). For their growth, most of conifers exhibit an NH_4^+ preference as the main N source (Kronzucker *et al.*, 1997; Warren and Adams, 2002; Hawkins and Robbins, 2010, Ortigosa *et al.*, 2020). However, the molecular mechanisms triggered by ammonium in maritime pine roots are largely unknown (Canales *et al.*, 2010). Microarray analysis of ammonium nutrition/excess in maritime pine roots showed differential expression patterns on several coding transcripts related to defense, stress response, transport process and N and carbohydrate metabolism (Canales *et al.*, 2010). This report is consistent with other reports on other model plant systems (Patterson *et al.*, 2010; Sun *et al.*, 2017). However, little is known about the transcriptional response of pine roots related to NH_4^+ nutrition (Canales *et al.*, 2010), vascular formation (Molina-Rueda *et al.*, 2015) and meristem development and maintenance (Brunoni *et al.*, 2019). The main goal of this work was to decipher the mechanisms involved during NH_4^+ uptake in the roots at transcriptional level, focusing on the root tip response, and its relationship with root development. This

Chapter 3. Introduction

information provides relevant data of great value for the sustainable management of forest nutrition and breeding.

Results

Metabolic status of maritime pine seedlings

In order to evaluate the metabolic status of pine seedlings in the stage in which they were going to be used to study the transcriptomic response in the root tip to the presence of NH_4^+ , a metabolite profiling was carried out. The metabolic status of the pine seedlings revealed a great abundance of amino acids that serve as nitrogen reserves such as L-arginine and L-asparagine in needles and stems, respectively (Figure 3.1).

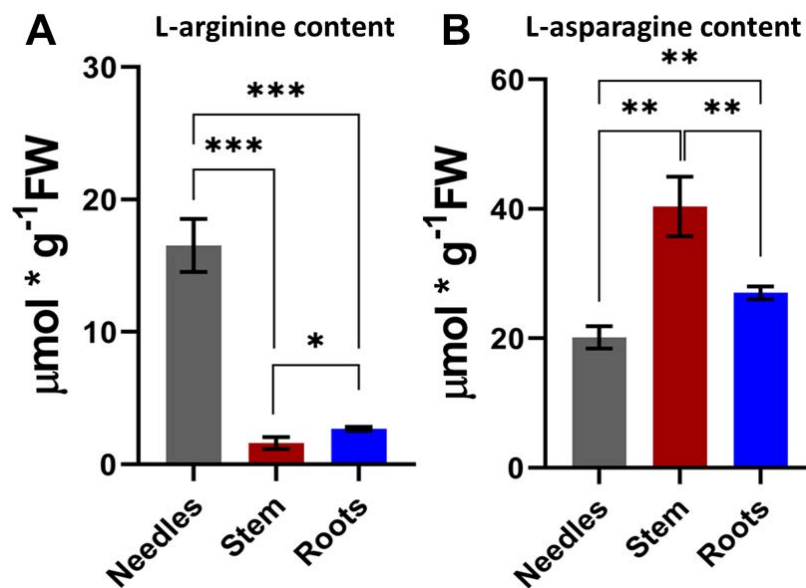


Figure 3.1. Abundance of L-arginine (A) and L-asparagine (B) in different 1-month old organs of maritime pine seedlings. Significant differences were determined with a t-test (* $P < 0.05$; ** $P < 0.01$; *** $P < 0.001$). Error bars show SE with $n = 3$.

Expression analysis of AMT gene family

As a first step to study the transcriptional response of pine roots to NH_4^+ application, the AMT family was analyzed. A sequence search analysis of AMTs based on the *Pinus pinaster* published transcriptomic data (Canales *et al.*, 2014; Cañas *et al.*, 2015; Cañas *et al.*, 2017) and unpublished maritime pine genome draft (Sterck *et al.*, unpublished) allowed us to identify four additional transcripts encoding AMT transporters in maritime pine (*PpAMT1.4*, *PpAMT2.4*, *PpAMT2.5* and *PpAMT2.6*) respect to those described in a previous work (Castro-Rodríguez *et al.*, 2016) (Figure 3.2). Phylogenetic analysis revealed that maritime pine AMT1 subfamily is composed by four members: *PpAMT1.1*, *PpAMT1.2*, *PpAMT1.3* and *PpAMT1.4*.

While maritime pine AMT2 subfamily is integrated by six members: *PpAMT2.1*, *PpAMT2.2*, *PpAMT2.3*, *PpAMT2.4*, *PpAMT2.5* and *PpAMT2.6*.

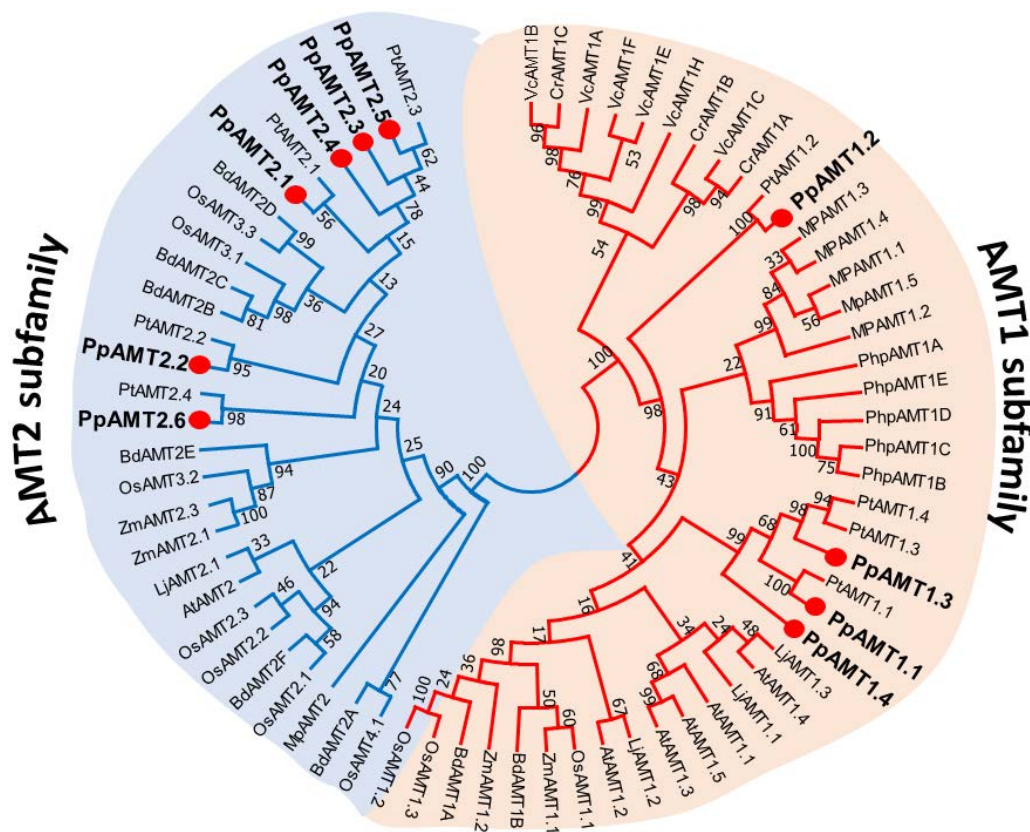
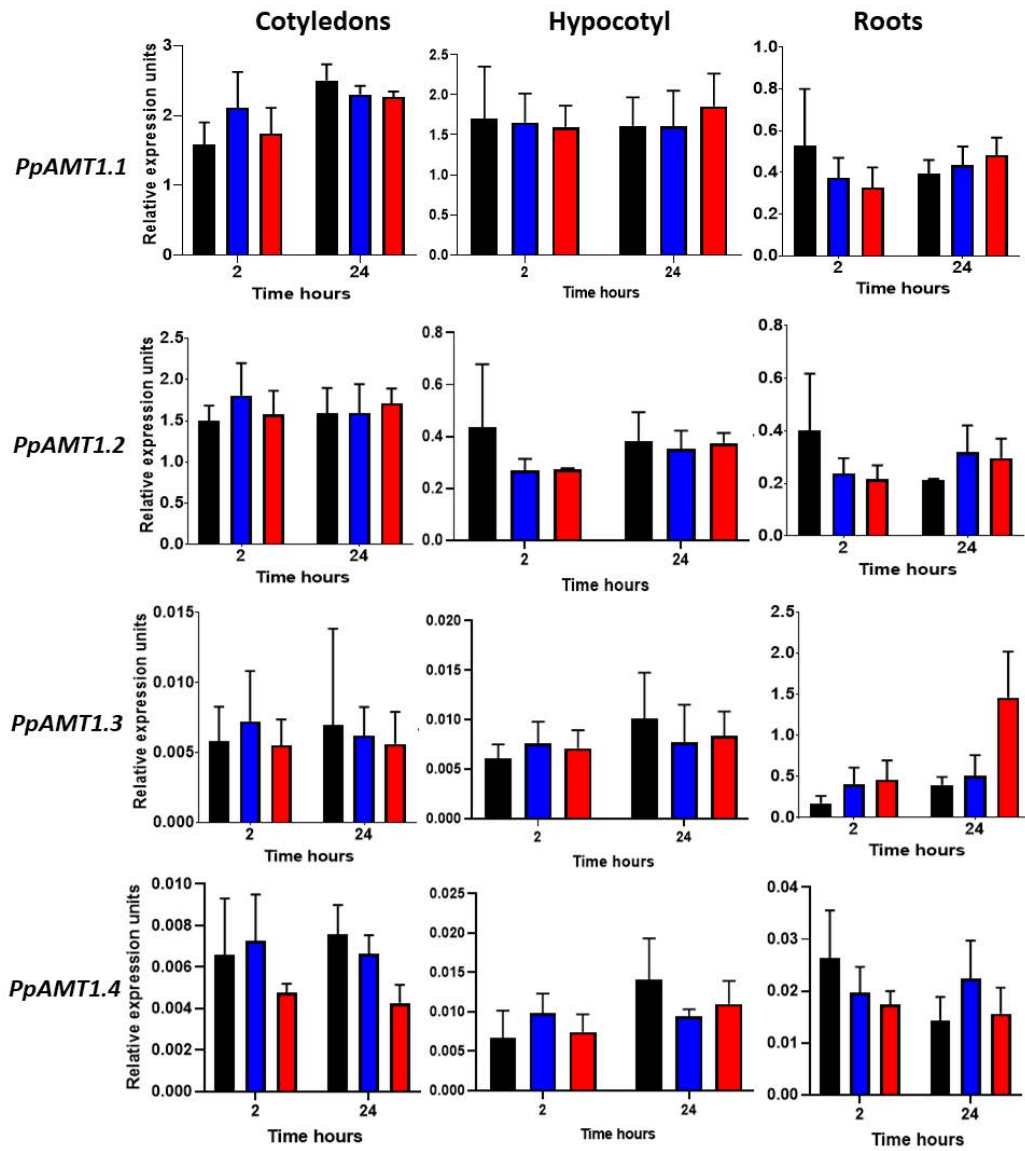


Figure 3.2. Phylogenetic tree of the AMT families including maritime pine members. The protein sequence alignment was made with Muscle (Edgar, 2004). The evolutionary history was inferred using the Neighbor-Joining method (Saitou and Nei, 1987). The bootstrap consensus tree inferred from 1000 replicates is taken to represent the evolutionary history of the taxa analysed (Felsenstein, 1985). Evolutionary analyses were conducted in MEGA7 (Kumar *et al.*, 2016). Abbreviations: At, *Arabidopsis thaliana*; Bd, *Brachypodium distachyon*; Cr, *Chlamydomonas reinhardtii*; Lj, *Lotus japonicus*, Mp, *Machantia polymorpha*; Os, *Oryza sativa*; Php, *Physcomitrella patens*; Pp, *Pinus pinaster*; Pt, *Pinus taeda*; Vc, *Volvox carteri*; Zm, *Zea mays*.

The gene expression patterns of individual members of the *PpAMT1* and *PpAMT2* subfamilies were determined on different organs of seedlings including cotyledons, hypocotyls and radicles, in response to in response to two levels of NH_4^+ supply, moderate (3 mM NH_4Cl) and low (0.1 mM NH_4Cl), at two different time points (2 and 24 hours post-irrigation) in order to evaluate the response of these genes

involved in NH_4^+ nutrition and to elucidate at what time could be more interesting to perform LCM on maritime pine root tips. The gene expression results are shown in the Figures 3.3 and 3.4.



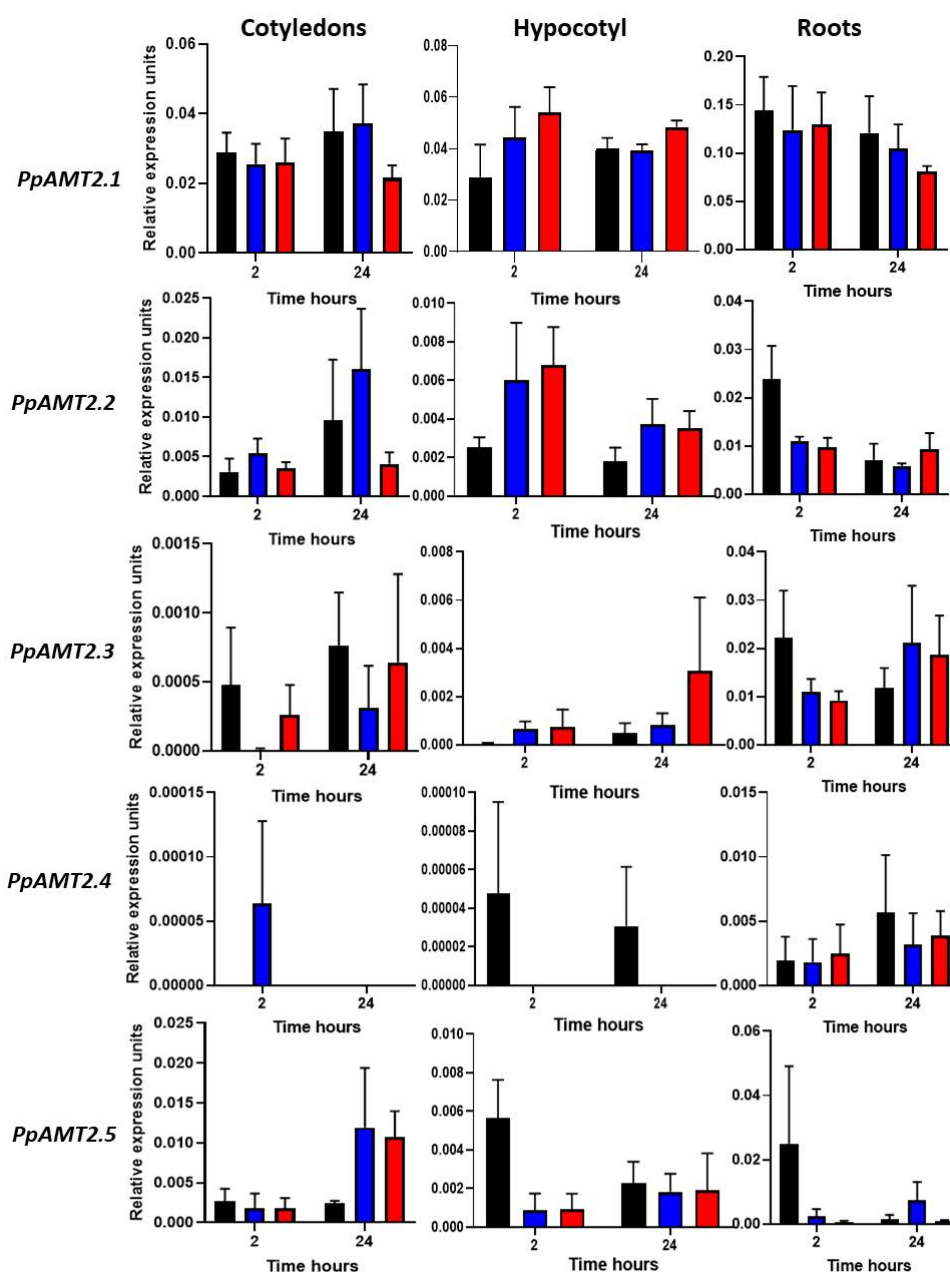


Figure 3.3. Gene expression of *PpAMT1* and *PpAMT2* transporter gene family under ammonium nutrition. One-month old seedlings were watered with water (control), 0.1 mM NH_4^+ (0.1) and 3 mM NH_4^+ (3). The different organs were harvested 2 h and 24 h after the treatment. Black columns correspond to control samples, blue columns to 0.1 mM samples and red lines to the 3 mM columns.

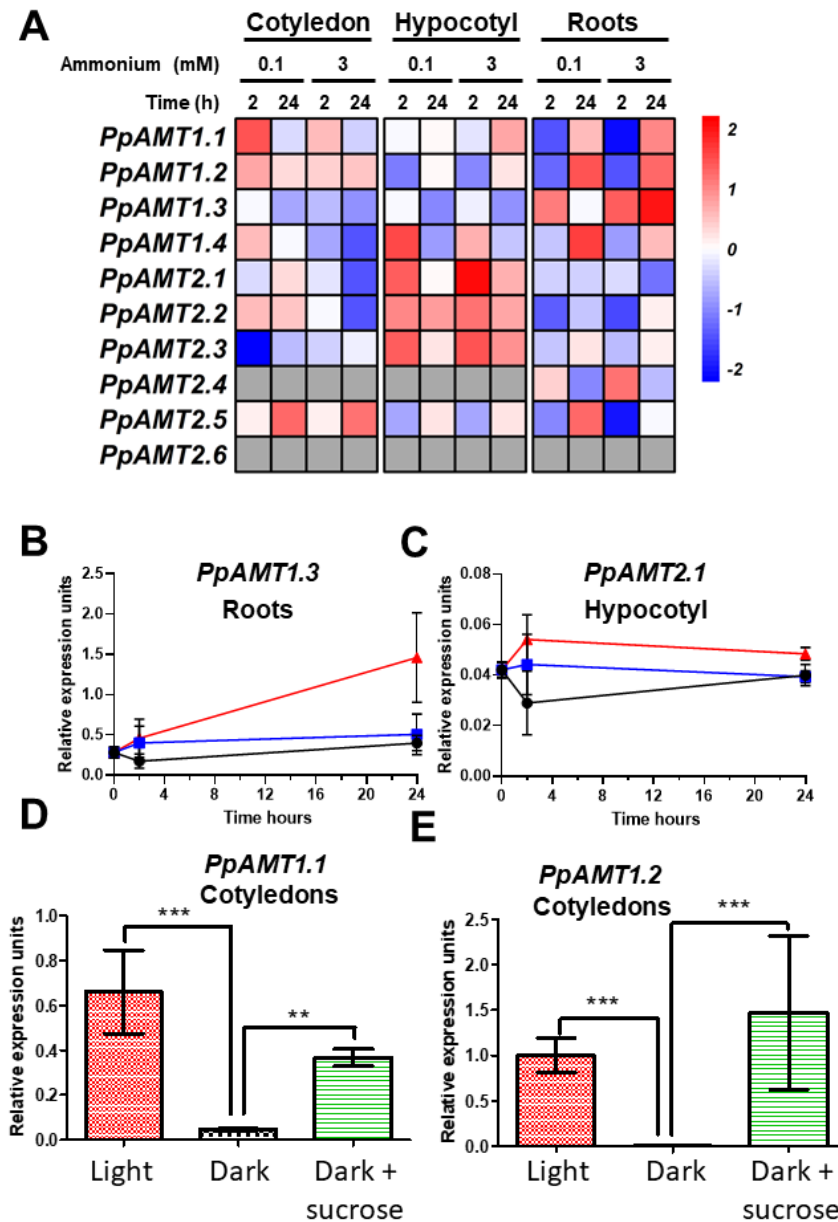


Figure 3.4. Gene expression of AMT transporter gene family in maritime pine under NH_4^+ nutrition. One-month old seedlings were watered with water (control), 0.1 mM NH_4^+ (0.1) and 3 mM NH_4^+ (3). The different organs were harvested 2 h and 24 h after the treatment. **A** Relative expression of AMT genes respect to the control samples. The logFC are presented in each cell of the heatmap. For each gene the logFC values have been scaled. **B** Gene expression profile of *PpAMT1.3* in roots. **C** Gene expression profile of *PpAMT2.1* in hypocotyl. Black lines correspond to control samples, blue lines to 0.1 samples and red lines to the 3 samples. **D** and **E** Gene expression profiles of *PpAMT1.1* and *PpAMT1.2* in different lighting conditions respectively. Red columns correspond to seedlings germinated and maintained in normal photoperiod (light), grey columns to seedlings germinated

and maintained in dark (dark) and green columns to seedlings germinated and maintained in dark and irrigated with 3 mM sucrose (dark+sucrose). Significant differences were determined with a one-way ANOVA (** $P < 0.01$; *** $P < 0.001$). Error bars show SE with $n = 3$.

The *PpAMT1.1*, *PpAMT1.2* expression levels were higher at cotyledons and hypocotyls and *PpAMT1.3* was mainly expressed at roots, as previously described (Castro-Rodríguez *et al.*, 2016) (Figure 3.4 A). *PpAMT1.4* exhibited low expression levels, being slightly larger at the roots (Figure 3.4A). All *PpAMT2* genes showed low transcript levels and *PpAMT2.6* was not detected in the samples examined. *PpAMT2.1* was the one with highest levels of expression in roots and hypocotyls (Figure 3.4A). Transcripts levels in response to NH_4^+ nutrition at different time points were not statistically significant in any case. However, at 24 hours the expression of *PpAMT1.3* increased in response to NH_4^+ nutrition in roots whereas a short-term increase in the levels of *PpAMT2.1* transcript was observed in hypocotyls (Figure 3.4B, C). Thus, the gene expression of *PpAMT1.3* in roots was used to validate the response of the pine seedlings under the nutritional experiments before to make the RNA sequencing.

Since *PpAMT1.1* and *PpAMT1.2* are specifically expressed in the aerial part of the seedlings it was interesting to investigate if these genes are regulated by light. Transcripts levels of *PpAMT1.1* and *PpAMT1.2* were examined at light, dark and dark plus 3 mM sucrose conditions (Figure 3.4D, E). The expression levels of both *PpAMT1* genes dramatically decreased in the cotyledons of the seedlings under dark conditions. When the seedlings under dark conditions were supplemented with 3 mM sucrose, the transcript levels of *PpAMT1.1* were one half of the initial values in light conditions (Figure 3.4D) meanwhile the levels of *PpAMT1.2* transcripts were completely restored (Figure 3.4E).

Tissue-specific dynamics of the root transcriptome in response to NH_4^+ nutrition

According to the expression results of *AMT* genes and mainly focused in *PpAMT1.3* expression profile observed (Figure 3.4B), root tips from seedlings irrigated with 3 mM NH_4^+ and harvested at 24 h were employed to isolate different tissues by LCM (root cap, RC; root meristem, RM; root developing cortex, RDC, and root

developing vessels, RDV) in order to study the local transcriptomic response to NH_4^+ nutrition in maritime pine roots.

The complete differential expression results are shown in the Dataset S3.1. A total of 295 DE transcripts were identified in the RNA-seq analysis, being RDC the tissue with the higher number of DE transcripts (107 upregulated and 70 downregulated), while RDV was the tissue with the lowest response (12 transcripts upregulated and none downregulated) (Figure 3.5). Interestingly, only 2 genes were upregulated, and none was downregulated in all root tissues. Both transcripts are different splicing isoforms from a common gene although there were no identifications for any of the transcripts after a *blastx* search in the nr database.

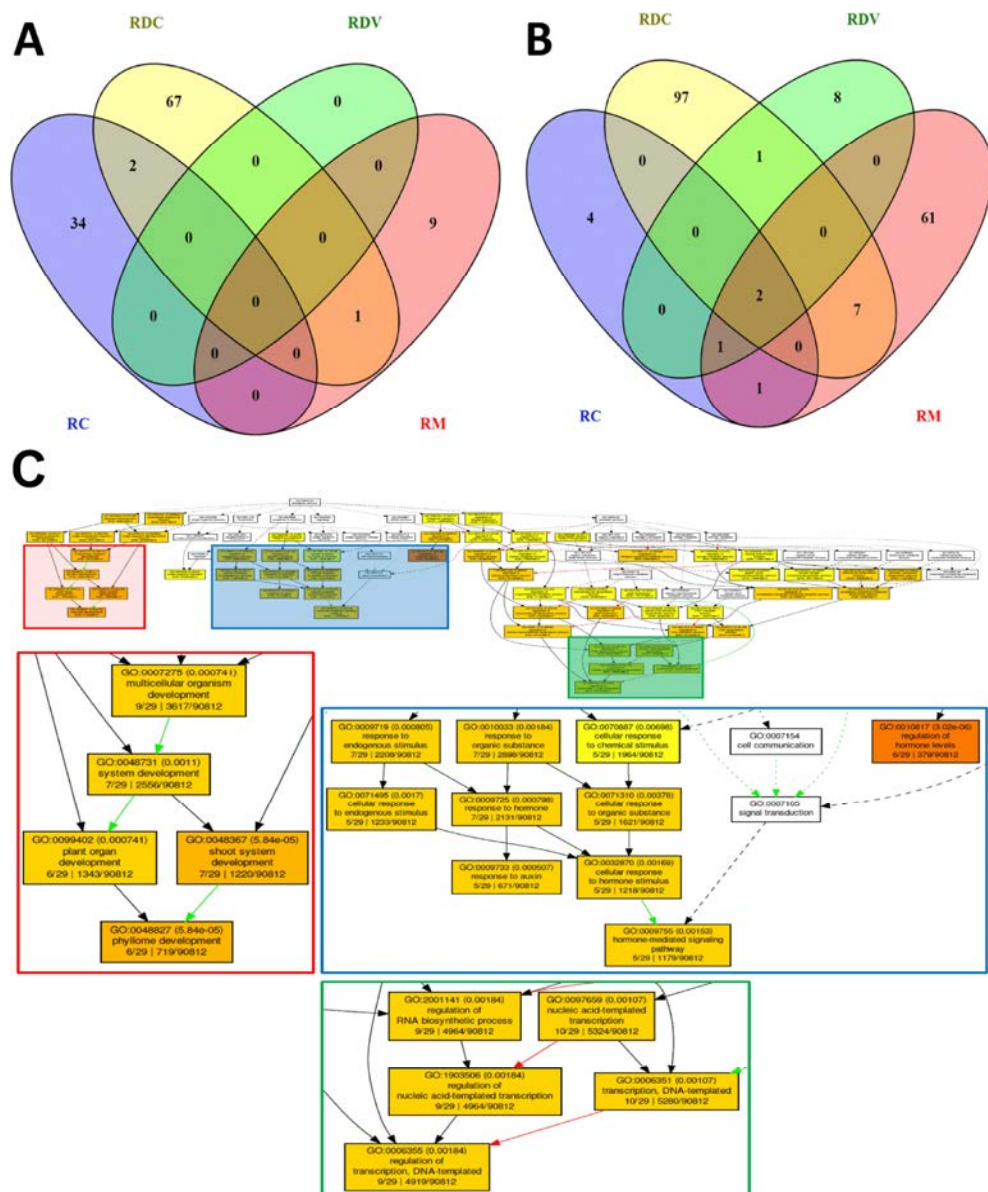


Figure 3.5. Venn diagram of DE transcripts and functional enrichment results in maritime pine root cap tissue (RC). **A.** Venn diagram of down-regulated DE

transcripts from LCM RNA-Seq. **B.** Venn diagram of up-regulated DE transcripts from LCM RNA-Seq. **C.** Functional enrichment of negative differential expressed (DE) transcripts from LCM RNA-Seq. Three biological process related to plant development (red box), hormone signalling pathway (blue box) and regulation of transcription (green box) are highlighted. RC: root cap; RM: root meristem; RDC:) root developing cortex; RDV: root developing vessels.

A summary of the main functional data derived from the RNA-seq of LCM samples is presented in the Figure 3.6 and Dataset S3.2. The complete results of Singular Enrichment Analysis (SEA) analyses are shown in Dataset S3.2. For BP category of downregulated DE transcripts in RDC only the “cytoskeleton organization” term (GO:0007010) was significant. Nevertheless, numerous enriched functions were significant for the upregulated transcripts in this tissue as those involved in defense responses such as “induction of programmed cell death” (GO:0012502), “chitin catabolic process” (GO:0006032), “defense response to bacterium” (GO:0042742) and fungus (GO:0050832), and “cell wall macromolecule catabolic process” (GO:0016998) but also those involved in hormone responses such as “response to abscisic acid” (GO:0009737). In the upregulated transcripts of RM, it was also observed a similar enrichment of the defense responses as found in RDC. Interestingly, RC was the tissue with more complex results revealing downregulation of developmental process, hormone pathways and transcription processes (Figures 3.5 and 3.6). It must be highlighted that 10 of the total 35 significant downregulated transcripts in RC were transcription factors. It was not possible to get functional enrichment results from DE transcripts neither upregulated nor downregulated from RDV due to the low number of differentially expressed transcripts.

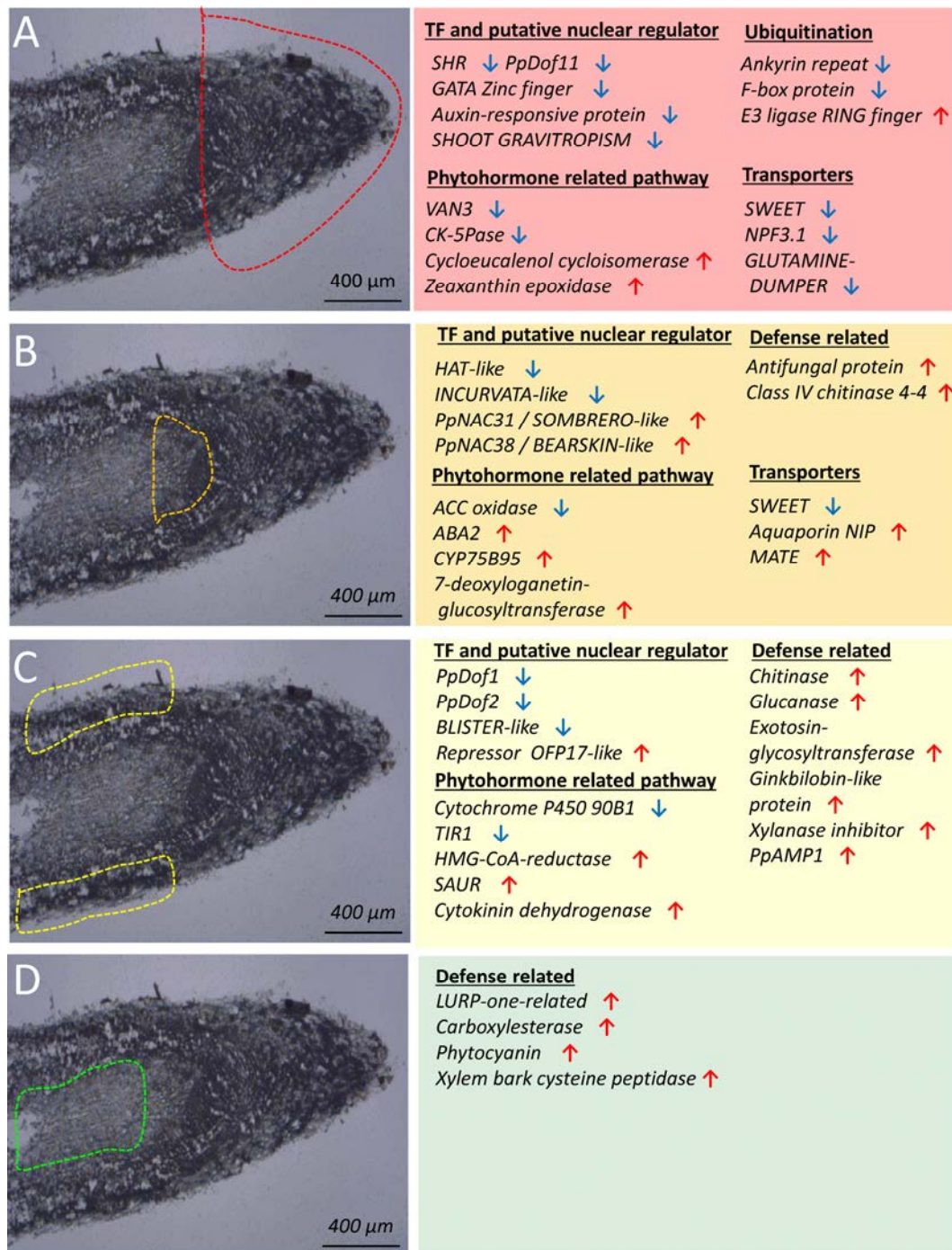
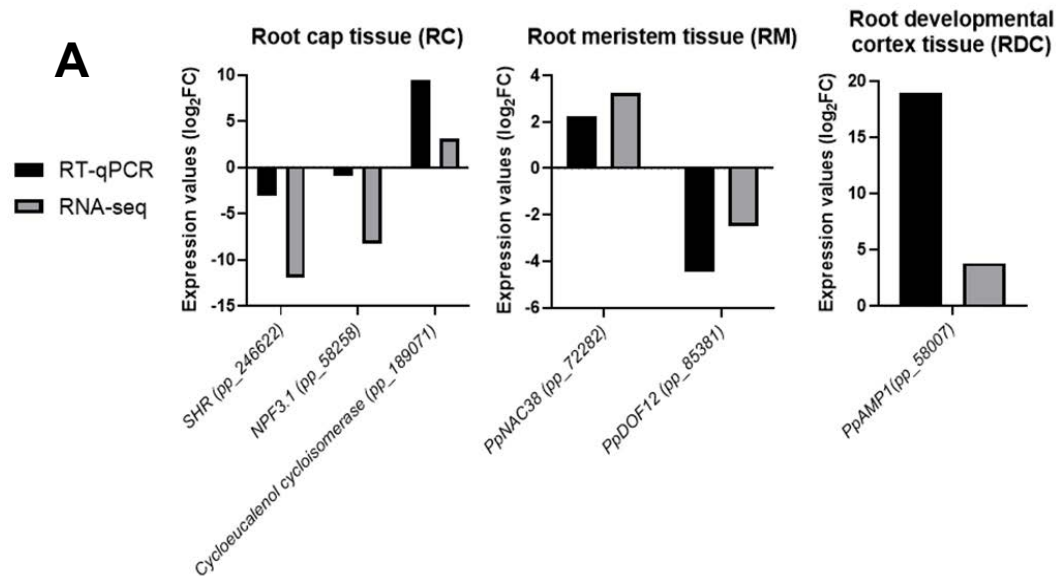


Figure 3.6. Resume of the main functional results obtained in the LCM RNA-Seq analysis. Functions and DE transcripts in (A) the root cap (RC), (B) root meristem (RM), (C) root developing cortex (RDC) and (D) root developing vessels (RDV). Blue arrows indicate downregulated transcripts, red arrows upregulated ones.

RT-qPCR analyses verification

In order to validate the LCM transcriptomic results, RT-qPCRs of *SHR* (pp_246622), *PpNAC38* (pp_72282), *PpAMP1* (pp_58007), *PpNPF3.1* (pp_58258) and the coding transcript for a cycloeucaleenol cycloisomerase enzyme (pp_189071) were performed. The same gene expression trend was observed when RT-qPCR and RNA-seq results were compared (Figure 3.7A). Analyzing expression values of selected DE across all tissues it was observed that *SHR* and the cycloeucaleenol cycloisomerase transcript expression were detected only in the control RC samples according to LCM RNA-seq results (Dataset 3.1) being the *SHR* downregulated and the cycloeucaleenol cycloisomerase upregulated. The expression profiles observed for *PpNAC38*, *PpAMP1* and *PpNPF3.1* are in line with LCM RNA-seq results (Dataset 3.1). In LCM RNA-seq results (Dataset 3.1) *PpNAC38*, showed its upregulation in all tissues except in RC what agrees with RT-qPCR results (Figure 3.7). The same tendency was observed for *PpAMP1* which expression levels showed to increase under NH₄⁺ presence (Figure 3.7 and Dataset 3.1). In the case of *PpNPF3.1*, RT-qPCR results (Figure 3.7) agrees with LCM RNA-seq results (Dataset 3.1) in RC, RM and RDV. However, its expression levels were not able to be detected in RDC where LCM RNA-seq results showed a decrease in its expression level (Dataset 3.1).



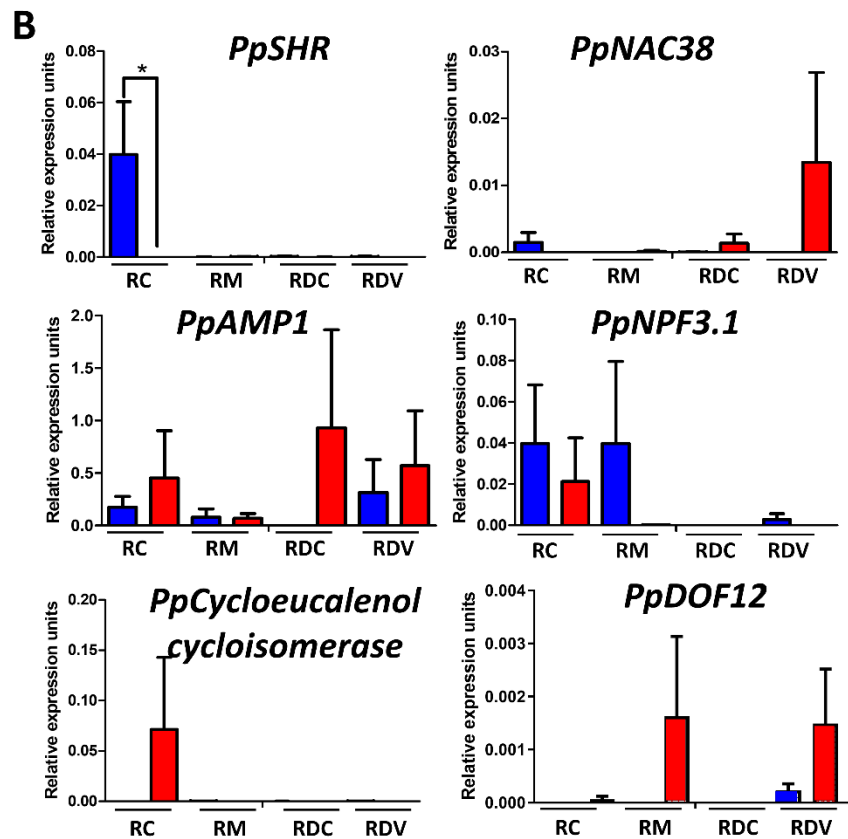


Figure 3.7. A. Comparison between RT-qPCR and RNA-seq results from identified DE transcripts in their respective tissue. **B.** RT-qPCR results from identified DE transcripts at LCM transcriptomic level in all root tip tissues. Blue columns correspond to control samples. Red columns correspond to samples supplied with 3 mM NH₄⁺. Significant differences were determined with a t-test (* *P*-value < 0.05).

Transcription factors in developmental processes

Additionally to the SEA analyses, the DE transcripts were individually analyzed looking for different kind of regulators such as transcription factors (TF), transcripts involved in phytohormone response or in ubiquitination. From a total of 295 DE transcripts, 31 TFs were identified (Dataset S3.1) in the root tip in response to NH₄⁺ nutrition. All the 10 TFs identified in RC were repressed in the presence of NH₄⁺. However, in RM and RDC 6 and 4 TF transcripts were downregulated while 5 and 6 TF transcripts were upregulated, respectively.

Interestingly, it was observed a strong downregulation of *SHORT ROOT* (SHR) in RC *INCURVATA-like* and Homeobox-leucine zipper protein *HAT-like* in RM both involved in meristem-developmental regulation, and also the TF identified in RC

as Zinc finger *C2H2 SHOOT GRAVITROPISM* related to gravitropism response. *SHR* was the most highly repressed TF (-11 logFC). Furthermore, it was observed the induction of two transcriptional repressors of different plant developmental aspects (3 logFC), *PpNAC31* identified as a *SOMBRERO-like NAC* TF and an *OFPI7-like* repressor, which change in expression pattern were localized in RM and RDC, respectively. In addition, novel TFs in maritime pine were identified. Two of them belong to *DOF*-family and were named as *PpDOF11* and *PpDOF12* being both down-regulated in RC and RM respectively. Phylogenetic analysis of these two new *DOF*-type TFs revealed that *PpDOF11* is grouped with *AtDOF1.4* (*AT1G28310*) and *OsDOF7.2* (*LOC_Os07g32510*) in subfamily E and *PpDOF12* is grouped with members of the subfamily A of *Pinus pinaster*: *PpDOF4*, *PpDOF7*, *PpDOF8* and *PpDOF10* (Figure 3.8, Table S3.1).

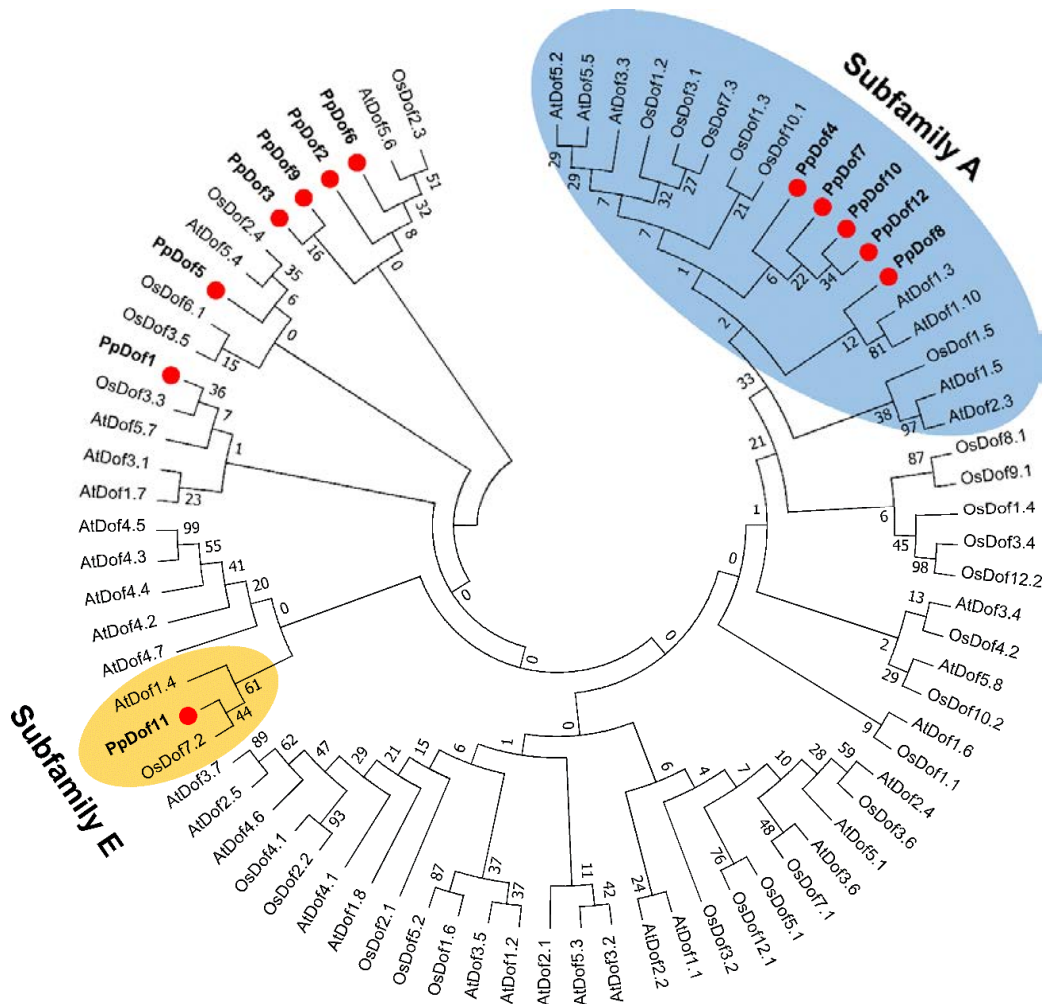


Figure 3.8. Phylogenetic tree of Dof transcription factor family in maritime pine, Arabidopsis and rice. The protein sequences employed to infer the phylogenetic tree are presented in the Table S3.1. The protein sequence alignment was made with

Muscle (Edgar, 2004). The evolutionary history was inferred using the Neighbor-Joining method (Saitou and Nei, 1987). The bootstrap consensus tree inferred from 1000 replicates is taken to represent the evolutionary history of the taxa analyzed (Felsenstein, 1985). Branches corresponding to partitions reproduced in less than 50% bootstrap replicates are collapsed. The evolutionary distances were computed using the Dayhoff matrix-based method (Schwarz and Dayhoff, 1979) and are in the units of the number of amino acid substitutions per site. The analysis involved 78 amino acid sequences. All positions containing gaps and missing data were eliminated. There were a total of 54 positions in the final dataset mainly corresponding to the Dof domain. Evolutionary analyses were conducted in MEGA7 (Kumar *et al.*, 2016). Abbreviations: At, *Arabidopsis thaliana*; Pp, *Pinus pinaster*; Os, *Oryza sativa*.

Additionally, it was identified a member of the NAC-family (*PpNAC38*) that was up-regulated in RM tissue. This TF has homology to BEARSKIN1 (AT1G33280) (e-value: $7e-96$) and BEARSKIN2 (AT4G10350) (e-value: $3e-97$) of *Arabidopsis thaliana* and it is framed within the NAC subfamily C (Figure 3.9).

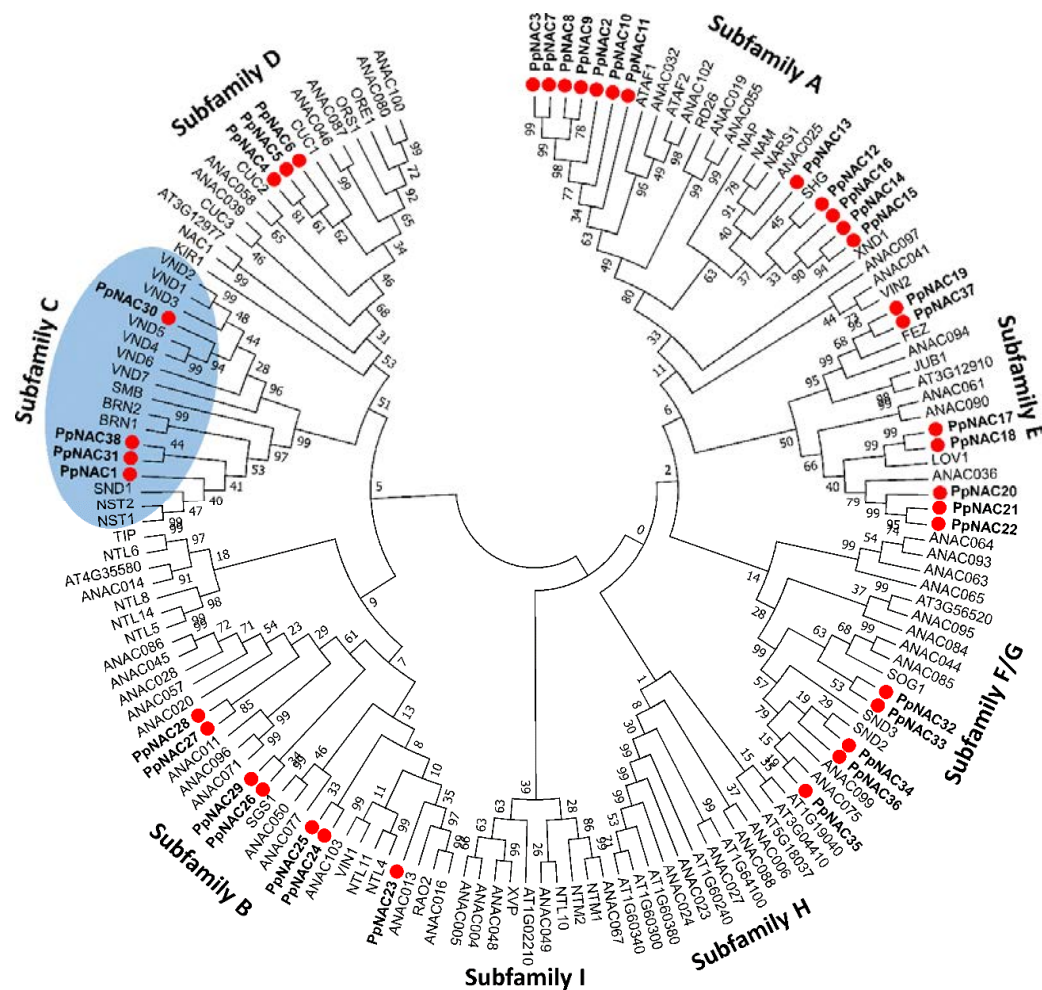


Figure 3.9. Phylogenetic tree of NAC transcription factor family in maritime pine and Arabidopsis. The protein sequences employed to infer the phylogenetic tree are presented in the Table S3.2. The protein sequence alignment was made with Muscle (Edgar, 2004). The evolutionary history was inferred using the Neighbor-Joining method (Saitou and Nei, 1987). The bootstrap consensus tree inferred from 1000 replicates is taken to represent the evolutionary history of the taxa analyzed (Felsenstein, 1985). Branches corresponding to partitions reproduced in less than 50% bootstrap replicates are collapsed. The evolutionary distances were computed using the Dayhoff matrix-based method (Schwarz and Dayhoff, 1979) and are in the units of the number of amino acid substitutions per site. The analysis involved 151 amino acid sequences. All positions with less than 80% site coverage were eliminated. That is, fewer than 20% alignment gaps, missing data, and ambiguous bases were allowed at any position. There were 261 positions in the final dataset. Evolutionary analyses were conducted in MEGA7 (Kumar *et al.*, 2016).

Phytohormone-related genes

Phytohormones play crucial roles in plant growth, development and response to biotic and abiotic stimulus. Twenty-six DE transcripts related to phytohormone pathways were identified of which 19 were upregulated and 7 were downregulated (Dataset S3.1). Cytokinin-related genes were the second most represented phytohormone-related transcripts; a strong repression of *cytokinin riboside 5'-monophosphate phosphoribohydrolase* (*pp_222714*) (-6.9 logFC), a cytokinin-activating enzyme, was observed in RC. But also, the upregulation of a *cytokinin dehydrogenase* (*pp_215376*), an enzyme that inactivates cytokinins was observed in RDC. The repression of transcripts related to brassinosteroids (BRs) and ethylene (ET) biosynthesis were also found, e.g. *cytochrome P450 90B1* (*pp_247190*) in RDC and *ACC oxidase* (*pp_202153*) in RM. In addition, transcripts related to gibberelins (GAs) response and abscisic acid (ABA) biosynthesis were upregulated, such as a *GASA gibberellin regulated cysteine rich protein* (*pp_111379*) in RDC and two *ABA2* coding transcripts with putative different subcellular localizations, that might be involved in ABA biosynthesis (*pp_198945*, mitochondrial, and *pp_209084*, cytosol) in RM and RDC, respectively.

Most of DE transcripts were related to auxin (IAA), some interesting examples are the downregulation of transcripts required to PIN transporters localization like *VAN3/FKD2*, *Auxin canal/PH2* (*pp_60103*) in RC and the upregulation of a *cycloeucaleanol cycloisomerase* (*pp_189071*) in RC, related with PIN transporters endocytosis. In addition, in RDC it was observed the repression of the auxin receptor *TIR1/AFB* (*pp_238715*) and a transcript for a *sulfotransferase* (*pp_208269*) that is similar to *SULT202B1* of *Arabidopsis thaliana* (*AT3G45070*) (e-value: 5e-72).

Ubiquitination related genes

Transcripts related to ubiquitination process were differentially expressed only in RC and RDC tissues. Expression values of the DE transcripts were more pronounced in RC compared to those observed in RDC (Dataset S3.1). In RC, an *E3 ubiquitin-protein ligase RING finger* (*pp_209433*) was markedly induced (9 logFC) and two possible *E3 ubiquitin ligase* coding transcripts were strongly repressed; one *ankyrin repeat protein* (*pp_233357*) and one *F-box protein* (*pp_87887*). In RDC, transcripts encoding for different *E3 ubiquitin-protein ligase*

Chapter 3. Results

RING finger (pp_222774) and a possible *E3 ubiquitin ligase ankyrin repeat protein* (pp_79846) were downregulated, while a transcript coding a putative *ubiquitin ligase F-box protein* was upregulated.

Defense-related genes

Related to defense response, transcripts for a nuclear localized *VQ motif containing protein* and *NPR1 interacting protein* were upregulated in RDC. Interestingly, the main defense response was observed in RDC, with the upregulation of a number of transcripts associated to antimicrobial activity (3 logFC) such as *Class I, II and IV chitinases* (pp_117806 and pp_72600pp_117812, pp_117813, pp_117816, pp_146696, pp_146697, pp_146699, pp_146700), *ginkbilobin-2 antifungal proteins* (pp_134773, pp_134774, pp_134777, pp_134778 and pp_252648), and small protein coding transcripts related to defense like *embryo-abundant protein, EAP* (pp_252647) and *antimicrobial peptide 1, AMP1* (pp_58007) as is shown in Dataset S3.1.

Discussion

Many plant species prefer nitrate over NH_4^+ as a source of inorganic N (Esteban *et al.*, 2016). In contrast, conifers and particularly maritime pine prefer NH_4^+ over nitrate (Warren and Adams, 2002; Ortigosa *et al.*, 2020). However, little is known about the effect of NH_4^+ on developmental processes and its potential action as signaling molecule in these species. In the present work, the root transcriptomic response to NH_4^+ nutrition has been studied in maritime pine.

The large amount of arginine and asparagine detected in pine seedlings (Figure 3.1) are coherent with those previously described (Cañas *et al.*, 2008) and reinforce the idea that ammonia acts more as a signal than as a nutrient at short time as pointed out Liu and von Wirén (2017) at least in this seedling stage.

Ammonium transporters family (AMTs)

To find a reference gene with an expression controlled by NH_4^+ nutrition the gene expression profiles of the AMT gene family were analyzed. First, the identification of new AMT encoded genes was carried out (*PpAMT1.4*, *PpAMT2.4*, *PpAMT2.5* and *PpAMT2.6*).

According to the expression characterization of the whole AMT family under NH_4^+ supply, the most responsive AMT gene was *PpAMT1.3* in roots (Figure 3.3 and Figure 3.4A). The transporter coding by *PpAMT1.3* was proposed to play an essential role in in root primary NH_4^+ uptake in maritime pine (Castro-Rodríguez *et al.*, 2016). In fact, there were no general changes in the expression in roots of the set of AMT genes, except for *PpAMT1.3* suggesting that the rest of AMT genes could be involved in NH_4^+ transport in determinate processes, tissues and developmental stages. This seems to agree with previous results where the NH_4^+ uptake in maritime pine roots was not restricted in short times (Ortigosa *et al.*, 2020). Thus, the gene expression analysis of AMT family pointed some interesting data on the potential roles of some members of the family. In pine seedlings, *PpAMT1.1* and *PpAMT1.2* were mainly expressed in cotyledons according with previous findings in maritime pine (Castro-Rodríguez *et al.*, 2016). Results shown in Figure 3.4D,E suggest that the expression of *PpAMT1.1* and *PpAMT1.2* is regulated by light and photosynthetic products. This is consistent with previous works demonstrating that *AtAMT1.1* (*AT4G13510*), *AtAMT1.2* (*AT1G64780*) and

AtAMT1.3 (*AT3G24300*) showed diurnal variation in their expression (Gazzarrini *et al.*, 1999). The light-dependent regulation is plausible because it is well known that to achieve NH_4^+ assimilation, a proper carbon skeleton flux, coming from photosynthetic metabolism is required (Vega-Mas *et al.*, 2019). All these data might evidence a tiny coordination of maritime pine *AMT* genes in order to adequate a proper NH_4^+ transport from roots to shoots. Functional complementation in *Arabidopsis* *AMT* mutants with pine genes could serve to further support their regulation and their potential roles in the control of NH_4^+ levels observed in needles of the seedlings exposed to NH_4^+ nutrition for a long-term (Ortigosa *et al.*, 2020).

Root transcriptome dynamics in response to NH_4^+ supply

To characterize and study the local transcriptomic response of maritime pine root tip to NH_4^+ supply, a low-input RNA-seq from LCM isolated samples was performed. The results of the *PpAMT* genes expression suggest a limited response at short times to the NH_4^+ supply in maritime pine entire roots, although the most responsive experimental condition was the exposure to a concentration of 3 mM for 24 hours (Figure 3.4). This condition was selected to study the local response to NH_4^+ in maritime pine root tips. The transcriptomic analysis of selected root tip tissues isolated by LCM suggest that NH_4^+ nutrition has a profound effect in root development (Figures 3.6 and 3.10, Dataset S3.1).

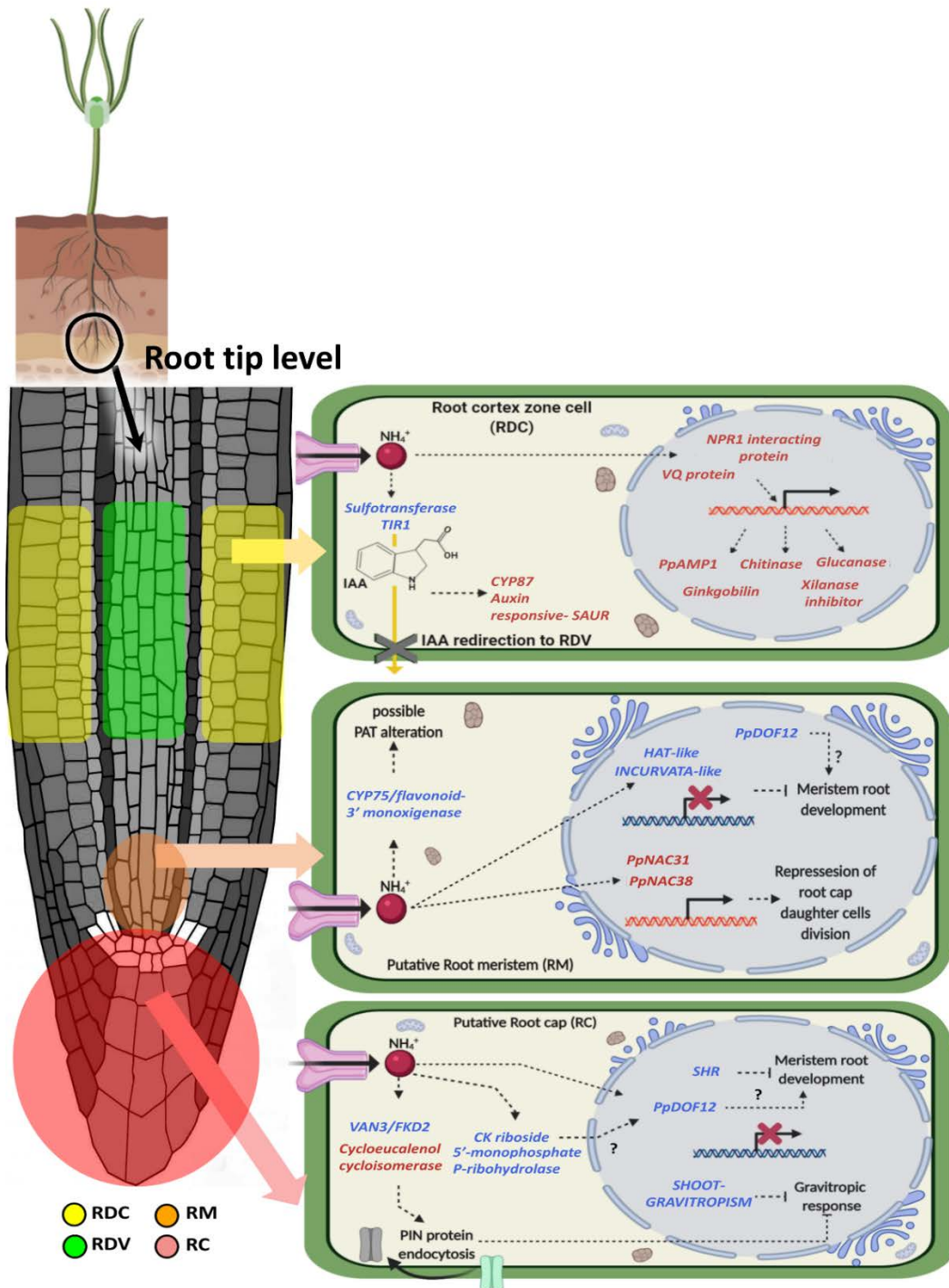


Figure 3.10. Schematic representation of transcriptional response induced by NH_4^+ supply in maritime pine seedling roots at short times. Transcripts in red letters are upregulated. Transcripts in blue letters are downregulated. The root tip tissues are the root cap (RC) root meristem (RM), root developing cortex (RDC) and root developing vessels (RDV).

NH_4^+ is well known to trigger defense response *in planta* (Patterson *et al.*, 2010; Fernández-Crespo *et al.*, 2012; Sun *et al.*, 2017; Ravazzolo *et al.*, 2020). The main response at RDC tissue involved defense related genes, this might be linked to the localized expression observed in the root cortex as suggest transcriptomic data in RDC (Figures 3.5C and 3.10, Dataset S3.1). The upregulation of the *antimicrobial peptide 1 (AMP1)* and *embryo abundant protein (EAP)* transcripts in RDC is consistent with the results previously published on maritime pine roots (Canales *et al.*, 2010). Moreover, the repression of *glutamine dumper (pp_143492 in RC)* and *SWEET transporters (pp_154562 in RC and pp_148437 in RM)* are also consistent to previous studies in maritime pine roots (Canales *et al.*, 2010). Additionally to transcripts coding proteins directly involved in defense, several regulators of this kind of response were also upregulated, for example a transcript coding for a *VQ motif containing protein (pp_194539)* and another one coding for a *NPR1-interacting protein (pp_117037)* in RDC (Figure 3.10, Dataset S3.1). Recently, it has been described that the VQ motif-containing proteins act as regulatory proteins interacting with WRKY TFs (Garrido-Gala *et al.*, 2019). In *Arabidopsis*, NH_4^+ induces expression changes of several WRKY TFs (Patterson *et al.*, 2010). Several of these WRKY TFs have been linked to the regulation of defense responses in plants (Pandey and Somssich, 2009; Rushton *et al.*, 2010; Wang *et al.*, 2020). In the same way, NPR1 (NONEXPRESSOR OF PR GENES1, AT1G64280) plays an important role in acquired and induced systemic resistance (Pieterse *et al.*, 1998). NPR1 was described to be a key regulator of plant defense signaling network, mediating crosstalk between salicylic acid and ethylene/ jasmonic acid responses (Backer *et al.*, 2019). Furthermore, WRKY TFs are also regulated by NPR1-dependent manner (Yu *et al.*, 2001). Additionally, ubiquitination has been described to mediate NPR1 turnover by ubiquitin ligase action (Spoel *et al.*, 2009). This could be in line with the induction of a NPR1-interacting protein because ubiquitination-related transcripts are down-regulated in RDC (Dataset S3.1). Based on these findings, the highly represented defense response observed in RDC, a cortical tissue, might be responsible of the defense response observed in roots because the entire root is mostly composed by the cortical and vascular tissues (Glimn-Lacy and Kaufman, 2006).

Transcription factors involved in maritime pine root development

Different studies suggest that RSA principally targets root system processes such as root elongation, root gravitropism and lateral root branching, appearing to occur in the root tip (Li *et al.*, 2014). It has been described that NH_4^+ alters RSA by root elongation inhibition and stimulating lateral root branching (Liu & von Wirén, 2017). In maritime pine seedlings, long-term N nutrition drives phenotypic changes on RSA, NH_4^+ supplied plants exhibited more biomass than nitrate-fed ones due to the increase in branched roots (Ortigosa *et al.*, 2020). In RC tissue, NH_4^+ caused a strong repression of *SHORT-ROOT (SHR)* (*pp_246622*), a GRAS-type TF involved in the regulation and coordination of root development including phloem differentiation (Helariutta *et al.*, 2000; Zhou *et al.*, 2010; Aichinger *et al.*, 2012; Kim *et al.*, 2020). Another group of TFs that control proper phloem development are DOFs, specifically those included in the subfamily named PHLOEM EARLY DOFs (PEARs) (Miyashima *et al.*, 2019). In the root tip transcriptomic analyses, four different maritime pine DOFs were significantly downregulated: *PpDOF11* (*pp_58878*) and *PpDOF12* (*pp_85381*) in RC and RM tissues respectively, and *PpDOF1* and *PpDOF2* in RDC. These TFs might play roles in developmental processes on the root meristem and the vascular zone according to the expression patterns observed (Figures 3.11 and 3.12).

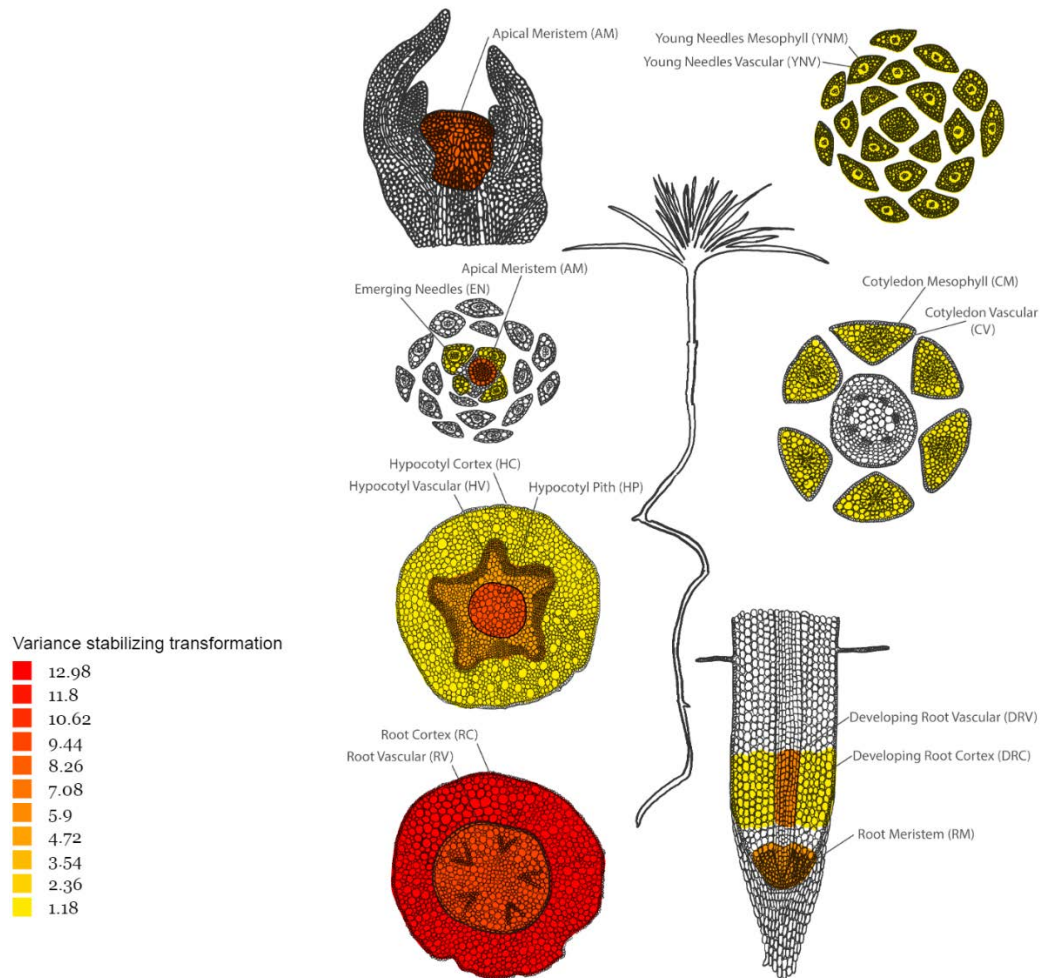


Figure S3.11. Expression atlas of *PpDOF11* in the tissues of one-month old seedlings (Cañas *et al.*, 2017).

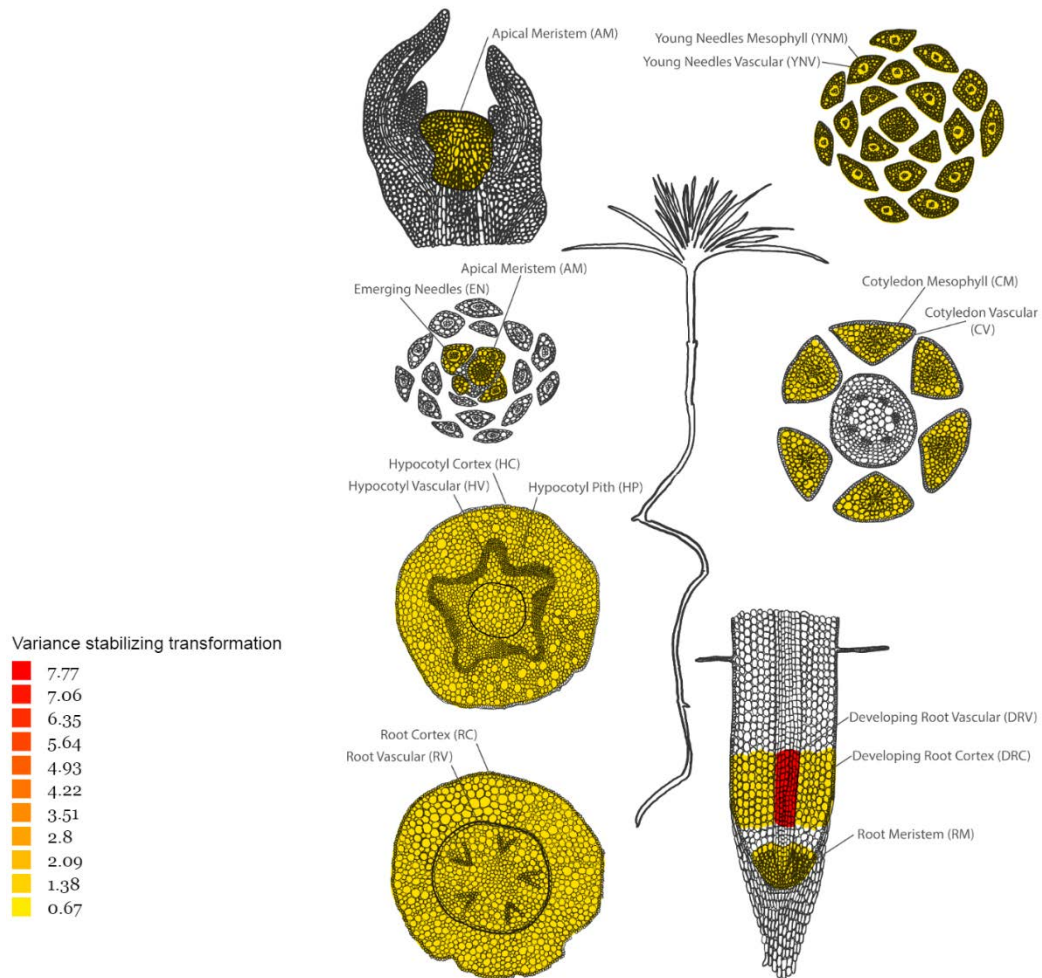


Figure S3.12. Expression atlas of *PpDOF12* in the tissues of one-month old seedlings (Cañas *et al.*, 2017).

In addition, Homeobox-leucine zipper (HD-Zip) and NAC-domain TFs also take part in the meristem development (Ochando *et al.*, 2006; Willemsen *et al.*, 2008; Bennett *et al.*, 2010, Kondo *et al.*, 2016). Two HD-Zip coding transcripts identified as *HAT-like* (*pp_141831*) and *INCURVATA-like* (*pp_85012*) that belong HD-Zip III class (Turchi *et al.*, 2013) were downregulated in RM tissue. In *Arabidopsis* several HATs play important roles in development (Aoyama *et al.*, 1995; Carlsbecker *et al.*, 2010; Roodbarkelari and Groot, 2017). Similar aspects have been observed for *INCURVATA* TFs, related to the regulation of meristem and procambial and vascular tissues maintenance and/or formation (Green *et al.*, 2005; Prigge *et al.*, 2005; Ochando *et al.*, 2006). Also in RM, the upregulation of two NACs TFs related to *SOMBRERO* (*SMB*) and *BEARSKIN* (*BRN*) (*PpNAC31* and *PpNAC38*, respectively) (Dataset S3.1, Table S3.2, Figure 3.9) is consistent with

previous GUS reporter analyses indicating that the expression patterns of *SMB*, *BRN1* and *BRN2* largely overlap in *Arabidopsis* roots (Bennett *et al.*, 2010). *SMB* has been described to repress stem cell-like divisions in the root cap daughter cells (Willemsen *et al.*, 2008; Bennet *et al.*, 2014; Kamiya *et al.*, 2016) and together with *BRN1* and *BRN2* regulates cellular maturation of root cap in *Arabidopsis* (Bennett *et al.*, 2010). The induction of *BRN* and *SMB* orthologues could reflect that under the presence of enough N there is no need to promote principal root elongation and growing in depth since the nutritional conditions are favorable.

Another well documented effect caused by NH_4^+ is the inhibition of root gravitropism which has been linked with the decrease of the *PIN2* auxin exporter expression (Liu *et al.*, 2013; Zou *et al.*, 2012; 2013). Interestingly, the upregulation of a transcript coding for a *cycloeucaleanol cycloisomerase* (*pp_189071*) in RC samples (Dataset S3.1), which is required for *PIN2* endocytosis (Men *et al.*, 2008) (Figure 3.7). This could suppose the molecular mechanism by which NH_4^+ affects *PIN2* levels and could be related to the gravitropic response and lateral root formation (Zou *et al.*, 2013). Additionally, it should be mentioned the downregulation of a zinc finger *C2H2 SHOOT GRAVITROPISM* (*pp_174625*) in the same tissue, RC (Figure 3.7, Dataset S3.1). Furthermore, it is tempting to hypothesize that in gymnosperms *SHOOT GRAVITROPISM* could be involved in the regulation of the amyloplast accumulation in graviperceptive cells and/or in the establishment of auxin gradients through the regulation of auxin biosynthesis and/or transport similarly to that occurs in *Arabidopsis* (Yamauchi *et al.*, 1997; Morita *et al.*, 2006; Tanimoto *et al.*, 2008).

Hormones and ubiquitin ligase-related genes in root developmental processes

In parallel to *SHR* pathway, auxin also takes an important role in the maintenance and cell fate of root stem cell niche (Zhou *et al.*, 2010; Bishopp *et al.*, 2011). Alteration in auxin transport by *PIN* proteins is thought to be one of the signals (Kim *et al.*, 2020). The results presented in this work are consistent with this idea because of the strong repression of *VAN3/PH2/FKD2* coding transcript in RC and RM (Dataset S3.1). In *Arabidopsis*, *FKD* genes (*FKD1* and *FKD2*, *AT3G63300* and *AT5G13300*, respectively) encode redundant PH domain proteins that respond to auxin and are crucial in vascular leaf pattern formation by the proper *PIN* transporters localization (Steynen and Schultz, 2003; Hou *et al.*, 2010). This

evidence suggests that an alteration in auxin transport is taking place in pine roots. In addition, a transcript upregulated in RM (*pp_203884*, Dataset S3.1) encodes a *CYP75/flavonoid 3'-monooxygenase*, which is an enzyme that catalyzes the 3'-hydroxylation of flavonoids, e.g. dihydrokaempferol into dihydroquercetin (Bark *et al.*, 2011). Flavonoids are known to affect polar auxin transport (PAT) (Peer and Murphy, 2007; Yin *et al.*, 2014) and, especially quercetin, down-regulate *SHR* and *HD-ZIP III* (Franco *et al.*, 2015). In RDC, the transcript levels of a *TIR1 auxin receptor* and a *sulfotransferase* were downregulated (Dataset S3.1). Previous reports showed that sulphated flavonoids revert the auxin inhibition efflux caused by flavonoids (Ananvoranich *et al.*, 1994; Teles *et al.*, 2018). Additionally, auxin can promote xylem related *HD-ZIP II* and *HD-ZIP III* transcription (Sessa *et al.*, 2018), which could relate the repression of the *HAT-like* and *INCURVATA-like* transcription factors with the alteration of auxin gradient in the root tip of maritime pine.

The response to auxin is triggered through targeted degradation of the transcriptional *AUX/IAA* repressors by the F-box ubiquitin E3 ligase protein SCF^{TIR1/AFB} (Gray *et al.*, 2001; Salehin *et al.*, 2015). The strong repression of a transcript coding a possible ubiquitin-ligase F-box protein in RC (Dataset S3.1) could be part of the molecular mechanism of the suggested polar auxin transport alteration, concordantly, there were no changes in the expression of the *AUX/IAA* repressors.

Auxin redirecting process from the QC region to the root elongation zone through the root cortex (Michniewicz *et al.*, 2007) is probably blocked according to our data in RC, RM and RDC (Figure 3.7). In this sense, the changes triggered by NH_4^+ and linked to auxin do not seem to involve the induction/repression of genes coding proteins involved in the biosynthesis or catabolism of this phytohormone.

Moreover, our results suggest that cytokinin (CK) activation does not take place according to the strong repression of a coding transcript for a *cytokinin riboside 5'-monophosphate phosphoribohydrolase* (*pp_222714*) in RC samples, which activates CK and has been related to control shoot meristem maintenance in rice (Kuroha *et al.*, 2009). This is also synchronized with the induction of a transcript coding for a *cytokinin dehydrogenase* (*pp_215376*) in RDC (Dataset S3.1), involved in CKs degradation (Werner *et al.*, 2003), and the repression of different *DOF* TFs (Dataset S3.1) (Figure 3.10). CKs have been highlighted as regulators of

procambial cell proliferation (Mähönen *et al.*, 2006; Bishopp *et al.*, 2011; De Rybel *et al.*, 2014). CK signaling promotes the expression of several *PEAR* (*DOF*) factors, (Mishayima *et al.*, 2019) that induce cell proliferation around protophloem-sieve element (PSE) cell files forming an organizer proximal to QC (Mishayima *et al.*, 2019). These findings suggest that NH_4^+ is affecting CK homeostasis related to vascular development of pine roots.

Gibberelins (GAs) also have been reported to be important in root meristem development (Ubeda-Tomás *et al.*, 2009). In *Arabidopsis*, the NPF3.1 transporter mediates GAs transport under N deficiency (David *et al.*, 2016) and the maritime pine transcript for the *NPF3.1* transporter (*pp_58258*) was downregulated in RC (Dataset S3.1). The repression of *NPF3.1* could be another aspect pointing out the importance of hormones affecting root meristem development, according to the TFs repressed in RC (Figure 3.7, Dataset S3.1).

ABA and ethylene have been also reported to be involved in NH_4^+ -responsive pathways in *Arabidopsis* (Li *et al.*, 2014). A recent work in rice demonstrates that endogenous ABA content alleviates NH_4^+ rice toxicity by the regulation of the SAPK9–bZIP20 pathway, which promotes NH_4^+ assimilation by the stimulation of the GS/GOGAT cycle and the enhance of antioxidant activity by boosting superoxide dismutase (SOD), ascorbate peroxidase (APX) and catalase (CAT) activities (Sun *et al.*, 2020a). The upregulation of several transcripts encoding ABA2 enzymes involved in ABA biosynthesis was observed in RM and RDC, and also two putative ABA induced TFs in RM, indicating that ABA could be involved in the maritime pine NH_4^+ response (Dataset S3.1). The repression of a *BLISTER-like* transcript (*pp_170664*) in RDC point out that glutathione-ascorbate cycle is not operative in the presence of NH_4^+ . *BLISTER* is a TF involved in the increase of ascorbate levels (Purdy *et al.*, 2011). In fact, transcripts variants coding for two different *L-gulonolactone oxidases* (e.g. *pp_183087* and *pp_234650*), the enzyme that produces ascorbate, were down-regulated in RC and RDC (Dataset S3.1). These results are consistent with the levels of oxidized glutathione (GSSG) observed under long term NH_4^+ supply (Ortigosa *et al.*, 2020). Taken together, these findings suggest that pine, as a gymnosperm with a high NH_4^+ tolerance, could present an alternative mechanism for the elimination of ROS. One possibility would implicate *glutathione-S-transferases* (*GSTs*) enzymes that are induced at 24 hours, because it is known that *GSTs* can intervene in different aspects such as the

mitigation of oxidative stress, detoxification processes and hormone transport (Gullner *et al.*, 2018). Regarding ethylene (ET), a transcript coding for an *ACC oxidase (ACO)* was found to be repressed in RM, what is consistent with the downregulation of *BLISTER-like* transcript since one of the *ACO* reaction substrates is ascorbate (Dataset S3.1). Interestingly, in rice roots have been described that ET is involved in NH_4^+ response by the induction of several *ethylene response factors (ERFs)* (Sun *et al.*, 2017).



Conclusions

The study of how the root of plants respond to NH_4^+ nutrition is complex task since it is a nutrient that can be toxic when supplied in excess. The results presented in this work have identified responses related with defense and phytohormone signaling but also revealed a possible molecular regulation mediated by NH_4^+ for the modification of root development and architecture (Figure 3.10).

It would be interesting to further study the extensive defense response exhibited by maritime pine roots under NH_4^+ supply (Figure 3.10) since pines have long life cycles and the modulation of the defensive response could be very useful for the viability of the silviculture of this species, especially during the seedling stage when the plant is more vulnerable (Losso *et al.*, 2019).

The expression profiles of genes related with hormones decipher the molecular mechanisms underlying changes in RSA phenotype previously observed in maritime pine roots under long-term NH_4^+ supply (Ortigosa *et al.*, 2020). Beside this, the study of the transcriptome dynamics in different root tissues provide new insights into the transcriptional network regulating root development in response to NH_4^+ nutrition such as the repression of crucial TFs involved in root meristem maintenance and development. In fact, this is one of the first reports in *planta* that links *SHR*, and other TFs and regulators proteins, to NH_4^+ nutrition and its phenotypic effect on root architecture (Jia and von Wirén, 2020), probably affecting the early vascular development. Based on the TF expression patterns and the literature, QC in maritime root tip might be located in RC (Figure 3.10). Moreover, the presence of functionally uncharacterized TFs in maritime pine that could be involved in the molecular mechanisms governing root elongation inhibition, agravitropic response and lateral root branching, encourage to address future studies to clarify all these hypotheses.

Supplemental material:

All the supplemental materials are provided in the folder Chapter 3 – Supplemental Material, accessible through this link:

https://drive.google.com/drive/folders/1AEqD4ZFnxzTMfi_19HG_3HRyAo-_Vua?usp=sharing

Chapter 3. Conclusions and Supplemental material

Dataset S3.1. LCM low-input RNA-seq differential expression results. DE transcripts up-regulated are in highlighted red. DE transcripts down-regulated are in highlighted blue. (Pendrive)

Dataset S3.2. LCM low-input RNA-seq functional enrichment of DE transcripts. Only conditions with significant functions are shown. (Pendrive)

Table S3.1. Protein sequences of Dof transcription factors in maritime pine, *Arabidopsis* and rice. (Pendrive)

Table S3.2. Protein sequences of NAC transcription factors in maritime pine and *Arabidopsis*. (Pendrive)

Chapter 4

Integrative metabolic, transcriptomic, epitranscriptomic and proteomic profiling of the response of maritime pine to ammonium nutrition

Francisco Ortigosa, César Lobato-Fernández, Concepción Ávila, Francisco M. Cánovas, Rafael A. Cañas.



Introduction

Important discoveries in the 20th century in the nascent field of molecular biology meant that during the 1970s the central dogma of molecular biology emerged (Crick, 1970). However, today it is known that the transcription and translation process are not always directly linked. Multiple factors intervene in the gene response and its regulation. Two good examples of this are the long non-coding RNAs (lncRNAs) (Cesana *et al.*, 2011; Liu *et al.*, 2015) and the micro-RNAs (miRNAs) (Chekulaeva and Filipowicz, 2009; Paul *et al.*, 2015). These members of the RNA family have been reported to regulate important aspects of both development and response to stimuli response, in all eukaryotic organisms (Chekulaeva and Filipowicz, 2009; Cesana *et al.*, 2011; Liu *et al.*, 2015; Paul *et al.*, 2015). A good example is the regulation of plant root development mediated by *miRNA160* (*miR160*). It has been described that *miR160* regulates the expression of several *auxin response factors* (*ARFs*) (*ARF10*, *ARF 16* and *ARF17*) in *Arabidopsis* and soybean (*Glycine max*) (Wang *et al.*, 2005; Nizampatnam *et al.*, 2015). *miR160* overexpression in *Arabidopsis* experiments alters the root system architecture (RSA), giving place to a decrease in the length of the principal root and an increase of lateral roots (Liu *et al.*, 2018). Therefore, *miR160* role has been linked to control the proper root cap development and to the gravitropic response (Wang *et al.*, 2005; Liu *et al.*, 2018). Several examples for a relevant role of miRNAs in the regulation of N nutrition have been described. In *Arabidopsis*, it was found that *miR167* was repressed by nitrate or glutamine/glutamate, leading to an increase of *AtARF8* expression level (Gifford *et al.*, 2008; Gutiérrez, 2012). These results in a greater initiation and emergence of lateral roots (Gifford *et al.*, 2008; Gutiérrez, 2012). In rice (*Oryza sativa*), it was observed that *OsmiR160* expression was higher under NH_4^+ nutrition than under NO_3^- nutrition (Li H *et al.*, 2016), linking the role of miRNAs involved in N metabolism to changes in RSA through the putative targets related to auxin pathway as it was described for *miR160* in *Arabidopsis thaliana* and soybean (Wang *et al.*, 2005; Nizampatnam *et al.*, 2015; Li, H *et al.*, 2016; Liu *et al.*, 2018).

However, these studies only represent a small part of the RNA metabolism. In recent years, an emerging discipline focused on the cellular and biological role of RNA chemical modification has emerged under the term *epitranscriptomics*. Chemical modifications are found in all RNA types such as transfer RNA (tRNA),

ribosomal RNA (rRNA), messenger RNA (mRNA) and small RNAs (RNAs) (Xiong *et al.*, 2017; Vandivier and Gregory, 2018). Until date, more than 160 different modifications have been identified in RNA (Shen *et al.*, 2019). From those, based on *Arabidopsis thaliana* mRNA epitranscriptome m⁷G, m⁶A, m¹A, m⁵C, hm⁵C, and uridylation modifications have been identified (Shen *et al.*, 2019). Due to the marriage between classical detection techniques of RNA modifications and high-throughput sequencing it has been able to determine that the most prevalent chemical modification present in messenger mRNAs is N⁶-methyladenosine (m⁶A), in both animals and plants (Fray and Simpson, 2015). m⁶A transcriptome-wide analysis revealed that the m⁶A mark in transcripts is predominantly localized near the stop codon and throughout the 3' untranslated region (UTR) (Shen *et al.*, 2019). A shared m⁶A methylation motif (RRACH [R = A/G; H = A/U/C]) between plants and other eukaryotic organisms has been described (Shen *et al.*, 2019) and m⁶A deposition, recognition and elimination is carried out by a large number of proteins (see Appendix 2). m⁶A sites have been described to be strongly conserved between *Arabidopsis* ecotypes (Luo *et al.*, 2014), suggesting m⁶A localization within the transcriptome plays important roles (Anderson *et al.*, 2018). Several cellular roles have been observed to be affected by the m⁶A presence, such as mRNA stability (Luo *et al.*, 2014; Shen *et al.*, 2016; Wei *et al.*, 2018) or translational efficiency (Luo *et al.*, 2014). In addition, the proper m⁶A deposition has been reported to be essential during *Arabidopsis* embryo development (Vespa *et al.*, 2004; Zhong *et al.*, 2008; Růžička *et al.*, 2017) as it has been described in order eukaryotic organisms (Wang *et al.*, 2014; Geula *et al.*, 2015). These evidences suggest that m⁶A mark intervenes in fundamental biological processes and underlies basic developmental programs in eukaryotes (Fray and Simpson, 2015; Vandivier and Gregory, 2018; Shen *et al.*, 2019). Furthermore, m⁶A has been also reported to be involved during biotic and abiotic plant stress-response (Martínez-Pérez *et al.*, 2017; Anderson *et al.*, 2018), fruit ripening (Zhou *et al.*, 2019), flowering transition (Duan *et al.*, 2017), leaf morphogenesis (Arribas-Hernández *et al.*, 2018), trichome development (Vespa *et al.*, 2004; Bodi *et al.*, 2012) and apical shoot meristem development (Shen *et al.*, 2016).

Nitrogen (N) is an essential element for plant development, as it is a key component of cellular constituents such as nucleic acids, proteins or phytohormones among others (Hawkesford *et al.*, 2012; Chapter 1). N uptake by plants from soil can be

carried out through inorganic forms such as nitrate (NO_3^-) or ammonium (NH_4^+) or through organic forms such as urea ($\text{CH}_4\text{N}_2\text{O}$), peptides or amino acids (Liu and von Wirén, 2017). For most plants crop species, NO_3^- is the preferred form (Crawford and Forde, 2002). However, for other plants like rice, tea or pine, NH_4^+ is the preferred form (Sasakawa and Yamamoto, 1978; Ruan *et al.*, 2016; Chapter 2). Although the knowledge of the miRNA regulation related to plant N nutrition is still poor, several works and reviews collect the information obtained about the role of miRNAs in response to the presence / absence of N, in favor of NO_3^- over NH_4^+ (Xu Z *et al.*, 2011; Nguyen *et al.*, 2015; Shahzad *et al.*, 2018; Kaur *et al.*, 2020). Nevertheless, nothing at all is known about the potential role of epitranscriptome modifications in the regulation of N nutrition.

The aim of the present work is to shed light about the short-time response of maritime pine roots to NH_4^+ nutrition elucidating whether a regulatory relationship exists between transcriptomics, miRNA, epitranscriptomic and proteomics. For this purpose, different widely extended, such as miRNA-seq, and novel omics approaches were used, such as wide transcriptome analyses by Direct RNA Sequencing (DRS) using Oxford Nanopore Technology (ONT) platform or MeRIP-seq.

Results

Metabolite profiling in response to ammonium nutrition

Potential changes in the levels of metabolites caused by short-term NH_4^+ nutrition were analyzed in maritime pine roots (Figure 4.1). First, no striking change patterns are observed in the levels of metabolites examined.

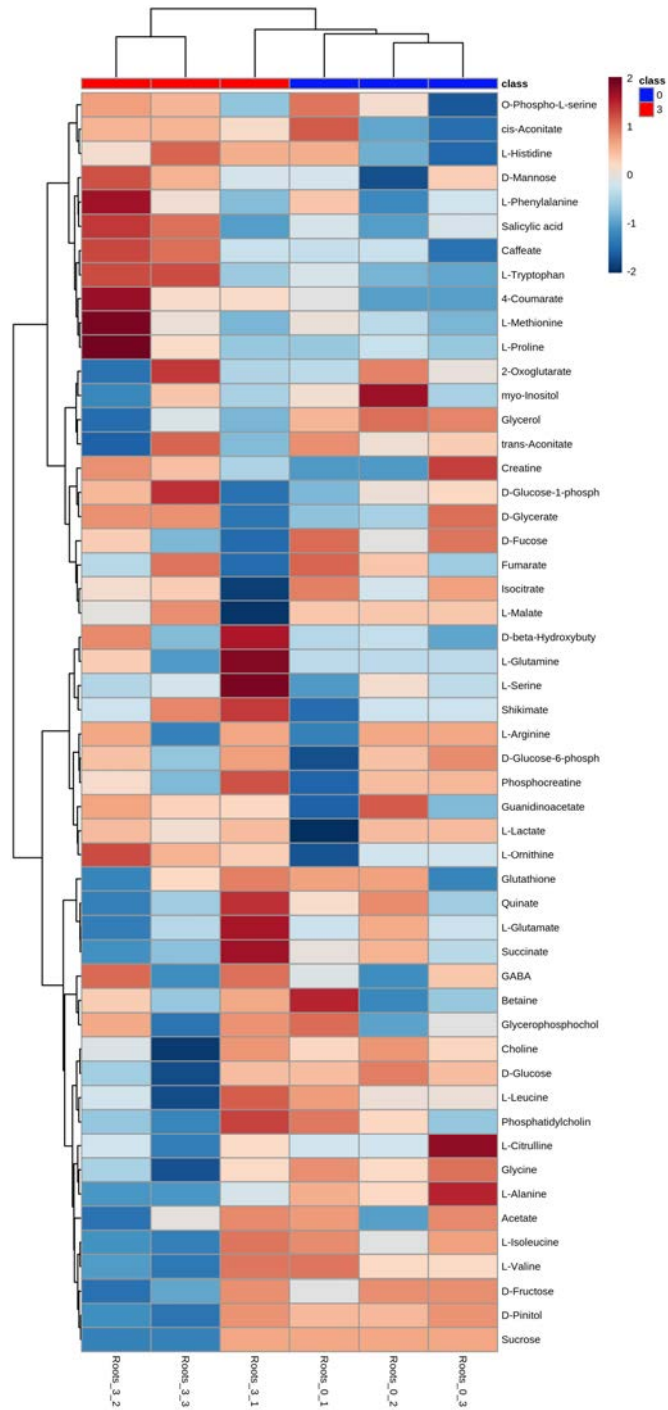


Figure 4.1. Heatmap of the root metabolite profiles analysed under ammonium condition (Root_3) and control condition (Root_0) at 24 hours.

However, a detailed study showed a statistically significant decrease in the levels of carbohydrates such as sucrose and glucose. In the same way it was observed a statistically significant increase of shikimate levels (Figure 4.2). In turn, although the results are not statistically significant, it was observed a slight trend for increased levels of glycolysis intermediary metabolites such as glucose-6 phosphate and glucose-1 phosphate and TCA anaplerotic pathway intermediates such as cis-aconitate, L-glutamate and GABA (Figure 4.2). In the same way, a positive trend in the accumulation of L-glutamine and L-methionine as well as in aromatic amino acids (L-phenylalanine and L-tryptophan) was observed in NH_4^+ -treated plants (Figure 4.2). In contrast, metabolites such as L-asparagine, isocitrate, 2-oxoglutarate and L-malate were observed to decrease (Figure 4.2). Full metabolite profiling data is available in Dataset 4.1.

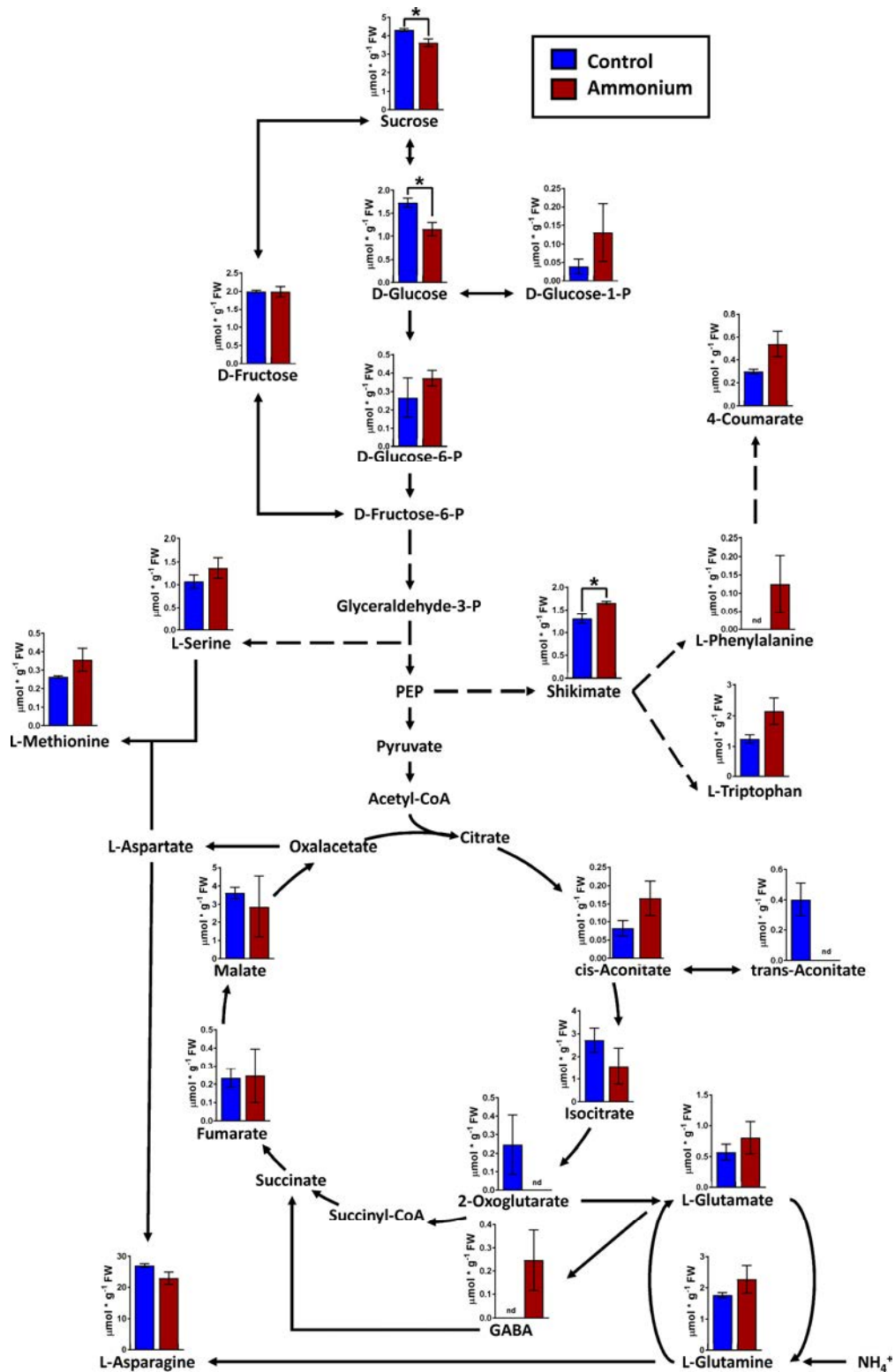


Figure 4.2. Main trend of metabolites in the roots of ammonium-untreated and ammonium-treated at 24 hours post-irrigation. Blue columns correspond to control plants; red columns correspond to 3 mM NH_4^+ supply. Differences between treatments were determined with a t-test. Significant differences are indicated with asterisks on top of the columns: * at $P < 0.05$. Error bars show SE with $n = 3$.

Direct RNA sequencing (DRS)

With the aim to corroborate our experimental design, RT-qPCRs of *PpAMT1.3* and *PpAMP1* were performed. The gene expression results showed that *PpAMT1.3* and *PpAMP1* were upregulated in response to ammonium nutrition (Figure 4.3) as described previous studies (Canales *et al.*, 2011; Castro-Rodríguez *et al.*, 2016, Chapter 3).

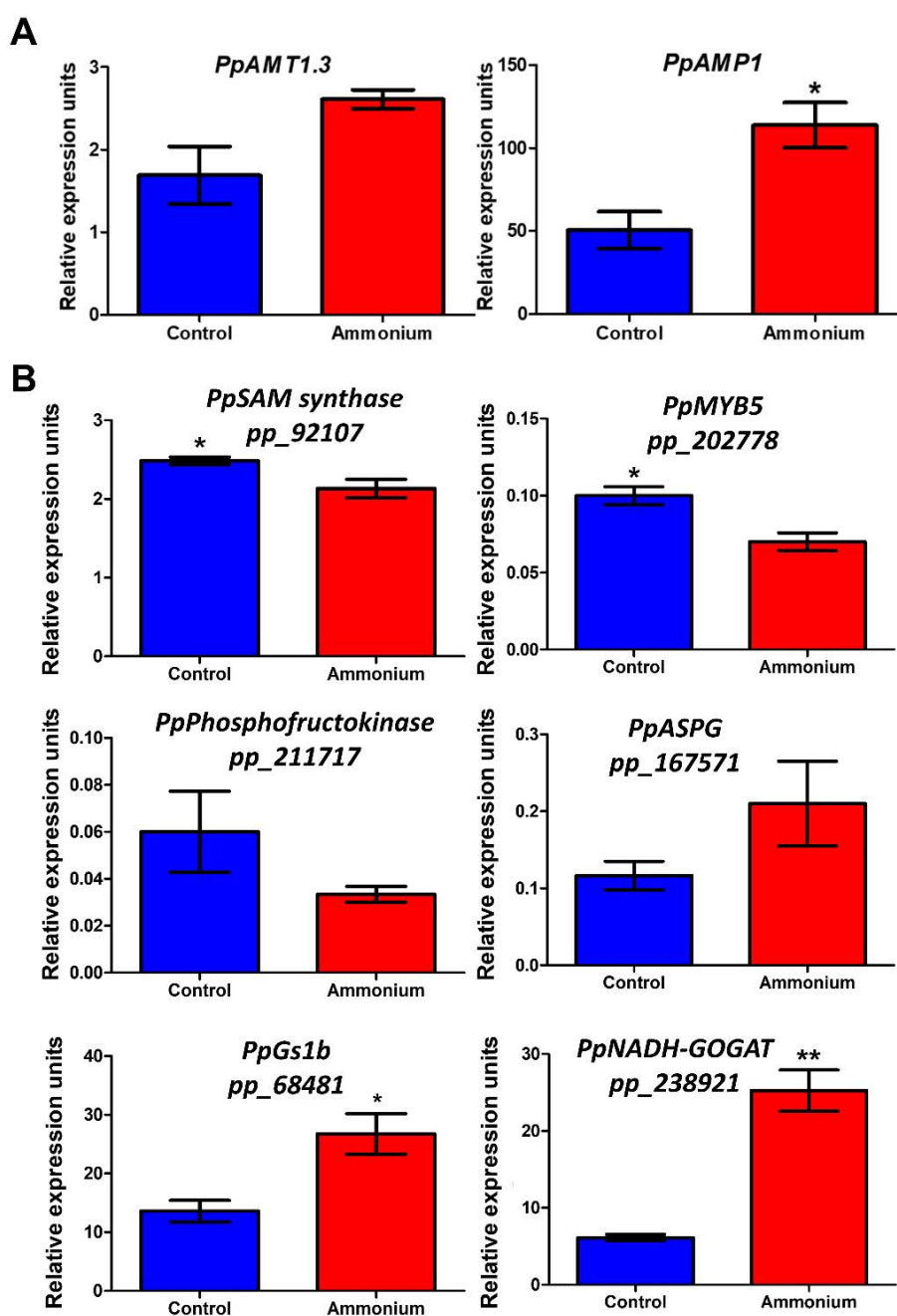


Figure 4.3. A. Gene expression of *Ammonium transporter 1.3* (*PpAMT1.3*) and *Antimicrobial peptide 1* (*PpAMP1*) genes in maritime pine under 3mM NH_4^+ presence. B. RT-qPCR results from six differentially expressed genes identified on

DRS transcriptomic data. Blue columns correspond to control samples. Red columns correspond to samples supplied with 3 mM NH_4^+ . Roots were harvested 24 hours post-irrigation. Significant differences were determined with a t-test (* $P < 0.05$; ** P -value < 0.01). Error bars show SE with $n = 3$.

ONT-DRS was performed using polyA mRNA from 1-month old maritime pine seedling roots (Figure 4.4). The complete sequencing results are shown in the Table 4.1. The read mean sizes were between 908 bp to 1059 bp (Figure 4.4). The longest reads were between 10298 bp to 14299 bp.

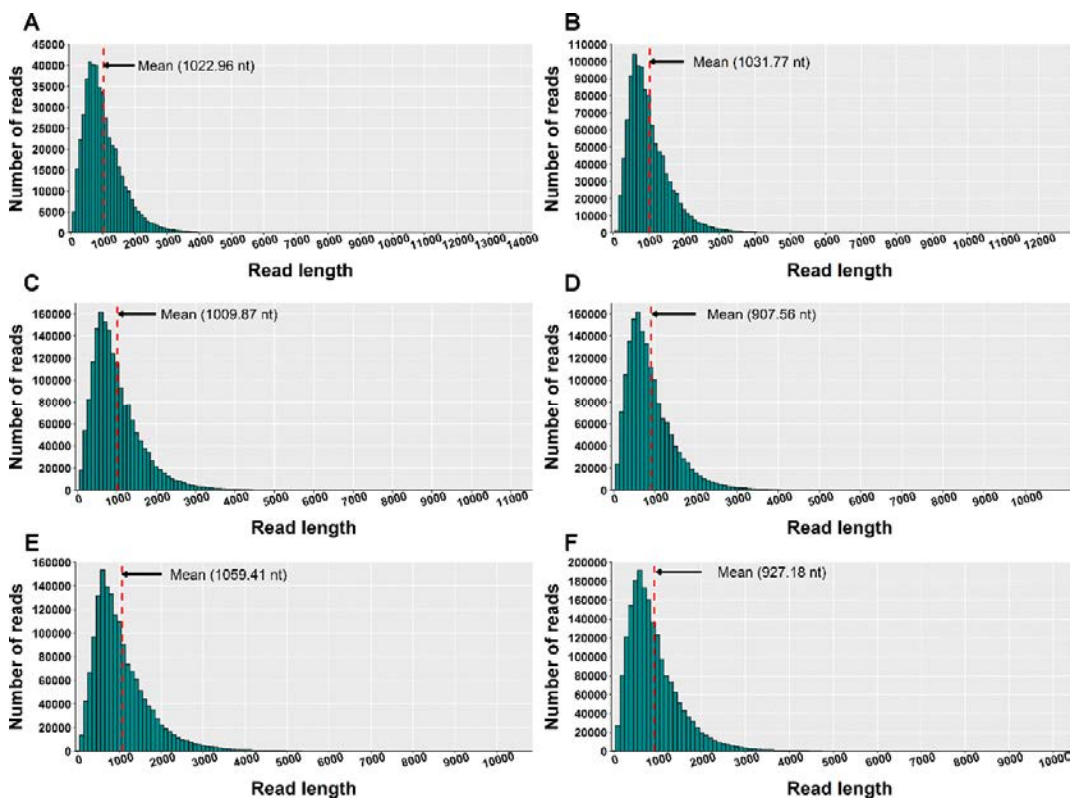


Figure 4.4. Number of reads and read size distribution obtained from direct RNA sequencing (DRS). A, C, and E graphs belong to control samples. B, D and F graphs belong to NH_4^+ -treated samples.

Table 4.1. Direct RNA sequencing information for each sample run.

Sample	Length read (mean, bp)	Length read (median, bp)	Maximum length read (bp)	Maximum quality per sample
C1	1022.96	887	14299	27.94
C2	1009.87	854	11465	29.37
C3	1059.41	889	10808	30.20
N1	1031.77	886	12834	14.32
N2	907.56	768	10951	29.96
N3	927.18	786	10298	30.50
Mean	993.13	845	11775.83	27.05

Differential expression analyses identified 350 differentially expressed (DE) transcripts. From the total DE obtained, 106 were upregulated and 244 were downregulated (Dataset 4.2). Singular Enrichment Analysis (SEA) was performed individually by each gene expression regulation (up- or downregulated transcripts) to classify the biological functions under NH_4^+ nutrition. The SEA global results are shown in Dataset 4.2. The results obtained for the GO terms of upregulated transcripts showed that the Biological Process (BP) terms “ammonia assimilation cycle” (GO:0019676), “glutamate biosynthetic process” (GO:0006537), “protein glutathionylation” (GO:0010731), “response to cadmium ion” (GO:0046686), “developmental growth” (GO:0048589), the Cellular Component (CC) term “chloroplast stroma” (GO:0009570), “cytosolic ribosome” (GO:0022626) and the Molecular Function (MF) “glutamate synthase (NADH) activity” (GO:0016040), “3 iron, 4 sulfur cluster binding” (GO:0051538), “FMN binding” (GO:0010181), “acylglycerol lipase activity” (GO:0047372) and “phospholipase activity” (GO:0004620) were over-represented (Figure S4.1). The significant biological functions of DE transcripts downregulated showed that BP terms “response to heat” (GO:0009408), “response to water deprivation” (GO:0009414), “protein folding” (GO:0006457), “ethylene-activated signaling pathway” (GO:0009873) and the MF terms “calcium ion binding” (GO:0005509), “transcription coactivator activity” (GO:0003713), “mRNA binding” (GO:0003729), “chaperone binding” (GO:0051087) and “transcription factor activity, sequence-specific DNA binding”

(GO:0003700) were over-represented (Figure S4.2). A more detailed study of the upregulated transcriptomic response revealed that transcripts of key genes encoding enzymes of the GS-GOGAT cycle, *PpGS1b* (pp_68481) and *PpNADH-GOGAT* (pp_238920) were upregulated. Furthermore, transcripts for genes involved in defense and cell wall remodeling were also upregulated. In relation with the defense-related response it is notable the upregulation of *PpAMP1* (pp_58005, pp_58008), *class IV chitinase* (pp_239593, pp_239598, pp_239600, pp_117809), different splicing coding forms of a *patatin-like protein 2* (pp_71017, pp_71018, pp_71019, pp_71020, pp_71022), *pathogenesis-related protein PR-1* (pp_87427) and a *defensin coding transcript* (pp_92119) (Dataset 4.2). It was also observed the upregulation of cell wall-related transcripts such of those encoding *expansin-A18* (pp_134987), *non-classical arabinogalactan protein 30* (pp_66323), probable *prolyl 4-hydroxylase 4* (pp_235715), *xyloglucan:xyloglucosyl transferase* (pp_68519) and different forms of *xyloglucan endotransglucosylase/hydrolase* (pp_66707, pp_66708, pp_68517). In contrast, the downregulation of different transcription factors (TFs) was observed (Dataset 4.2) such as *ethylene response factors (ERFs)* (pp_58625, pp_58626, pp_86737, pp_96228, pp_96234), a *trihelix transcription factor ASIL2* (pp_59947), a *MYB coding transcript* (pp_202778) and a nucleus localized coding *RPW8 domain-containing protein* (pp_142311). In the same sense, it was observed the repression of different splicing forms of an *auxin-repressed protein/dormancy-auxin associated protein coding transcript* (pp_58457, pp_58458, pp_58459, pp_58461, pp_58462, pp_58463), as well as for carbohydrate metabolism enzymes like *pyruvate decarboxylase* (pp_78343, pp_123611, pp_126347) and *sucrose synthase* (pp_144843).

To verify DRS results, RT-qPCRs for six additional genes to *PpAMT1.3* and *PpAMP1* were performed (Figure 4.3). Three of the transcripts analyzed were downregulated (pp_92107, pp_202778 and pp_211717), whereas the rest of the differentially expressed genes (DEGs) were upregulated (pp_167571, pp_68481 and pp_238921) under NH_4^+ nutrition. The differential expressions observed with DRS-RNA-seq were generally confirmed in the RT-qPCR data (Figure 4.3B) (Dataset 4.2).

Differential proteomics

To study the relationship between transcription and translation, a study of differential proteomics was carried out. Proteomics analyses revealed that 114 proteins were differentially regulated by ammonium (Dataset 4.3). Thirty eight of the 114 proteins identified were over-represented, while 76 proteins were under-represented under NH_4^+ nutrition. For the purpose of elucidating the biological roles of the identified proteins, SEA analyses were performed (Dataset 4.3). Results obtained showed an over-representation of the BP terms “cell redox homeostasis” (GO:0045454), “protein complex assembly” (GO:0006461), “cellular macromolecular complex assembly” (GO:0034622), “translation” (GO:0006412), “cellular response to oxidative stress” (GO:0006979) and “defense response to bacterium” (GO:0042742), CC terms such as “cytosolic ribosome” (GO:0022626), “small ribosomal subunit” (GO:0015935), “nucleolus” (GO:0005730), “chloroplast” (GO:0009507) and MF terms “structural constituent of ribosome” (GO:0003735) and “enzyme regulator activity” (GO:0030234) were over-represented (Figure S4.3). In contrast, in under-represented protein enrichment results it was observed an over-representation of BP terms “ribosome assembly” (GO:0042255), “ATP metabolic process” (GO:0046034), “translation” (GO:0006412), “response to metal ion” (GO:0010038), “oxidation-reduction process” (GO:0055114), CC terms “cytosol” (GO:0005829), “apoplast” (GO:0048046), “chloroplast” (GO:0009507), “ribosome” (GO:0005840) and MF terms “oxidoreductase activity, acting on the aldehyde or oxo group of donors, NAD or NADP as acceptor” (GO:0016620), “structural constituent of ribosome” (GO:0003735), “GTPase activity” (GO:0003924) and “GTP binding” (GO:0005525) (Figure S4.4).

Both transcript and protein levels of ATP-dependent 6-phosphofructokinase 2 were downregulated in response to NH_4^+ . Also, a S-adenosylmethionine synthetase coding transcript (pp_92107) and a methionine synthase enzyme were downregulated. Interestingly, similar NH_4^+ effects were found on ubiquitin-related transcripts and proteins (pp_97223, pp_119746, pp_136832, pp_136833, pp_136834, pp_136835, pp_140029, pp_153165, pp_153168, pp_197054, pp_224539, among other), being transcripts and proteins less abundant (Dataset 4.2, Dataset 4.3). In contrast, it was found upregulation of transcripts and proteins for profilin (pp_71321, pp_166621) and ribosomal subunit (pp_43165, pp_43167,

pp_194661, pp_209639, pp_209640, pp_236316, pp_236318, pp_236320, pp_236928), where pp_236316 was found in both transcriptomic and proteomic results (Dataset 4.2, Dataset 4.3). Similar results were obtained for transcripts and proteins involved in the regulation of hydrogen peroxide levels such as peroxidases and peroxiredoxin (pp_136236, pp_136239, pp_204103, pp_245532) (Dataset 4.2, Dataset 4.3). Interestingly, an inverse link between transcriptomic and proteomic approach was observed upregulation/over-representation of glycine-rich RNA-binding proteins (pp_197347, pp_197348, pp_197349, pp_197350, pp_211512, pp_211516, pp_221956) (Dataset 4.2, Dataset 4.3) and also for cysteine biosynthesis related transcript (cysteine synthase fragment) (pp_152995) and protein (S-adenosyl-L-homocysteine hydrolase) (pp_41646).

No direct evidences between transcriptomic and proteomic information were observed for the TCA-related enzymes, being mainly down-represented at proteomic level (pp_116289, pp_153216, pp_153217) (Dataset 4.2, Dataset 4.3).

miRNA-seq

To further explore the regulation of the response of maritime pine seedlings to NH_4^+ nutrition small RNA sequencing was performed in the same samples analyzed previously. A total of 32,711 putative miRNAs were identified using Mirnova software (Vitsios *et al.*, 2017) (Dataset 4.2). For only 617 putative miRNAs of the total were predicted a precursor in the genome (Dataset 4.2). The sizes of the putative miRNAs were between 12 and 33 nucleotides (nt) although only between 16 and 28 nt there were a significant number of miRNA and reads (Figure 4.5A, B). Most of the miRNA were 21 nt in length (71%) followed very far by the miRNAs with 22 nt (10.91%). However, the expression differences between the 21 nt miRNAs and the rest of miRNAs were lower, mainly considering the miRNAs higher than 21 nt. This is because the reads of 21 nt miRNAs corresponded only to the 40.5% of the total reads. Along the miRNA sequences the amount of A+U decreased from 5' to 3' mainly due to the diminution of A and the increasing of C (Figure 4.5C). The proportions of A+U were higher than 50% in all the positions from the 1 (64.71%) to 17 (53.67%) and in the single sites 21 (52.05%) and 22 (50.95%). This proportion was the lowest in the position 19 (33.69%). In the first base (5'), A was presented in more than 25% except in the 20 nt length miRNAs (24.58%) (Figure 4.5D). C was always lower than 25% except for 16 (26.09%), 18

(26.35%) and 27 nt (26%) miRNAs. In the case of G its bias was around 25% in every case except for 21 (14.56%), 22 (14.8%), 23 (18.66%) and 28 nt (20.37%) miRNAs. In the last case, U bias in this site was generally significantly lower than 25% except for 20, 24 and 28nt (24.65-25.93%) miRNAs, but especially very high for 21 (36.95%), 22 (41.28%) and 23 nt (32.53%) miRNAs (Figure 4.5D).

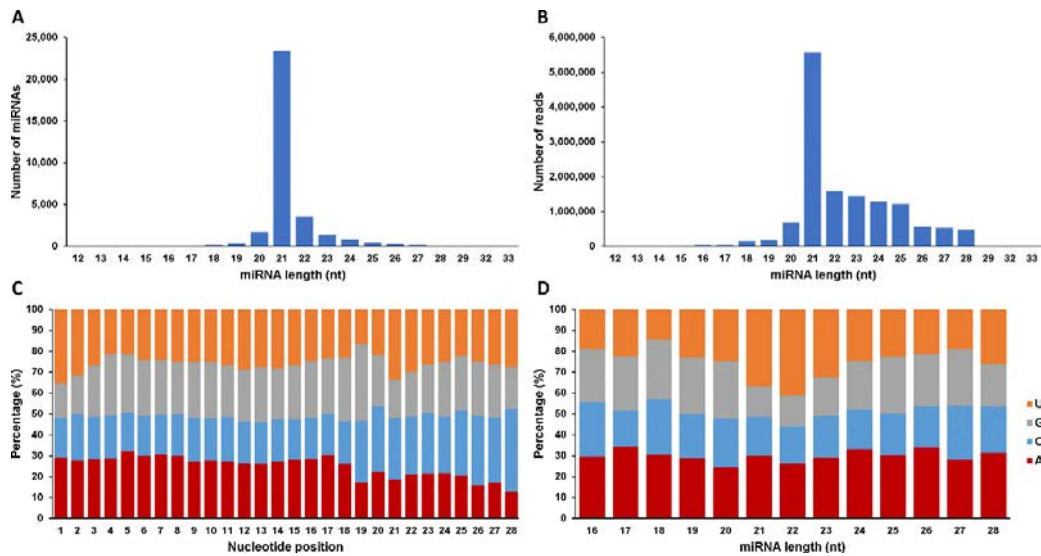


Figure 4.5. miRNA abundance and nucleotide distribution along the miRNA. A, Abundance of the predicted miRNAs considering their length. B, Number of miRNAs by length. C, Nucleotide bias along the different sequence positions of the predicted miRNAs. The sequence positions after 28 were not considered because the low number of miRNAs higher than 28 nucleotides. D, Nucleotide bias in the first sequence position of the predicted miRNAs. The miRNAs with sequences lower than 16 or higher than 28 nucleotides were not considered because the low number of miRNAs with these lengths.

Differential expression analysis revealed a total of 22 DE miRNAs (MIRs). Of the total, 6 MIRs were induced while 16 were repressed (Dataset 4.2). SEA analyses were performed for the mRNA targets of the DE miRNAs (Dataset 4.2). Functional enrichment of the up-regulated MIRs targets revealed the over-representation of BP terms “chloroplast accumulation movement” (GO:0009904), “chloroplast avoidance movement” (GO:0009903), “cell wall modification” (GO:0042545), “carboxylic acid metabolic process” (GO:0019752), “meiotic DNA double-strand break formation” (GO:0042138), “transcription elongation from RNA polymerase II promoter” (GO:0006368), CC term “DSIF complex” (GO:0032044) and MF

terms “oxidoreductase activity, acting on paired donors, with oxidation of a pair of donors resulting in the reduction of molecular oxygen to two molecules of water” (GO:0016717), “mRNA binding” (GO:0003729) and “S-formylglutathione hydrolase activity” (GO:0018738) (Figure S4.5). On the other hand, the SEA analyses of repressed DE MIRs targets in the presence of ammonium showed an enrichment in the BP terms “mRNA export from nucleus” (GO:000640), “SCF-dependent proteasomal ubiquitin-dependent protein catabolic process” (GO:0031146), “protein autophosphorylation” (GO:0046777), “brassinosteroid biosynthetic process” (O:0016132), “negative regulation of cellular carbohydrate metabolic process” (GO:0010677), “regulation of cell morphogenesis involved in differentiation” (GO:0010769), “defense response signaling pathway, resistance gene-dependent” (GO:0009870) and “abscisic acid-activated signaling pathway” (GO:0009738), CC terms “transcription export complex” (GO:0000346) and MF terms “thiol-dependent ubiquitin-specific protease activity” (GO:0004843), “ADP binding” (GO:0043531), “progesterone 5-alpha-reductase activity” (GO:0050213) and “Rho guanyl-nucleotide exchange factor activity” (GO:0005089) (Figure S4.6, Dataset 4.2).

Interestingly, a deeper study revealed that the upregulated transcripts *PpGS1b* (pp_68481) and defensin 5.1 (pp_92119) were targets of the statistically significant downregulated *MIR217* and *MIR1073*, respectively. Both *MIR217* and *MIR1073* showed a putative inhibitory action by cleavage (Dataset 4.2).

Differential DRS epitranscriptomics

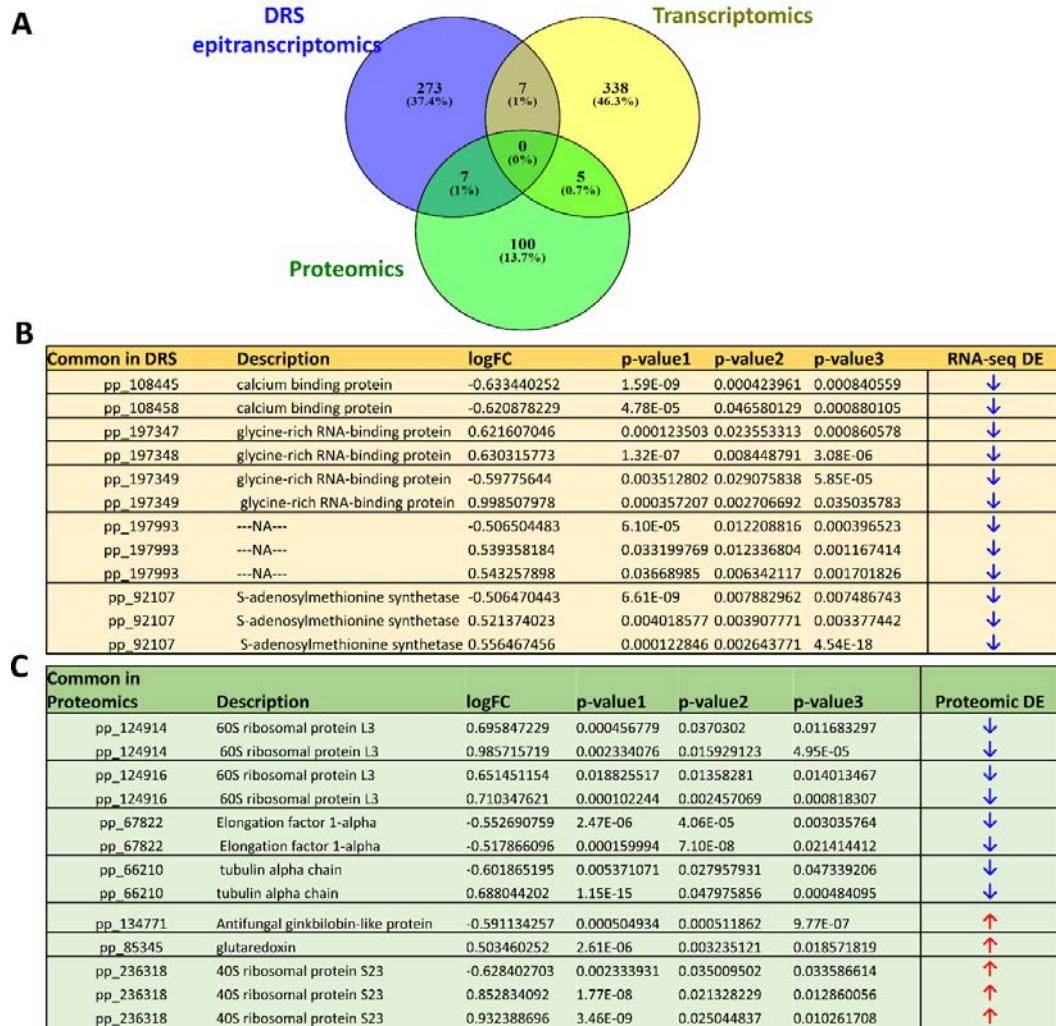
As a first differential epitranscriptomic approximation DRS results were explored with Tombo software to identify the chemical modified nucleotide in the mRNAs. After the bioinformatic analyses, 513 statistically significant putative modified nucleotides were obtained in 283 transcripts (Dataset 4.4). In order to infer the possible regulated processes, SEA analyses were carried out (Dataset S4.4 and Figure S4.7). Thus, the enriched terms in the over-modified transcripts were the BP term “organonitrogen compound metabolic process” (GO:1901564), and, the CC terms “cytosolic ribosome” (GO:0022626) and “ribosomal subunit” (GO:0044391). For over-modified transcripts MF terms were not found. However, results from under-modified transcripts showed an over-representation of BP terms “chitin catabolic process” (GO:0006032), “translation” (GO:0006412), “translational

elongation” (GO:0006414), “cell wall macromolecule catabolic process” (GO:0016998), “hydrogen peroxide catabolic process” (GO:0042744), “water transport” (GO:0006833), “killing of cells of other organism” (GO:0031640), CC terms “cytosolic large and small ribosomal subunit” (GO:0022625 and GO:0022627, respectively), “extracellular space” (GO:0005615), “cytoskeleton” (GO:0005856) and MF terms, “translation elongation factor activity” (GO:0003746), “translation initiation factor activity” (GO:0003743), “chitinase activity” (GO:0004568), “structural constituent of ribosome” (GO:0003735) and “antioxidant activity” (GO:0016209), among others (Figure S4.7).

The comparison of statistically significant results from transcriptomic and proteomic analyses revealed that 7 DE transcripts and 7 DE proteins were in common with DRS differential epitranscriptomic results (Figure 4.6A). Interestingly, all common transcripts were differentially modified whose DE expression data revealed a general repression for all common transcripts (Figure 4.6B) (Dataset 4.2). Meanwhile 4 differentially modified transcripts common with proteomic results were under-represented and the other 3 over-represented (Figure 4.6C) (Dataset 4.4). In addition, a more exhaustive data search revealed that several splicing forms of DE transcripts and proteins were also differentially modified, such as *ACC oxidase* (*pp_162588*), *40S ribosomal protein S23* (*pp_236318*), *isocitrate dehydrogenase* (*pp_153221*), *sucrose synthase* (*pp_144839*) or *L-asparaginase beta subunit* (*pp_167572*) among others (Dataset 4.4).

The GO terms comparison between general epitranscriptomics and the other omics techniques revealed that 74 GO terms were shared (Figure 4.6D). In order to study whether there is any relationship between the 74 common GO terms in these three layers of information, they were compared with the GO terms of the over / under modified sequences. This comparison allowed us to observe that 6 GO terms were specifically related to over-modified sequences and related to BP terms cytoplasmic translation (“GO:0002181”), regulation of transcription, DNA-templated (“GO:0006355”) and sequestering of actin monomers (“GO:0042989”) and MF terms binding (“GO:0005488”) and magnesium ion binding (“GO:0000287”) (Figure 4.6F). In addition, 5 GO terms were specifically related to under-modified sequences which were related to BP term protein transport (“GO:0015031”), MF terms calcium ion binding (“GO:0005509”), peroxidase activity (“GO:0004601”),

protein heterodimerization activity (“GO:0046982”) and CC term cell wall (“GO:0009505”) (Figure 4.6F).



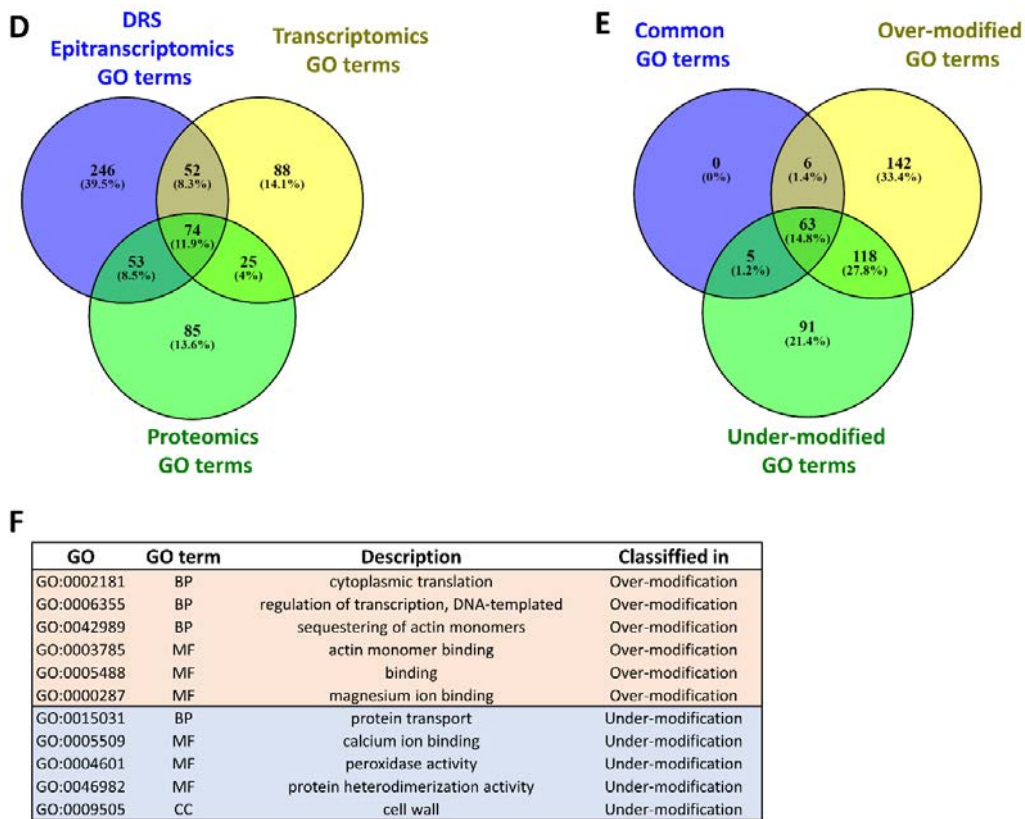


Figure 4.6. A. Comparison between differentially modified transcripts (blue) with transcriptomic (yellow) and proteomic (green) results. B. Common transcripts identified between epitranscriptomic and transcriptomic analyses. C. Common transcripts identified between epitranscriptomic and proteomic analyses. Red arrows indicated an upregulation/overrepresentation at transcriptomic and protein levels, respectively. Blue arrows indicated a downregulation/underrepresentation at transcriptomic and protein layers, respectively. D. GO terms comparison between epitranscriptomics, transcriptomics and proteomics layer. E. Comparison between the common 74 GO terms found in the different layers of information and GO terms of over- and undermodified transcripts identified at our general epitranscriptomic approach. F. Description of the specific GO terms related to over-modified transcripts (orange) and under-modified transcripts (blue).

Differential m⁶A epitranscriptomics

m⁶A mRNA immunoprecipitation followed by RNA sequencing (MeRIP-seq) revealed that an average of ~15300 putative m⁶A sites were enriched at the control root samples, whereas an average of ~13000 putative m⁶A sites were enriched at the ammonium root samples. After filtering process was performed, fifty-one

differentially m⁶A sites enriched on coding 38 different transcripts including splicing variants were detected (Dataset S4.5). Thus, more than one putative m⁶A site in some transcripts were found (Figure 4.7A,C) (Dataset S4.5).

The localization of the differentially modified sequences revealed that m⁶A mark is more frequently to be localized in 3'-UTR regions (~ 92.1 %) than in CDS regions (~ 7.8 %) (Figure 4.7A,B,C,D,E) (Dataset 4.5). The putative m⁶A sites in these transcripts were identified using the BERMP software (Huang *et al.*, 2018) (Dataset 4.5). Most of the predicted m⁶A sites were in the peak regions identified in the MeRIP-seq were identified. Analyzing this sites with the Motif-based sequence analysis tool, also known as MEME, (Bailey *et al.*, 2015) a consensus sequence motif for putative m⁶A sites was identified: RRACH (where R = G/A, H = A/C/U, bold letter stands for adenosine being modified to m⁶A) (Figure 4.7F).

Any of the transcripts with the DE m⁶A marks correspond to DE transcripts or proteins. Nevertheless, a general negative correlation (-0.62 and *P*-value <0.0001) was observed between higher m⁶A deposition and their respective expression values (Figure 4.7A) (Dataset 4.5). Among the transcripts with DE m⁶A marks were *histone-lysine N-methyltransferase ATX2 with Jas TPL-binding domain* (*pp_116019*, *pp_116021*), *mitogen-activated protein kinase homolog MMK1* (*pp_143730*, *pp_143731*), *photosystem II 22 kDa protein* (*pp_215461*, *pp_215464*) or *methylesterase* (*pp_243770*) among others (Figure 4.7A) (Dataset 4.5). All putative DE m⁶A marks were *in silico* tested using BERMP tool and *Arabidopsis thaliana* methylome as a reference (Huang Y *et al.*, 2018)) (Dataset 4.5). It was observed a high confidence values for most putative DE m⁶A marks detected (Dataset 4.5).

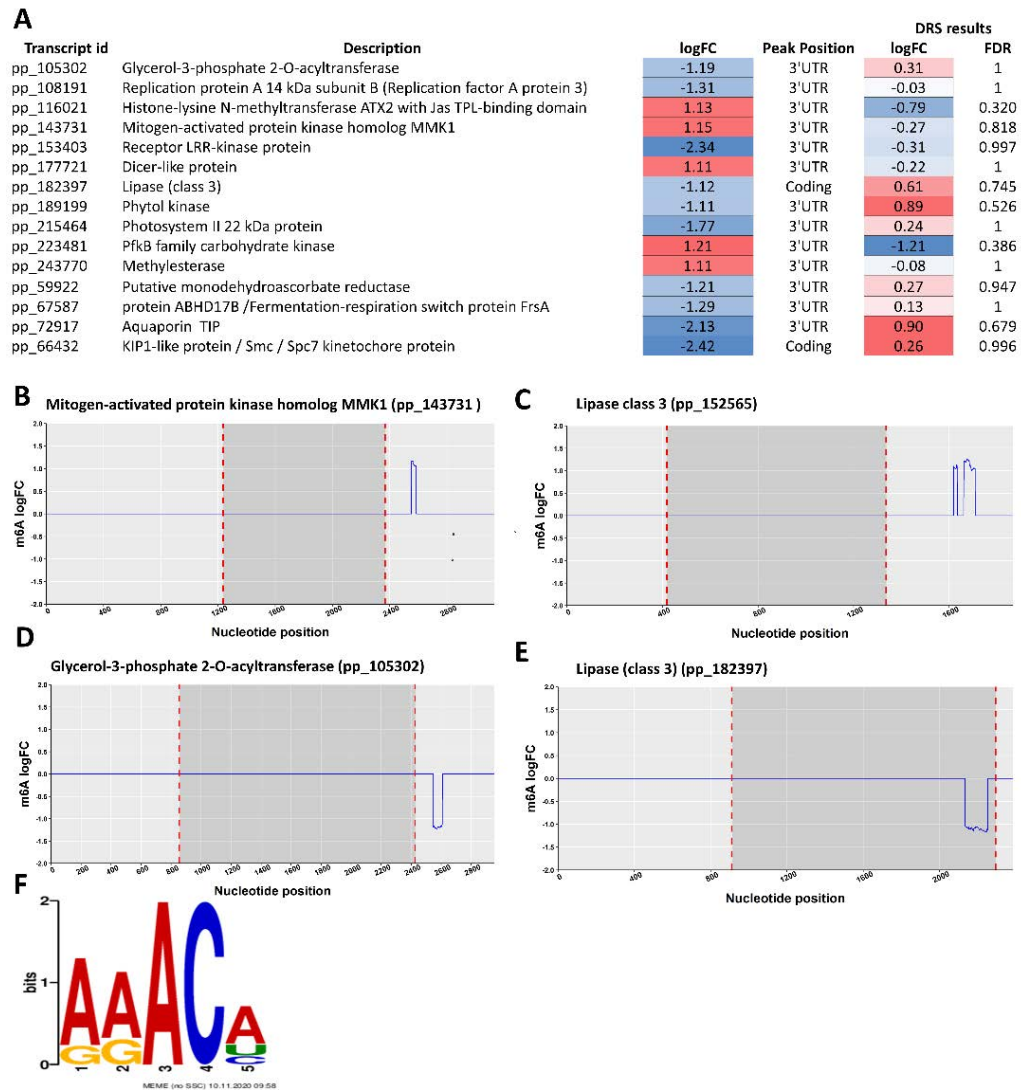


Figure 4.7. A. Brief summary from differential epitranscriptomic results (MeRIP-seq results) and DRS results in pine roots exposed to 3mM NH₄Cl at 24 hours. B-E Representation of the m⁶A changes (m⁶A log FC) across the transcript. The shaded area refers to the coding sequence (CDS). F Consensus motif identified in differential epitranscriptomic results. Complete data are available on Dataset 4.5.

Discussion

Nitrogen (N) form part of important biomolecules essential for life, such as nucleotides, proteins and cofactors among others as well as for the proper plant growth and development (Xu *et al.*, 2012, Chapter 1). It is worth mentioning that the responses observed in the transcriptome, epitranscriptome proteome and metabolome profiling are possibly reflecting that NH_4^+ acts as a signal at short times as described in Chapter 3. Accordingly, it was expected that the most profound changes would be detected at transcriptome level and the effect of NH_4^+ would be diluted in the rest

Carbon and nitrogen metabolism related genes

Post-translational regulatory mechanisms provide rapid regulation of multiple pathways and processes in plants (Jacquot *et al.*, 2017; O’Leary and Planxton, 2020; Sulis and Wang, 2020). One of the best well described mechanisms related to NH_4^+ uptake regulation involves the phosphorylation/dephosphorylation of AMTs (Hao *et al.*, 2020). The modification of the AtAMT1.1 threonine residue 460 (T460) marks the switch between the active or inactive state of the ammonium transporter (Loqué *et al.*, 2007). The protein kinase CIPK23 (calcineurin B-like interacting protein kinase 23) has been shown to phosphorylate T460 of the AtAMT1.1 and AtAMT1.2 in a CBL-1 (calcineurin B-like protein, Ca^{2+} sensor) dependent manner (Straub *et al.*, 2017). Consistently, our DRS results showed a wide repression of three *CBL-interacting protein kinase* coding transcripts (*pp_91958*, *pp_91963* and *pp_236381*) and several *calcium binding protein* coding transcripts (i.e.: *pp_146235*, *pp_108447*, *pp_108460*, *pp_108462*) (Dataset 4.2). These results could imply the regulation of NH_4^+ uptake at transcriptional level to the proper N acquisition and assimilation. No statistically significant changes of AMT proteins were observed probably due to post-transcriptional regulatory importance of AMT activity (Dataset 4.3).

The inorganic N incorporated from the soil must be assimilated to become part of the biomolecules. It is well known that for an optimum N assimilation, a proper provision of C skeletons is strongly required (Lam *et al.*, 1996). Likewise, and in relation to the high interconnection degree between the metabolism of N and C, the whole roots DRS results showed the downregulation of a transcript encoding

sucrose synthase (*pp_144843*). Concomitantly with the lower sucrose levels, a glucose consumption and an increase of glucose 6-phosphate levels observed in roots (Figure 4.2A). In addition, it was observed a decreased expression levels of gene for *ATP-dependent 6-phosphofructokinase* (*pp_211717*, *PFK*) (Dataset 4.2). Furthermore, the same effect was observed at proteomic level (*pp_211715*) (Dataset 4.3). Phosphofructokinase is a key regulatory enzyme in plant glycolysis that controls the carbon flow to this pathway (Mustroph *et al.*, 2007; Yao and Wu, 2016). *A priori*, this result is the opposite that those observed in *Arabidopsis* leaves under NH_4^+ -nutrition (Borysiuk *et al.*, 2018). This finding is in line with epitranscriptomic results where it was observed the over-modification of the *carbohydrate kinase PfkB family* transcript (*pp_223481*). However, maritime pine seedlings exhibit a strong preference for NH_4^+ and roots are able to uptake and accumulate large NH_4^+ amounts (Chapter 2). Different PFK patterns observed could be due to modulation of glycolysis, both at the transcriptomic and epitranscriptomic levels, to provide C skeletons for inorganic N assimilation.

In turn, in maritime pine roots, the transcriptomic response reveals the downregulation of transcripts encoding *pyruvate decarboxylase* (*PDC*) enzymes (*pp_78343*, *pp_123611*, *pp_126347*, *pp_163572*) and *alcohol dehydrogenase* (*ADH*) (*pp_105643*, *pp_179993*, *pp_203818*, *pp_203819*, *pp_247833*, *pp_247834*, *pp_247837*) (Dataset 4.2), being the corresponding protein to *pp_203818* downrepresented at proteomic level as well (Dataset 4.3). It is well known that plants under low oxygen conditions regulate their metabolism, inducing the fermentation pathway (Mithran *et al.*, 2014) in which *PDC* and *ADH* activities are essential resulting in pyruvate consumption producing acetaldehyde. After that, acetaldehyde is reduced to ethanol with the concomitant oxidation of *NADH* to *NAD*⁺ by alcohol dehydrogenase (*ADH*) (Kürsteiner *et al.*, 2003; Mithran *et al.*, 2014). The repression observed of *PDC* and *ADH* suggests that NH_4^+ could be involved in ensuring two things: i) a sufficient pool of pyruvate obtained during glycolysis, as pointed out the lower sucrose and glucose levels and higher glucose 6-phosphate (Figure 4.2A). This could lead to obtaining enough *NADH* and 2-oxoglutarate through TCA cycle for N assimilation according to the increased levels of cis-aconitate, L-glutamate and L-glutamine found in roots under NH_4^+ nutrition (Figure 4.2A) and ii) the overrepresentation of TIM mitochondrial transporter proteins (*pp_105401*, *pp_105402*) (Dataset 4.3). TIM proteins are part of the

TIM/TOM complex that is involved in nuclear coding proteins translocation through the mitochondrial membrane to be used in oxidative phosphorylation (Alberts *et al.*, 2013), which could mean that mitochondria are fully active. In addition, differential epitranscriptomic results showed that transcripts involved in the *fermentation-respiration switch* (*pp_67583* and *pp_67587*) were downmodified probably to favour cellular respiration pathway as our data proposes. This data suggest that regulation of the respiration/fermentation pathway might be coordinated at both transcriptomic and epitranscriptomic level.

Besides, root L-glutamine levels in the presence of NH_4^+ correlated well with the up-regulation of *glutamine synthetase* (*GS*) and *NADH-glutamate synthase* (*NADH-GOGAT*) transcripts (Figure 4.3B, Dataset 4.2), which is consistent with previous transcriptomic reports (Li *et al.*, 2017; Sun *et al.*, 2017; Huan *et al.*, 2018; Tang *et al.*, 2019). However, no overrepresentation of *GS* and *NADH-GOGAT* was observed at proteomic level (Dataset 4.2 and Dataset 4.3). Similar results in proteomics of NH_4^+ nutrition have been observed before (Marino *et al.*, 2016; Coletto *et al.*, 2019) and as well as the lack of correlation between relative expression values of *GS* transcripts and activity during long term NH_4^+ supply, discussed on Chapter 2, where it is hypothesized that the response to the N form could be regulated through a post-transcriptional (translational or post-translational) mechanism (Chapter 2). Based on our miRNA-seq results, we identified a differentially downregulated miRNA (*MIR217*) that targets *PpGS1b* transcript (*pp_68481*) (Dataset 4.2). This finding is consistent with the upregulation of *PpGS1b* transcripts discussed previously. No evidences of the regulation of *GS* gene expression by miRNAs were found in plants. Further functional experiments are strongly required in order to validate this finding and to assess its biological role under nitrogen nutrition.

ROS related genes.

Several reports have shown that NH_4^+ or even its assimilated products may act as stress signalling molecules, activating several mechanisms and pathways related to the reactive oxygen species (ROS) accumulation (de Souza *et al.*, 2016). Protection against oxidative stress is one of the different roles that GABA is thought to play in plant and non-plant cells (Bouche and Fromm, 2004; Fait *et al.*, 2008; Cesetti *et al.*, 2012). Interestingly, GABA levels were detected only in NH_4^+ -treated roots

according with previous NH_4^+ -fed plant reports (Carroll *et al.*, 1994; Coletto *et al.*, 2019). Nevertheless, no evidences were observed for transcript upregulation and/or protein overrepresentation of glutamate decarboxylase (GAD) (Dataset 4.2 and Dataset 4.3), which is coherent with the work of Menz *et al.* (2016) in *Arabidopsis*. In this study, they did not observe the up-regulation of *GAD* coding genes at transcriptomic level but GAD proteins were differentially phosphorylated in roots under NH_4^+ deprivation (Menz *et al.*, 2016) suggesting that, like in human cells, GAD post-translational modification could be important for GAD activity (Chou *et al.*, 2017). A recent work focused on salinity and osmotic stress in rice, showed that the high tolerance to these stresses is closely associated with the capability of GABA to influence ROS levels by inducing antioxidant enzymes, secondary metabolism and their transcription level (Sheteiwy *et al.*, 2019). Epitranscriptomically, several antioxidant coding transcripts were identified to be differentially modified (*catalase* and *ascorbate peroxidase*) (Dataset 4.4). These enzymatic activities were described to be increased under NH_4^+ presence (Patterson *et al.*, 2010; Sun *et al.*, 2020). However, differentially expression patterns of these transcripts/proteins were observed neither transcriptomic nor proteomic results. Additionally and related to secondary metabolism, it was observed an upregulation of transcripts related to secondary metabolism, such as those encoding for *4-coumarate-CoA ligase* (*pp_153265*), *anthocyanidin reductase ((2S)-flavan-3-ol-forming)-like* (*pp_179044*) and *caffeoyl-CoA O-methyltransferase* (*pp_153042*) as well as higher levels of secondary metabolites such as shikimate, L-phenylalanine and 4-coumarate (Figure 4.2B).

In addition to the possible role of *MIR217* regulating *PpGS1b* gene expression, *MIR217* also targets a repressed MYB-like transcription factor (FT) identified in our database as *PpMYB5* (*pp_202778*) (Dataset 4.2, Chapter 3). This transcription factor share homology with MYB4 of *Arabidopsis thaliana* (*AtMYB4*) (e-value: $2e-87$), being a possible orthologue of MYB5 of *Picea glauca* (*PgMYB5*), as phylogenetic analysis revealed (Bedon *et al.*, 2007). *AtMYB4* functions as a repressor of target genes related to UV-B stress (Mitra *et al.*, 2019). However, it is known that many R2R3-MYB FTs are involved in other pathways such as secondary metabolism related to phenylpropanoid pathway (Hichri *et al.*, 2011) and lignifying process in gymnosperm (Bedon *et al.*, 2007). The downregulation of both *PpMYB5* and *MIR217* could be involved in the regulation of these pathways of

secondary metabolism as the upregulation of *4-coumarate-CoA ligase* (*pp_153265*), *anthocyanidin reductase ((2S)-flavan-3-ol-forming)-like* (*pp_179044*) and *caffeoyl-CoA O-methyltransferase* (*pp_153042*) seems to indicate (Dataset 4.2). Furthermore, it is necessary to propose the possibility that PpMYB5 may also regulate the expression of *PpGS1b*, as has been demonstrated for other MYB TFs in maritime pine, such as PpMYB1, PpMYB4 and PpMYB8 (Craven-Bartle *et al.*, 2013).

Related to antioxidant activity putatively enhanced by GABA, at proteomic level the over-representation of two glutaredoxin proteins (*pp_85340* and *pp_85345*) and a peroxiredoxin-2E-1 (*pp_125224*) was observed. These proteins (glutaredoxins and peroxiredoxins) are involved in the reversible oxidation-reduction process of -SH radicals (Li, 2014; Liebthal *et al.*, 2018). Furthermore, it was observed the induction of several *glutathione S-transferase* transcripts under NH_4^+ supply (*pp_105375*, *pp_105380*, *pp_105381*, *pp_105382*, *pp_105383*, *pp_105385*, *pp_235801*, *pp_235803*, *pp_235810*) (Dataset 4.2). Recently, similar results have also been observed in rice seedlings under NH_4^+ excess and they have been attributed to lead the detoxification of the oxidants via reductive glutathione (Su *et al.*, 2020). These evidences might support the role of GABA on ROS protection by inducing different antioxidative pathways to protect from their deleterious effects and avoid cellular oxidation, at least on cysteine thiol-group (-SH) in maritime pine. Studies focused on NH_4^+ and GABA supply in maritime pine seedlings could shed light to determine a potential link between the presence of GABA under NH_4^+ supply and the activation of these pathways. In addition, it was observed the upregulation of transcripts involved in phospholipid biosynthesis such as those encoding for *phosphoethanolamine N-methyltransferase* (*pp_15256*, *pp_152569*, *pp_152570*) and *choline kinase* (*pp_128668*). It is known that ROS can affect membrane integrity (Gupta and Huang 2014) and therefore, it would be interesting to perform comparative lipidomic studies to examine if changes in lipidic composition are a characteristic feature in NH_4^+ -tolerant/sensitive plants.

Defense related genes

Nitrogen status is often related to plant disease emergence and plant immunity (Walters and Bingham, 2007; Fagard *et al.*, 2014). NH_4^+ is well known to induce the upregulation of defense genes *in planta* (Patterson *et al.*, 2010; Fernández-

Crespo *et al.*, 2012; Sun *et al.*, 2017; Ravazzolo *et al.*, 2020, Chapter 3). At transcriptomic level, DRS results evidenced an important induction of defense genes in maritime pine roots under NH_4^+ supply (Dataset 4.2).

The upregulation of the *antimicrobial peptide 1 (AMP1)* (*pp_58005* and *pp_58008*) and *pathogenesis-related protein (PR-1)* (*pp_87427*) transcripts are consistent with the microarray results previously published on maritime pine roots (Canales *et al.*, 2010) and with Chapter 3. AMP family is composed by different small secreted cysteine-rich peptides (Silverstein *et al.*, 2007). Pine AMP proteins are known to inhibit fungal pathogen development (Asiegbu *et al.*, 2003; Ekramoddoullah, 2005, Jaber *et al.*, 2018). According with data presented in Chapter 3, a wide induction of several genes with reported direct antimicrobial activity was observed (Dataet 4.2) such as those encoding for splicing forms of *class IV chitinase* transcripts (*pp_239593*, *pp_239598*, *pp_239600*) (Patel and Goyal, 2017), a *defensin5.1* coding transcript (*pp_92119*) (Stotz *et al.*, 2009), a *beta-lactamase* transcript (*pp_223924*) (Saeidi *et al.*, 2015) and a *thaumatin-like protein* (*pp_127651*) (Yan *et al.*, 2017). Similar tendency was observed at proteomic level for several ginkbilobin antifungal protein (*pp_134771*, *pp_134773* and *pp_252648*) (Wang and Ng, 2000). Finally, we found that the up-regulated defensin5.1 (*pp_92119*) was identified as a target of the repressed *MIR1073* (Dataset 4.3). This finding is a clear evidence of the direct regulation link between plant-defense response regulation by *MIR* genes (Liu SR *et al.*, 2017) and NH_4^+ presence.

The wide induction of defense related genes observed under NH_4^+ supply highlights how important this kind of genes could be for conifers at their natural environment since conifers have adapted to living in suboptimal environments for most plants where nutrient availability is a limiting factor for their growth and development (Farjon 2018).

Ethylene related genes

The physiological implication of ethylene (ET) in NH_4^+ response is still poorly understood. Transcriptomic studies carried out in rice described that under NH_4^+ excess, ET could be one of the major regulatory molecules activating the MAPK (mitogen-activated protein kinase) signal-transduction pathway in roots (Sun *et al.*, 2017). ABA and ET have been assessed to be the major regulatory molecules responding to NH_4^+ excess (7.5 mM $(\text{NH}_4)_2\text{SO}_4$), activating the MAPK signal-

transduction pathway (Sun *et al.*, 2017). According to our results, no evidence of this pathway activation was observed. However, two splicing members of *MAPK* (mitogen-activated protein kinase) were overmodified (*pp_143730* and *pp_143731*). This observation could be one of the reasons why this route was not found in our experimental model. Another reason would be that in our experimental conditions the NH_4^+ supply does not turn out to be excessive but rather enough, constituting a molecular evidence of what had been previously described about this nutritional condition (Canales *et al.*, 2010).

Additionally, Li and coworkers (Li G *et al.*, 2013) described in *Arabidopsis* that shoot-supplied NH_4^+ (SSA) promoted ET biosynthesis only in shoots, resulting in a reduction of the lateral root formation process due to *AUX1* (auxin transporter 1) repression. Interestingly, the ethylene receptor-defective mutant *etr1-3* was more resistant compared to wild-type under SSA, whereas the ethylene-overproduction mutants *xbat32* and *eto1-1* exhibited a more acute phenotype (Li G *et al.*, 2013). These data might point out that ET biosynthesis is involved in detrimental NH_4^+ -related phenotypes such as reduction in the number of lateral roots (LRs). Only few reports described that the application of ET biosynthesis and action inhibitors improved symptoms of NH_4^+ toxicity affecting root system architecture (RSA) (Barker and Corey, 1991; Feng and Barker, 1992a,b; Li G *et al.*, 2013). A comparison of the root transcriptomic response and differential proteomics results revealed that at short time (24 hours), NH_4^+ provokes a decrease for ethylene-related transcripts and proteins. Several ET TFs were downregulated at transcriptomic level while proteomic results revealed that the ACC oxidase enzyme (1-aminocyclopropane-1-carboxylate oxidase, also known as ACO) was downrepresented (Dataset 4.3). ACC oxidase is the enzyme responsible for the final stage in the biosynthesis of ethylene in higher plants (John *et al.*, 1999), whereas the putative root ET reduction could imply the down-regulation of different ethylene-response factors (*ERFs*) (*pp_58625*, *pp_586256*, *pp_86737*, *pp_96228*, *pp_96234*) observed at transcriptomic level (Dataset 4.2) and in LCM RNA-seq results (Chapter 3). Furthermore, according to our general epitranscriptomic results a splicing *ACC oxidase* transcript (*pp_162588*) exhibited a putative pseudouridine (Ψ) nucleotide differentially modified and located in the 3'-UTR. (Dataset 4.4). It is described that Ψ is a frequent chemical modification in coding and non-coding RNAs (Chen and Witte, 2020) and it is shown to be dynamically regulated upon

stress conditions in yeast and mammalian transcriptomes (Li X *et al.*, 2016). Ψ marks have been related to several RNA process such as RNA stability, RNA secondary structures or translation (Li X *et al.*, 2016). Although, *pp_162588* is differentially modified additional technique approaches are required in order to validate its biological importance regulating ACC oxidase splicing form expression. Additionally, another possible relation that could be taken into account is ET pathway and the translation process. It is described that ET signaling affects gene translation in different ways (Merchante *et al.*, 2015). This evidence may be one possible explanation of the different patterns observed in both ribosome related transcripts and proteins and their respective enrichment results (Dataset 4.2, Dataset 4.3). Be that as it may, these findings are consistent with those described above and suggest a link between what we did observe on RSA of maritime pine seedlings at long term NH_4^+ -supply and the IAA transport alteration proposed in Chapter 3 in the presence of NH_4^+ , consistent with the wide repression response of splicing forms identified as *auxin induced proteins* (*pp_58457*, *pp_58458*, *pp_58459*, *pp_58461*, *pp_58462*, *pp_58463*) (Dataset 4.2).

Differential epitranscriptomics and m⁶A epitranscriptomics

First, the lack of correlation between ONT general epitranscriptomic and MeRIP-seq results (Dataset 4.4 and Dataset 4.5) may be due to the technical approach performed, as data coverage and processing are different. However, the differential epitranscriptomic approximation revealed that protein translation was the most affected process (Figure S4.7) (Dataset 4.4). It is well known that ribosome post-transcriptional modifications are fundamental to global ribosome topology and functions (Taoka *et al.*, 2018). This evidence suggests that NH_4^+ might alter translation through changes in the modification status of ribosomal subunit transcripts (Dataset 4.4) (Figure S4.7). In addition, it is needed to point out that ET balance could be one of the players in this response, according to what has been discussed above (Merchante *et al.*, 2015).

The putative m⁶A sites were mainly located in the 3' untranslated region (3'UTR), which have the RRACH consensus motif (Figure 4.7F). Despite the *in-silico* validation of the DE m⁶A marks, it would be advisable to carry out a complementary check to validate these results. Be that as it may, these results are consistent with those previously performed on eukaryotic cells (Meyer *et al.*, 2012;

Fray and Simpson, 2015; Vandivier and Gregory, 2018). The negative correlation between epitranscriptomic and transcriptomic data suggests a possible role of m⁶A mediating mRNA stability, which also agrees with m⁶A roles previously reported (Luo *et al.*, 2014; Shen *et al.*, 2016; Wei *et al.*, 2018).

The absence of a direct epitranscriptomic relationship between transcriptomic or proteomic data could be attributed to the time variable due to it is described an increased in transcriptome changes over time (Patterson *et al.*, 2010; Sun *et al.*, 2017; Yang *et al.*, 2018).

Thus, these results might suggest that the short-term regulation (24 hours post-irrigation) caused by NH₄⁺ presence may have a greater relevance at the post-translational level (Menz *et al.*, 2016). In addition to the epitranscriptomic results discussed in this section and above, a deeper study of MeRIP-seq results revealed another possible link. For example, the over-modified *histone-lysine N-methyltransferase ATX2 with Jas TPL-binding domain (ATX2) splicing variants (pp_116019 and pp_116021)* and the *histone H3 downregulation (pp_244922)* (Dataset 4.2, Dataset 4.5). In *Arabidopsis*, it has been reported that AtATX2 dimethylates 'Lys-4' of histone H3 (H3K4me2), being this modification a specific tag for epigenetic transcriptional activation (Pien *et al.*, 2008; Saleh *et al.*, 2008; Shafiq *et al.*, 2014).



Conclusions

To understand the regulation of the response of maritime pine to ammonium availability it is necessary to carry out a holistic study involving transcriptomics, epitranscriptomics, proteomics and metabolomics. According to our data integration, it was observed that NH_4^+ is acting as signal molecule (Chapter 3) triggering a root systemic response that mainly involved changes in key pathways such as carbon and nitrogen metabolism, defense response or ET signaling pathway. Interestingly, ET-related response observed was different from that of previously reported in other NH_4^+ tolerant plants such as rice (Sun *et al.*, 2017). Furthermore, it was observed that a differential m⁶A deposition might play a key regulatory role on the MAPK signal-transduction pathway. In addition, differential epitranscriptomic approaches showed that posttranscriptional marks might play important roles regulating translational process and gene expression. In turn, a differentially expressed miR was identified in the presence of NH_4^+ whose putative target was *PpGSIb*. More experimental efforts might demonstrate its biological implication, which could constitute a biotechnological tool of paramount importance (Zhang and Wang, 2015).

In summary, the reported data constitutes an important advance in the current understanding on how nitrogen nutrition is regulated in conifers. In addition, the present study reveals key points on the ammonium nutrition stimulus and provide new insights on how the response differs between biological systems.

Supplemental material:

All the supplemental materials are provided in the folder Chapter 4 – Supplemental Material, accessible through this link:

https://drive.google.com/drive/folders/1qx5s3J-t0H1CAC4gtq9AYq_qA9NoJmuW?usp=sharing

Dataset S4.1. Normalized data from root metabolite profiling. (Pendrive).

Dataset S4.2. This dataset includes: whole root DRS differential expression results. DE transcripts up-regulated are in highlighted red. DE transcripts down-regulated are in highlighted blue. SEA Whole root DRS differential repressed transcripts results. SEA Whole root DRS differential upregulated transcripts results.

Significant DE miRNA's target prediction results. Putative miRNA's precursor prediction results. Putative miRNA's precursor prediction results. SEA Whole root DRS differential repressed miRNA targets results. SEA Whole root DRS differential over-expressed miRNA targets results. (Pendrive).

Dataset S4.3. This dataset includes: whole root DRS differential proteomics results. DE proteins/peptides up-regulated are in highlighted red. DE proteins/peptide down-regulated are in highlighted blue. SEA results from Whole root DRS differential proteomics under-represented results. SEA results from Whole root DRS differential proteomics over-represented results. (Pendrive).

Dataset S4.4. This dataset includes: whole root DRS differential modification results. DE transcripts over-modified are in highlighted red. DE transcripts under-modified are in highlighted blue. Specific GO terms related to differentially modified transcripts. Whole root common DRS differential modification and DRS transcriptomic and proteomic results. Whole root DRS differential over-modified transcripts results. Whole root DRS differential under-modified transcripts results. (Pendrive).

Dataset S4.5. This dataset includes: whole root significant peaks after RIP-seq analysis. m⁶A peaks in ammonium samples are highlighted in red. m⁶A peaks in control samples are highlighted in blue. Transcripts variants from a same gene are highlighted in yellow. Predicted methylation sites near the RIP peaks. BERMP web server was used to determine putative m⁶A sites. (Pendrive).

Supplemental Figures:

All the supplemental figures are provided in the folder Chapter 4 – Supplemental Material, accessible through this link:

https://drive.google.com/drive/folders/1qx5s3J-t0H1CAC4gtq9AYq_qA9NoJmuW?usp=sharing

Supplemental Figure 4.1 (Figure S4.1). Functional enrichment results (SEA) of positive differential expressed (DE) transcripts from Direct RNA Sequencing results. (Pendrive).

Supplemental Figure 4.2 (Figure S4.2). Functional enrichment results (SEA) of negative differential expressed (DE) transcripts from Direct RNA Sequencing results. (Pendrive).

Supplemental Figure 4.3 (Figure S4.3). Functional enrichment results (SEA) of overrepresented proteins from differential proteomic results. (Pendrive).

Supplemental Figure 4.4 (Figure S4.4). Functional enrichment results (SEA) of underrepresented proteins from differential proteomic results. (Pendrive).

Supplemental Figure 4.5 (Figure S4.5). Functional enrichment results (SEA) of overrepresented MIR targets from miRNA-seq results. (Pendrive).

Supplemental Figure 4.6 (Figure S4.6). Functional enrichment results (SEA) of underrepresented MIR targets from miRNA-seq results. (Pendrive).

Supplemental Figure 4.7 (Figure S4.7). Functional enrichment results (SEA) of overmodified and undermodified transcripts from Direct RNA Sequencing epitranscriptomic results. (Pendrive)



General Discussion



In the last few years, an international trend has emerged in science education towards approaches based on the relationship between the teaching of concepts and the needs of the real world, making science education more meaningful, relevant and motivating for graduate students (Wieringa *et al.*, 2011).

It is well known that, in each university career, students must carry out practices so that they can develop and apply the knowledge they have acquired in their theoretical classes, being this even more important in scientific-technical careers (Van Son *et al.*, 2014). Likewise, practical classes play a key role in the learning of new knowledge and the establishment of the already acquired ones. On many occasions, practical classes are based on archaic approaches that have nothing to do with the needs in an academic and / or labor world. Chapter 1 shows the development of a practical protocol that not only helps undergraduate students to understand the importance of nitrogen (N) acquisition and metabolism for plants, but also helps them to understand and relate the knowledge of the theoretical lessons taught, through the training of practical skills in the laboratory (extracting proteins, performing enzymatic activities, isolating RNA or studying gene expression, among others) (Chapter 1). This means that students not only reinforce their knowledge on N metabolism, but also acquire experience in the handling of current laboratory techniques that present a high horizontal transference between their formal teaching and their hypothetical future work possibilities. Thus, Chapter 1 shows that N constitutes a limiting and essential macronutrient for plant development (Marschner, 2012; Buchanan, 2015, Chapter 1).

For most plant species of agronomic interest, ammonium (NH_4^+) based nutrition as the main source of N can produce toxic effects that are able to compromise their growth and development (Esteban *et al.*, 2016; Liu and von Wirén, 2017). Among a set of phenotypic effects, it could be mentioned: decrease in vegetative growth, alteration in the root apparatus / aerial apparatus relationship, chlorosis in leaves and changes in root architecture stands out (Esteban *et al.*, 2016). These effects become evident, generally, when NH_4^+ concentration applied is within the millimolar range (Liu and von Wirén, 2017) being associated with several causes such as the ionic content imbalance due to the alteration of the incorporation process of other cations (K^+ , Ca^{2+} or Mg^{2+}), intracellular alkalization, extracellular acidification, alteration of the hormonal balance and oxidative stress, among the

main causes (Esteban *et al.*, 2016). Nevertheless, considering the differential biomass accumulation and ^{15}N incorporation rate, maritime pine exhibited a strong preference for NH_4^+ over other alternative sources of N (Chapter 2).

Different root transcriptomic analysis in various NH_4^+ -sensitive/tolerant plant models have shown that the response to NH_4^+ nutrition is highly dynamic and time dependent, observing that the number of differentially expressed genes (DEGs) increases as the time of exposure to this element increases (Patterson *et al.*, 2010; Canales *et al.*, 2010; Sun *et al.*, 2017; Yang *et al.*, 2018; Tang *et al.*, 2019). This transcriptome dynamics is in accordance with the results obtained in the short-term regulation of gene expression in roots of *Pinus pinaster* exposed to NH_4^+ nutrition; the different omics responses studied although notable were not exacerbated (Chapter 3 and 4). Thereby, induction of the defensive response (Chapter 3 and 4) constitutes one of the main characteristics observed at transcriptional level what agrees with data reported in other plant species (Patterson *et al.*, 2010; Sun *et al.*, 2017). In addition, a wide range of responses to NH_4^+ nutrition were observed such as the upregulation of N assimilating enzymes (Figure D.1), oxidative stress and pathways involved in secondary metabolism (Chapter 3 and 4) (Patterson *et al.*, 2010; Canales *et al.*, 2010; Sun *et al.*, 2017; Yang *et al.*, 2018; Tang *et al.*, 2019). Related to N assimilation, it is well known that the GS/GOGAT cycle constitutes the main pathway for the incorporation of inorganic nitrogen into amino acids (Bernard and Habash, 2009). Several *GSI* overexpression studies have been performed to improve NUE (nitrogen use efficiency) and for phytoremediation obtaining promising results for biotechnological applications (Habash *et al.*, 2011; Castro-Rodríguez *et al.*, 2016b, Hu *et al.*, 2018; Gao *et al.*, 2019). In Chapter 4, we identified a DE miRNA (*miR217*) that present *PpGSIb* as target (Chapter 4) (Figure D.1). To our knowledge, this finding constitutes the first report of the miRNAs role that putatively regulates specifically a GS isogene. It would be interesting to study the expression patterns of *miR217* under different N conditions (suboptimal or excessive) to elucidate its biotechnological potential in the manipulation of the N assimilatory pathway through anti-miRNA technology (Eamens and Wang, 2011).

The increase in intracellular levels of reactive oxygen species (ROS) and oxidative stress due to the high presence of NH_4^+ has also been reported (Patterson *et al.*, 2010; Esteban *et al.*, 2016; Liu and von Wirén, 2017; Sun *et al.*, 2020). Superoxide

dismutase (SOD), catalase (CAT), glutathione reductase (GR) and ascorbate peroxidase (APX) activities have been determined to be crucial in order to prevent ROS deleterious effects (Patterson *et al.*, 2010; Sun *et al.*, 2020). Neither transcriptomic nor proteomic analyses showed significant changes in any of these antioxidant enzymes. However, the occurrence of epitranscriptomics modifications suggest that regulation of the gene expression is in some way mediated by chemical modifications in RNA (Chapter 3 and 4). The integration of the results obtained in short-term experiments (24 hours) suggests that GABA play an important role in modulating ROS levels in a first stage (Chapter 4) where antioxidant genes seemed to be finely regulated, as pointed out by epitranscriptomic data and their absence in transcriptomic and proteomic analyses (Chapter 4). It has been described that in the presence of NH_4^+ , *Arabidopsis* roots have a higher content of both oxidized ascorbate and oxidized glutathione (GSSG) (Patterson *et al.*, 2010). These molecules are key metabolites within the ascorbate-glutathione cycle, one of the main routes for the elimination of ROS in plants (Milter, 2002). However, metabolite profiling in the roots of maritime pine in presence of NO_3^- or NH_4^+ during a long-term period did not show a fully support to what it was previously observed in *Arabidopsis*. In maritime pine, higher levels of GSSG were observed in the roots treated with NO_3^- (Chapter 2). According to the literature, ROS can act as a signal that affect primary root elongation (Liu and von Wirén, 2017; Jia and von Wirén, 2020). All above results strongly suggest that ROS levels at long-term conditions could be one of the reasons for the differences in root biomass observed on the N nutrition characterization work (Chapter 2). This makes the oxidative response an interesting point deserving attention in future studies.

In addition, our root microdissection transcriptomic results showed that NH_4^+ triggers important changes in the expression levels of several transcription factors (FTs) involved in root growth and development, such as *PpSHR*, *PpNAC31*, *PpNAC38* and DOFs (putative PEAR-like *PpDOF11* and *PpDOF12*), among others (Chapter 3) (Figure D.1). Further functional studies could shed light about the importance of these FTs in maritime pine root growth and maintenance since their relationship with NH_4^+ has been proposed for the first time in the present work (Chapter 3). Furthermore, comparative microdissection and functional studies in other model plants such as rice, wheat or *Arabidopsis* could provide new insights

on how NH_4^+ is affecting the expression of these genes and their cross importance regulating NH_4^+ -associated root phenotypes.

Moreover, it is notable to mention that other factors that probably are involved in NH_4^+ -root system architecture (RSA) are phytohormones, specially auxin (IAA) and ethylene (ET) (Chapter 3 and 4). Regarding IAAs, several reports described that inhibition of root elongation is accompanied by a loss in root gravitropism affecting the activity of the root meristem (Zou *et al.*, 2012; Liu Y *et al.*, 2013). This effect seems to be related to delayed lateral auxin redistribution, the potassium carrier TRH1 pathway and affecting auxin transporters expression in *Arabidopsis* (Li B *et al.*, 2011; Zou *et al.*, 2012, 2013). These findings are coherent with an alteration of IAA transport that is proposed in Chapter 3 (Figure D.1), although it is suggested that the molecular mechanism may be different. These mechanisms probably involve the modulation of auxin transporters localization, at least at the time point analyzed (Chapter 3). Likewise, ET is known to be implicated in lateral root (LR) formation and may affects AUX1 (IAA transporter) function (Negi *et al.*, 2008, 2010). It is described that high levels of ET in the root environment can promote both acropetal and basipetal auxin transport in roots, preventing the localized accumulation of auxin needed to drive LRs production (Negi *et al.*, 2008; Lewis *et al.*, 2011). Interestingly, our complete root multi-omics study pointed out that maritime pine root decreased ET response under NH_4^+ nutrition (Chapter 4). This fact constitutes the opposite response observed in *Arabidopsis*, an NH_4^+ -sensitive plant (Li G *et al.*, 2013), or in rice, an NH_4^+ -tolerant plant (Sun *et al.*, 2017). This response could be related to the alteration of the auxin distribution proposed in Chapter 3 due to NH_4^+ alters IAA transport, and having been described that IAA transport is partially restored when antagonists of ET perception (Ag^+) are applied (Li G *et al.*, 2013). Dual role of IAA and ET could be one reason for the RSA differences observed (Chapter 2). It is true that in the whole root results, no changes were observed in gene expression, modifications of RNA and protein levels of the transcripts proposed to be involved in the alteration of IAAs distribution (Chapter 3). This can be explained by a dilution effect of their expression levels, since changes in the expression patterns of these transcripts were specifically located in the root cortex zone (RDC), a highly localized area of the root apex (Chapter 3 and 4). Interestingly,

the integration of multiomic results obtained in Chapter 4 results suggest a reconfiguration of the ribosomal proteins and elongation factors that include all biological levels although this is more accused in epitranscriptomics and proteomics (Figure D.1) (Dataset 4.2, 4.3, 4.4) (Chapter 4). This suggests that NH_4^+ nutrition promotes a general translation activation to support the root growth of maritime pine seedlings observed under long term NH_4^+ supply (Chapter 2). This kind of effects over ribosomal protein composition and proteins involved in translation has been previously observed in different conditions including plant mineral nutrition (Wang *et al.*, 2013; Prinsi and Espen, 2018). The obtained data suggest that the modification in these elements can be mediated in an important proportion by the epitranscriptomic modifications in the transcripts of these proteins (Figure D.1). As one of the main points, these changes could influence the ribosome functions and performance. Although, more research efforts are required to functionally validate this observation.

Be that as it may, these evidences show the relevant role of phytohormones in modulating root growth and development in *Pinus pinaster*, at least in the presence of NH_4^+ . Similar medium- and long-term studies could provide information about the modulation of the responses observed in short-term experiments. Furthermore, in order to get a complete idea of the processes that are being carried out, it would be necessary to study the rest of the sections in the plant. Thanks to the implementation of these approaches, the way is paved to carrying out functional studies that contrast these evidences. As well as the study of the response of the maritime pine roots to other nitrogen sources, which would provide information about the specificity of the response observed.

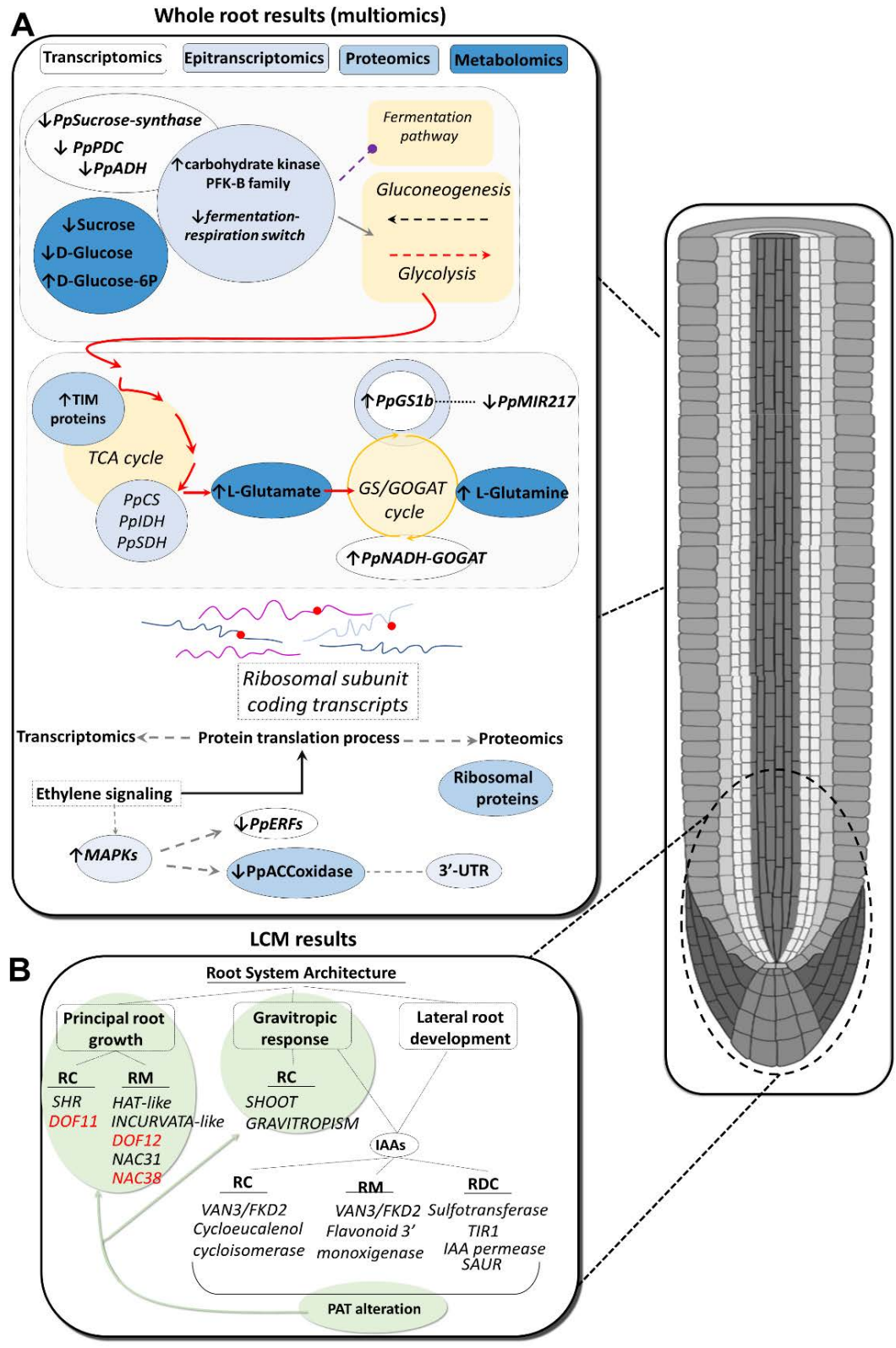


Figure D.1. Schematic representation of the main omics results obtained in Chapter 4 and Chapter 3 (from the top to the bottom). A. Results from integration of multiomics approaches pointed out an important relationship between transcriptomic, epitranscriptomic, proteomic and metabolite content data. Protein

translation process was the most affected term by differentially epitranscriptomic modifications. B. Ammonium affects to the expression of several transcription factors and auxins (IAAs) related transcripts probably related to root system architecture processes.



Conclusions



1. The laboratory experience on plant nitrogen nutrition designed and executed in this work enables undergraduate and graduate students to develop interdisciplinary technical and scientific skills, from agronomy and plant physiology to biochemistry and molecular biology.
2. Ammonium and nitrate are alternative sources of inorganic N for maritime pine nutrition. In roots, ammonium is more efficiently incorporated than nitrate being the main organ involved in the accumulation of an excess of ammonium whereas the stem is the main organ involved in the accumulation of excess nitrate.
3. Ammonium nutrition promotes a greater increase in maritime pine root biomass than nitric nutrition. The nitrogen status of needles was higher in ammonium nutrition than in nitric nutrition.
4. The data of the present work support that ammonium acts as a signal molecule in the development stage of maritime pine studied.
5. The application of capture laser microdissection followed by NGS (Next Generation Sequencing) allowed the identification of new transcripts not included in the pre-existing transcriptomic databases of maritime pine, such as *PpNAC38*, *PpDOF11* or *PpDOF12*.
6. Ammonium influences, directly or indirectly, the gene expression of transcription factors involved in root architecture, such as *PpSHORT-ROOT* or *PpSHOOT-GRAVITROPISM*.
7. Ammonium causes changes in the gene expression of transcripts linked to the metabolism and transport of important phytohormones in root system architecture (auxins, cytokinins and ethylene).
8. The integration of changes in transcriptome, epitranscriptome and proteome revealed a regulatory role of ammonium in different pathways such as carbon and nitrogen metabolism, in defensive response, in ethylene-mediated signaling pathway and in ribosome protein composition.



Material and Methods



Plant material and growth conditions

Tomato plants (Chapter 1)

Cherry tomato (*Solanum lycopersicum* var. *cerasiforme*) seeds were sowed in plastic pots (10 cm diameter) with vermiculite as the inert substrate. The seeds were irrigated with distilled water. The seedlings and plants were cultivated in a growth room at 25°C and 50/70% relative humidity with a 16/8 h photoperiod.

A week after emergence, the seedlings were irrigated with 40 mL of ¼ Hoagland solution (Hoagland and Arnon, 1950). This process was repeated once a week during the following two weeks. Additionally, the plants were also irrigated with distilled water once a week, 3-4 days after fertilization.

The plants were divided in two groups: optimal N supply (N+) and low N supply (N-). Each plant of the N+ group was irrigated with 80 mL of complete Hoagland solution once every two weeks. Each plant of the N- group was irrigated with 80 mL of low N Hoagland solution once every two weeks:

- Complete Hoagland solution: 3 mM KNO₃; 2 mM Ca(NO₃)₂•4H₂O; 0.1 mM chelated Fe (Sequestrene 138 Fe G100, Syngenta); 1mM MgSO₄•7H₂O; 0.5 mM (NH₄)H₂PO₄; 1X micronutrients solution (0.046 mM H₃BO₃, 0.013 mM MnCl₂•4H₂O, 0.8 mM ZnSO₄•7H₂O, 0.3 mM CuSO₄•5H₂O, 0.1 mM Na₂MoO₄•2H₂O).
- Low N Hoagland solution: 0.5 mM KNO₃; 2mM KCl, 2 mM CaCl₂; 0.1 mM chelated Fe (Sequestrene 138 Fe G100, Syngenta); 1mM MgSO₄•7H₂O; 0.5 mM KH₂PO₄; 1X micronutrients solution (0.046 mM H₃BO₃, 0.013 mM MnCl₂•4H₂O, 0.8 mM ZnSO₄•7H₂O, 0.3 mM CuSO₄•5H₂O, 0.1 mM Na₂MoO₄•2H₂O).

The plants were watered with distilled water during the weeks without irrigation with Hoagland solution. This procedure was maintained for eight weeks (Figure M1). The final amount of N supplied to N+ plants was 0.045 g and to N- plants 0.006 g.

Materials and Methods

Days	Sowing (D0)	D7	D14	D21	D28	D35	D42	D49	D56	D63	D70	D77	D84	D91	D98-D101
Water	100 mL	80 mL					80 mL		80 mL		80 mL		80 mL		Harvest and lab practice
Hoagland 1/4			40 mL	40 mL	40 mL										
Complete Hoagland							80 mL		80 mL		80 mL		80 mL	80 mL	
Low N Hoagland							80 mL		80 mL		80 mL		80 mL	80 mL	

Days	D98	D99	D100	D101
Plant weighing				
Plant material frozen				
Protein extraction				
Protein Quantification				
SDS-PAGE				
Western blotting				
Chlorophyll meas.				
RNA extraction				
RNA quantification				
RT-qPCR				

Figure M1. Time schedule including plant irrigation and the main laboratory techniques or objectives. Light blue squares correspond to actions applied for all the samples. Red squares correspond to the group of plants treated with optimal N amount. Orange squares correspond to the group of plants treated with low N amount.

The tomato plants were harvested in the laboratory. Four plants were harvested for each treatment, one plant by each student working group. The roots were rinsed in water to eliminate vermiculite. Next, the plants were dried off with a paper cloth. The tomato plants were sectioned in two parts (shoots and roots) using a scalpel. The shoots and roots were weighed in an electronic scale, and the results were annotated. The samples were kept on ice until used for protein extraction. Samples for total RNA extraction were flash frozen in liquid nitrogen and stored at -80°C until use.

Pine seedlings (Chapter 2)

Maritime pine seeds (*Pinus pinaster* Ait.) from Sierra Bermeja (Estepona, Spain) (ES20, Ident.–11/12) were obtained from the *Área de Recursos Genéticos Forestales* of the Spanish *Ministerio de Agricultura, Pesca y Alimentación*. Pine seeds were imbibed in distilled water for 48 h under continuous aeration and germinated with vermiculite as an inert substrate. Pine seedlings were cultivated in a growth chamber with a 16/8 h light/dark photoperiod, light intensity of $125 \mu\text{mol m}^{-2} \text{s}^{-1}$, constant temperature of $26\text{--}27^{\circ}\text{C}$, and 75%–80% relative humidity. Forty seedlings aged one month were randomly transplanted into forestall seedbeds for each experimental condition. The seedlings were grown in a greenhouse from February to April of 2019 at a mean temperature of 25°C and 50/70% relative humidity with a 16/8-h photoperiod (*Instituto de Hortifruticultura Subtropical y*

Mediterránea, IHSM La Mayora UMA-CSIC). Each group was irrigated twice per week with 40 mL of the corresponding N solution or 40 mL of distilled water. Five experimental conditions were tested: 8 mM NH₄Cl; 6 mM NH₄Cl – 2 mM KNO₃; 4 mM NH₄Cl – 4 mM KNO₃; 2 mM NH₄Cl – 6 mM KNO₃; 8 mM KNO₃. After 60 days of treatment, seedlings were subdivided and harvested in three random groups. The seedlings were divided into three different sections (cotyledon, hypocotyl, and roots). Each section was weighed and immediately frozen in liquid N₂. For the N uptake analyses, one-month-old seedlings grown in vermiculite and only irrigated with distilled water were used. They were separated into two groups. One group was fed with 7.5 mM of ¹⁵N-labelled ammonium and the second one with 7.5 mM of ¹⁵N-labelled nitrate. The plants were harvested at different times after nutrient application: 0, 15, 30, 60, 120, and 240 min. Each organ was isolated, weighed, and immediately frozen in liquid N₂. Three biological replicates were taken. Each replicate consisted of a pool of five seedlings. All samples were stored at –80 °C until powdering with a mixer mill MM400 (Retsh, Haan, Germany) and further analyses were conducted.

Pine seedlings (Chapters 3 and 4)

Maritime pine seeds (*Pinus pinaster* Ait.) from “Sierra Segura y Alcaraz” (Albacete, Spain) were provided by the *Área de Recursos Genéticos Forestales* of the Spanish *Ministerio de Agricultura, Pesca y Alimentación*. Seed germination was carried out following the protocol described elsewhere (Cañas *et al.*, 2006). Seedlings were grown in vermiculite in plant growth chambers under 16 h light photoperiod, a luminal intensity of 100 μmol m⁻² s⁻¹, a constant temperature of 25 °C and watered twice a week with distilled water. One-month old maritime pine seedlings were used for the experiments. Pine seedlings were randomly subdivided into three different groups, relocated into forestall seedbeds and irrigated with 80 mL of a solution that contains macro- and micronutrients without any N source (1.16 mM KCl; 0.63 mM KH₂PO₄; 0.35 mM MgSO₄·7H₂O; 0.17 mM CaCl₂·H₂O; 80 μM EDTA-FeSO₄; 25.9 μM H₃BO₃; 10.2 μM MnCl₂·4H₂O; 1.3 μM ZnSO₄·7H₂O; 0.7 μM CuSO₄·5H₂O; 0.1 μM Na₂MoO₄·2H₂O). After three days of acclimation, the control group was irrigated with 80 mL of water (C), and the second group was supplied with 80 mL of 0.1 mM NH₄Cl (0.1) and the third group was supplied with 80 mL of 3 mM NH₄Cl (3). Root samples were collected before

the irrigation and at two different time points after the treatments (2 and 24 hours) and immediately frozen in liquid N (Figure M2).

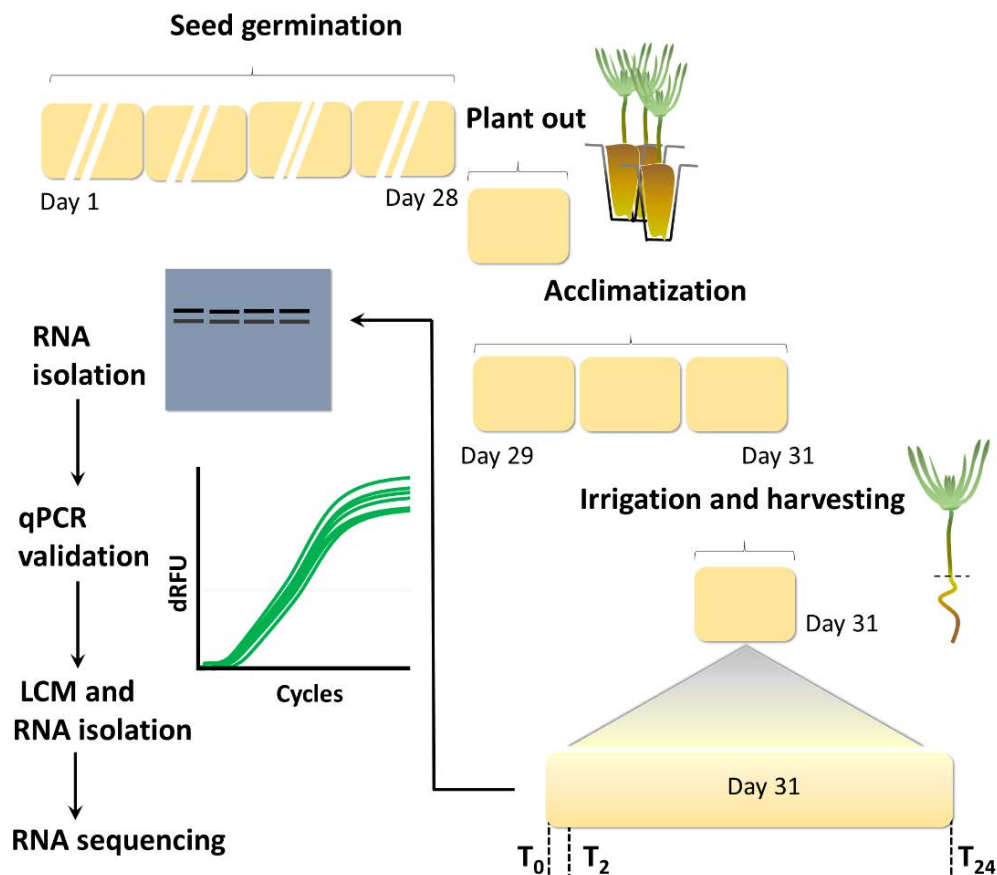


Figure M2. Experimental procedure scheme.

Ten seedlings were collected and pooled per each sample. The same experiment was carried out three independent times. The screening condition and adequate development of each experiment was verified through the gene expression analysis by RT-qPCR of a control gene, *PpAMT1.3* (GenBank Accession KC807909) following previous results of Castro-Rodríguez *et al.* (2016). Additionally, in order to perform laser capture microdissection (LCM) technique in the most responsive condition, seedling's root tips were cut and tissues of 5-6 mm were imbibed in a specimen holder with Tissue-Tek optimal cutting temperature embedding medium (Sakura Finetek, Alphen aan den Rijn, The Netherlands) and immediately frozen in liquid N for cryostat sectioning. Frozen samples were stored at -80°C until use.

Protein extraction

The tomato samples were completely disrupted by grinding in a precooled mortar (on ice) with extraction buffer (50 mM Tris-HCl pH 8, 2 mM EDTA, 20 mM 2-mercaptoethanol and 2% (w/v) polyvinyl(poly)pyrrolidone (PVPP)) and fine sea sand. The sample and buffer ratio should be 1/4 (w/v) for leaves and 1/2 (w/v) for roots. The sample and fine-sea-sand ratio should be 1/0.5 (w/w) for leaves and 1/0.25 for roots.

The protein extracts were placed into 1.5-mL Eppendorf tubes and centrifuged during 10 min at 4°C and 22,000 g. Supernatants were collected in clean tubes and stored on ice until use.

Soluble proteins of pine seedlings were extracted using 100 mg of sample ground powder for stem and roots and 50 mg in the case of needles. The extraction was performed by adding 1 mL of extraction buffer (50 mM Tris-HCl pH 8, 1 mM EDTA, 10 mM MgCl₂, 0.5 mM dithiothreitol (DTT), 20% (w/v) glycerol, 0.1% (v/v) Triton X-100, 1% (w/v) polyvinylpyrrolidone (PVP), and 1% (w/v) polyvinyl(poly)pyrrolidone (PVPP)) and 30 mg of fine sea sand. The resulting extract was centrifuged at 12,000 g for 30 min at 4 °C.

The soluble protein amounts were measured following the Bradford method (Bradford, 1976) with the Bradford Protein Assay reagent (Bio-Rad, Ca, USA). For tomato samples two different dilutions, 1/800 and 1/1600, of protein extracts were used for analysis. A protein standard curve was obtained with six increasing concentrations of bovine serum albumin (BSA): 1, 2, 4, 6, 8 and 10 µg/mL respectively.

Dilutions of protein extracts as well as the BSA standard curve, were measured in triplicate. Next, 200 µL of the Bradford Protein Assay reagent was added to 800 µL of each protein sample. The final solutions were incubated for 15 min.

The colorimetric assay was determined at 595 nm in a spectrophotometer. The soluble protein amount was calculated based on the linear regression of the BSA standard curve.

Enzyme Activity Measures

GS activity was measured using the transferase assay described in a previous report (Cánovas *et al.*, 1984). The reaction mix contained 500 µL of 0.2 M Tris-HCl pH 8, 100 µL of 0.6 M NH₂OH (pre-equilibrated to pH 7 with NaOH), 100 µL of 1 M

Materials and Methods

glutamate, 100 μL of 62.5 mM ATP, 100 μL of 0.3 M MgSO_4 and 100 μL of protein extract in a final volume of 1 mL. For pine samples the final reaction volume was adjusted to 150 μL and the assay was developed in microtiter plates. For each sample a control reaction was prepared without glutamate. The autozero was obtained with the entire reaction solution without protein extract. The reaction was initiated with addition of the protein extract. The reaction mixes were incubated at 37°C for 15 min. The reaction was stopped with the addition of 350 μL of GS-STOP solution (10% (w/v) $\text{FeCl}_3 \cdot 6\text{H}_2\text{O}$ in 0.2 N HCl; 24% (w/v) trichloroacetic acid; and 50% (w/v) HCl). The solution was mixed by inversion. The tubes were centrifuged at 4000 g for 5 min. The supernatants were recovered and their absorbances recorded on a spectrophotometer at 540 nm. The reaction product is L- γ -glutamylhydroxamate and an extinction coefficient of 298 $\text{M}^{-1}\text{cm}^{-1}$ was used to calculate GS activity. GS activity in tomato samples was determined only in the leaves because a protein that inhibits GS reaction has been previously reported to be present in tomato roots (Gallardo and Cánovas, 1992).

For estimation of glutamate dehydrogenase (GDH, EC 1.4.1.2) activity, the NADH-GDH assay was used (Turano *et al.*, 1996). The reaction was developed with 180 mM Tris-HCl pH 8, 5 mM $(\text{NH}_4)_2\text{SO}_4$, 0.1 mM CaCl_2 , 2 mM NADH and 15.6 mM 2-oxoglutarate in a final volume of 250 μL . The reaction was launched with the addition of 2-oxoglutarate. Aspartate aminotransferase (AspAT, EC 2.6.1.1) and alanine aminotransferase (AlaAT, EC 2.6.1.2) activities were measured following Gibon *et al.* (2004) in a final reaction volume of 100 μL . For AspAT the reaction mix contained 100 mM Tris-HCl pH 7.8, 50 mM L-aspartate, 0.07 mM pyridoxal phosphate (PLP), 0.25 mM NADH, 0.6 U of malate dehydrogenase and 5 mM 2-oxoglutarate. The reaction was launched with the addition of 2-oxoglutarate. For AlaAT the reaction mix contained 100 mM Tris-HCl pH 8, 25 mM L-alanine, 0.25 mM pyridoxal phosphate (PLP), 3.75 mM NADH, 1.5 U of lactate dehydrogenase and 5 mM 2-oxoglutarate. The three enzymatic reactions were measured continuously following the NADH oxidation through absorbance determinations at 340 nm. The amount of NADH oxidized by the reaction was calculated using a NADH standard with 0-187.5 nmol in range.

SDS-PAGE and western blotting analysis

Loading buffer was added to a final concentration of 1X (30 mM Tris-HCl, pH 6.8, 1% (w/v) sodium dodecyl sulfate (SDS), 10% (v/v) glycerol, 0.001% (w/v) bromophenol blue, 0.5 M 2-mercaptoethanol) for samples used in SDS-PAGE and western blotting. The samples containing the loading buffer can be stored at -20°C until use.

The samples with loading buffer were boiled for 5 min and subjected to electrophoresis in 12.5% (w/v) SDS-polyacrylamide gels (Laemli, 1979). Twenty micrograms of proteins were loaded in each well. Five microliters of All Blue Precision Plus Protein™ Prestained Standard (BioRad) was used as marker ladder for each gel.

Polyacrylamide gels for protein profiles were stained with Coomassie blue solution (0.1% (w/v) Coomassie R-250, 10% (v/v) acetic acid, 40% (v/v) methanol) for 25 minutes and then destained overnight (2% (v/v) acetic acid, 40% (v/v) methanol). Images of the SDS-PAGE gels were obtained in a ChemiDoc XRS+ (Bio-Rad).

For western analysis, the gels were equilibrated for 10 min in Towbin transfer buffer (25 mM Tris, 192 mM glycine pH 8.3, 20% methanol) (Towbin *et al.*, 1979) and electroblotted to nitrocellulose membrane (Amershan Protran Premium 0.45 NC), in a Trans-Blot® Turbo™ Transfer System (Bio-Rad) following the manufacturer instructions (18 V during 32 min).

The membranes were blocked for 1 h with 5% (w/v) of non-fat milk powder dissolved in tween-phosphate buffered saline (TPBS): 1X PBS (140 mM NaCl, 3 mM KCl, 5 mM Na₂HPO₄, 1.47 mM KH₂PO₄, pH 7.4) with 0.05% (v/v) Tween-20. After blocking, the membranes were incubated overnight at 4°C with antiserum against pine GS1 (Cantón *et al.*, 1996) diluted in TPBS with 0.05% (w/v) of bovine serum albumin (BSA) (dilution 1:5,000). The membranes were washed three times with TPBS. Antigen-antibody complexes were detected with a goat anti-rabbit IgG-HRP (Santa Cruz Biotechnologies). The membranes were incubated for 2 h at room temperature with peroxidase-conjugated secondary antibodies diluted in TPBS with 0.05% (w/v) BSA (dilution 1:10,000). Finally, the membranes were washed twice with TPBS and then twice with phosphate buffered saline (PBS). Immunodetection was visualized with the Supersignal West Pico Chemiluminescent Substrate (Thermo) following manufacturer's instructions. The membranes were incubated

with a mix 1:1 (v:v) of Stable Peroxide Solution and the Luminol/Enhancer for 3–5 min. The images were captured with a ChemiDoc XRS+ (Bio-Rad).

Chlorophyll measurement

Fifty microliters of crude extract from a leaf protein extraction were mixed with 950 μ L of 80% (v/v) acetone for subsequent chlorophyll quantification. The crude protein extract was collected with cut micropipette tips. The tubes were well vortexed and stored overnight at 4°C in dark conditions. After incubation, the sample was centrifuged at 22,000 g and 4°C for 10 min. The supernatant was recovered and the absorbances at 663 nm and 647 nm were measured on a spectrophotometer. The chlorophyll content was calculated as follows (Lichtenthaler and Buschmann, 2001):

$$\text{Chlorophyll A (CHLA; } \mu\text{g/mL)} = \text{Abs}_{663,2\text{nm}} * 12,25 - \text{Abs}_{646,8\text{nm}} * 2,79$$

$$\text{Chlorophyll B (CHLB; } \mu\text{g/mL)} = \text{Abs}_{646,8\text{nm}} * 21,5 - \text{Abs}_{663,2\text{nm}} * 5,1$$

$$\text{Total chlorophylls (CHL; } \mu\text{g/mL)} = \text{CHLA} + \text{CHLB}$$

Total RNA extraction

Total RNA was extracted following the protocol described by Canales *et al.* (2012). In a 1.5-mL Eppendorf tube, approximately 100 mg of each frozen and powdered tissue (one-two spatula tips) was extracted with 600 μ L of preheated (65°C) CTAB extraction buffer (3% (w/v) cetyltrimethylammonium bromide (CTAB), 100 mM Tris pH 8, 2 M NaCl, 30 mM ethylenedinitrilotetraacetic acid (EDTA), 2% (w/v) polyvinylpyrrolidone (PVP), 2% (w/v) polyvinylpolypyrrolidone PVPP, and 4% (v/v) 2-mercaptoethanol). The samples were well mixed and incubated for 6 min at 65°C in a water bath. The same volume of chloroform/isoamyl alcohol (24:1) was immediately added (600 μ L) to the tube. The samples were well-mixed and centrifuged for 10 min at 22,000 g at 4°C. The supernatant was recovered in a new 1.5-mL Eppendorf tube, and an equal volume of 4 M LiCl was added and mixed by inversion. The samples were incubated at 4°C overnight. After the incubation, the samples were centrifuged at 22,000 g for 25 min at 4°C to pellet the RNA. The supernatant was eliminated, and the pellet was washed with 1 mL of 70% ethanol (centrifugation at 22,000 g for 10 min at 4°C), air dried for 15 min and resuspended in 50 μ L of sterilized distilled water. A treatment with RQ1 RNase-Free DNase (Promega, Wis, USA) was applied to remove genomic DNA from the RNA

samples. Total RNA quantification and purity were estimated using a NanoDrop ND-1000 spectrophotometer at 260 nm and 280 nm (Thermo Scientific, MA, USA), and RNA integrity was checked by agarose gel. For sequencing, RNA quality was also determined in a Bioanalyzer 2100 (Agilent, Santa Clara, CA, USA). The concentration was verified with a Qubit 4 Fluorometer (Invitrogen, Paisley, UK) and Qubit RNA BR, Broad-Range, Assay Kit (Invitrogen, Paisley, UK).

In the Chapter 1, for the RNA measures, dilutions (1/100) of the RNA samples were made in sterilized distilled water. The dilutions were placed in UVette® 220 nm – 1,600 nm cuvettes (Eppendorf, Germany) for the absorbance measures. For the concentration determination, the RNA coefficient of 40 µg/mL was used. The RNA quality was determined by the 260 nm/280 nm ratio (higher when the ratio is nearest to 2).

RT-qPCR analyses

Chapter 1

The GS gene expression was determined by RT-qPCR using the iTaq™ Universal One-Step RT-qPCR Kit (Bio-Rad, CA USA). The primers are shown in Table M1 (at the end of this section). The total RNA samples were diluted to a final concentration of 5 ng/µL. In a qPCR plate, 10 ng of total RNA (2 µL) were loaded in each well. A master mix was prepared and added (8 µL) to the wells containing total RNA (5 µL of iTaq universal SYBR Green [2x] (Bio-Rad, CA USA), 0.125 µL of iScript-rt (Bio-Rad, CA USA), 0.5 µL of primer mix (10 µM each) and 2,375 µL of nuclease-free water). The plate was placed in a CFX384 Touch™ Real-Time PCR Detection System (Bio-Rad, CA USA) and the reaction was developed as follows: 10 min at 50°C (reverse-transcription reaction); 3 min at 95°C (polymerase activation); 1 s at 95°C; and 5 s at 60°C. The two last steps were repeated 40 times. The qpcR package for the R environment (Ritz and Spiess, 2008) was used to estimate the gene expression from the raw fluorescence data. The MAK3 model was used to calculate the initial template fluorescence D0, which does not require the use of efficiencies in the qPCR assay. The results were normalized to the reference gene, *SICAC* (Solyc08g006960.2.1) (Expósito-Rodríguez *et al.*, 2008).

Chapters 2-4

Reverse transcription reactions were performed using iScript™ Reverse Transcription Supermix (Bio-Rad, CA, USA) using 1 µg of total RNA. The qPCR reactions were carried out using 5 ng of cDNA and SsoFast™ EvaGreen® Supermix (Bio-Rad, CA, USA) in a final volume of 10 µL. The reactions were developed on a C1000™ Thermal Cycler with a CFX384™ Touch Real-Time PCR Detection System (Bio-Rad, CA, USA) under the following conditions: 3 min at 95°C (1 cycle), 1 s at 95°C, and 5 s at 60°C (50 cycles), with a melting curve from 60°C to 95°C. The raw fluorescence data were analysed as described above. Expression data were normalized to two reference genes, *SKP1/ASK1* and *SLAP*, that were previously tested for RT-qPCR experiments in maritime pine (Granados *et al.*, 2016). For the qPCR analysis, three biological replicates and three technical replicates per sample were used. Primers used for qPCR in each chapter are presented in Table M1 (at the end of this section).

Laser capture microdissection (LCM), RNA isolation and low-input RNA-seq

LCM procedure was carried through as previously described (Cañas *et al.*, 2014). Full step protocol is described below: 1 day before cryosectioning, root tip samples were tempered at -20°C. Thirty micrometers thick sections were cut using a cryostat (CM1950, Leica Biosystems, Wetzlar, Germany) at -20°C and mounted on PET-membrane 1.4 µm steel frame (Leica Biosystems, Wetzlar, Germany). The PET-membrane containing samples were stored at -80°C until use.

Before microdissection, samples were fixed in cold 70% ethanol for 30 seconds, embedding medium was removed in DEPC-treated water for 2 min and refixed in cold 100% ethanol for 2 minutes. Afterwards, samples were air dried and used for microdissection. A laser microdissector (LMD 7000, Leica, Wetzlar, Germany) was used for microdissection. The samples obtained were placed into 0.5 mL tube caps containing 20 µL of lysis buffer from the RNAqueous-Micro RNA Isolation Kit (Ambion, USA) and all samples were placed at -80°C. Four different tissue areas were isolated by microdissection approximatively corresponding to the root cap (RC), meristem (RM), developing cortex (RDC) and developing vessels (RDV) areas.

All RNA extractions from the microdissection procedure were carried out using manufacturer's instruction protocol (non-LCM) for the RNAqueous-Micro RNA

Isolation Kit (Ambion, USA). RNA quality, DNA contamination and first quantification were performed via RNA Pico Assay for the 2100 Bioanalyzer (Agilent, Santa Clara, CA, USA). Quantification was verified via a Qubit RNA BR (Broad-Range) Assay Kit (Invitrogen, Paisley, UK). RNA samples with RNA integrity number (RIN) higher than 7 were used for subsequent RNA sequencing, mRNA amplification and cDNA synthesis.

The low input RNA-seq was carried out by Novogen (HK). The cDNA synthesis and amplification, and the library preparation was made with the SMART-Seq™ v4 Ultra™ Low Input RNA Kit for Sequencing (Takara, Mountain View, CA, USA) following the manufacturer's instructions. RNA sequencing was made in a NovaSeq 6000 sequencer according to the manufacturer's instructions for paired-end reads (Illumina, San Diego, CA, USA). The 24 samples were sequenced producing paired-end reads of 150 bp length. The sequencing output is shown in the Table M2.

Table M2. LCM low-input RNA sequencing results

Sample	Raw bases (Gb)	Final bases (Gb)	Raw reads (M)	Final reads (M)
A1T24_3_RC	11.92	9.9	79.47	68.01
A1T24_3_RDC	13.37	10.62	89.12	73.18
A1T24_3_RDV	11.64	9.6	77.58	66
A1T24_3_RM	12.83	10.58	85.52	72.75
A1T24_C_RC	13.39	10.99	89.24	75.87
A1T24_C_RDC	13.43	11.15	89.51	76.79
A1T24_C_RDV	12.41	10.3	82.73	70.78
A1T24_C_RM	11.66	9.69	77.76	66.58
A3T24_3_RC	12.16	9.96	81.08	68.83
A3T24_3_RDC	13.12	10.68	87.5	73.88
A3T24_3_RDV	13.23	10.83	88.2	74.94
A3T24_3_RM	12.82	10.67	85.46	73.55
A3T24_C_RC	13.22	10.86	88.13	75.16
A3T24_C_RDC	13.58	11.18	90.52	77.17
A3T24_C_RDV	12.48	10.38	83.23	71.75
A3T24_C_RM	12.9	10.62	85.98	73.28
A4T24_3_RC	13.71	11.44	91.42	78.82
A4T24_3_RDC	13.94	11.44	92.96	78.86
A4T24_3_RDV	14.87	12.19	99.11	84.48
A4T24_3_RM	12.45	10.32	82.97	71.08
A4T24_C_RC	15.67	12.79	104.46	88.36
A4T24_C_RDC	12.98	10.67	86.51	73.8
A4T24_C_RDV	12.47	10.39	83.13	71.54
A4T24_C_RM	12.89	10.47	85.4	71.87

The raw reads were trimmed (quality and contamination) using SeqTrimBB software (<https://github.com/rafnunser/seqtrimbb>). Only the pairs in which both reads passed the quality test were further analysed ($Q > 20$). Trimmed reads are shown in the Table M2. These reads were assembled using Trinity 2.11.0 (Haas *et al.*, 2013). Contigs lower than 400 pb were eliminated, for the rest of contigs the redundancy was reduced using CD-HIT-EST software (Fu *et al.*, 2012). The final transcriptome was used as the reference for the read mapping that was performed with BWA using the MEM option (Li and Durbin, 2009). The read count was obtained with the python script *sam2counts* (<https://github.com/vsbuffalo/sam2counts>). Differentially expressed (DE) transcripts were identified using the edgeR package for R, the transcripts were normalised by cpm and filtered; 2 cpm in at least 2 samples (Robinson *et al.*, 2010). Each sample was from a single seedling in a different experimental replicate. The

samples were basically grouped by tissue and nutritional condition (Figure M2), thus only the transcripts with $FDR < 0.05$ and the three experimental replicates with the same expression sense than the final logFC (positive or negative) were considered as differentially expressed.

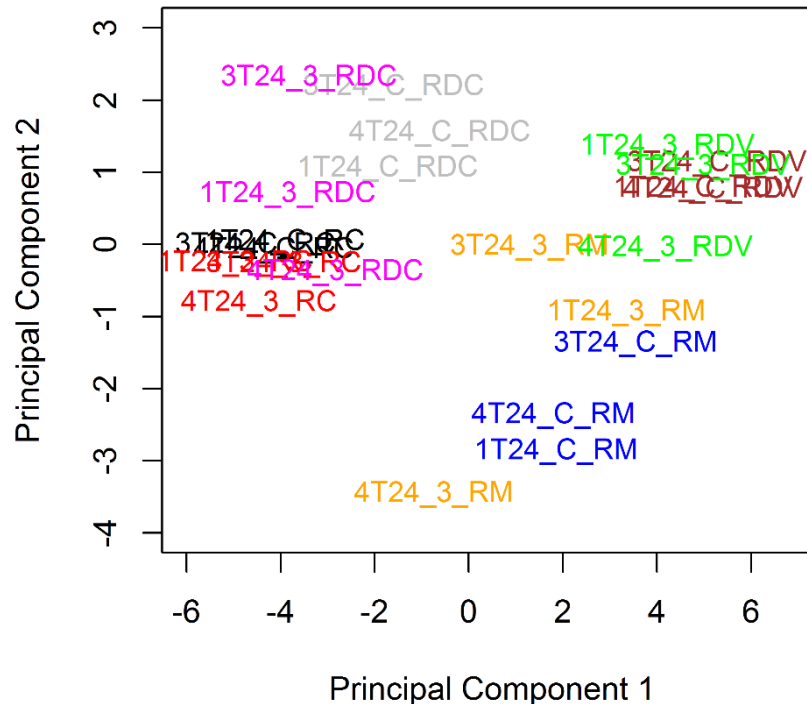


Figure M2. Multidimensional scaling plot (MDS) of LCM samples.

Functional annotation and enrichment analyses

The final assembled transcriptome was functionally annotated with BLAST2GO (Götz *et al.*, 2008) using DIAMOND software with *blastx* option (Buchfink *et al.*, 2015). The NCBI's plants-*nr* database (NCBI Resource Coordinators, 2016) was the subject in the search. Blast results were considered valid with $e\text{-value} < 1.0E\text{-}6$. Singular enrichment analysis (SEA) of the GO terms was made in the AGRIGO v2.0 web tool under standard parameters using as GO term reference the whole assembled transcriptome annotation (Tian *et al.*, 2017).

cDNA amplification from LCM RNA samples

As a result of RNA extraction from LCM samples, 1 ng of total RNA were retrotranscribed and amplified. In order to perform convenient relative gene expression analysis by qPCR, the cDNA synthesis and amplification protocol was carried out using Conifer RNA Amplification (CRA+) protocol previously described by (Cañas *et al.*, 2014). In order to monitor and control the amplification

Materials and Methods

process, the ERCC RNA Spike-in kit (ThermoFisher, Waltham, MA, EEUU) was used according to manufacturer's instructions (Figure M3).

First-strand cDNA synthesis 1 ng of total RNA was added to a mix containing 1 μ M dNTPs and 1 μ M polTdeg primer in a final volume of 7 μ L. Reaction mixtures were incubated in a thermal cycler for 5 minutes at 65°C. Subsequently, temperature was decreased to 50°C keeping tubes in the thermal cycler at 50°C for 1-3 minutes. Afterwards, 3 μ L RT mixture-1 (2 μ L of 5 \times first-strand buffer, 8.30 mM of MgCl₂, 0.5 μ L RevertAid H Minus Reverse Transcriptase (Thermo Scientific, Waltham, MA, EEUU) was added and reaction mix was gently mix by pipetting. All reaction tubes were incubated during 60 minutes at 50°C. When incubation time was ended, 10 μ L of RT mixture-2 (2 μ L of 5 \times first-strand buffer, 5.1 μ L nuclease-free water, 8.30 mM MgCl₂, 6 μ M MnCl₂ (100 mM), 1.95 mM PlugOligo-Adapter primer and 0.5 μ L RevertAid H Minus Reverse Transcriptase (Thermo Scientific, Waltham, MA, EEUU) was added to each tube. Reaction mixture was gently mixed by pipetting and incubated for 90 minutes at 42°C. The synthesized ss-cDNA was purified using the NucleoSpin® Gel and PCR Clean-up kit (Macheray-Nagel, Düren, Germany) according to the manufacturer's instructions.

The ds-cDNA was obtained by nested PCR reactions using the primer pairs Amp-ATTB1.1 / Amp-ATTB2.1 and AmpATT-1.2 / Amp-ATTB2.2, respectively. First PCR (PCR-1) reactions were performed in a total volume of 25 μ L, using 11.5 μ L of purified ss-cDNA, 2X iProof™ HF Master Mix (BioRad, CA, USA) and 1 mM Amp-ATTB1.1 and Amp-ATTB2.1 primer pairs. The result obtained was diluted 35 times with nuclease-free water and several second PCR (PCR-2) reactions were performed using 1 μ L of diluted ds-cDNA from PCR-1 step, 1 mM Amp-ATTB1.2 and Amp-ATTB2.2 primer pairs and 2X iProof™ HF Master Mix (BioRad, CA, USA) in a total volume of 50 μ L. Several reactions were pooled and purified using NucleoSpin® Gel and PCR Clean-up kit (Macheray-Nagel, Düren, Germany) according to the manufacturer's instructions. The quantity of the amplified ds cDNA was determined using the Qubit 4 Fluorometer (Invitrogen, Paisley, UK) and Qubit dsDNA BR Assay Kit (Invitrogen, Paisley, UK) and the quality of the final amplifications were corroborated by 1% (p/v) agarose gel electrophoresis. The primers used for cDNA synthesis and amplification are listed in the Table M1 (at the end of this section).

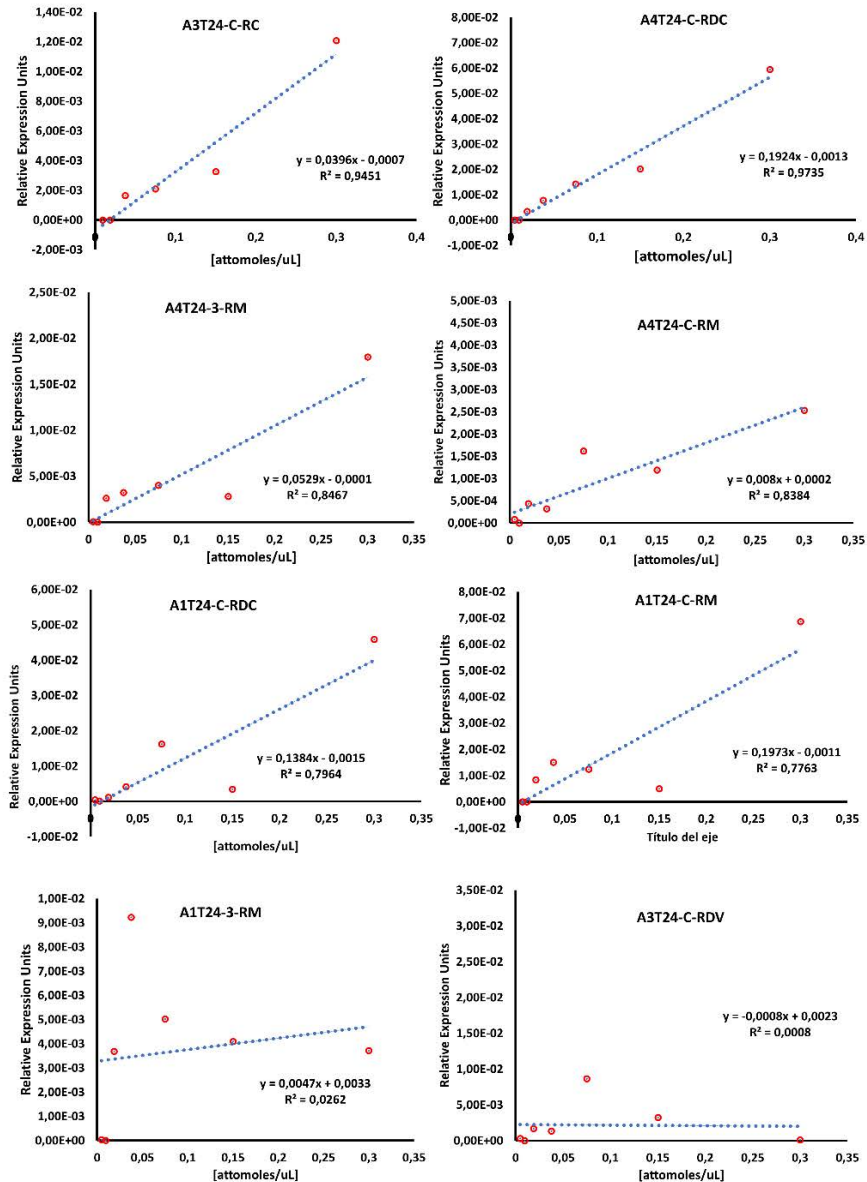


Figure M3. ERCC amplification control for LCM samples.

mRNA isolation and preparation

Only samples with a RIN value > 7 were selected to mRNA isolation. polyA mRNA isolation was performed using Dynabeads™ mRNA Purification Kit (Invitrogen, Paisley, UK) following the manufacturer's instructions. This process was carried out twice per sample to avoid rRNA contamination. Purity of the polyA mRNA was determined through the 260/280 and 260/230 ratios. polyA mRNA quality was also determined in a Bioanalyzer 2100 (Agilent, Santa Clara, CA, USA). The concentration was verified with a Qubit 4 Fluorometer (Invitrogen, Paisley, UK) and Qubit RNA HS, High Sensitivity, Assay Kit (Invitrogen, Paisley, UK). Before to proceed with RIP-seq, the polyA mRNA was physically fragmented using a

sonicator (cycle 1, 80% amplitude for 30 seconds during 5 minutes for each sample) to obtain a mean size around 150 nt verified in a Bioanalyzer 2100 (Agilent, Santa Clara, CA, USA).

Direct RNA sequencing (DRS) and differential epitranscriptomic analysis

Nanopore libraries for DRS were prepared from 1.65 up to 2.18 µg of isolated polyA mRNA using the nanopore Direct RNA Sequencing kit (SQK-RNA001, Oxford Nanopore Technologies, ONT) according to manufacturer's instructions. The poly(T) adapter ligation to the polyA mRNA was performed using T4 DNA ligase (New England Biolabs) in the Quick Ligase reaction buffer (New England Biolabs) for 15 min at room temperature. First-strand cDNA synthesis was carried with SuperScript III Reverse Transcriptase (Thermo Fisher Scientific) using the oligo(dT) adapter. The RNA-cDNA hybrid obtained was purified using Agencourt RNAClean XP magnetic beads (Beckman Coulter). The DRS adapter was ligated to polyA mRNA using T4 DNA ligase (New England Biolabs) in the Quick Ligase reaction buffer (New England Biolabs) for 15 min at room temperature followed by a second purification step using Agencourt beads (as described above). Finally, DRS libraries were loaded onto a R9.4 SpotON Flow Cells (Oxford Nanopore Technologies) and sequenced until complete nanopores depletion, around 24 hours of run time. Basecalling was carried out with ONT Guppy software (<https://community.nanoporetech.com>). The resultant reads were filtered by quality ($Q > 8$) using an in-house Python script. Read alignment was made with minimap2 software (Li H, 2018) using root transcriptome of maritime pine as reference. The alignment parameters were adjusted for direct RNA sequencing (*-uf* and *-kl4*). Differentially expressed (DE) transcripts were identified using the edgeR package for R, the transcripts were normalised by cpm and filtered; 2 cpm in at least 2 samples (Robinson *et al.*, 2010). The transcripts with $FDR < 0.05$ were considered as differentially expressed.

ONT-DRS reads with a $Q > 9$ were used for *de novo* modification detection with the TOMBO software (Stoiber *et al.*, 2016). The total mapped reads per base and the number of modified bases in each position were obtained using the *text_output_browser_file* method with the options *coverage* and *fraction*. Only the positions with at least 50 mapped reads were employed for subsequent analyses. A Fischer exact test was carried out for each transcript position to determine the

differential expression of modified bases among control and NH₄⁺ supplied samples. The transcript positions with a P-value < 0.05 and a logFC > 0.5 were considered as differentially modified.

miRNA isolation and miRNA-seq

Using grounded powder roots, total RNA was isolated using Norgen Biotek Plant/Fungi Total RNA Purification kit (Norgen Biotek, Thorold, ON, Canada). Total RNA concentration and purity were determined with a Nanodrop ND1000 (Thermo Scientific, Waltham, MA, USA). Purity was determined through the 260/280 and 260/230 ratios. The concentration was verified with a Qubit 4 Fluorometer (Invitrogen, Paisley, UK) and Qubit RNA BR, Broad-Range, Assay Kit (Invitrogen, Paisley, UK). RNA quality was further confirmed using agarose gel electrophoresis and using the RNA Pico Assay for the 2100 Bioanalyzer (Agilent, USA). RNA samples with an RNA integrity number (RIN) higher than 7 were used for miRNA-Seq. The miRNA isolation and sequencing were carried out by FASTERIS (Plan-les-Ouates, Switzerland). Three micrograms of total RNA were used to isolated miRNAs by polyacrylamide gels in order to select sequences with a size between 18 and 30 bp. RNA libraries for sequencing were prepared using the TruSeq small RNA kit (Illumina, San Diego, CA, USA) according to the manufacturer’s instructions. The 21 samples were sequenced on an Illumina HiSeq 4000 as single-end reads of 50 bp length. The sequencing results are presented in the Table M3.

Table M3. miRNA-seq sequencing results.

Sample	Yield (Mb)	Reads (Millions)	Q30 (%)
A1T24C	810	16.22	98.48
A1T24-3	1027	20.55	98.49
A3T24C	655	13.12	98.45
A3T24-3	873	17.48	98.44
A4T24C	826	16.53	98.34
A4T24-3	879	17.58	98.51

The read quality trimming and the miRNA identification was made using Mirnova software with universal plant prediction model without a reference species (Vitsios *et al.*, 2017). The precursor prediction was made with miRDeep-P2 (Kuang *et al.*, 2019) using a genome assembly draft of maritime pine (Sterck *et al.*, unpublished).



Materials and Methods

The miRNA read count was improved with CD-HIT (Fu *et al.*, 2012). The differential expression analysis of the miRNA was made using the edgeR package for R, the miRNAs were normalised by cpm and filtered; 20 cpm in at least 2 samples (Robinson *et al.*, 2010). Only the miRNAs with *P*-values < 0.05 and the three experimental replicates with the same expression sense than the final logFC (positive or negative) were considered as differentially expressed. The prediction of targets for differential expressed miRNA was carried out with the psRNATarget software (Dai *et al.*, 2018).

Differential proteomics analysis

Protein extraction

The proteins were extracted following the protocol described by González Fernández *et al.* (González Fernández *et al.*, 2014). The extractions were carried out with 200 mg of sample. Protein content was determined using a commercially kit (Protein Assay Dye Reagent; Bio-Rad, CA, USA) and bovine serum albumin as a standard (Bradford, 1976). Protein extracts were cleaned-up in 1D SDS-PAGE at 10% polyacrilamde as described in Valledor and Weckwerth, 2014. Samples were loaded onto the stacking gel and 80 V was applied until the electrophoresis front reached the resolving gel. The run was stopped when the protein extract had entered 1 cm into the resolving gel and the gel was stained with Commasie Blue. Protein bands were cut off, diced and kept in water at 4°C until digestion.

Protein digestion

Protein digestion were carried out in the Proteomics Facility at Research Support Central Service, University of Cordoba. Briefly, gel dices were distained in 200 mM ammonium bicarbonate (AB)/50% acetonitrile for 15 min followed by 5 min in 100 % acetonitrile. Protein was reduced by addition of 20 mM dithiothreitol in 25 mM AB and incubated for 20 min at 55 °C. The mixture was cooled down to room temperature, followed by alkylation of free thiols by addition of 40 mM iodoacetamide in 25 mM AB, in the dark for 20 min and the gel pieces were then washed twice in 25 mM AB. Proteolytic digestion was performed by addition of Trypsin (Promega, Madison, WI) at 12.5 ng/μL of enzyme in 25 mM AB and incubated at 37 °C overnight. Protein digestion was stopped by addition of

trifluoroacetic acid at 1% final concentration and the digested samples were finally Speedvac dried.

nLC-MS2 analysis

Protein analysis were carried out in the Proteomics Facility at Research Support Central Service, University of Cordoba. Nano-LC was performed in a Dionex Ultimate 3000 nano UPLC (Thermo Scientific) with a C18 75 μm x 50 Acclaim Pepmam column (Thermo Scientific). The peptide mix was previously loaded on a 300 μm x 5 mm Acclaim Pepmap precolumn (Thermo Scientific) in 2% acetonitrile/0.05% TFA for 5 min at 5 $\mu\text{L}/\text{min}$. Peptide separation was performed at 40°C for all runs. Mobile phase buffer A was composed of water, 0.1% formic acid. Mobile phase B was composed of 20% acetonitrile, 0.1% formic acid. Samples were separated at 300 nL/min. Elution conditions were: 4-35%B for 60 min; 35-55% B for 3 min; 55-90% B for 3 min followed by 8 min wash at 90% B and a 12 min re-equilibration at 4%B. Total time of chromatography was 85 min.

Eluting peptide cations were converted to gas-phase ions by nano electrospray ionization and analysed on a Thermo Orbitrap Fusion (Q-OT-qIT, Thermo Scientific) mass spectrometer operated in positive mode. Survey scans of peptide precursors from 400 to 1500 m/z were performed at 120K resolution (at 200 m/z) with a 4×10^5 ion count target. Tandem MS was performed by isolation at 1.2 Da with the quadrupole, CID fragmentation with normalized collision energy of 35, and rapid scan MS analysis in the ion trap. The AGC ion count target was set to 2×10^3 and the max injection time was 300 ms. Only those precursors with charge state 2–5 were sampled for MS2. The dynamic exclusion duration was set to 15 s with a 10-ppm tolerance around the selected precursor and its isotopes. Monoisotopic precursor selection was turned on. The instrument was run in top 30 mode with 3 s cycles, meaning the instrument would continuously perform MS2 events until a maximum of top 30 non-excluded precursors or 3s, whichever is shorter.

Protein database creation for identification method

For the protein database obtaining the root transcriptome of *Pinus pinaster* was used (Manuscript 3). The transcriptome was translated into the six open reading frames with transeq tool (Madeira *et al.*, 2019). The output peptides chains were filtered

Materials and Methods

by length, deleting those less than 50 amino acids (Romero-Rodríguez *et al.*, 2014) (Method SX). To reduce the redundancy of proteins in the database, CD-HIT-EST with a 99% identity filter was used (Fu *et al.*, 2012).

Protein identification and relative quantification

The raw data were processed using Proteome Discoverer (version 2.3, Thermo Scientific). MS2 spectra were searched with SEQUEST engine against Pinus pinaster proteome reference database. In silico peptide lists were created using the followings settings: reagent used for protein digestion was trypsin, a maximum of two missed internal cleavage sites per peptide, precursor mass tolerance of 10 ppm and fragment mass tolerance of 0.75 Da per fragment ions. Only peptides with a high confidence ($FDR \leq 0.01$) and minimum XCorr of 2 were selected. The identified proteins were filtered by a minimum of two different peptides. Minora algorithm was used to determine relative quantification. This algorithm detects and quantify isotopic clusters using LC/MS peaks in each data set, regardless of whether they are associated with a peptide spectral matches (PSMs). The protein identification with redundancy is considered by Proteome Discoverer software. Proteins sharing peptides were grouped and all those groups without a unique peptide were removed. Normalization and scaling were made with Proteome Discoverer software. Differentially expressed (DE) proteins were identified using the edgeR package for R (Robinson *et al.*, 2010). The proteins with $FDR < 0.05$ were considered as differentially expressed. The resultant proteins were annotated using BLAST with *blastp* option against NCBI's non-redundant database (Camacho *et al.*, 2008) and BLAST2GO software (Götz *et al.*, 2008). Proteins with the same sequence annotation and quantification profile across the samples was considered the same protein selecting the protein with the longest sequence.

Elemental Analysis and NUE Component Estimation

Ground powder (100 mg) of cotyledons, hypocotyls, and roots was dried at 70°C for 48 h in an oven. Total C and N contents in different sections of pine seedlings were determined in triplicate by an elemental macro-analyzer Leco truSpec CHNS (Leco Corporation, St. Joseph, MI) at the Atomic Spectrometry Unit, University of Málaga. ¹⁵N determinations were performed by mass spectrometry using a Flash IRMS Elemental Analyzer (EA-IRMS), Delta V IRMS, Conflo IV Universal

Interface (Thermo Scientific, MA, USA). The N content and biomass of the samples were used to calculate the nitrogen utilization efficiency (NUtE; Biomass / N supplied) and nitrogen uptake efficiency (NUpE; N content / N supplied) (Good *et al.*, 2004).

Free Amino Acids, Ammonium, Nitrate, and Nitrite Contents

Free amino acids and ammonium were extracted with 2% 5-sulfosalicylic acid (Ferrario-Méry *et al.*, 1998). A hundred mg of each powdered sample was extracted in 1 mL of 2% 5-sulfosalicylic acid. The samples were mixed by vortex and centrifuged at 22,000 g for 15 min at 4°C. The recovered supernatant was used for soluble amino acid and ammonium quantifications. Soluble amino acids were determined using the procedure described by Sun *et al.* (2006) with a spectrophotometrical measure at 570 nm. The colorimetric reactions were developed with 10 µL of extracted sample, 190 µL of water and 200 µL of fresh combined solution A:B (4:1). Solution A was composed by 2 g of ninhydrin and 0.3 g of hydrantine dissolved in 75 mL of DMSO. Solution B was 4 M sodium acetate pH 5.2. The reaction solutions were incubated at 95°C during 30 min. Then they were put in ice during the addition of 1 mL of 50% ethanol. The samples were cooled in ice during 30 min before the spectrophotometrical determination. Free ammonium was measured using the Berthelot reaction (phenol hypochlorite assay) with a spectrophotometrical measure at 635 nm (Husted *et al.*, 2000). The reaction mix contained 10 µL of extracted sample, 100 µL of 330 mM sodium phenolate pH 13, 100 µL of fresh 0.01% (w/v) sodium nitroprusside and 100 µL of fresh 1.6% (v/v) bleach/sodium hypochlorite. The mix was incubated during 40 min at room temperature. The amount in each sample was determined using an ammonium standard solution with 0-20 nmol in range. Nitrate and nitrite measures were performed as described by García-Robledo *et al.* (2014). Nitrite was determined spectrophotometrically at 540 nm after a colorimetric reaction using Griess' reactive (equal volumes of 60 mM sulfanilamide in 1.2 N HCl and 4 mM N-(1-naphthyl) ethylenediamine dihydrochloride) after 20 min incubation at room temperature. Nitrate was reduced to nitrite with 2% vanadium (III) chloride (VCl₃) in 6N HCl, and the produced nitrite was measured as described above. Nitrite was measured prior the nitrate reduction with the aim of determining the basal nitrite present in the samples. Nitrite and nitrate contents were calculated based on a

standard curve using commercial sodium nitrite from Sigma-Aldrich (MO, USA).

Metabolite Profiling

The metabolites for $^1\text{H-NMR}$ analysis were extracted following the protocol previously described by Kruger *et al.* (2008). Two hundred milligrams of frozen powder were used for extractions with 500 μL of cold 1 M HClO_4 . The samples were vigorously mixed by vortexing and incubated during 30 min on ice. Then, the extracts were centrifuged at 25.000 g and 4°C during 15 min. The supernatant was recovered, and the resultant pellet was resuspended in 500 μL of cold 1 M HClO_4 and centrifuged at 25.000 g and 4°C during 15 min. This new supernatant was recovered and combined with the former one. The samples were neutralized with 2 M KOH until reach pH 5-6. The neutralized extracts were incubated 30 min on ice and then centrifuged at 25.000 g and 4°C during 15 min. The supernatant was recovered and lyophilized. After this, the samples were resuspended in 1 mL of 25 mM NaH_2PO_4 - 25mM Na_2HPO_4 pH 7.5, the pH of the samples was adjusted to 7.5 and they were centrifuged at 14.000 g and 4°C during 10 min. Then the samples were lyophilized again. Finally, the resultant pellets were resuspended in 1 mL D_2O with 3mM sodium 3-(trimethylsilyl)propionate-2,2,3,3d4 (TSP) and centrifuged at 14.000 g and 4°C during 10 min. The resultant supernatant was used for the $^1\text{H-NMR}$ analysis. These analyses were performed on a Bruker ASCEND™ 400 MHz NMR Spectrometer (Bionand, *Centro Andaluz de Nanomedicina y Biotecnología*, Málaga, Spain). The 1D- $^1\text{H-NMR}$ spectrum for each sample was obtained as previously described by Cañas *et al.* (2015). Spectra were acquired using the composite pulses sequence zgcppr with 1 s water presaturation delay, 8 kHz spectral width, 32 k data points, 16 scans and a recycle time of 8 s. Quantitative analysis of the NMR spectra was performed using LCMModel software (Linear Combination of Model Spectra) (Provencher, 1993) and a previously generated reference metabolite spectral library (Cañas *et al.*, 2015). The internal reference was an electronically generated signal, ERETIC (electronic reference to access in vivo concentrations) (Akoka *et al.*, 1999). The metabolite amounts were determined at millimolar concentrations. The metabolite contents were analyzed with MetaboAnalyst 4.0 (Chong *et al.*, 2018). Data were normalized using the quantile method, then log transformation and mean centered. MetaboAnalyst 4.0 was used to construct a Heatmap and perform a *t*-test with the metabolite data.

Statistics

In Chapter 2, biomass and root:shoot ratio results are presented in boxplots including minimum, maximum, and median values. For the rest of experiments, the mean values for three pools of plants with standard errors ($SE = SD/\sqrt{(n-1)}$) are presented. Statistical analyses were performed using Prism 5 (Graphpad, CA, USA) except for metabolite data that were analyzed using MetaboAnalyst 4.0 (Chong *et al.*, 2018). Differences among organs were not statistically analyzed. For each organ and whole seedling, nutritional differences were statistically analyzed to reduce problems with distribution and variance of data. In this line, one-way ANOVA was used for the analyses of all data except for ^{15}N incorporation and metabolite profile assuming that data met ANOVA conditions. When one-way ANOVA was significant, a Newman-Keuls multiple comparison test was carried out. The ^{15}N incorporation time experiment was analyzed using two-way ANOVA (mixed model) with a Bonferroni post-test determining significant differences in nutrition conditions between the global time experiment and each individual time point. Root metabolite profiles were analyzed using *t*-tests. In every case, significant differences were considered when $p < 0.05$ except for *t*-test analyses, where FDR < 0.05 was assumed.

Phylogenetic analyses

Evolutionary analyses were performed in MEGA7 (Kumar *et al.*, 2016). The protein sequence alignment was made with Muscle (Edgar, 2004). The evolutionary history was inferred using the Neighbor-Joining method (Saitou and Nei, 1987). The bootstrap consensus tree inferred from 1000 replicates is taken to represent the evolutionary history of the taxa analyzed (Felsenstein, 1985).

MeRIP-seq

To perform the N^6 -methyladenosine (m^6A) RNA immunoprecipitation, fragmented polyA mRNA in a range of 3.15 - 6 μg was used. Samples were precipitated with 1/10 of the total volume of sodium acetate (3M, pH5.2), 1/14 of the total volume of molecular grade glycogen (5mg/mL) (Invitrogen, Paisley, UK) and 2.5 volumes of cold molecular grade absolute ethanol. Subsequently, samples were incubated at -

Materials and Methods

80 °C overnight. After that, samples were centrifuged at 14.000 rpm for 30 minutes on a precooled ultra-centrifuge. Pellets were washed with 70% ethanol. The final pellets obtained were dried at room temperature for 10 minutes and resuspended in molecular grade distilled water (10 µL of molecular grade distilled water (Ambion, Austin, TX, USA) per 1 µg of polyA mRNA used). Samples were mixed with 10 µL of RNaseOUT (Life Technologies, Carlsbad, CA, USA), 200 µL 5X IP buffer (50 mM Tris HCl pH7.4, 750 mM NaCl, 0.5% vol/vol Igepal[CA-6300]) and 5 µL of m⁶A antibody (ab151230, Abcam, Cambridge, UK). The volume of the samples was brought up to 1 mL with molecular grade distilled water. Then, samples were incubated at 4°C for 3 hours. During the time of the immunoreaction, DynabeadsTM protein-A beads (Invitrogen, Paisley, UK) were prepared using 1X IP buffer supplemented with molecular grade BSA (0.5 mg/mL) (Sigma, San Luis, MO, USA). Protein-A beads solution was rotated at 4°C for 2 hours. Then, 100 µL of protein-A beads was added to each immunoreaction tube and incubated at 4°C for 2 hours. Subsequently, samples were spin down, and the resulting pellets were washed three times with 1X IP buffer. For each pellet, 95 µL of proteinase K buffer (5 mM Tris pH 7.5, 1 mM EDTA, 0.25% SDS) and 5 µL of molecular grade proteinase K (Invitrogen, Paisley, UK) was added. Proteinase K reactions were incubated at 50°C for 45 minutes and mixed every 10 minutes. Afterwards, samples were spun down, and pellets were washed twice with 300 µL of 1X IP buffer. The resulting mixtures were precipitated (as described above). Finally, pellets were resuspended in 20 µL of molecular grade distilled water. Final m⁶A-RNA immunoprecipitation yield was quantified using Qubit RNA HS, High Sensitivity, Assay Kit (Invitrogen, Paisley, UK). Total amount from 80 up to 130 ng were obtained.

The RIP sample sequencing was carried out by Novogen (HK). The cDNA synthesis and amplification, and the library preparation was made with the SMART-SeqTM v4 UltraTM Low Input RNA Kit for Sequencing (Takara, Mountain View, CA, USA) following the manufacturer's instructions. RNA sequencing was made in a NovaSeq 6000 sequencer according to the manufacturer's instructions for paired-end reads (Illumina, San Diego, CA, USA). The 6 samples were sequenced producing single-end reads of 150 bp length. The sequencing output is shown in the Table M4.

Table M4. MeRIP-seq sequencing results.

Samp le	Raw yield (Gb)	Raw reads (Millions)	Final yield (Gb)	Trimmed reads (Millions)
C1	14.26	95.08	11.04	83.59
C2	13.14	87.58	10.62	79.75
C3	13.72	91.44	10.81	79.74
N1	13.18	87.89	10.66	80.65
N2	13.82	92.14	11.71	85.82
N3	12.93	86.21	10.67	78.93

The raw reads were trimmed (quality and contamination) using SeqTrimBB software (<https://github.com/rafnunser/seqtrimbb>). Only the pairs in which both reads passed the quality test were further analysed ($Q > 20$). Trimmed reads are shown in the Table M4. The final transcriptome was used as the reference for the read mapping that was performed with BWA using the MEM option (Li and Durbin, 2009). The read count was obtained with the python script *sam2counts* (<https://github.com/vsbuffalo/sam2counts>). Differentially expressed (DE) transcripts were identified using the edgeR package for R, the transcripts were normalised by cpm and filtered; 2 cpm in at least 2 samples (Robinson *et al.*, 2010). The root transcriptome (Chapter 3) was used as the reference for the read mapping that was performed with BWA using the MEM option (Li and Durbin, 2009). The read count was obtained with the python script *sam2counts* (<https://github.com/vsbuffalo/sam2counts>). The m⁶A peak identification was made using PeakRanger software (Feng *et al.*, 2011) with DRS reads as reference. The counts of bases in the peaks for each sample were normalized by the counts from the DRS ($(\text{base counts} / \text{DRS transcript CPM}) * \text{Mean CPM of the sample}$). Differentially expressed (DE) m⁶A peaks were identified using the edgeR package for R, the transcripts were normalised by cpm and filtered; 2 cpm in at least 2 samples (Robinson *et al.*, 2010). The peaks with $\text{FDR} < 0.05$ were considered as differentially expressed. The putative m⁶A sites in these transcripts were identified using the BERMP software (Huang *et al.*, 2018). The resultant sites were analysed with the motif-based sequence analysis tool (MEME) (Bailey *et al.*, 2015) in order to identify a consensus sequence motif for putative m⁶A sites.

Table M.1. Primer sequences used in each chapter.

Primer Name	Identifier	Sequence (5' – 3')	Chapter
qSIGS1.1-F	Solyc04g014510.2	TAGGCACAAGGAGCACATTG CA	1
qSIGS1.1-R		TTCCTTCTCCGTGTCTCTTCCC	1
qSIGS1.2-F	Solyc11g011380.1	GAAGCACAAAGAACACATAG CT	1
qSIGS1.2-R		TGCCTTCTCTGTGTCTCTTCC A	1
qSIGS1.3-F	Solyc05g051250.2	AAGGCACAAAGAGCACATTG CT	1
qSIGS1.3-R		TGCCTTCTCTGTATCTCTACC T	1
qSIGS1.4-F	Solyc12g041870.1	GAGGCACAAGGAACATATTG TT	1
qSIGS1.4-R		AGCTTTTTTCCATCTCCCTTCC A	1
qSIGS2-F	Solyc01g080280.2	TCGCCACAAGGAACATATAA GT	1
qSIGS2-R		TTCCTTCTCAGTGTCACGCCC C	1
qSICAC-F	Solyc08g006960.2.1	CCTCCGTTGTGATGTA ACTGG	1
qSICAC-R		ATTGGTGAAAGTAACATCA TCG	1

*Reference gene and primers from Expósito-Rodríguez *et al.* (2008).

Primer Name	Identifier [*]	Sequence (5' – 3')	Chapter
SKP1/ASK1-F	unigene18128	ATGCTGGACAGGCTTTGAAC	2
SKP1/ASK1-R	unigene18128	GAGTTGCTCCGAGATCTTTACA	2
SLAP-F	unigene1135	AGTATGCTAAGGAATCGTGCCT	2
SLAP-R	unigene1135	GTCCATAATTACACACGAACAGA	2
qNR-F	unigene1771	ATCCCCTCCCACATCCTGTTAT	2
qNR-R	unigene1771	ACAGAGATCAGGAGTGCTCAAT	2
qNiR-F	unigene2952	TTCCAATTCTCATCCATCGCCA	2
qNiR-R	unigene2952	TCGGCTAAGCTATTGGAGAACT	2
qGS1a-F	isotig10070	ATCGAGGAGCTTCAGTTAGAGTGG	2
qGS1a-R	isotig10070	TGGTCGTCTCAGCAATCATAGAAGT	2
qGS1b-F	unigene10503	CCCAATTGTTTGTGGGGGATA	2
qGS1b-R	unigene10503	CTGAATGACAACTAGACACTG	2
qFd_GOGAT-F	unigene9110	ATTTGTTGCCATAGTGTGAGCG	2
qFd_GOGAT-R	unigene9110	GGTCTCCAGGTCTAGAGGATGT	2
qNADH_GOGAT-F	isotig26980	CATAACAAGCCACTCACATGCC	2
qNADH_GOGAT-R	isotig26980	CTTGGACCAGGTAGTTGATGCT	2
qAlaAT1-F	unigene1013	GTGCTTATTTTATGTCTGGGCAAC	2
qAlaAT1-R	unigene1013	GCACTACCAACCTGCAAACCTAG	2
qAlaAT2-F	isotig29148	ACCTGATGCGAGTTGTATGAAAC	2
qAlaAT2-R	isotig29148	GCTGTTATGGGAGAGAGGGC	2
qGGT-F	isotig28624	TGTTTGGTTTGGTTCAGGACTC	2
qGGT-R	isotig28624	ACTATACAGCACCGCAGACATT	2
qAspAT1-F	unigene4809	GCCTGAACAAAGATCAAGTTGCA	2
qAspAT1-R	unigene4809	GTTTTAGAGCTCAGACCTGCCA	2
qAspAT2-F	unigene17743	TGACTCCAGAGCAAGTTGACC	2
qAspAT2-R	unigene17743	TGCCAAGTATTCAACATTGCCG	2
qAspAT3-F	isotig09767	GAAGCACCTGACATCACATTGG	2
qAspAT3-R	isotig09767	ATGAAAGATCGGTAAGCAGCCA	2

*Cañas *et al.*, 2017.

Materials and Methods

Primer Name	Identifier [*]	Sequence (5' – 3')	Chapter
Amp-ATTB1.1	-	TGCTCGGGGACAACCTTTGTACAA	3
Amp-ATTB2.1	-	GGCGGCCGCACAACCTTTGTACAA	3
Amp-ATTB1.2	-	TCGTCGGGGACAACCTTT- GTACAAAAAAGTTGG	3
Amp-ATTB2.2	-	GGCGGCCGCACAATTTGTACAA- GAAAGTTGGGTTTTTTT	3
polTdeg	-	AACAGTGGTATCAACGCAGAGTACT- TTTGTTTTTTTTCTTTTTTTTTTVN	3
PugOligo- Adapter	-	AAGCAGTGGTATCAAC- GCAGAGTACGGGGG	3
qpp-AMT1.1-F	unigene25006	TGGTGCAGAAGACAATGATGATG	3
qpp-AMT1.1-R	unigene25006	ACCACGTACACACCCATTACT	3
qpp-AMT1.2-F	c107097	TTGGCAGAGAGGAAGAGACG	3
qpp-AMT1.2-R	c107097	CGTCGGGAAGTGAATGGTCA	3
qpp-AMT1.3-F	isotig52198	GCACAAATTCATCCCACGGG	3
qpp-AMT1.3-R	isotig52198	TCAACGTTACCCACACCACA	3
qpp-AMT1.4-F	unigene18567	GCAGCCAGTTATAAGCAGGG	3
qpp-AMT1.4-R	unigene18567	TGACAAAGAGAACCCCGTCT	3
qpp-AMT2.1-F	unigene5961	TTCGTAGCTTGCAGGAGGTG	3
qpp-AMT2.1-R	unigene5961	ACCCTCTCTTCATCCGGCTA	3
qpp-AMT2.2-F	isotig45956	TGAGGAAAGCAGGGGATATGTC	3
qpp-AMT2.2-R	isotig45956	TTCAAGGACCAAGGCTAACAAA	3
qpp-AMT2.3-F	isotig44966	GTAGCTCGGGTTAGGTTCCAG	3
qpp-AMT2.3-R	isotig44966	CATTCACGCCCTGATATGCC	3
qpp-AMT2.4-F	177558926r	GTGGCTTGCAGGTTGTGTAC	3
qpp-AMT2.4-R	177558926r	TGGAGTCAGATTGTAGCCCC	3
qpp-AMT2.5-F	176992561r	AGCGGTTCCAGAGGAGCAAC	3
qpp-AMT2.5-R	176992561r	TCCTACAGCCAAACCACAC	3
qpp-AMT2.6-F	177135176r	TGAAATAAGTGTGCGCTGG	3
qpp-AMT2.6-R	177135176r	CTGCCAGCAACGATGTAGAC	3
qpp-AMP1-F	pp_58007	AAAGGCGTTGCTCAGACCC	3
qpp-AMP1-R	pp_58007	GCCAACTACTTAGACGTGCCT	3
qpp-SHR-F	pp_246622	CAAGTGAAGTACCCGACCCC	3
qpp-SHR-R	pp_246622	TTGAAGCCCATCGACGTGA	3

qpp-NAC38-F	pp_72282	TCTTATACTGCCTGCTTGCTTG	3
qpp-NAC38-R	pp_72282	GTACGCATGGATTGGAGTGATA	3
qpp-NPF3.1-F	pp_58258	TCCCCACCAACCTCAACAGAG	3
qpp-NPF3.1-R	pp_58258	CCACAACGAAAGGCTTGTAGGT	3
qpp-cycloeucaleanol cycloisomeraseF	pp_189071	GATCCCCAAATGGATACAAAGA	3
qpp-cycloeucaleanol cycloisomeraseR	pp_189071	GTTTTCTTCCACATTGCACAAG	3
qpp-DOF12-F	pp_85381	ACCCTTATGCCTGTAACAATGG	3
qpp-DOF12-R	pp_85381	AGTACTGAACCCCGCAATACAT	3
qERCC-130-F	-	TCTGACGGGACAAGGGATCA	3
qERCC-130-R	-	ATTTCTGATATGGCGGCGGT	3
qERCC-2-F	-	GGGTCCATCAGTTGTCCGTA	3
qERCC-2-R	-	GTCCTTACAAGTCCGCTCCT	3
qERCC-96-F	-	CTTGCGCCAATTATCGAGCT	3
qERCC-96-R	-	AGTGTAGGACTCGTCGCATT	3
qERCC-4-F	-	ACATCTTCATAAGGGGTTGGGT	3
qERCC-4-R	-	TGGGGAAATTTGGGAAGCAGT	3
qERCC-46-F	-	TTCGGTGGCAGTATGGGATT	3
qERCC-46-R	-	ACAACACCAACGTCGCAAAAA	3
qERCC-136-F	-	CGCCAGTTTCCCGTGTATCT	3
qERCC-136-R	-	TCTTTCGGTCCAGTGCTTCC	3
qERCC-108-F	-	AGATATGCCATGCGTGCTGT	3
qERCC-108-R	-	CGCGTCGATAAGGTCACAGA	3
qERCC-116-F	-	GCTTATCGGGCCTGCTACAT	3
qERCC-116-R	-	GCTACCAGATCACCGCAGTT	3
qERCC-95-F	-	GGCTTAACCGCTATCGCTCT	3
qERCC-95-R	-	CGGCTTTGTGGGATGAGGTT	3
SIAP-F	pp_199988	AGTATGCTAAGGAATCGTGCCT	3
SIAP -R	pp_199988	GTCCATAATTACACACGAACAGA	3
SKP1/ASK1-F	unigene18128	ATGCTGGACAGGCTTTGAAC	3
SKP1/ASK1-R	unigene18128	GAGTTGCTCCGAGATCTTTACA	3



*Canales *et al.*, 2014; Cañas *et al.*, 2017

Primer Name	Identifier [*]	Sequence (5' – 3')	Chapter
qpp-AMT1.3-F	isotig52198	GCACAAATTCATCCCACGGG	4
qpp-AMT1.3-R	isotig52198	TCAACGTTACCCACACCACA	4
qpp-AMP1-F	pp_58007	AAAGGCGTTGCTCAGACCC	4
qpp-AMP1-R	pp_58007	GCCAACTACTTAGACGTGCCT	4
qpp_GS1b-F	pp_68481	CCAATTGTTTGTGGGGGATA	4
qpp_GS1b-R	pp_68481	CTGAATGACAACTAGACACTG	4
qNADH_GOGAT-F	pp_238921	CATAACAAGCCACTCACATGCC	4
qNADH_GOGAT-R	pp_238921	CTTGACCAGGTAGTTGATGCT	4
qMYB5-F	pp_202778	ATCGTGTGGAAGGAATGAGC	4
qMYB5-R	pp_202778	AATGCCTTGATTGCCACTCT	4
qpp_Pfk-F	pp_211717	AAATGGTACAGGTGGAGGACA	4
qpp_Pfk-R	pp_211717	GGCTTCCCACGAACATAAAA	4
qpp_ASPG-F	pp_167571	CCCTGCCAGGTTCACTTAAA	4
qpp_ASPG-R	pp_167571	ATCAGTTGGAGACCGCAGTT	4
qpp_SAM synthase-F	pp_92107	CTGTGCCCTCTTCATCCAGT	4
qpp_SAM synthase-R	pp_92107	GCCATTACAGCCCACAGAAT	4

*Cañas *et al.*, 2017.

Appendix 1



Appendix 1.1. Last version of the practical handout for the students without western blotting procedure.

Introduction

The correct nutrition of a plant is marked to a large extent by the availability of different nutrients and the ability of the plant to use them. Since ancient times, it is well known that well-fertilized plants grow more and better, allowing higher agricultural yields (Marschner 2012). But the lack of a certain element can cause a series of symptoms on the plant phenotype. Thus, there is a series of markers of the nutritional status of the plant. These markers can be of physiological, biochemical, metabolic or molecular kind (Marschner 2012).

Among the most important elements for plant nutrition we found nitrogen (N). N is the most abundant metabolizable element after C, H and O constituting an essential part of amino acids, nitrogenous bases, chlorophylls, etc. (Buchanan et al., 2015).

Objective

The objective of the present teaching laboratory activity is to demonstrate the importance of the nutrient supply to plants using different markers for it.

1. Different nutritional markers will be measured (soluble proteins, chlorophylls, biomass and glutamine synthetase activity) in plants grown with different contributions of N.
2. In these plants the expression of the different genes of the glutamine synthetase family in tomato will be measured.

Evaluation

From the experimental results, the student must write a scientific document with explanations about the observations. The document must consist of a maximum of 5 pages in A4 typeface Arial 12 and line spacing 1.15. It must include the following sections:

- **Introduction** (maximum a half page).

- **Results** (includes the description and presentation of results: tables, graphs ...)
- **Discussion** (interpretation of the results based on the bibliography).
- **Bibliography**.

Part 1. Measurement of physiological and biochemical nutritional markers in plants grown under different nutritional conditions

Materials and reagents

- Water bath (37 °C)
- Vortex
- Aluminum foil
- Ice boxes
- Spectrophotometer
- Mortar
- Fine washed sea sand
- Benchtop centrifuge
- Refrigerated centrifuge
- Scalpel
- 250 mL beakers
- Acetone 80%
- Bradford reagent
- BSA solution 0.25 mg/mL
- Polivinylpyrrolidone (PVPP)
- Extraction buffer (50mM Tris-HCl pH 8, 2mM EDTA, add before using 20mM 2-mercaptoethanol)
- 0.2 M Tris-HCl buffer, pH 8
- NH₂OH (Hydroxylamine) 0.6 M neutralized, pH 7
- Sodium glutamate 1 M
- ATP 62.5 mM
- MgSO₄ 0.3 M
- GS Stop reagent:
 - 10% (w / v) FeCl₃·6H₂O in 0.2 N HCl
 - 24% (w / v) aqueous trichloroacetic acid
 - 50% (w / v) HCl

- Tomato plants (cherry variety) grown during two months in different nutritional conditions:

Control: complete Hoagland solution (Hoagland & Arnon 1950), N (0.04515 g).

N0.5: medium with reduced N, N (0.00595 g).

Procedures

A. SAMPLE PROCESSING

Every student group must choose only one plant from a treatment (normal N or low N).

1. The roots must be washed with abundant distilled water for removing all the attached vermiculite.
2. The roots must be dried up. For that purpose, is essential to use drying paper.
3. Both shoots and roots must be weighed independently. The results must be recorded.
4. The samples must be kept on ice until processing.

B. OBTAINING OF TOMATO EXTRACTS

1. Put the mortar to cool on ice.
2. Weigh 1 g of fresh tomato leaves. Weigh 0.5 g of fine sea sand per gram of leaves. Weigh 0.2 g of PVPP for each gram of tissue. For roots weigh 0.5 g of tissue and 0.5 g of fine sea sand and 0.2 g of PVPP.
3. Cut into small pieces and put them in the cold mortar. Add the fine sea sand and the PVPP. **Add 4 mL of extraction buffer per gram of leaves. Add 2mL of extraction buffer per gram of leaves.** Homogenize with the mortar as much as possible while keeping the mortar on ice.
4. Put the crude extract in Eppendorf tubes and keep them cold until centrifugation. **Estimate the obtained volume with a micropipette (P1000).**
5. Take 50 μ L of leaf crude extract and add them to 950 μ L of cold 80% acetone into a new Eppendorf tube. Mix well in a vortex, cover the tube with aluminum foil

Appendix 1

and store in the refrigerator (4°C) until the next day (**measurement of chlorophylls**).

6. Centrifuge for 10 minutes at 13,000 rpm in a refrigerated centrifuge at 4 °C.
7. Collect the supernatant and use it as the enzymatic extract. **Estimate the obtained volume with a micropipette (P1000).**

C. QUANTIFICATION OF SOLUBLE PROTEINS (Bradford 1976)

1. Prepare different dilutions of the protein extracts (for leaf samples 1/800 and 1/1600; for root samples 1/200 and 1/100). Samples must be prepared for the Bradford assay by **triplicate**. The final volume of each replica must be 800 µL.
2. A standard curve must be prepared from a stock solution of albumin (BSA) at 0.25 mg/mL. The final concentrations of the standard must be: 1, 2, 4, 6, 8 and 10 µg/mL. The standard must be made by **triplicate**. The final volume of each replica must be 800 µL.
3. Add 200 µL of Bradford reagent to each tube (blank, standard and samples), mix well by inversion and incubate for 15 min at room temperature.
4. Measure the absorbance at 595 nm of each tube. The amount of soluble proteins in the extracts must be recorded. The soluble protein amount must be calculated using the standard (Lambert-Beer law).

D. GLUTAMINE SYNTHETASE ENZYME ACTIVITY DETERMINATION, SYNTHETASE ASSAY (Gallardo & Cánovas, 1992).

1. Prepare the following reaction mixes in Eppendorf tubes. Add the solution in the following order and mix the solutions by gently pipetting:

	TrisHCl 0.2M	NH ₂ OH	Glu	ATP	MgSO ₄	
	H ₂ O	(pH 8)	0.6M	1 M	62.5 mM	0.3 M
Tube	(mL)	(mL)	(mL)	(mL)	(mL)	(mL)
Blank	0.1	0.5	0.1	0.1	0.1	0.1
LB	0.1	0.5	0.1	-	0.1	0.1
1	-	0.5	0.1	0.1	0.1	0.1
2	-	0.5	0.1	0.1	0.1	0.1
3	-	0.5	0.1	0.1	0.1	0.1

2. Start the reaction with the addition of 0.1 mL leaf protein extract. Leave the tubes in a water bath at 37 °C for 15 minutes.
3. Stop the reaction by adding 0.35 mL of GS stop reagent. Mix well in a vortex.
4. Centrifuge the tubes at 5,000 rpm for 5 minutes at room temperature. Transfer the supernatant to a new tube.
5. Measure the absorbance of the supernatant against the blank at **540 nm**. Use the molar extinction coefficient for the reaction product (**L-Glutamic acid γ -monohydroxamate; 298 M⁻¹cm⁻¹; Lambert-Beer law**) to calculate the GS activity level.

F. CHLOROPHYLL MEASURE (LicLtentLaler & BuscLmann, 2001).

1. **From the point 4 of the OBTAINING OF TOMATO EXTRACTS:** Take 50 μ L of leaf crude extract and add it to 950 μ L of cold 80% acetone. Mix well in a vortex, cover the tube with aluminum foil and store in a refrigerator (4°C) until the next day.
2. Centrifuge the tubes for 10 min at 13,000 rpm.

3. Use the supernatants to measure the absorbance spectrum from 300 nm to 700 nm.

DO: 663.2nm (or 663 nm depending to the spectrophotometer units)

DO: 646.8nm (or 647 nm depending to the spectrophotometer units)

4. Calculate the different chlorophylls:

Total chlorophylls ($\mu\text{g/mL}$) = $C_a + C_b$

Chlorophyll A ($C_a; \mu\text{g/mL}$) = $\text{DO}_{663.2\text{nm}} * 12.25 - \text{DO}_{646.8\text{nm}} * 2.79$

Chlorophyll B ($C_b; \mu\text{g/mL}$) = $\text{DO}_{646.8\text{nm}} * 21.5 - \text{DO}_{663.2\text{nm}} * 5.1$

Questions

Put together all the results from all the student groups and:

- Calculate the NUE.
- Calculate the mg of soluble proteins per g of fresh weight (FW).
- Calculate the μg of chlorophylls per g of fresh weight (FW).
- Calculate the glutamine synthetase (GS) activity expressed in μmol of product per minute and per g of fresh weight (FW).
- Compare and explain the results obtained for both treatments (normal N and low N supply).

Part 2. Determination of molecular nutritional markers in plants grown under different nutritional conditions

Materials and reagents

- Ice boxes
- Spectrophotometer
- Benchtop centrifuge
- Refrigerated centrifuge
- Small metal spatula
- Scalpel
- Vortex
- 250 mL beakers
- Mortar

- Liquid nitrogen
- RNA extraction buffer (Tris-HCl 100 mM pH 8, EDTA 30 mM, NaCl 2M, CTAB (cetyltrimethylammonium bromide) 3%, PVP (polyvinylpyrrolidone) 2%, PVPP (polyvinylpolypyrrolidone) 2%, β -mercaptoethanol 4%)
- Chloroform/isoamyl alcohol (24:1) (stock 4°C)
- Lithium chloride 4M (stock 4°C)
- Ethanol 70% (stock -20°C)
- Nuclease free MilliQ water
- Spectrophotometer cuvettes (UVette® 220 nm–1,600 nm Eppendorf 0030106318)
- iTa^q™ Universal SYBR® Green One-Step Kit de Biorad (100 x 20 μ L 1725150)
- 96 well qPCR plates and plastic seals

-PRIMERS:

Gene	Primer	Sequence	Identifier
SIGS1.1	qSIGS1.1-F	TAGGCACAAGGAGCACATTGCA	Solyc04g014510.2
	qSIGS1.1-R	TTCCTTCTCCGTGTCTCTTCCC	
SIGS1.2	qSIGS1.2-F	GAAGCACAAAGAACACATAGCT	Solyc11g011380.1
	qSIGS1.2-R	TGCCTTCTCTGTGTCTCTTCCA	
SIGS1.3	qSIGS1.3-F	AAGGCACAAAGAGCACATTGCT	Solyc05g051250.2
	qSIGS1.3-R	TGCCTTCTCTGTATCTCTACCT	
SIGS1.4	qSIGS1.4-F	GAGGCACAAGGAACATATTGTT	Solyc12g041870.1
	qSIGS1.4-R	AGCTTTTTCCATCTCCCTTCCA	
SIGS2	qSIGS2-F	TCGCCACAAGGAACATATAAGT	Solyc01g080280.2
	qSIGS2-R	TTCCTTCTCAGTGTACGCCCC	
SICAC*	qSICAC-F	CCTCCGTTGTGATGTAAGTGG	Solyc08g006960.2. 1
	qSICAC-R	ATTGGTGAAAGTAACATCATCG	

*Reference gene and primers from Expósito-Rodríguez *et al.* (2008).

Procedures

A. TOTAL RNA EXTRACTION FROM TOMATO

1. Weigh 0.5 g of fresh tomato leaves or roots.
2. Cold the mortar with liquid N and putt the tissue sample into the mortar.
3. Grind the sample to fine powder and with a previously cold spatula (with liquid N) take two tips of powder (around 100 mg) and introduce it in an Eppendorf tube.
4. In the fume extractor, add 600 µL of extraction buffer heated to 65°C to the sample and mix vigorously until all the tissue be completely dissolved (by



vortexing). Incubate the tubes for 6 minutes at 65°C and vortex them every 2 minutes. The tubes must be on the bench-top when the buffer is added, not on ice.

4. Add 600 µL of chloroform:isoamyl alcohol and mix well (all in the fume hood). Leave the tubes on ice for 1 to 2 minutes.

5. Centrifuge for 10 minutes at 13,000 rpm in a refrigerated centrifuge at 4 °C.

6. Collect the supernatant (400 µL) in a new tube.

7. Add one volume of 4M LiCl (400 µL). **Mix well for inversion and store the tube in the fridge until the next day.**

8. Centrifuge at 13,000 rpm for 25 min at 4 °C. Discard the supernatant, should have a typical nucleic acid pellet.

9. Add 1 mL of cold 70% ethanol and, **without disturbing the pellet**, centrifuge at 13,000 rpm at 4°C for 10 minutes.

10. Remove all the supernatant with a pipette (**as much as possible**) and let the pellet dry on the table. No more than 15 minutes.

11. Resuspend the pellet in 50 µL of nuclease free MilliQ water. Use vortex and pipetting to resuspend the pellet.

B. SPECTROPHOTOMETRIC QUANTIFICATION OF TOTAL RNA

1. Make a 1/100 dilution of the RNA extract in 500 µL of nuclease free water. Measure absorbance at 230 nm, 260 nm and 280 nm using the cuvettes UVette®.

2. Calculate the concentration and total amount of RNA in the extraction. For RNA, the coefficient to be used is 40 µg/mL per unit Absorbance at 260 nm. Calculate the quality of RNA using the ratios 260/280 (it must be near 2) and 260/230 (it must be near 2.5)

3. Calculate the volume needed to take 5 ng of total RNA. If it is necessary to dilute, make a dilution in such a way that the RNA concentration remains at 2.5 ng/µL.

C. MEDIDA DE LA EXPRESIÓN GÉNICA POR RT-qPCR

1. Design the qPCR plate (all students together). Put three technical replicas per sample. Must be enough reactions to analyze the 5 GS genes and the reference gene *SICAC*.

2. Add 2 µL of diluted RNA (2.5 ng/µL) in each well to be used.

Appendix 1

3. Prepare a mastermix **for each gene to analyze**. Reaction mixture for each well:

<i>iTaq universal SYBR Green (2x)</i>	5 μ L
<i>iScript-rt</i>	0.125 μ L
<i>For. and rev. Primer mix (10 μM)</i>	0.5 μ L
<u>H₂O nuclease-free</u>	<u>2.375 μL</u>
Total	8 μ L

4. Add the specific reaction mix to each well.

5. Seal the plate, centrifuge to eliminate bubbles and put it in the thermal cycler.

6. Reaction parameters:

	Time	Temperature	Cycles
RT reaction	10 min	50°C	
Taq activation	3 min	95°C	
Denaturation	1 s	95°C	40 cycles
Extension	5 s	60°C	
<i>Melting curve</i>	Increase 0.5°C / 2 s (65-95°C)		

7. Recover the data from the thermal cycler and calculate the expression of the GS genes according to the values of the normalizing gene.

- For the determination of gene expression, the raw fluorescence data of each reaction will be adjusted to the MAK2 model, which does not require assumptions about the amplification efficiency of the oligos of a quantitative PCR assay (qPCR) (Boggy & Wolf 2010). The initial concentration (parameter D0) for each gene will be deduced from the MAK2 model using the qpcR package for the R environment (Ritz & Spiess 2008) and the data will be normalized with the expression of the reference gene *SICAC*.

Questions

Using the data obtained by all the student groups:

- Calculate the gene expression of tomato GS genes.
- Compare and explain the results obtained for both treatments (normal N and low N supply).

Appendix 1.2. Rubric for students' report.

Evaluation standard	Description	Points allotted	Maximum student's performance
Use of scientific language	Correct use of scientific language using the terms properly	10	In the better results the student must use the correct scientific term in every case
Report structure	Student's ability to stick to the structure of a scientific work	10	The structure is well adjusted with the appropriate modifications to the work carried out (Introduction, Results, Discussion and References)
Tables and figures	Student's ability to draw tables and figures from the results in the most appropriate way	35	The results are presented in tables and/or figures according to their nature and that of the methods used to obtain them showing the statistical significance in the numerical results and they are presented in a logical order in the report
Discussion	Ability to discuss based on the results and previous knowledge regarding the researched subject	35	The student must understand the results (positives or negatives) and discuss its biological insight in relationship to the theoretical concepts about plant nitrogen nutrition and previous scientific publications in this research area
References and cites use	Correct use of the bibliography and its inclusion in the form of citations in the text, considering the topicality and adequacy of the bibliography to the text and the results	10	Students must master the bibliography about plant nitrogen nutrition, they must cite appropriately the publications in the text, which must be updated and fully adequate to the results to be discussed

Appendix 1.3. Questionnaire for experience in plant nitrogen nutrition.

Assign a score from 1 to 5 to each question (1- Strongly Disagree / 5 - Strongly Agree)

1. The teaching laboratory activity has been well organized.
2. The teaching laboratory activity has been useful to develop my skills in Biochemistry and Molecular Biology techniques.
3. The teaching (laboratory activity) has helped me to understand the theoretical concepts about plant nitrogen nutrition.
4. After the teaching laboratory activity, I will be able to apply the concepts about plant nitrogen nutrition to the real practice.
5. This teaching laboratory activity will help me in my professional career.
6. Please include any comments about your experience in the teaching laboratory activity. The best aspects, suggestions, opinions.



Appendix 2

N⁶-methyladenosine modifications in the mRNA of plants: facts and works. Incidence and functional relevance of N⁶-methyladenosine in plant mRNA

Francisco Ortigosa, Concepción Ávila, Francisco M.

Cánovas, Rafael A. Cañas.



Introduction

The existence of chemical modifications in RNA nucleosides has been known for more than five decades since the discovery of pseudouridine (Ψ) in 1956 (Grosjean, 2005). Since then, modifications in RNA nucleosides have been found to be more abundant and varied compared to DNA modifications. Up to 160 modifications have been described in RNA molecules (Boccaletto *et al.*, 2017). These chemical modifications can be present on ribosomal (rRNA), transfer (tRNA) and messenger (mRNA) RNAs, but they also are present in small RNAs (Lan *et al.*, 2018). Overall, they are caused by cellular and physiological processes, even though some physical or chemical agents can also alter the structure of nucleosides causing mutations. These changes generate both, a wide genetic and regulatory diversity, shaping a still poorly known layer of information between transcriptome and proteome.

So far, nucleoside modifications in tRNA (Chen *et al.*, 2010; Tuorto *et al.*, 2012; Hienzsche *et al.*, 2013) and even in rRNA have been well studied (Sharma and Lafontaine, 2015; Sloan *et al.*, 2017). However, much less is known about modifications in mRNA, although epitranscriptomic studies in *Arabidopsis thaliana* have revealed the existence of RNA modifications such as N⁷-methylguanosine (m⁷G), 5-methylcytosine (5mC), and N⁶-methyladenosine (m⁶A) (Nichols, 1979; Yang *et al.*, 2019; Fray, 2015) (Figure 1a). These RNA modifications have been described to influence cellular processes such as mRNA splicing (Xiao W. *et al.*, 2016), turnover (Ke *et al.*, 2017), translation (Wang X. *et al.*, 2015; Peer *et al.*, 2019), stabilization (Wang Y. *et al.*, 2014; Wang X. *et al.*, 2014) and localization (Lesbriel *et al.*, 2018; Lesbriel and Wilson, 2019) (Figure 1b). At physiological level, the m⁶A has been involved in the response to abiotic stresses (Anderson *et al.*, 2018) and in diverse developmental processes (Fray, 2015; Vandivier and Gregory, 2018). Their influence on development means that these modifications can have a great impact on crop yield, since they could determine biomass accumulation, and production of seeds and fruits.

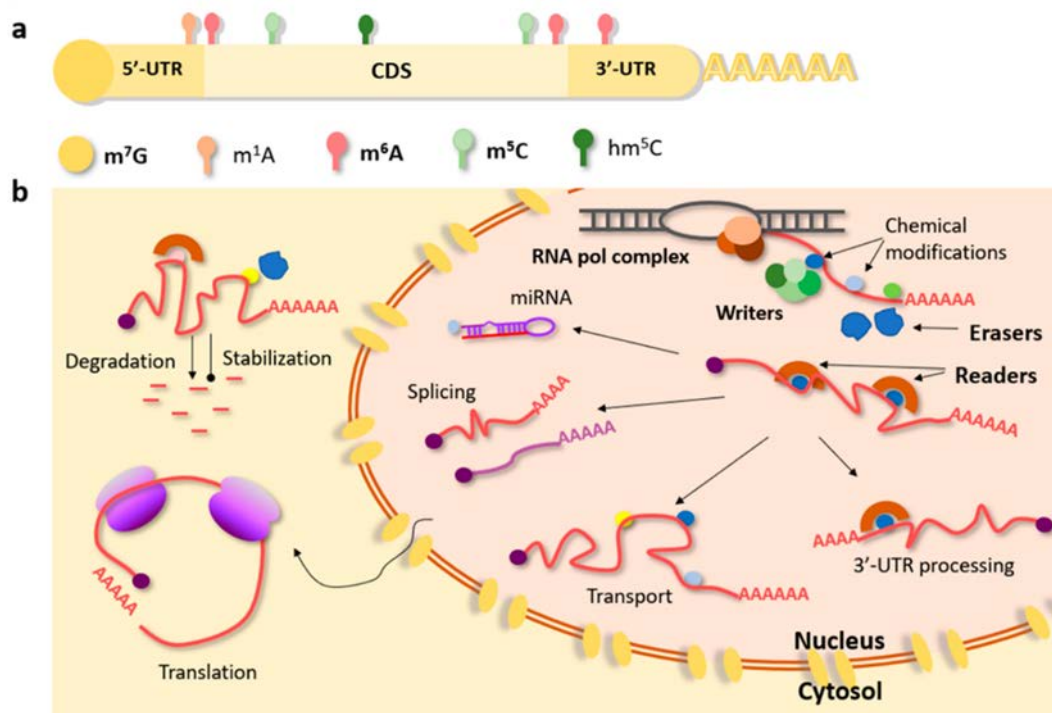


Figure 1. Chemical modification of plant transcripts a) Position of chemical modifications found into the mRNA: m^7G , N⁷-methylguanosine; m^1A , N¹-methyladenosine; m^6A , N⁶-methyladenosine; m^5C , 5-methylcytosine; and hm^5C , 5-hydroxymethylcytosine. Chemical modifications in bold have been reported to be present in plants. b) mRNA processes affected by chemical modifications in plants.

Among the chemical modifications on mRNA nucleosides, the N⁶-methyladenosine (m^6A) is the most abundant and best characterized in eukaryotic cells (Clancy *et al.*, 2002; Li K. *et al.*, 2020;) including plants (Zhong *et al.*, 2008; Li Y. *et al.*, 2014; Růžička *et al.*, 2017; Shi *et al.*, 2018; Yue *et al.*, 2019), and even in virus (Krug *et al.*, 1976; Kennedy *et al.*, 2016). The studies of m^6A modifications in mRNA using non-sequencing and sequencing procedures have allowed shedding light on the functions of the m^6A modification. The present review summarizes the catalogue of proteins involved in the m^6A dynamics, the biological functions of this chemical modification and the different strategies for studying the m^6A modification in the mRNA of plants. This new playground can let to understand the failure of new transgenic lines or how to improve the yield in new crop lines.

1. m⁶A: Writing, reading and erasing in plants

Until now the m⁶A modification has only been studied in a few model and crop plants such as *Arabidopsis* (Zhong *et al.*, 2008; Růžicka *et al.*, 2017), rice (Li Y. *et al.*, 2014), wheat (Kennedy and Lane, 1979), oat (Haugland and Cline, 1980) and maize (Luo J. *et al.*, 2020). Although m⁶A modification can be found within the coding region of the transcript, the greatest number of these modifications are concentrated in the 3'-untranslated region (UTR (Dominissini *et al.*, 2012; Luo G. *et al.*, 2014; Shen L. *et al.*, 2016; (Luo J. *et al.*, 2020). Moreover, the m⁶A/A ratio varies with development stages and tissues (Bährle *et al.*, 2007; Zhong *et al.*, 2008; Bodi *et al.*, 2012). In eukaryotes, including plants, most of the adenine methylation sites are found in the conserved consensus sequence RRACH (R=A/G, A=m⁶A, H=A/C/U) (Dominissini *et al.*, 2012; Yue *et al.*, 2019). The m⁶A modification is reversible that is performed by the action of conserved protein complexes. Three types of protein effectors are found to be involved in m⁶A dynamics: (i) *writers*: enzymes responsible for producing this kind of methylation; (ii) *readers*: those are able to recognize the m⁶A in the mRNA and promote the cellular response; and (iii) *erasers*: demethylases that converts m⁶A in A.

1.1 Writers and their biological implications

The adenine methylation process is known as *writing*. A protein complex known as methylome, which uses S-adenosyl methionine as methyl group donor, is responsible of the modification. This protein complex has been extensively studied in animals (Steve-Puig *et al.*, 2020). The methylome is less known in plants where there are some unidentified elements and lack some homologs to proteins of the animal methylome (Fray, 2015; Yue *et al.*, 2019). In plants, the writing process is performed by a methylome integrated by the adenosine methyltransferase catalytic subunit MTA (*At4g10760*, METTL3 human homolog) (Zhong *et al.*, 2008), the adenosine methyltransferase non-catalytic subunit MTB (*At4g09980*, METTL14 human homolog) (Růžicka *et al.*, 2017), the not-well known subunit MTC (*AT1G19340*, METTL4 human homolog) (Yue *et al.*, 2019), the regulatory subunit FIP37 (*At3g54170*, WTAP human homolog) (Zhong *et al.*, 2008; Shen L. *et al.*, 2016), the E3 ubiquitin-protein ligase HAKAI (*At5g01160*) (Růžicka *et al.*, 2017)

Appendix 2. 1. m6A: Writing, reading and erasing in plants

and the subunit VIRILIZER, VIR (*At3g05680*, VIRMA human homolog) (Růžička *et al.*, 2017) (Figure 2a)

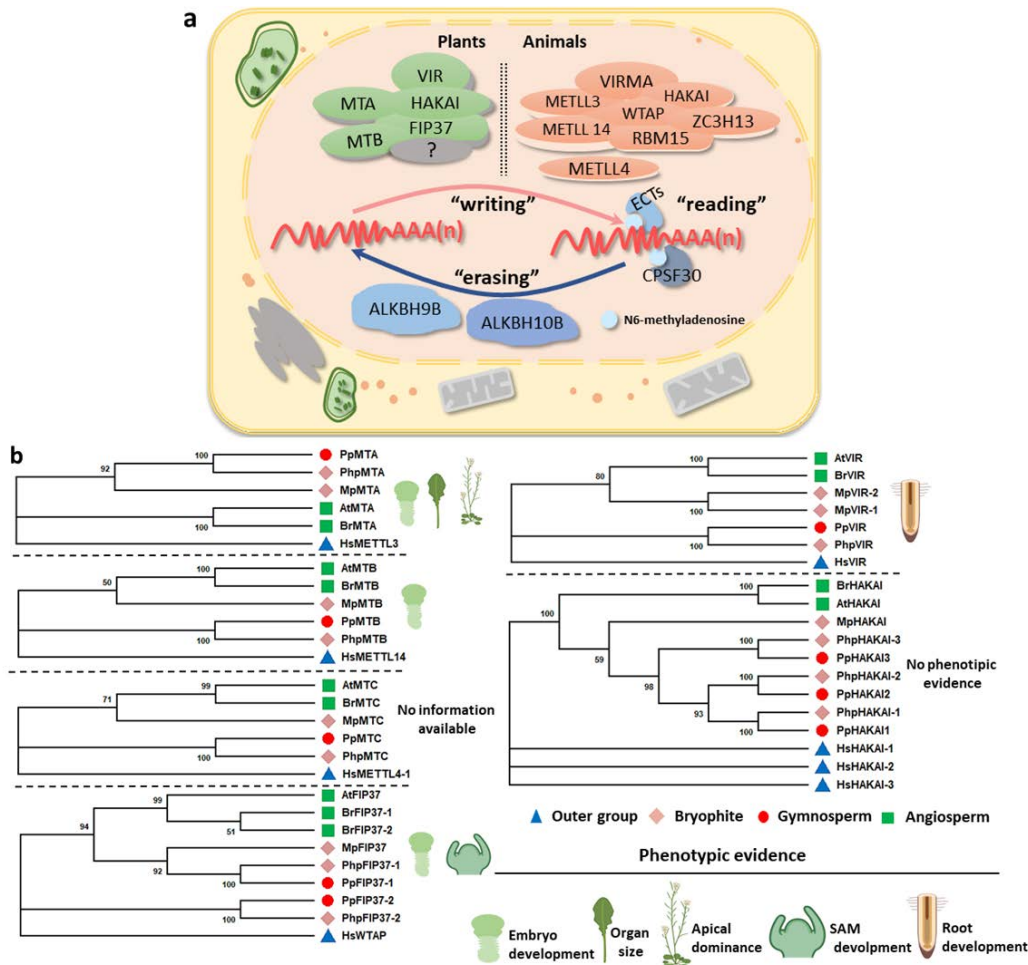


Figure 2. The methylome complex in plants. a) Comparison of plant and animal methylome complexes. b) Phylogenetic analysis and biological implication of proteins involved in *Arabidopsis thaliana* plant methylome. Phylogenetic analysis was conducted using MEGAX and the Maximum Likelihood (ML) method was adopted with 1000 bootstrap replications. *Arabidopsis thaliana* (At), *Brassica rapa* (Br), *Marchantia polimorpha* (Mp) and *Physcomitrella patens* (Php) protein sequences were obtained from Yue *et al.* 2019. *Pinus pinaster* (Pp) protein sequences were obtained from Congenie database. *Homo sapiens* (Hs) protein sequences were obtained from nr NCBI database. Phenotypic evidences are illustrated according to previously published information (Zhong *et al.*, 2008; Bodi *et al.*, 2012; Růžička *et al.*, 2017; Shen L. *et al.*, 2016).

The role of m⁶A in the mRNA of plants appears to be essential. This has been demonstrated through functional characterization of different proteins involved in

the plant methylome complex (Figure 2b). Zhong *et al.* (2008) demonstrated using *Arabidopsis* knockouts of *MTA* and *FIP37* genes that the proteins encoded were necessary for the proper development of embryos. Additionally, the *MTA* expression presented a tissue-dependent distribution, being associated with meristematic tissues such as the apical meristem, the root tip and reproductive organs. The knockdown of *MTB* displayed that plant fitness was disturbed with a concomitant decrease of plant height (Růžička *et al.*, 2017). Null variants of *MTA*, *MTB*, *FIP37* and *VIR* have been proved to be embryonic lethal (Zhong *et al.*, 2008; Růžička *et al.*, 2017). Moreover, plant lines with reduced expression of *MTA*, *MTB*, *FIP37* and *VIR* exhibited lower levels of m⁶A compared with wild-type plants which resulted in loss of the apical dominance, lower growth rate, abnormal root development and increase of trichomes in the branches (Bodi *et al.*, 2012; Růžička *et al.*, 2017).

The function of the plant FIP37 differs of WTAP in humans since it cannot be related to the mRNA splicing process (Zhong *et al.*, 2008; Bodi *et al.*, 2012; Shen L. *et al.*, 2016). Additionally, it has been observed that the deletion of *FIP37* involves a significant decrease in the proportion of m⁶A modification within the stop codon and the 3'-UTR region, while the 5'-UTR region was less affected (Zhong *et al.*, 2008; Bodi *et al.*, 2012). Phenotypically, it is observed that on plants with reduced FIP37, apical meristem suffers an aberrant increase in size and appears abnormal leaf primordia. Interestingly, FIP37 might play a key role indispensable for the regulation of the cell division in the shoot stem cells, because a change in m⁶A levels produces a shift in the amount of key transcripts of regulatory processes (WUSCHEL, *WUS*; *At2g17950* and SHOOTMERISTEMLESS, *STM*; *At1g62360*) (Yue *et al.*, 2019; Shen L. *et al.*, 2016). Additionally, m⁶A is involved in limiting mRNA chimera formation of recently duplicated genes. These are targets of the m⁶A-assisted polyadenylation (m-ASP). According to this, increase of mRNA chimera for m-ASP targets in *Arabidopsis* mutants for *FIP37* with decreased m⁶A has been observed (Pontier *et al.*, 2019).

Considering the low conservation of the machinery for m⁶A editing among the different life lineages, it is likely that some of their integrating factors have not yet been identified in the plant methylome. A possible example of this could be FPA (*At2g43410*), an RNA-binding protein that shows a low degree of homology with

human RBM15 in the RNA binding domain (Arribas-Hernández and Brodersen, 2020). FPA regulates flowering time in *Arabidopsis* via a pathway independent of daylength, by using RNA-mediated chromatin silencing of the floral repressor FLC (FLOWERING LOCUS C), mainly taking part in the polyadenylation process (Bäurle *et al.*, 2007; Hornyik *et al.*, 2010) although its involvement in m⁶A deposition has not yet been demonstrated.

These proteins are essential for a normal development, so it is of paramount importance to study how these proteins perform their regulatory function, and in turn how they are regulated by environmental and nutritional stimuli. This information will give a more complete and complex vision of the role of the plant methylome that can lead to future crop improvements.

1.2 Erasers and their biological implications

Transcriptome-wide analysis has revealed that the appearance and disappearance of the m⁶A modification is a dynamic and reversible process (Luo G. *et al.*, 2014). The elimination of m⁶A modification in the mRNA is called *erasing* and is carried out by enzymes that belong to the ALKBH demethylase family (Jia *et al.*, 2012; Zheng *et al.*, 2013; Duan *et al.*, 2017). Thirteen ALKBH proteins are encoded in the *Arabidopsis* genome (Mielecki *et al.*, 2012), but only for two of them, ALKBH9B (*At2g17970*) and ALKBH10B (*At4g02940*) there are experimental evidences confirming that they catalyze the release of the methyl group from the m⁶A modifications (Duan *et al.*, 2017; Martínez-Pérez *et al.*, 2017). *ALKBH* genes display differential expression throughout tissues (Arribas-Hernández and Brodersen, 2020) as well as different subcellular localizations (Mielecki *et al.*, 2012). Some authors have pointed out that this could imply functional specializations and regulations (Burguess *et al.*, 2016; Shen L. *et al.*, 2019). Subcellular localization approaches have revealed that AtALKBH9B accumulates in cytoplasmatic granules, which colocalize with small interfering RNA (siRNA) bodies (cytoplasmic domains where siRNAs are generated after conversion to double-stranded RNA by the cellular RNA-dependent RNA polymerase 6, RDR6) (Martínez de Alba *et al.*, 2015) and associate with P bodies (cytoplasmic domains that contain proteins involved in diverse posttranscriptional processes, such as mRNA degradation, nonsense-mediated mRNA decay (NMD) and RNA-mediated

gene silencing) (Eulalio *et al.*, 2007). This finding suggests that AtALKBH9B activity might be linked to mRNA silencing and/or mRNA decay processes (Arribas-Hernández *et al.*, 2018). In fact, it has been demonstrated that mRNAs with m⁶A are more stable because this mark inhibits a site-specific cleavage related with the methylation site RRACH (Anderson *et al.*, 2018).

On the other hand, m⁶A modification is also important in the infection caused by virus. The alfalfa mosaic virus (AMV) is an example of this. AMV causes necrosis and yellow mosaics on a large variety of plant species. The AMV genome consists of three single-stranded RNAs of positive sense polarity and has been shown to present m⁶A marks (Martínez-Pérez *et al.*, 2017). It was found that *AtALKBH9B* knockout plants exhibited increased levels of m⁶A deposition on viral RNAs, affecting virus accumulation and facilitating a systemic infection (Martínez-Pérez *et al.*, 2017). It has been demonstrated that AMV coat protein can recruit AtALKBH9B, suggesting the functional importance of the coat protein in the development of virus pathology (Martínez-Pérez *et al.*, 2017). In future applications, these proteins could be used as targets against plant viruses, since m⁶A modifications may play important roles in the pathogen-host response.

In the case of AtALKBH10B, it has been observed that this *eraser* intervenes in the flowering transition and vegetative growth (Mielecki *et al.*, 2012), stabilizing mRNA from FLOWERING LOCUS T (FT, *At1g65480*) and its up-regulators, SQUAMOSA PROMOTER BINDING PROTEIN-LIKE 3 and 9 (SPL3, *At2g33810*; SPL9, *At2g42200*). The increased methylation level promotes accelerated mRNA degradation of these transcripts in *Arabidopsis* (Duan *et al.*, 2017). In this context, this protein family has a tremendous biotechnological potential.

1.3 Readers and biological implications

m⁶A-binding proteins, also known as readers, carry out the identification of this epitranscriptomic mark. These proteins bind specifically to m⁶A-modified nucleotides in RNA mediating post-transcriptional regulation. Several *readers* have been identified to date. The best understood are the YTH domain-containing proteins. YTH domain is highly conserved among all eukaryotic organisms and it is particularly widespread in plants (Zhang *et al.*, 2010). The YTH proteins are

divided in two subfamilies, YTHDC and YTHDF, with nuclear and mainly cytoplasmic localization, respectively. In *Arabidopsis* and rice genomes, 13 and 14 YTH genes were identified respectively, but their functions are mostly uncharacterized (Fray, 2015, Yue *et al.*, 2019). The *Arabidopsis* proteins contain a highly conserved C-terminal region and have been termed as Evolutionarily Conserve C-Terminal Region (ECT). AtECT1 – AtECT11 belong to YTHDF clade and AtECT12 and AtECT13 belong to YTHDC clade (Arribas-Hernández *et al.*, 2018; Scutenaire *et al.*, 2018; Arribas-Hernández and Brodersen, 2020). It has been observed that three tryptophan residues are essential for their m⁶A binding capacity (Trp411, Trp465, and Trp470) forming a hydrophobic pocket where the m⁶A is accommodated (Theler *et al.*, 2014; Xu C. *et al.*, 2014; Zhu *et al.*, 2014). AtECT2 is the homolog of human YTHDF1, YTHDF2 and YTHDF3 proteins which have cytoplasmic localization. Nevertheless, AtECT2 is present in both cytoplasm and nucleus (Wei L. *et al.*, 2018). Using formaldehyde cross-linking and immunoprecipitation the identification of AtECT2 RNA binding sites have been possible. They are mainly located in 3'-UTR regions. It has also been possible to identify a plant-specific m⁶A motif: URUAY (R = G/A, Y = U/A, where over 90% sites were UGUAY) (Wei *et al.*, 2018). UGUA sequence has been reported to be a polyadenylation signal (Shen Y. *et al.*, 2008). Thus, two possible roles have been proposed for AtECT2 according to its localization. AtECT2 generates an increase in the transcripts carrying the m⁶A modification and it is also involved in trichome development, suggesting a AtECT2 role in cytoplasm increasing mRNA stability (Wei *et al.*, 2018).

Furthermore, a role for AtECT2 has been proposed in the nucleus, according to the recognition of UGUA sites. This could be related to mRNA stability through its possible role as a mediator for an alternative polyadenylation and 3'-UTR process (Wei *et al.*, 2018). Additional work showed that AtECT2/3/4 are required for the proper plant aerial organogenesis, acting redundantly for normal leaf morphogenesis and its proper timing (Arribas-Hernández *et al.*, 2018).

Another possible actor is AtCPSF30 (CLEAVAGE AND POLYADENYLATION SPECIFICITY FACTOR 30, *At1g30460*) that harbor an YTH domain unique in plants, which presence is generated by alternative splicing (Fray, 2015; Reichel *et al.*, 2019; Arribas-Hernández and Brodersen, 2020). A role for AtCPSF30 has been

proposed as part of a protein complex that acts in the formation of 3' ends of the mRNA, where m⁶A is frequently present. (Fray, 2015; Burgess *et al.*, 2016; Hunt *et al.*, 2012; Chakrabarti and Hunt, 2015). This hypothesis suggests that m⁶A would play a certain role in the formation of 3' end of mRNA during the process of polyadenylation although it must be corroborated experimentally.

In animals, proteins that do not carry the YTH domain has been related with m⁶A-related regulation, especially during splicing events. Two potential classes of *readers* or related partners are the SR and hnRNP proteins. SR are proteins that recognize the pre-mRNA cis-acting elements (ESEs) and participate in splicing processes. The SR proteins SPLICING FACTOR 3 and 10 (SRSF3 and SRSF10) show competitive binding to the known reader YTHDC1 (Xiao W. *et al.*, 2016). The ability of SRSF3 to bind mRNA increases when interacts with YTHDC, promoting the inclusion of exons. In contrast, this interaction blocks SRSF10 RNA binding process preventing exon exclusion (Xiao W. *et al.*, 2016). On the other hand, SRSF2 has been shown to have preference for binding mRNAs containing m⁶A sites and its RNA binding sites often overlap with m⁶A sites although it has not been shown that it interacts with YTHDC1 (Zhao X. *et al.*, 2014). This might indicate that additional proteins may be involved in the process such as SRSF3 and SRSF10. Heterogeneous nuclear ribonucleoproteins (hnRNP) represent a large family of RNA-binding proteins (RBP) related to multiple processes. It has been proved that hnRNPA2B1 binds to RNAs carrying m⁶A and its biochemical footprint matches the m⁶A consensus motif modulating alternative splicing events (Alarcón *et al.*, 2015-a). Furthermore, hnRNPA2B1 binds to m⁶A in a cluster of primary-miRNA (pri-miRNA) interacting with DGCR8 microRNA microprocessor complex promoting pri-miRNA processing (Alarcón *et al.*, 2015-a). In animals, this is an example of the complexity inherent in the regulation mediated by m⁶A modifications and the proteins involved. To our knowledge, there is no experimental evidence of *reader* proteins without YTH domain in plants. Nevertheless, it is possible to speculate with the existence of a cluster of proteins that have not yet been characterized in plants and involved in the recognition of m⁶A and / or in the cellular function derived from it.

1.4. Existence of m⁶A in chloroplast and mitochondria

Marks of m⁶A have also been found in organellar transcripts (Wan *et al.*, 2015; Shen L. *et al.*, 2016; Wang Z. *et al.*, 2017; Murik *et al.*, 2019). The m⁶A motif in chloroplast and mitochondria transcriptomes shares homology with the nuclear core motif (RRACH), which strongly suggests similar and conserved mechanisms between the organelles and the nuclear epitranscriptome (Wang Z. *et al.*, 2017). Marks of m⁶A have been found in different types and regions of mitochondrial transcripts (mtRNAs) of *Arabidopsis thaliana* and *Brassica oleracea*, including coding sequences, introns, UTRs, and non-coding RNAs mainly near the start codon. These results suggest that this epitranscriptome mark may be related to the translation capacity of mitochondrial mRNAs (Wang Z. *et al.*, 2017). According to the differences in m⁶A transcripts patterns between organelles and nucleus, the editing process may be different in these cell compartments although additional proteins involved in organellar m⁶A cycle have not been identified.

1.5 Other biological roles

The biological implications of m⁶A are less known in plants than in animals. Overall, modifications in RNA could play roles in all RNA processing steps. In eukaryotic organisms other than plants, the m⁶A mark is involved in diverse RNA processes such as splicing (Xiao W. *et al.*, 2016; Louloui *et al.*, 2018), turnover (Ke *et al.*, 2017), stabilization (Wang, Y. *et al.*, 2014; Wang, X. *et al.*, 2014), localization (Lesbriel *et al.*, 2018; Lesbriel and Wilson, 2019), translation (Meyer *et al.*, 2015; Yu *et al.*, 2018), miRNAs (Alarcón *et al.*, 2015-b; Michlewski and Caceres, 2019), ncRNAs (Patil *et al.*, 2016; Warda *et al.*, 2017) and RNA structure (Patil *et al.*, 2016). However, in plants little information is available on processes such as translation (Wang, Y. *et al.*, 2015; Luo, JH. *et al.*, 2020), splicing (Delaney *et al.*, 2006; Pontier *et al.*, 2019) and alternative polyadenylation (Fray, 2015; Delaney *et al.*, 2006; Pontier *et al.*, 2019). Comparatively, mRNA stabilization has been much more studied (Martínez-Pérez *et al.*, 2017; Anderson *et al.*, 2018; Wei, L. *et al.*, 2018; Yue *et al.*, 2019).

At physiological level, there are different processes related to m⁶A modifications. Parker and coworkers observed that m⁶A was associated to circadian and seasonal rhythms (Parker *et al.*, 2020) and have been reported the link between m⁶A into

Appendix 2. 1. m⁶A: Writing, reading and erasing in plants

stress responses (Anderson *et al.*, 2018). Interestingly, saline stress conditions caused an increase in the m⁶A marks located in the stop codon and in the 3'-UTR of transcripts coding for proteins involved in the response to saline and osmotic stresses resulting in increased stability (Anderson *et al.*, 2018).

2. Detecting m⁶A modifications

Several technical approaches have been developed to identify and study m⁶A modifications (Dominissini *et al.*, 2012; Molinie *et al.*, 2016; Aschenbrenner *et al.*, 2018). A summary is shown on Table 1.

Table 1. Technical approaches to study m⁶A RNA modification.

Method	Application	Antibody	References
m ⁶ A dot blot	Semiquantitative detection	+	Molinie <i>et al.</i> , 2016; Shen, L. <i>et al.</i> , 2016; Shen, L. <i>et al.</i> , 2017; Wang, X. <i>et al.</i> , 2017; Nagarajan <i>et al.</i> , 2019
m ⁶ A-seq/Me-RIP-seq	Quantification and dynamics on transcriptome	+	Dominissini <i>et al.</i> , 2012; Meyer <i>et al.</i> , 2012; Dominissini <i>et al.</i> , 2013; Meng <i>et al.</i> , 2014; Warda <i>et al.</i> , 2017; Zeng <i>et al.</i> , 2018
m ⁶ A-LAIC-seq	Quantification of the m6A stoichiometry	+	Molinie <i>et al.</i> , 2016
m ⁶ A-CLIP/miCLIP	Quantification and dynamics on transcriptome	+	Ke <i>et al.</i> , 2015; Linder <i>et al.</i> , 2015
PA-m ⁶ A-seq	Quantification and dynamics on transcriptome	+	Chen, K. <i>et al.</i> , 2015
LC-MS/MS	Detection and quantification	-	Shen, L. <i>et al.</i> , 2016; Yuan, 2017
TLC	Detection and quantification	-	Zhong <i>et al.</i> , 2008; Liu, N. <i>et al.</i> , 2013; Bodi and Fray, 2017
HRM	Detection	-	Golovina <i>et al.</i> , 2014
SELECT	Detection and percentage determination at specific site	-	Xiao, Y. <i>et al.</i> , 2018
SCARLET	Percentage determination at specific site	-	Liu, N. <i>et al.</i> , 2013; Liu N, <i>et al.</i> , 2016;

DART-seq	Quantification and dynamics on transcriptome	-	Meyer, 2019
----------	--	---	-------------

The methodological approaches used to study m⁶A RNA modification can be divided in antibody-dependent and antibody-free methods. Among methodologies using antibodies, the m⁶A dot blot is useful to observe global changes in m⁶A levels. Nevertheless, it is restricted to qualitative analysis without the possibility to characterize m⁶A changes in the individual transcripts (Molinie *et al.*, 2016; Shen, L. *et al.*, 2016) (Figure 3a). For that reason, the most widely used techniques combine both antibody specificity and high throughput sequencing. This allows determinations of m⁶A profiles between samples at individual transcript level. Before the immunoprecipitation, the RNA is usually fragmented (approximate sizes of 100-200 nt). This allows the bioinformatic identification of conserved sites and domains for m⁶A. The immunoprecipitation of methylated RNA using specific m⁶A antibodies and subsequent deep sequencing (m⁶A-seq/MeRIP-seq) allows comparative, quantitative and localized studies (Dominissini *et al.*, 2012; Meyer *et al.*, 2012) (Figure 3b.1). MeRIP-seq presents three major drawbacks: a considerable amount of input RNA is usually required (e.g. several micrograms of poly(A)-RNA). It has low resolution, which makes difficult to evaluate and identify the actual m⁶A site and may not directly assess the false positives (McIntyre *et al.*, 2019). Alternatively, the m⁶A-level and isoform-characterization sequencing technique (m⁶A-LAIC-seq) does not require RNA fragmentation (Molinie *et al.*, 2016) (Figure 3b.2). This method relies on sequencing full-length transcripts in both m⁶A-positive and negative fractions after the RNA immunoprecipitation step, allowing quantification of m⁶A levels with spike-in RNAs as an internal standard. This approach permits to examine the differential use of (non)/methylated isoform (Molinie *et al.*, 2016). Despite this, the m⁶A-LAIC-seq is unable to identify the m⁶A sites or domains. In contrast, there is a group of methods that combine UV crosslinking and massive sequencing techniques such as m⁶A-CLIP (crosslinking immunoprecipitation) (Ke *et al.*, 2015), miCLIP (m⁶A individual-nucleotide-resolution crosslinking and immunoprecipitation) (Linder *et al.*, 2015) (Figure 3b.3) and PA-m⁶A-seq (photo-crosslinking-assisted m⁶A sequencing) (Chen, K. *et*

al., 2015) (Figure 3b.4). Using these technologies, the identification of m⁶A nucleosides is not restricted to a consensus motif allowing a properly or at least more accurate identification of m⁶A sites. UV light is used to establish a crosslinking between RNA fragments and m⁶A antibodies, which avoids losses of antibodies bound to m⁶A during the washing steps. This results in increased RNA recovery that improves the massive sequencing output.

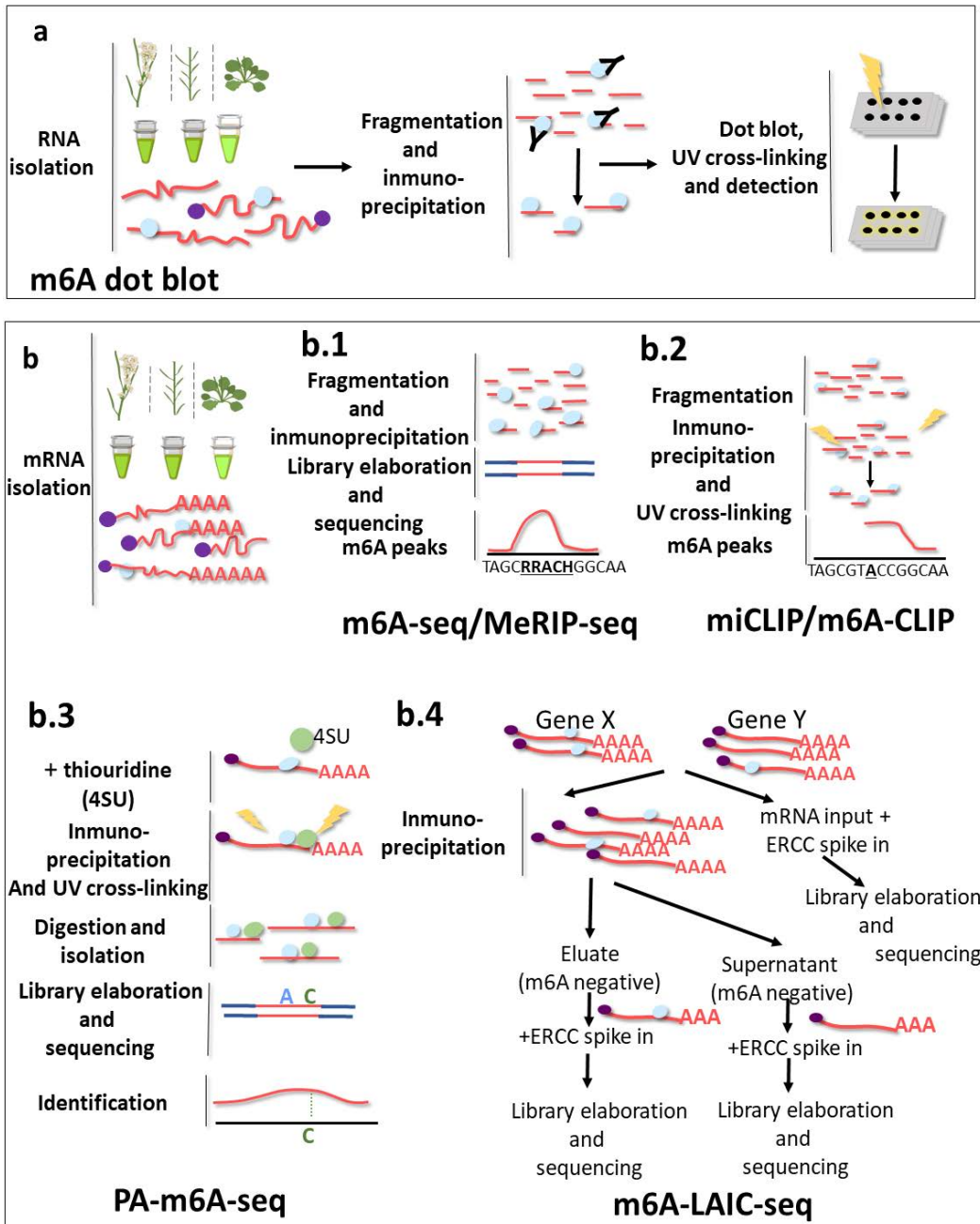


Figure 3. Schematic m⁶A Antibody based detection approaches. **a)** Total m⁶A detection, m⁶A dot blot (Nagarajan *et al.*, 2019). **b)** High throughput sequencing m⁶A detection, b.1) m⁶A-seq/MeRIP-seq (Dominissini *et al.*, 2012; Meyer *et al.*,

2012), b.2) m⁶A-LAIC-seq (Molinie *et al.*, 2016), b.3) miCLIP/m⁶A-CLIP (Ke *et al.*, 2015; Linder *et al.*, 2015), and b.4) PA-m⁶A-seq (Chen, K. *et al.*, 2015).

As previously mentioned, a common limitation for methods based on the use of antibodies and allowing a global mapping of the methylation sites is the large amount of initial RNA required. Thus, these methods used to be not feasible for limited quantity samples, even if the improvements in these methodologies have allowed to reduce the required amount (Merkurjev *et al.*, 2018; Weng, Y. *et al.*, 2018; Zeng *et al.*, 2018). At the same time, it is necessary to keep in mind that anti-m⁶A antibodies can generate cross reactions because they can recognize the structurally similar cap modification N⁶,2'-O-dimethyladenosine (m⁶Am). Thus, in cases where the immunoprecipitation process is used, false positive results can be obtained.

Alternative methodologies that do not use anti-m⁶A antibodies have been developed. Mass spectrometry constitutes a sensitive method in order to detect m⁶A, permitting the detection at poor abundance. RNA needs to be fragmented and separated in order to allow the detection through tandem mass spectrometers. However, this approach does not allow differentiation between the m⁶A of the mRNA and the m⁶A of the rRNA or snRNA (Thüring *et al.*, 2017; Zaccara *et al.*, 2019). Two-dimensional thin layer chromatography (TLC) method makes possible to separate different biochemicals on the basis of their relative attractions to the stationary and mobile phases. Using RNase T1 digestion and a 2D thin-layer chromatography has been possible to quantify the amount of m⁶A (Zhong *et al.*, 2008; Jia, G. *et al.*, 2012; Bodi and Fray, 2017). Other options are HRM (high-resolution melting analysis) (Golovina *et al.*, 2014) (Figure 4a) and SELECT (single-base elongation- and ligation-based qPCR amplification method) (Xiao, Y. *et al.*, 2018) (Figure 4b). HRM is a simple alternative to detect m⁶A residues in a specific area of the RNA that relies on the previous knowledge of the m⁶A modification site (Golovina *et al.*, 2014). The presence of m⁶A reduces the melting temperature of the RNA / DNA duplex. A previous quick screening to optimize conditions to perform the assay is required (Golovina *et al.*, 2014). The HRM assay allows to determine the modification grade of a determined known site comparing two or more samples. While SELECT is based on the fact that m⁶A hinders the activity of single base elongation by DNA polymerases and the efficiency of the

Appendix 2. 2. Detecting m⁶A modifications

nick ligation by the DNA ligase (Xiao, Y. *et al.*, 2018). Two DNA primers with PCR adapters anneal to RNA leaving a gap opposite to m⁶A. The m⁶A modifications on the RNA selectively prevent single base elongation mediated by the *Bst* DNA polymerase from the probe. Although this step is not fully efficient, the following nick ligation step filters them out because any m⁶A mark inhibits the ligation step. This produces a decrease in the quantity of products obtained. The presence of the m⁶A is observed by the comparison of the qPCR results of the control sample against the problem sample since the amplification of samples with m⁶A modification should be retarded. This approach allows the m⁶A position resolution and quantification with single nucleotide precision (Xiao, Y. *et al.*, 2018). The SCARLET method (Site-specific cleavage and radioactive labeling followed by ligation-assisted extraction and thin-layer chromatography) constitutes an approach to settle the exact localization of m⁶A at any mRNA/lncRNA of interest at a single nucleotide resolution (Liu, N. *et al.*, 2013) (Figure 4c). This technique combines site-specific cleavage of each m⁶A site of a candidate transcript by combined RNase H site-specific cleavage, followed by a radiolabeling step, performing a splinted ligation to a 116-mer DNA oligo and a final RNase A/T1 digestion. Denaturing PAGE is used to isolate the ligation product: individual nucleotides are digested by nuclease P1 and m⁶A is detected by TLC (Liu, N. *et al.*, 2013). The main SCARLET limitation is that works only on one mRNA/lncRNA candidate because the complexity of the procedure involves different steps and radioactivity labeling, but it is also possible to parallelize several experiments at the same time (Liu, N. *et al.*, 2016). Until now the techniques mentioned above have in common that they are not used to carry out global studies. However, in 2019 Meyer published a new antibody-free method called DART-seq (deamination adjacent to RNA modification targets) in animal cells (Meyer, 2019) (Figure 4d). DART-seq is based on the fact that the cytidine deaminase APOBEC1 induces deamination C→U. This protein is fused to YTH domain from YTHDF2 protein that binds m⁶A sites. The cells are transformed with a DNA construction that allows the expression of this fusion protein (APOBEC1-YTH), which induces the deamination C→U of sites adjacent to m⁶A residues. The changes in the sequence are detected by standard RNA-seq (Meyer, 2019). This approach avoids the problems derived from the use of antibodies described before although requires genetic transformation of the organism. Additionally, it is possible to perform this method with a low RNA

quantity. Other possibility is the use of this method for the localization of m⁶A modifications in different cellular compartments targeting APOBEC1-YTH fusion protein. Even potentially can be used together with single-cell isolation and library preparation methods to achieve single-cell m⁶A detection (Meyer, 2019).

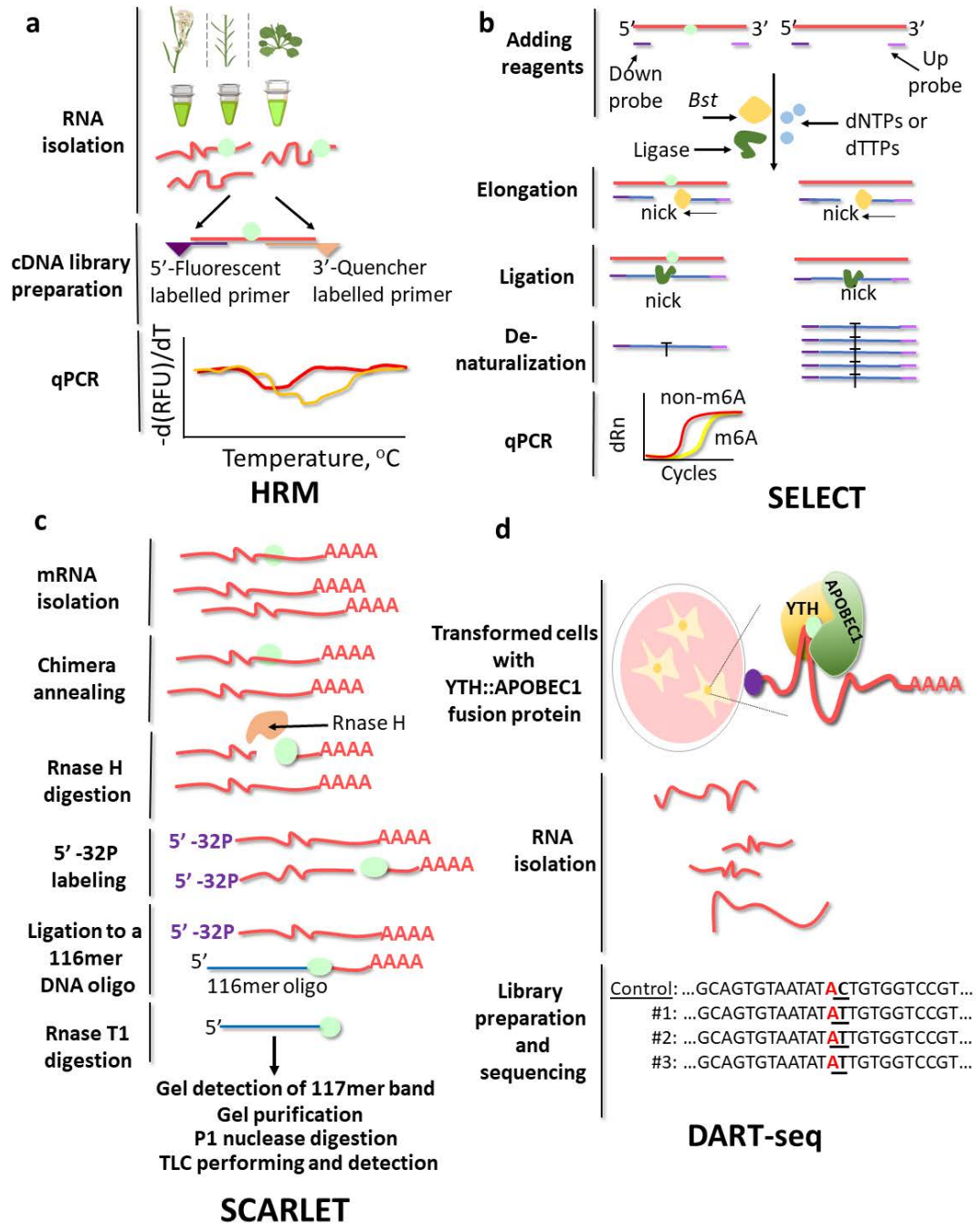


Figure 4. Schematic m⁶A Antibody non-based detection approaches. **a)** High-resolution melting analysis (Golovina *et al.*, 2014). **b)** Single-base elongation- and ligation-based qPCR amplification method (SELECT) (Xiao, Y. *et al.*, 2018). **c)** Site-specific cleavage and radioactive labeling followed by ligation-assisted

Appendix 2. 2. Detecting m⁶A modifications

extraction and thin-layer chromatography (SCARLET) (Liu, N. *et al.*, 2013). **d**) Deamination adjacent to RNA modification targets (DART-seq) (Meyer, 2019).

Regardless of the approach, they all have the same common characteristic that is inherent in the very nature of the RNA and that to obtain reliable results on m⁶A modification in mRNAs it is essential to efficiently remove contaminants from tRNAs and rRNAs. Therefore, transcriptome-wide mapping protocols are currently most used.

In recent years, and with the release of the Oxford Nanopore Technology (ONT) platform, there is the potential to directly detect chemical modifications in the original nucleotide (Xiong *et al.*, 2017; Zhao *et al.*, 2019). The direct-RNA sequencing (DRS) method developed by ONT avoids amplification biases (Garalde *et al.*, 2018) providing a more complete and complex view of RNA modifications. In ONT-DRS, an ionic current pass through the biological nanopore (bacterial CsgG amyloid secretion protein) and the device detects the changes in current generated when RNA strand crosses the nanopore. This information is translated downstream into nucleotide sequences through a bioinformatic procedure known as base-calling. A feature that stands out in this methodology is the base-caller programs that allow translating changes in the current into the specific nucleotide sequence. There are different base-callers, it is possible to use the base-callers provided by Oxford Nanopore on the Metrichor cloud computing platform (e.g.: Guppy, Albacore), but several research groups are generating other alternatives (David *et al.*, 2016; Boža *et al.*, 2017). These softwares are based on artificial intelligent approaches to translate current signals into nucleotides including their modifications. Now, they need to be improved in order to achieve higher accuracy because that is one of their main weaknesses. This would allow to draw a more complex picture at transcriptome and epitranscriptome levels. Another limitation is that bioinformatic tools for detecting RNA chemical modifications are scarce. Tombo (Stoiber *et al.*, 2016), EpiNano (Liu, H. *et al.*, 2019) or MINES (Lorenz *et al.*, 2020) are, up to date, the only reported tools to identify modified nucleotides in RNA and they are mainly limited to m⁶A, but it is also possible the detection of m⁵C using Tombo. Currently, this emerging technology must be complemented by second generation sequencing to obtain sufficiently robust results. Therefore, the ONT-DRS is postulated as a highly valuable alternative to perform both

transcriptomic and epitranscriptomic studies, although software analysis should be implemented.

3. Future perspectives

The molecular bases underlying the biological roles of m⁶A must be studied because little is known about this topic, especially in plants. Research efforts are required to shed light on the biological importance of the m⁶A modification and to answer the most asked questions such as: Why are some types of RNAs methylated and not others? Why are certain localized sites modified? What are the roles of modified sites in RNA processing? Because of this, epitranscriptomics constitutes a novel field of study full of challenges and possibilities, which will undergo a significant boom in the coming years, revealing how the epitranscriptome regulates and can be dynamically regulated affecting the transcriptome. Additional research efforts on m⁶A modification in crop species can provide valuable information to further improve crop performance



References



- Abiko T, Obara M, Ushioda A, Hayakawa T, Hodges M, Yamaya T. 2005.** Localization of NAD-isocitrate dehydrogenase and glutamate dehydrogenase in rice roots: candidates for providing carbon skeletons to NADH-glutamate synthase. *Plant and cell physiology*, **46**:1724-1734.
- Aichinger E, Kornet N, Friedrich T, Laux T. 2012.** Plant stem cell niches. *Annual Review of Plant Biology*, **63**: 615-636.
- Agrawal A, Cashore B, Hardin R, Shepherd G, Benson C, Miller D. 2013.** *Economic contributions of forests*. Background paper, 1.
- Akoka S, Barantin L, Trierweiler M. 1999.** Concentration measurement by proton NMR using the ERETIC method. *Analytical Chemistry*, **71**:2554-2557.
- Alarcón CR, Goodarzi H, Lee H, Liu X, Tavazoie S, Tavazoie SF. 2015a.** HNRNPA2B1 is a mediator of m6A-dependent nuclear RNA processing events. *Cell*, **162**: 1299-1308.
- Alarcón CR, Lee H, Goodarzi H, Halberg N, Tavazoie SF. 2015b.** N6-methyladenosine marks primary microRNAs for processing. *Nature* **519**: 482–485.
- Allúe Andrade JL. 1990.** Mapa de Subregiones Fitoclimáticas de España Peninsular y Balear. *Ministerio para la Transición Ecológica y el Reto Demográfico*.
- Alberts B, Bray D, Hopkin K, Johnson AD, Lewis J, Raff M, Roberts K, Walter P. 2013.** Essential cell biology. *Garland Science*.
- Álvarez C, Ángeles Bermúdez M, Romero LC, Gotor C, García I. 2012.** Cysteine homeostasis plays an essential role in plant immunity. *New Phytologist*, **193**: 165-177.
- Ananvoranich S, Varin L, Gulick P, Ibrahim R. 1994.** Cloning and regulation of flavonol 3-sulfotransferase in cell-suspension cultures of *Flaveria bidentis*. *Plant Physiology*, **106**: 485-491.
- Anderson SJ, Kramer MC, Gosai SJ, Yu X, Vandivier LE, Nelson AD, Anderson ZD, Beilstein MA, Fray RG, Lyon E, Gregory BD. 2018.** N6-methyladenosine inhibits local ribonucleolytic cleavage to stabilize mRNAs in *Arabidopsis*. *Cell Reports*, **25**: 1146-1157.
- Andrade SL, Dickmanns A, Ficner R, Einsle O. 2005.** Crystal structure of the archaeal ammonium transporter Amt-1 from *Archaeoglobus fulgidus*. *Proceedings of the National Academy of Sciences*, **102**: 14994-14999.
- Aoyama T, Dong CH, Wu Y, Carabelli M, Sessa G, Ruberti, I, Morelli G, Chua NH. 1995.** Ectopic expression of the Arabidopsis transcriptional activator Athb-1 alters leaf cell fate in tobacco. *The Plant Cell*, **7**: 1773-1785.
- Aranda I, Alía R, Ortega U, Dantas ÂK, Majada J. 2010.** Intra-specific variability in biomass partitioning and carbon isotopic discrimination under moderate drought stress in seedlings from four *Pinus pinaster* populations. *Tree Genetics & Genomes*, **6**: 169-178.

Araya T, Kubo T, von Wirén N, Takahashi H. 2015. Statistical modeling of nitrogen-dependent modulation of root system architecture in *Arabidopsis thaliana*. *Journal of Integrative Plant Biology*, **58**: 254-265.

Ariz I, Asensio AC, Zamarreño AM, García-Mina JM., Aparicio-Tejo PM, Moran JF. 2013. Changes in the C/N balance caused by increasing external ammonium concentrations are driven by carbon and energy availabilities during ammonium nutrition in pea plants: the key roles of asparagine synthetase and anaplerotic enzymes. *Physiologia Plantarum*, **148**: 522-537.

Arribas-Hernández L, Bressendorff S, Hansen MH, Poulsen C, Erdmann S, Brodersen P. 2018. An m6A-YTH module controls developmental timing and morphogenesis in Arabidopsis. *The Plant Cell*, **30**: 952-967.

Arribas-Hernández L, Brodersen P. 2020. Occurrence and functions of m6A and other covalent modifications in plant mRNA. *Plant Physiology*, **182**: 79-96.

Aschenbrenner J, Werner S, Marchand V, Adam M, Motorin Y, Helm M, Marx A. 2018. Engineering of a DNA polymerase for direct m6A sequencing. *Angewandte Chemie International Edition*, **57**: 417-421.

Asiegbu FO, Choi W, Li G, Nahalkova J, Dean RA. 2003. Isolation of a novel antimicrobial peptide gene (*Sp-AMP*) homologue from *Pinus sylvestris* (Scots pine) following infection with the root rot fungus *Heterobasidion annosum*. *FEMS Microbiology Letters*, **228**: 27-31.

Avila C, Suárez MF, Gómez-Maldonado J, Cánovas FM. 2001. Spatial and temporal expression of two cytosolic glutamine synthetase genes in Scots pine: functional implications on nitrogen metabolism during early stages of conifer development. *The Plant Journal*, **25**: 93-102.

Babourina O, Voltchanskii K, McGann B, Newman I, Rengel Z. 2007. Nitrate supply affects ammonium transport in canola roots. *Journal of Experimental Botany*, **58**: 651-658.

Bai L, Zhou Y, Ma X, Gao L, Song CP. 2014a. Arabidopsis CAP1-mediated ammonium sensing required reactive oxygen species in plant cell growth. *Plant Signaling & Behavior*, **9**: e29582.

Bai L, Ma X, Zhang G, Song S, Zhou Y, Gao L, Miao Y, Song CP. 2014b. A receptor-like kinase mediates ammonium homeostasis and is important for the polar growth of root hairs in *Arabidopsis*. *The Plant Cell*, **26**: 1497-1511.

Bailey TL, Johnson J, Grant CE, Noble WS. 2015. The MEME suite. *Nucleic Acids Research*, **43**: 39-49.

Barker AV, Corey KA. 1991. Interrelations of ammonium toxicity and ethylene action in tomato. *Horticultural Science*, **26**: 177-180.

Backer R, Naidoo S, van den Berg N. 2019. The NONEXPRESSOR OF PATHOGENESIS-RELATED GENES 1 (NPR1) and related family: mechanistic insights in plant disease resistance. *Frontiers in Plant Science*, **10**: 102.

- Bäurle I, Smith L, Baulcombe DC, Dean C. 2007.** Widespread role for the flowering-time regulators FCA and FPA in RNA-mediated chromatin silencing. *Science*, **318**: 109-112.
- Bedon F, Grima-Pettenati J, Mackay J. 2007.** Conifer R2R3-MYB transcription factors: sequence analyses and gene expression in wood-forming tissues of white spruce (*Picea glauca*). *BMC Plant Biology*, **7**: 17.
- Beier MP, Obara M, Taniai A, Sawa Y, Ishizawa J, Yoshida H, Tomita N, Yamanaka T, Ishizuka Y, Kudo S, et al. 2018.** Lack of ACTPK 1, an STY kinase, enhances ammonium uptake and use, and promotes growth of rice seedlings under sufficient external ammonium. *The Plant Journal*, **93**: 992-1006.
- Bennett T, van den Toorn A, Sanchez-Perez GF, Campilho A, Willemsen V, Snel B, Scheres B. 2010.** SOMBRERO, BEARSKIN1, and BEARSKIN2 regulate root cap maturation in *Arabidopsis*. *The Plant Cell*, **22**: 640-654.
- Bennett T, van den Toorn A, Willemsen V, Scheres B. 2014.** Precise control of plant stem cell activity through parallel regulatory inputs. *Development*, **141**: 4055-4064.
- Bernard SM, Habash, DZ. 2009.** The importance of cytosolic glutamine synthetase in nitrogen assimilation and recycling. *New Phytologist*, **182**: 608-620.
- Bijlsma RJ, Lambers H, Kooijman SALM. 2000.** A dynamic whole-plant model of integrated metabolism of nitrogen and carbon. 1. Comparative ecological implications of ammonium-nitrate interactions. *Plant and Soil*, **220**: 49-69.
- Birol I, Raymond A, Jackman SD, Pleasance S, Coope R, Taylor GA, Saint Yuen MM, Keeling CI, Brand D, Vandervalk BP, et al. 2013.** Assembling the 20 Gb white spruce (*Picea glauca*) genome from whole-genome shotgun sequencing data. *Bioinformatics*, **29**: 1492-1497.
- Bishopp A, Help H, El-Showk S, Weijers D, Scheres B, Friml J, Benkova E, Mähönen AP, Helariutta Y. 2011.** A mutually inhibitory interaction between auxin and cytokinin specifies vascular pattern in roots. *Current Biology*, **21**: 917-926.
- Bloom AJ, Asensio JSR, Randall L, Rachmilevitch S, Cousins AB, Carlisle EA. 2012.** CO₂ enrichment inhibits shoot nitrate assimilation in C₃ but not C₄ plants and slows growth under nitrate in C₃ plants. *Ecology*, **93**: 355-367.
- Boccaletto P, Machnicka MA, Purta E, Piątkowski P, Bagiński B, Wirecki TK, de Crécy-Lagard V, Ross R, Limbach PA, Kotter A, et al. 2017.** MODOMICS: a database of RNA modification pathways. 2017 update. *Nucleic Acids Research*, **46**: 303-307.
- Boczulak SA, Hawkins BJ, Roy R. 2014.** Temperature effects on nitrogen form uptake by seedling roots of three contrasting conifers. *Tree Physiology*, **34**: 513-523.
- Bodi Z, Fray RG. 2017.** Detection and quantification of N⁶-Methyladenosine in messenger RNA by TLC. *RNA Methylation*. Humana Press, New York, NY: 79-87.

Bodi Z, Zhong S, Mehra S, Song J, Graham N, Li H, May S, Fray RG. 2012. Adenosine methylation in *Arabidopsis* mRNA is associated with the 3' end and reduced levels cause developmental defects. *Frontier in Plant Science*, **3**:48.

Boggy GJ, Woolf PJ. 2010. A mechanistic model of PCR for accurate quantification of quantitative PCR data. *PloS One*, **5**: e12355.

Bohnsack MT, Sloan KE. 2018. The mitochondrial epitranscriptome: the roles of RNA modifications in mitochondrial translation and human disease. *Cellular and molecular life sciences*, **75**: 241-260.

Borysiuk K, Ostaszewska-Bugajska M, Vaultier MN, Hasenfratz-Sauder MP, Szal B. 2018. Enhanced formation of methylglyoxal-derived advanced glycation end products in *Arabidopsis* under ammonium nutrition. *Frontiers in Plant Science*, **9**, 667.

Bostick DL, Brooks III CL. 2007. Deprotonation by dehydration: the origin of ammonium sensing in the AmtB channel. *PLoS Computational Biology* **3**: e22.

Bouche N, Fromm H. 2004. GABA in plants: just a metabolite? *Trends in Plant Science*, **9**: 110-115.

Boža V, Brejová B, Vinař T. 2017. DeepNano: deep recurrent neural networks for base calling in MinION nanopore reads. *PloS One*, **12**.

Bradford MM. 1976. A rapid and sensitive method for the quantitation of microgram quantities of protein utilizing the principle of protein-dye binding. *Analytical Biochemistry*, **72**: 248-254.

Breullin-Sessoms F, Floss DS, Gomez SK, Pumplin N, Ding Y, Levesque-Tremblay V, Noar RD, Daniels DA, Bravo A, Eaglesham JD, et al. 2015. Suppression of arbuscule degeneration in *Medicago truncatula* phosphate transporter4 mutants is dependent on the ammonium transporter 2 family protein AMT2; 3. *The Plant Cell*, **27**: 1352-1366.

Bright RM, Strømman AH. 2009. Life cycle assessment of second generation bioethanols produced from Scandinavian boreal forest resources: A regional analysis for middle Norway. *Journal of Industrial Ecology*, **13**: 514-531.

Britto DT, Kronzucker HJ. 2013. Ecological significance and complexity of N-source preference in plants. *Annals of Botany*, **112**: 957-963.

Brown DE, Rashotte AM, Murphy AS, Normanly J, Tague BW, Peer WA, Taiz L, Muday GK. 2001. Flavonoids act as negative regulators of auxin transport in vivo in *Arabidopsis*. *Plant physiology*, **126**: 524-535.

Brunoni F, Ljung K, Bellini C. 2019. Control of root meristem establishment in conifers. *Physiologia Plantarum*, **165**: 81-89.

Buchanan BB, Grissem W, Jones RL. 2015. Biochemistry and molecular biology of plants (2nd Edition). *John Wiley & Sons, Inc.*, Chichester, UK.

- Buchfink B, Xie C, Huson DH. 2015.** Fast and sensitive protein alignment using DIAMOND. *Nature Methods* **12**: 59-60.
- Burban C, Petit RJ. 2003.** Phylogeography of maritime pine inferred with organelle markers having contrasted inheritance. *Molecular Ecology*, **12**: 1487-1495.
- Burgess A, David R, Searle IR. 2016.** Deciphering the epitranscriptome: A green perspective. *Journal of Integrative Plant Biology*, **58**:822-835.
- Bustin SA, Benes V, Garson JA, Hellemans J, Huggett J, Kubista M, Mueller R, Nolan T, Pfaffl MW, Shipley GL et al. 2009.** The MIQE guidelines: minimum information for publication of quantitative real-time PCR experiments. *Clinical Chemistry* **55**: 611-622.
- Butcher TB. 2007.** Achievements in forest tree genetic improvement in Australia and New Zealand 7: Maritime pine and Brutian pine tree improvement programs in Western Australia. *Australian Forestry*, **70**: 141-151.
- Camacho C, Coulouris G, Avagyan V, Ma N, Papadopoulos J, Bealer K, Madden TL. 2008.** BLAST+: architecture and applications. *BMC Bioinformatics*, **10** :421.
- Canales J, Bautista R, Label P, Gómez-Maldonado J, Lesur I, Fernández-Pozo N, et al. 2014.** De novo assembly of maritime pine transcriptome: implications for forest breeding and biotechnology. *Plant Biotechnology Journal*, **12**: 286-299.
- Canales J, Rueda-López M, Craven-Bartle B, Avila C, Cánovas FM. 2012.** Novel insights into regulation of asparagine synthetase in conifers. *Frontiers in Plant Science*, **3**.
- Canales J, Avila C, Canovas FM. 2011.** A maritime pine antimicrobial peptide involved in ammonium nutrition. *Plant, Cell & Environment*, **34**: 1443-1453.
- Canales J, Flores-Monterrosso A, Rueda-López M, Avila C, Cánovas FM. 2010.** Identification of genes regulated by ammonium availability in the roots of maritime pine trees. *Amino Acids*, **39**: 991-1001.
- Cánovas FM., Avila C, Cantón FR, Canas RA, de la Torre F. 2007.** Ammonium assimilation and amino acid metabolism in conifers. *Journal of Experimental Botany*, **58**: 2307-2318.
- Cánovas FM, Cantón FR, Gallardo F, García-Gutiérrez A, de Vicente A. 1991.** Accumulation of glutamine synthetase during early development of maritime pine (*Pinus pinaster*) seedlings. *Planta* **185**: 372-378.
- Cánovas F, Valpuesta V, Núñez de Castro I. 1984.** Characterization of glutamine synthetase from tomato leaves. *Plant Science Letters*, **37**:79-85.
- Cantón FR, Suárez MF, Cánovas FM. 2005.** Molecular aspects of nitrogen mobilization and recycling in trees. *Photosynthesis Research*, **83**: 265-278.
- Cantón FR, Suárez MF, Jose-Estanyol M, Cánovas FM. 1999.** Expression analysis of a cytosolic glutamine synthetase gene in cotyledons of Scots pine seedlings: developmental, light regulation and spatial distribution of specific transcripts. *Plant Molecular Biology*, **40**: 623-634.

References

Cantón FR, Garcia-Gutierrez A, Crespillo R, Cánovas FM. 1996. High-level expression of *Pinus sylvestris* glutamine synthetase in *Escherichia coli*: Production of polyclonal antibodies against the recombinant protein and expression studies in pine seedlings. *FEBS Letters*, **393**: 205-210.

Cañas RA, Pascual MB, Fernando N, Ávila C, Cánovas FM. 2019. Resources for conifer functional genomics at the omics era. In *Advances in Botanical Research*. Academic Press, **89**: 39-76.

Cañas RA, Li Z, Pascual MB, Castro-Rodríguez V, Ávila C, Sterck L, et al. 2017. The gene expression landscape of pine seedling tissues. *The Plant Journal*, **91**: 1064-1087.

Cañas RA, Yesbergenova-Cuny Z, Simons M, Chardon F, Armengaud P, Quilleré I, Cukier C, Gibon Y, et al. 2017. Exploiting the genetic diversity of maize using a combined metabolomic, enzyme activity profiling, and metabolic modeling approach to link leaf physiology to kernel yield. *The Plant Cell*, **29**: 919-943.

Cañas RA, De la Torre F, Pascual MB, Avila C, Cánovas FM. 2016. Nitrogen economy and nitrogen environmental interactions in conifers. *Agronomy*, **6**: 26.

Cañas RA, Feito I, Fuente-Maqueda JF, Avila C, Majada J, Canovas F M. 2015a. Transcriptome-wide analysis supports environmental adaptations of two *Pinus pinaster* populations from contrasting habitats. *BMC Genomics*, **16**: 909.

Cañas RA, Canales J, Muñoz-Hernández C, Granados JM, Ávila C, García-Martín ML, Cánovas FM. 2015b. Understanding developmental and adaptive cues in pine through metabolite profiling and co-expression network analysis. *Journal of Experimental Botany*, **66**: 3113-3127.

Cañas RA, Canales J, Gómez-Maldonado J, Ávila C, Cánovas FM. 2014. Transcriptome analysis in maritime pine using laser capture microdissection and 454 pyrosequencing. *Tree Physiology*, **34**: 1278-1288.

Cañas RA, Quilleré I, Christ A, Hirel B. 2009. Nitrogen metabolism in the developing ear of maize (*Zea mays*): analysis of two lines contrasting in their mode of nitrogen management. *New Phytologist*, **184**: 340-352.

Cañas RA, Villalobos DP, Díaz-Moreno SM, Cánovas FM, Cantón FR. 2008. Molecular and functional analyses support a role of ornithine- δ -aminotransferase in the provision of glutamate for glutamine biosynthesis during pine germination. *Plant Physiology*, **148**: 77-88.

Cañas RA, de la Torre F, Cánovas FM, Cantón FR. 2007. Coordination of *PsAS1* and *PsASPG* expression controls timing of re-allocated N utilization in hypocotyls of pine seedlings. *Planta*, **225**: 1205-1219.

Cañas RA, de la Torre F, Canovas FM, Canton FR. 2006. High levels of asparagine synthetase in hypocotyls of pine seedlings suggest a role of the enzyme in re-allocation of seed-stored nitrogen. *Planta*, **224**: 83-95.

- Cao Y, Glass AD and Crawford, NM. 1993.** Ammonium inhibition of *Arabidopsis* root growth can be reversed by potassium and by auxin resistance mutations *aux1*, *axr1*, and *axr2*. *Plant Physiology*, **102**: 983-989.
- Carlsbecker A, Lee JY, Roberts CJ, Dettmer J, Lehesranta S, Zhou J, Lindgren O, Moreno-Risueno MA, Vatén A, Thitamadee S, et al. 2010.** Cell signalling by microRNA165/6 directs gene dose-dependent root cell fate. *Nature*, **20**: 316-321.
- Carroll AD, Fox GG, Laurie S, Phillips R, Ratcliffe RG, Stewart GR. 1994.** Ammonium assimilation and the role of [gamma]-aminobutyric acid in pH homeostasis in carrot cell suspensions. *Plant Physiology*, **106**: 513-520.
- Castro-Rodríguez V, Cañas RA, de la Torre FN, Pascual MB, Avila C, Cánovas FM. 2017.** Molecular fundamentals of nitrogen uptake and transport in trees. *Journal of Experimental Botany*, **68**: 2489-2500.
- Castro-Rodríguez V, Assaf-Casals I, Pérez-Tienda J, Fan X, Avila C, Miller A, Cánovas FM. 2016.** Deciphering the molecular basis of ammonium uptake and transport in maritime pine. *Plant, Cell & Environment*, **39**: 1669-1682.
- Castro-Rodríguez V, García-Gutiérrez A, Canales J, Canas RA, Kirby EG, Avila C, Cánovas FM. 2016b.** Poplar trees for phytoremediation of high levels of nitrate and applications in bioenergy. *Plant Biotechnology Journal*, **14**:299-312.
- Cesana M, Cacchiarelli D, Legnini I, Santini T, Sthandier O, Chinappi M, Tramontano A, Bozzoni I. 2011.** A long noncoding RNA controls muscle differentiation by functioning as a competing endogenous RNA. *Cell*, **147**: 358-369.
- Cesetti T, Ciccolini F, Li Y. 2012.** GABA not only a neurotransmitter: osmotic regulation by GABAAR signaling. *Frontiers in Cellular Neuroscience*, **6**:3.
- Chakrabarti M, Hunt AG. 2015.** CPSF30 at the interface of alternative polyadenylation and cellular signaling in plants. *Biomolecules*, **5**, 1151–1168.
- Chaffey NJ. (Ed.). 2002.** Wood formation in trees: cell and molecular biology techniques. *CRC Press*.
- Chapman EJ, Estelle M. 2009.** Mechanism of auxin-regulated gene expression in plants. *Annual Review of Genetics*, **43**: 265-285.
- Chekulaeva M, Filipowicz W. 2009.** Mechanisms of miRNA-mediated post-transcriptional regulation in animal cells. *Current Opinion in Cell Biology*, **21**: 452-460.
- Chen M, Witte CP. 2020.** A kinase and a glycosylase catabolize pseudouridine in the peroxisome to prevent toxic pseudouridine monophosphate accumulation. *The Plant Cell*, **32**: 722-739.
- Chen P, Jäger G, Zheng B. 2010.** Transfer RNA modifications and genes for modifying enzymes in *Arabidopsis thaliana*. *BMC Plant Biology*, **10**: 201.
- Chen TH and Murata AN. 2011.** Glycinebetaine protects plants against abiotic stress: mechanisms and biotechnological applications. *Plant, Cell & Environment*, **34**: 1-20.

References

Chen K, Lu Z, Wang X, Fu Y, Luo GZ, Liu N Han D, Dominissini D, Dai Q, Pan T, et al. 2015. High-resolution N6-methyladenosine (m6A) map using photocrosslinking-assisted m6A sequencing. *Angewandte Chemie International Edition*, **54**: 1587-1590.

Chevalier C, Bourgeois E, Just D, Raymond P. 1996. Metabolic regulation of asparagine synthetase gene expression in maize (*Zea mays* L.) root tips. *The Plant Journal*, **9**: 1-11.

Chiasson DM, Loughlin PC, Mazurkiewicz D, Mohammadidehcheshmeh M, Fedorova EE, Okamoto M, et al. 2014. Soybean *SATI* (Symbiotic Ammonium Transporter 1) encodes a bHLH transcription factor involved in nodule growth and NH₄⁺ transport. *Proceedings of the National Academy of Sciences*, **111**: 4814-4819.

Chong J, Soufan O, Li C, Caraus I, Li S, Bourque G, Wishart DS, Xia J. 2018. MetaboAnalyst 4.0: towards more transparent and integrative metabolomics analysis. *Nucleic Acids Research*, **46**: 486-494.

Chou CC, Modi JP, Wang CY, Hsu PC, Lee YH, Huang KF, Wang AHJ, Nan C, Huang X, Wei, J. 2017. Activation of brain L-glutamate decarboxylase 65 isoform (GAD65) by phosphorylation at threonine 95 (T95). *Molecular Neurobiology*, **54**: 866-873.

Clancy MJ, Shambaugh ME, Timpte CS, Bokar JA. 2002. Induction of sporulation in *Saccharomyces cerevisiae* leads to the formation of N 6-methyladenosine in mRNA: a potential mechanism for the activity of the IME4 gene. *Nucleic Acids Research*, **30**: 4509-4518.

Clarke JT, Warnock RC, Donoghue PC. 2011. Establishing a time-scale for plant evolution. *New Phytologist*, **192**: 266-301.

Coleto I, Vega-Mas I, Glauser G, González-Moro MB, Marino D, Ariz I. 2019. New insights on *Arabidopsis thaliana* root adaption to ammonium nutrition by the use of a quantitative proteomic approach. *International Journal of Molecular Sciences*, **20**: 814.

Cooper RJ. 2003. World markets for coniferous forest products: recent trends and future prospects. *Acta Horticulturae*, **615**: 349 – 353.

Couturier J, Montanini B, Martin F, Brun A, Blaudez D, Chalot M. 2007. The expanded family of ammonium transporters in the perennial poplar plant. *New Phytologist*, **174**: 137-150.

Craven-Bartle B, Pascual MB, Cánovas FM, Ávila C. 2013. A Myb transcription factor regulates genes of the phenylalanine pathway in maritime pine. *The Plant Journal*, **74**: 755-766.

Crawford NM, Forde BG. 2002. Molecular and developmental biology of inorganic nitrogen nutrition. *The Arabidopsis Book/American Society of Plant Biologists*, 1.

Crick F. 1970. Central dogma of molecular biology. *Nature*, **227**:561-563.

- Crisp MD, Cook LG. 2011.** Cenozoic extinctions account for the low diversity of extant gymnosperms compared with angiosperms. *New Phytologist*, **192**: 997-1009.
- Critchfield WB, Little EL. 1966.** Geographic distribution of the pines of the world. *US Department of Agriculture, Forest Service*, **991**.
- Cui H, Levesque MP, Vernoux T, Jung JW, Paquette AJ, Gallagher KL., Wang JY, Blilou I, Scheres B, Benfey PN. 2007.** An evolutionarily conserved mechanism delimiting SHR movement defines a single layer of endodermis in plants. *Science*, **316**: 421-425.
- Curtis TY, Bo V, Tucker A, Halford NG. 2018.** Construction of a network describing asparagine metabolism in plants and its application to the identification of genes affecting asparagine metabolism in wheat under drought and nutritional stress. *Food and Energy Security*, **7**: e00126.
- Dai X, Zhuang Z, Zhao PX. 2018.** psRNATarget: a plant small RNA target analysis server (2017 release). *Nucleic Acids Research*. **46**: 49-54.
- David LC, Berquin P, Kanno Y, Seo M, Daniel-Vedele F, Ferrario-Méry S. 2016.** N availability modulates the role of NPF3. 1, a gibberellin transporter, in GA-mediated phenotypes in *Arabidopsis*. *Planta*, **244**: 1315-1328
- David M, Dursi LJ, Yao D, Boutros PC, Simpson JT. 2016.** Nanocall: an open source basecaller for Oxford Nanopore sequencing data. *Bioinformatics*, **33**: 49-55.
- Davis AS, Jacobs DF. 2005.** Quantifying root system quality of nursery seedlings and relationship to outplanting performance. *New Forests*, **30**: 295-311.
- De Rybel B, Adibi M, Breda AS, Wendrich JR, Smit ME, Novák O, Yamaguchi N, Yoshida S, Isterdael GV, Palovaara J, et al. 2014.** Integration of growth and patterning during vascular tissue formation in *Arabidopsis*. *Science*, **345**.
- de Souza Miranda R, Gomes-Filho E, Prisco JT, Alvarez-Pizarro JC. 2016.** Ammonium improves tolerance to salinity stress in *Sorghum bicolor* plants. *Plant Growth Regulation*, **78**: 121-131.
- Delaney KJ, Xu R, Zhang J, Li QQ, Yun KY, Falcone DL, Hunt AG. 2006.** Calmodulin interacts with and regulates the RNA-binding activity of an *Arabidopsis* polyadenylation factor subunit. *Plant Physiology*, **140**: 1507-1521.
- Dominissini D, Moshitch-Moshkovitz S, Schwartz S, Salmon-Divon M, Ungar L, Osenberg S, Cesarkas K, Jacob-Hirsch J, Amariglio N, Kupiec M, et al. 2012.** Topology of the human and mouse m⁶A RNA methylomes revealed by m⁶A-seq. *Nature*, **485**: 201.
- Dominissini D, Moshitch-Moshkovitz S, Salmon-Divon M, Amariglio N, Rechavi G. 2013.** Transcriptome-wide mapping of N 6-methyladenosine by m⁶A-seq based on immunocapturing and massively parallel sequencing. *Nature Protocols*, **8**: 176.

References

Duan HC, Wei LH, Zhang C, Wang Y, Chen L, Lu Z, Chen PR, He C, Jia G. 2017. ALKBH10B is an RNA N6-methyladenosine demethylase affecting *Arabidopsis* floral transition. *The Plant Cell*, **29**:2995–3011.

Dubois F, Tercé-Laforgue T, Gonzalez-Moro MB, Estavillo JM, Sangwan R, Gallais A, Hirel B. 2003. Glutamate dehydrogenase in plants: is there a new story for an old enzyme?. *Plant Physiology and Biochemistry*, **41**: 565-576.

D'Apuzzo E, Rogato A, Simon-Rosin U, El Alaoui H, Barbulova A, Betti M, et al. 2004. Characterization of three functional high-affinity ammonium transporters in *Lotus japonicus* with differential transcriptional regulation and spatial expression. *Plant Physiology*, **134**: 1763-1774.

Eamens AL, Wang MB. 2011. Alternate approaches to repress endogenous microRNA activity in *Arabidopsis thaliana*. *Plant Signaling & Behavior*, **6**: 349-359.

Eastern Himalayan subalpine conifer forests. Terrestrial Ecoregions. World Wildlife Fund.

Edgar RC. 2004. MUSCLE: multiple sequence alignment with high accuracy and high throughput. *Nucleic Acids Research* **32**: 1792-1797.

Edgar R, Domrachev M, Lash AE. 2002. Gene Expression Omnibus: NCBI gene expression and hybridization array data repository. *Nucleic Acids Research* **30**: 207-210.

Ekramoddoullah AKM. 2005. Molecular tools in the study of the white pine blister rust (*Cronartium ribicola*) pathosystem. *Canadian Journal of Plant Pathology*, **27**: 510–520.

El-Azaz J, de la Torre F, Pascual MB, Debille S, Canlet F, Harvengt L, Trontin JF, Avila C, Cánovas FM. 2020. Transcriptional analysis of arogonate dehydratase genes identifies a link between phenylalanine biosynthesis and lignin biosynthesis. *Journal of Experimental Botany*, **71**: 3080-3093.

Ellison D, Morris CE, Locatelli B, Sheil D, Cohen J, Murdiyarso D, Gutierrez V, van Noordwijk M, Creed IF, Pokorny J, et al. 2017. Trees, forests and water: Cool insights for a hot world. *Global Environmental Change*, **43**: 51-61.

Engelsberger WR, Schulze WX. 2012. Nitrate and ammonium lead to distinct global dynamic phosphorylation patterns when resupplied to nitrogen-starved *Arabidopsis* seedlings. *The Plant Journal*, **69**: 978-995.

Esteban R, Ariz I, Cruz C, Moran JF. 2016. Mechanisms of ammonium toxicity and the quest for tolerance. *Plant Science*, **248**: 92-101.

Esteve-Puig R, Bueno-Costa A, Esteller M. 2020. Writers, readers and erasers of RNA modifications in cancer. *Cancer Letters*, **474**: 127-137.

Eulalio A, Behm-Ansmant I, Schweizer D, Izaurralde E. 2007. P-body formation is a consequence, not the cause, of RNA-mediated gene silencing. *Molecular and Cellular Biology*, **27**: 3970-3981.

- Expósito-Rodríguez M, Borges AA, Borges-Pérez A, Pérez JA. 2008.** Selection of internal control genes for quantitative real-time RT-PCR studies during tomato development process. *BMC Plant Biology*, **8**: 131.
- Fait A, Fromm H, Walter D, Galili G, Fernie AR. 2008.** Highway or byway: the metabolic role of the GABA shunt in plants. *Trends in Plant Science*, **13**: 14-19.
- Fagard M, Launay A, Clément G, Courtial J, Dellagi A, Farjad M, Krapp A, Soulié MC, Masclaux-Daubresse, C. 2014.** Nitrogen metabolism meets phytopathology. *Journal of Experimental Botany*, **65**:5643-5656.
- FAO F. 2018.** The State of the World's Forests 2018. Forest pathways to sustainable development.
- Farjon A. 2018.** The Kew review: conifers of the world. *Kew Bulletin*, **73**: 8.
- Farjon A, Filer D. 2013.** An atlas of the world's conifers: an analysis of their distribution, biogeography, diversity and conservation status. *Brill*.
- Felsenstein J. 1985.** Confidence limits on phylogenies: An approach using the bootstrap. *Evolution*. **39**, 783-791.
- Feng J, Barker AV. 1992a.** Ethylene evolution and ammonium accumulation by nutrient-stressed tomatoes grown with inhibitors of ethylene synthesis or action. *Journal of Plant Nutrition*, **15**: 155-167.
- Feng J, Barker AV. 1992b.** Ethylene evolution and ammonium accumulation by tomato plants under water and salinity stresses. Part II. *Journal of Plant Nutrition*, **15**: 2471-2490.
- Fernández-Crespo E, Camañes G, García-Agustín P. 2012.** Ammonium enhances resistance to salinity stress in citrus plants. *Journal of Plant Physiology*, **169**: 1183-1191.
- Ferrario-Méry S, Valadier MH, Foyer CH. 1998.** Overexpression of nitrate reductase in tobacco delays drought-induced decreases in nitrate reductase activity and mRNA. *Plant Physiology*, **117**: 293-302.
- Foli S, Reed J, Clendenning J, Petrokofsky G, Padoch C, Sunderland T. 2014.** To what extent does the presence of forests and trees contribute to food production in humid and dry forest landscapes?: a systematic review protocol. *Environmental Evidence*, **3**:15.
- Fontaine JX, Tercé-Laforgue T, Armengaud P, Clément G, Renou JP, Pelletier S, Catterou M, Azzopardi M, Gibon Y, Lea PJ, et al. 2012.** Characterization of a NADH-dependent glutamate dehydrogenase mutant of *Arabidopsis* demonstrates the key role of this enzyme in root carbon and nitrogen metabolism. *The Plant Cell*, **24**: 4044-4065.
- Fox H, Doron-Faigenboim A, Kelly G, Bourstein R, Attia Z, Zhou J, Moshe Y, Moshelion M, David-Schwartz R. 2018.** Transcriptome analysis of *Pinus halepensis* under drought stress and during recovery. *Tree Physiology*, **38**: 423-441.
- Franco DM, Silva EM, Saldanha LL, Adachi SA, Schley TR, Rodrigues TM, Dokkedal AL, Nogueira FTS, de Almeida LFR. 2015.** Flavonoids modify root

References

growth and modulate expression of SHORT-ROOT and HD-ZIP III. *Journal of Plant Physiology*, **188**:89-95.

Fray RG, Simpson GG. 2015. The *Arabidopsis* epitranscriptome. *Current Opinion in Plant Biology*, **27**:17-21.

Fu L, Niu B, Zhu Z, Wu S, Li W. 2012. CD-HIT: accelerated for clustering the next generation sequencing data. *Bioinformatics*. **28**: 3150-3152.

Fundación HAZI - HAZI Fundazioa 2019. Nuevas perspectivas del *Pino pinaster* en España.

Gaertner M, Den Breeyen A, Hui C, Richardson DM. 2009. Impacts of alien plant invasions on species richness in Mediterranean-type ecosystems: a meta-analysis. *Progress in Physical Geography*, **33**: 319-338.

Galinha C, Hofhuis H, Luijten M, Willemsen V, Blilou I, Heidstra R, Scheres B. 2007. PLETHORA proteins as dose-dependent master regulators of *Arabidopsis* root development. *Nature*, **449**:1053-1057.

Gallardo F, Cánovas FM. 1992. A macromolecular inhibitor of glutamine synthetase activity in tomato root extracts. *Phytochemistry*, **31**: 2267-2271.

Ganz P, Ijato T, Porrás-Murillo R, Stührwohldt N, Ludewig U, Neuhäuser B. 2020. A twin histidine motif is the core structure for high-affinity substrate selection in plant ammonium transporters. *Journal of Biological Chemistry*, jbc-RA119.

Ganz P, Mink R, Ijato T, Porrás-Murillo R, Ludewig U, Neuhäuser B. 2019. A pore-occluding phenylalanine gate prevents ion slippage through plant ammonium transporters. *Scientific Reports*, **9**: 1-9.

Gao K, Zhou T, Hua Y, Guan C, Zhang Z. 2020. Transcription factor WRKY23 is involved in ammonium-induced repression of *Arabidopsis* primary root growth under ammonium toxicity. *Plant Physiology and Biochemistry*.

Gao Y, de Bang TC, Schjoerring JK. 2019. Cisgenic overexpression of cytosolic glutamine synthetase improves nitrogen utilization efficiency in barley and prevents grain protein decline under elevated CO₂. *Plant Biotechnology Journal*, **17**: 1209-1221.

Garalde DR, Snell EA, Jachimowicz D, Sipos B, Lloyd JH, Bruce M, Pantic N, Admassu T, James P, Warland A, et al. 2018. Highly parallel direct RNA sequencing on an array of nanopores. *Nature Methods*, **15**: 201.

García-Gutiérrez A, Dubois F, Cantón FR, Gallardo F, Sangwan RS, Cánovas FM. 1998. Two different modes of early development and nitrogen assimilation in gymnosperm seedlings. *The Plant Journal*, **13**: 187-199.

García-Robledo E, Corzo A, Papaspyrou S. 2014. A fast and direct spectrophotometric method for the sequential determination of nitrate and nitrite at low concentrations in small volumes. *Marine Chemistry*, **162**: 30-36.

- Garrido-Gala J, Higuera JJ, Muñoz-Blanco J, Amil-Ruiz, F, Caballero JL. 2019.** The VQ motif-containing proteins in the diploid and octoploid strawberry. *Scientific Reports*, **9**: 1-16.
- Gaspar MJ, Velasco T, Feito I, Alfa R, Majada J. 2013.** Genetic variation of drought tolerance in *Pinus pinaster* at three hierarchical levels: a comparison of induced osmotic stress and field testing. *PLoS One*, **8**: e79094.
- Gaufichon L, Rothstein SJ, Suzuki A. 2016.** Asparagine metabolic pathways in *Arabidopsis*. *Plant and Cell Physiology*, **57**: 675-689.
- Gazzarrini S, Lejay L, Gojon A, Ninnemann O, Frommer WB, von Wirén N. 1999.** Three functional transporters for constitutive, diurnally regulated, and starvation-induced uptake of ammonium into *Arabidopsis* roots. *The Plant Cell*, **11**:937-947.
- Geula S, Moshitch-Moshkovitz S, Dominissini D, Mansour AA, Kol N, Salmon-Divon M, Hershkovitz V, Peer E, Mor N, Manor YS, et al. 2015.** m6A mRNA methylation facilitates resolution of naive pluripotency toward differentiation. *Science*, **347**:1002–1006.
- Gibon Y, Blaesing OE, Hannemann J, Carillo P, Höhne M, Hendriks JH, et al. 2004.** A robot-based platform to measure multiple enzyme activities in *Arabidopsis* using a set of cycling assays: comparison of changes of enzyme activities and transcript levels during diurnal cycles and in prolonged darkness. *The Plant Cell*, **16**: 3304-3325.
- Giehl RF, Laginha AM, Duan F, Rentsch D, Yuan L, von Wirén N. 2017.** A critical role of AMT2; 1 in root-to-shoot translocation of ammonium in *Arabidopsis*. *Molecular Plant*, **10** : 1449-1460.
- Gifford ML, Dean A, Gutierrez RA, Coruzzi GM, Birnbaum KD. 2008.** Cell-specific nitrogen responses mediate developmental plasticity. *Proceedings of the National Academy of Sciences*, **105**:803-808.
- Gion JM, Lalanne C, Le Provost G, Ferry-Dumazet H, Paiva J, Chaumeil P, Frigerio JM ; Brach J, Barré A, et al. 2005.** The proteome of maritime pine wood forming tissue. *Proteomics*, **5**: 3731-3751.
- Glassman SI, Peay KG, Talbot JM, Smith DP, Chung JA, Taylor J W, Vilgalys R, Bruns TD. 2015.** A continental view of pine-associated ectomycorrhizal fungal spore banks: a quiescent functional guild with a strong biogeographic pattern. *New Phytologist*, **205**: 1619-1631.
- Glimn-Lacy J, Kaufman PB. 2006.** Root Tissues. In: Botany Illustrated. Springer, Boston, MA.
- González Fernández R, Redondo I, Jorrín-Novo JV. 2014.** Making a protein extract from plant pathogenic fungi for gel- and LC-based proteomics. *Plant Proteomics: Methods and Protocols, 2nd Edition*, **1072**: 93-109.
- Good AG, Beatty PH. 2011.** Fertilizing nature: a tragedy of excess in the commons. *PLoS Biology*, **9**: e1001124.

References

Good AG, Shrawat A K, Muench DG. 2004. Can less yield more? Is reducing nutrient input into the environment compatible with maintaining crop production?. *Trends in Plant Science*, **9**: 597-605.

Götz S, García-Gómez JM, Terol J, Williams TD, Nagaraj SH, Nueda MJ, Robles M, Talón M, Dopazo J, Conesa A. 2008. High-throughput functional annotation and data mining with the Blast2GO suite. *Nucleic Acids Research* **36**: 3420-3435.

Gough CM. 2011. Terrestrial Primary Production: Fuel for Life. *Nature Education Knowledge*, **3**:28.

Granados JM, Ávila C, Cánovas FM, Cañas RA. 2016. Selection and testing of reference genes for accurate RT-qPCR in adult needles and seedlings of maritime pine. *Tree Genetics & Genomes*, **12**: 1-15.

Granstedt RC, Huffaker RC. 1982. Identification of the leaf vacuole as a major nitrate storage pool. *Plant Physiology*, **70**: 410-413.

Gray WM, Kepinski S, Rouse D, Leyser O and Estelle M. 2001. Auxin regulates SCF TIR1-dependent degradation of AUX/IAA proteins. *Nature*, **414**: 271-276.

Greb T. 2020. Plant Development: How Phloem Patterning Occurs. *Current Biology*, **30**: 217-219.

Green KA, Prigge MJ, Katzman RB, Clark SE. 2005. CORONA, a member of the class III homeodomain leucine zipper gene family in *Arabidopsis*, regulates stem cell specification and organogenesis. *The Plant Cell*, **17**: 691-704.

Grosjean H. 2005. Fine-tuning of RNA functions by modification and editing. *H. Grosjean (Ed.). Berlin, Heidelberg: Springer*, **24**: 442.

Gruffman L, Ishida T, Nordin A, Näsholm T. 2012. Cultivation of Norway spruce and Scots pine on organic nitrogen improves seedling morphology and field performance. *Forest Ecology and Management*, **276**:118-124.

Grunewald W, Friml J. 2010. The march of the PINs: developmental plasticity by dynamic polar targeting in plant cells. *The EMBO Journal*. **29**: 2700-2714.

Gruswitz F, Chaudhary S, Ho JD, Schlessinger A, Pezeshki B, Ho CM, Sali A, Westhoff CM, Stroud RM. 2010. Function of human Rh based on structure of RhCG at 2.1 Å. *Proceedings of the National Academy of Sciences*, **107**: 9638-9643.

Guether M, Neuhäuser B, Balestrini R, Dynowski M, Ludewig U, Bonfante P. 2009. A mycorrhizal-specific ammonium transporter from *Lotus japonicus* acquires nitrogen released by arbuscular mycorrhizal fungi. *Plant Physiology*, **150**: 73-83.

Gullner G, Komives T, Király L, Schröder P. 2018. Glutathione S-transferase enzymes in plant-pathogen interactions. *Frontiers in Plant Science*, **9**: 1836.

- Guo JH, Liu XJ, Zhang Y, Shen JL, Han WX, Zhang WF, Christie P, Goulding KWT, Vitousek PM, Zhang FS. 2010.** Significant acidification in major Chinese croplands. *Science*, **327**: 1008-1010.
- Gupta B, Huang B. 2014.** Mechanism of salinity tolerance in plants: physiological, biochemical, and molecular characterization. *International Journal of Genomics*, **2014**:701596.
- Gutiérrez RA. 2012.** Systems biology for enhanced plant nitrogen nutrition. *Science*, **336**:1673-1675.
- Habash DZ, Massiah AJ, Rong HL, Wallsgrave RM, Leigh RA. 2001.** The role of cytosolic glutamine synthetase in wheat. *Annals of Applied Biology*, **138**: 83-89.
- Hachiya T, Sakakibara H. 2017.** Interactions between nitrate and ammonium in their uptake, allocation, assimilation, and signaling in plants. *Journal of Experimental Botany*, **68**: 2501-2512.
- Hall DE, Robert JA, Keeling CI, Domanski D, Quesada AL, Jancsik S, Kuzyk MA, Hamberger B, Borchers CH, Bohlmann J. 2011.** An integrated genomic, proteomic and biochemical analysis of (+)-3-carene biosynthesis in Sitka spruce (*Picea sitchensis*) genotypes that are resistant or susceptible to white pine weevil. *The Plant Journal*, **65**: 936-948.
- Hamrick JL, Godt MJW, Sherman-Broyles SL. 1992.** Factors influencing levels of genetic diversity in woody plant species. In *Population genetics of forest trees*. Springer, Dordrecht: 95-124.
- Hao DL, Zhou JY, Yang SY, Qi W, Yang KJ, Su YH. 2020.** Function and regulation of ammonium transporters in plants. *International Journal of Molecular Sciences*, **21**: 3557.
- Haugland RA, Cline MG. 1980.** Post-transcriptional modifications of oat coleoptile ribonucleic acids: 5'-terminal capping and methylation of internal nucleosides in poly(A)-rich RNA. *European Journal of Biochemistry*, **104**:271–277.
- Hawkesford M, Horst W, Kichey T, Lambers H, Schjoerring J, Møller IS, White P. 2012.** Functions of macronutrients. In *Marschner's mineral nutrition of higher plants*, Academic Press, 135-189.
- Hawkins BJ, Robbins S. 2010.** pH affects ammonium, nitrate and proton fluxes in the apical region of conifer and soybean roots. *Physiologia Plantarum*, **138**: 238-247.
- Helariutta Y, Fukaki,H, Wysocka-Diller J, Nakajima K, Jung J, Sena G, Hauser MT, Benfey PN. 2000.** The SHORT-ROOT gene controls radial patterning of the Arabidopsis root through radial signaling. *Cell*, **101**: 555-567.
- Hichri I, Barrieu F, Bogs J, Kappel C, Delrot S, Lauvergeat V. 2011.** Recent advances in the transcriptional regulation of the flavonoid biosynthetic pathway. *Journal of Experimental Botany*, **62**: 2465-2483.
- Hienzs A, Deiml C, Reiter V, Carell T. 2013.** Total synthesis of the hypermodified RNA bases wybutosine and hydroxywybutosine and their

References

quantification together with other modified RNA bases in plant materials. *Chemistry—A European Journal*, **19**: 4244-4248.

Hirel B, Krapp A. 2020. Nitrogen utilization in plants biological and agronomic importance. *Encyclopedia of Biological Chemistry*. 3rd Edition. Elsevier, In press.

Hirel B, Lea PJ. 2001. Ammonia assimilation. In *Plant nitrogen*. Springer, Berlin, Heidelberg; 79-99.

Hoagland DR, Arnon DI. 1950. The water-culture method for growing plants without soil. *Circular. California Agricultural Experiment Station*, **347**: 1-32, (2nd edit).

Högberg MN, Briones MJ, Keel SG, Metcalfe DB, Campbell C, Midwood AJ., et al. 2010. Quantification of effects of season and nitrogen supply on tree below-ground carbon transfer to ectomycorrhizal fungi and other soil organisms in a boreal pine forest. *New Phytologist*, **187**: 485-493.

Hoopen FT, Cui TA, Pedas P, Hegelund JN, Shabala S, Schjoerring JK, Jahn TP. 2010. Competition between uptake of ammonium and potassium in barley and *Arabidopsis* roots: molecular mechanisms and physiological consequences. *Journal of Experimental Botany*, **61**: 2303-2315.

Hornyik C, Terzi LC, Simpson GG. 2010. The spen family protein FPA controls alternative cleavage and polyadenylation of RNA. *Developmental cell*, **18**: 203-213.

Hou H, Erickson J, Meservy J, Schultz EA. 2010. FORKED1 encodes a PH domain protein that is required for PIN1 localization in developing leaf veins. *The Plant Journal*, **63**: 960-973.

Hu M, Zhao X, Liu Q, Hong X, Zhang W, Zhang Y, Sun L, Li H, Tong, Y. 2018. Transgenic expression of plastidic glutamine synthetase increases nitrogen uptake and yield in wheat. *Plant Biotechnology Journal*, **16**: 1858-1867.

Huang H, Yao Q, Xia E, Gao L. 2018. Metabolomics and transcriptomics analyses reveal nitrogen influences on the accumulation of flavonoids and amino acids in young shoots of tea plant (*Camellia sinensis* L.) associated with tea flavor. *Journal of Agricultural and Food Chemistry*, **66**: 9828-9838.

Huang Y, He N, Chen Y, Chen Z, Li L. 2018. BERMP: a cross-species classifier for predicting m6A sites by integrating a deep learning algorithm and a random forest approach. *International Journal of Biological Sciences*, **14**: 1669.

Hunt AG, Xin, D, Li QQ. 2012. Plant polyadenylation factors: conservation and variety in the polyadenylation complex in plants. *BMC Genomics*, **13**, 641.

Husted S, Hebborn CA, Mattsson M, Schjoerring JK. 2000. A critical experimental evaluation of methods for determination of NH₄⁺ in plant tissue, xylem sap and apoplastic fluid. *Physiologia Plantarum*, **109**: 167-179.

Informe de la ONU 2019. Creciendo a un ritmo menor, se espera que la población mundial alcanzará 9.700 millones en 2050 y un máximo de casi 11.000 millones alrededor de 2100. *COMUNICADO DE PRENSA*.

- Iqbal A, Qiang D, Alamzeb M, Xiangru W, Huiping G, Hengheng Z, et al. 2020. Untangling the molecular mechanisms and functions of nitrate to improve nitrogen use efficiency. *Journal of the Science of Food and Agriculture*, **100**: 904-914.
- Jaber E, Kovalchuk A, Raffaello T, Kerio S, Teeri T, Asiegbu FO. 2018. A gene encoding scots pine antimicrobial protein Sp-AMP2 (PR-19) confers increased tolerance against *Botrytis cinerea* in transgenic tobacco. *Forests*, **9**: 10.
- Jacquot A, Li Z, Gojon A, Schulze W, Lejay L. 2017. Post-translational regulation of nitrogen transporters in plants and microorganisms. *Journal of Experimental Botany*, **68**: 2567-2580.
- Jahn TP, Møller AL, Zeuthen T, Holm LM, Klærke DA, Mohsin B, Kühlbrandt W, Schjoerring JK. 2004. Aquaporin homologues in plants and mammals transport ammonia. *FEBS Letters*, **574**: 31-36.
- Jia G, Fu Y, Zhao X, Dai Q, Zheng G, Yang Y, Yi C, Lindahl T, Pan T, Yang YG. 2012. Corrigendum: N6-Methyladenosine in nuclear RNA is a major substrate of the obesity-associated FTO. *Nature Chemical Biology*, **8**: 1008.
- Jia Z, von Wirén N. 2020. Signaling pathways underlying nitrogen-dependent changes in root system architecture: from model to crop species. *Journal of Experimental Botany*, **71**: 4393-4404.
- Jiao X, Wang H, Yan J, Kong X, Liu Y, Chu J, Chen X, Fang R, Yan Y. 2020. Promotion of BR biosynthesis by miR444 is required for ammonium-triggered inhibition of root growth. *Plant Physiology*, **182**: 1454-1466.
- John P, Reynolds EA, Prescott AG, Bauchot AD. 1999. ACC Oxidase in the Biosynthesis of Ethylene. In: Kanellis A.K., Chang C., Klee H., Bleecker A.B., Pech J.C., Grierson D. (eds) *Biology and Biotechnology of the Plant Hormone Ethylene II*. Springer, Dordrecht.
- Kang HI, Lee HO, Lee IH, Kim IS, Lee SW, Yang TJ, Shim D. 2019. Complete chloroplast genome of *Pinus densiflora* Siebold & Zucc. and comparative analysis with five pine trees. *Forests*, **10**: 600.
- Kamada-Nobusada T, Makita N, Kojima M, Sakakibara H. 2013. Nitrogen-dependent regulation of de novo cytokinin biosynthesis in rice: the role of glutamine metabolism as an additional signal. *Plant and Cell Physiology*, **54**: 1881-1893.
- Kamiya M, Higashio SY, Isomoto A, Kim JM, Seki M, Miyashima S, Nakajima K. 2016. Control of root cap maturation and cell detachment by BEARSKIN transcription factors in *Arabidopsis*. *Development*, **143**: 4063-4072.
- Kaur K, Duhan N, Singh J, Kaur G, Vikal Y. 2020. Computational identification of maize miRNA and their gene targets involved in biotic and abiotic stresses. *Journal of Biosciences*, **45**: 1-17.
- Ke S, Pandya-Jones A, Saito Y, Fak JJ, Vågbo CB, Geula S, Hanna JH, Black DL, Darnell Jr JE, Darnell, R. B. 2017. m6A mRNA modifications are deposited in nascent pre-mRNA and are not required for splicing but do specify cytoplasmic turnover. *Genes & Development*, **31**: 990-1006.

Ke S, Alemu EA, Mertens C, Gantman EC, Fak JJ, Mele A, Haripal B, Zucker-Scharff I, Moore MJ, Park CY, et al. 2015. A majority of m6A residues are in the last exons, allowing the potential for 3' UTR regulation. *Genes & Development*, **29**: 2037-2053.

Kennedy TD, Lane BG. 1979. Wheat embryo ribonucleates. XIII. Methyl-substituted nucleoside constituents and 5'-terminal dinucleotide sequences in bulk poly (A)-rich RNA from imbibing wheat embryos. *Canadian Journal of Biochemistry*, **57**: 927-931.

Kennedy EM, Bogerd HP, Kornepati AV, Kang D, Ghoshal D, Marshall JB, Poling BC, Tsai K, Gokhale NS, Horner SM, et al. 2016. Posttranscriptional m6A editing of HIV-1 mRNAs enhances viral gene expression. *Cell Host & Microbe*, **19**: 675-685.

Kerr PS, Rufty TW, Huber SC. 1985. Changes in nonstructural carbohydrates in different parts of soybean (*Glycine max* [L.] Merr.) plants during a light/dark cycle and in extended darkness. *Plant Physiology*, **78**: 576-581.

Khademi S, O'Connell J, Remis J, Robles-Colmenares Y, Miercke LJ, Stroud RM. 2004. Mechanism of ammonia transport by Amt/MEP/Rh: structure of AmtB at 1.35 Å. *Science*, **305**: 1587-1594.

Kim H, Zhou J, Kumar D, Jang G, Ryu KH, Sebastian J, Miyashima S, Helariutta Y, Lee JY. 2020. SHORTROOT-Mediated Intercellular Signals Coordinate Phloem Development in *Arabidopsis* Roots. *The Plant Cell*, **32**; 1519-1535.

Kimble JM, Rice CW, Reed D, Mooney S, Follett RF, Lal R. 2007. Soil carbon management: Economic, environmental and societal benefits. *CRC Press*.

Kondo Y, Nurani AM, Saito C, Ichihashi Y, Saito M, Yamazaki K, Mitsuda N, Ohme-Takagi M, Fukuda H. 2016. Vascular Cell Induction Culture System Using *Arabidopsis* Leaves (VISUAL) Reveals the Sequential Differentiation of Sieve Element-Like Cells. *The Plant Cell*, **28**: 1250-1262.

Koprivova A, Kopriva S. 2014. Molecular mechanisms of regulation of sulfate assimilation: first steps on a long road. *Frontiers in Plant Science*, **5**, 589.

Koyama LA, Kielland K. 2019. Black spruce assimilates nitrate in boreal winter. *Tree Physiology*, **39**: 536-543.

Kronzucker HJ, Siddiqi MY, Glass AD, Kirk GJ. 1999. Nitrate-ammonium synergism in rice. A subcellular flux analysis. *Plant Physiology*, **119**: 1041-1046.

Kronzucker HJ, Siddiqi MY, Glass AD. 1997. Conifer root discrimination against soil nitrate and the ecology of forest succession. *Nature*, **385**: 59-61.

Kronzucker HJ, Siddiqi MY, Glass AD. 1996. Kinetics of NH_4^+ influx in spruce. *Plant Physiology*, **110**: 773-779.

Krug RM, Morgan MA, Shatkin AJ. 1976. Influenza viral mRNA contains internal N6-methyladenosine and 5'-terminal 7-methylguanosine in cap structures. *Journal of Virology*, **20**: 45-53.

- Kruger NJ, Troncoso-Ponce MA, Ratcliffe RG. 2008.** ^1H NMR metabolite fingerprinting and metabolomic analysis of perchloric acid extracts from plant tissues. *Nature Protocols*, **3**: 1001-1012.
- Kuang Z, Wang Y, Li L, Yang X. 2019.** miRDeep-P2: accurate and fast analysis of the microRNA transcriptome in plants. *Bioinformatics*, **35**: 2521-2522.
- Kumar A, Silim SN, Okamoto M, Siddiqi MY, Glass AD. 2003.** Differential expression of three members of the AMT1 gene family encoding putative high-affinity NH_4^+ transporters in roots of *Oryza sativa* subspecies indica. *Plant, Cell & Environment*, **26**: 907-914.
- Kumar R, Taware R, Gaur VS, Guru SK, Kumar A. 2009.** Influence of nitrogen on the expression of TaDof1 transcription factor in wheat and its relationship with photo synthetic and ammonium assimilating efficiency. *Molecular Biology Reports*, **36**: 2209.
- Kumar S, Stecher G, Tamura K. 2016.** MEGA7: Molecular Evolutionary Genetics Analysis version 7.0 for bigger datasets. *Molecular Biology and Evolution*, **33**: 1870-1874.
- Kuroha T, Tokunaga H, Kojima M, Ueda N, Ishida T, Nagawa S, Fukuda H, Sugimoto K, Sakakibara H. 2009.** Functional analyses of LONELY GUY cytokinin-activating enzymes reveal the importance of the direct activation pathway in *Arabidopsis*. *The Plant Cell*, **21**: 3152-3169.
- Kürsteiner O, Dupuis I, Kuhlemeier C. 2003.** The pyruvate decarboxylase1 gene of *Arabidopsis* is required during anoxia but not other environmental stresses. *Plant Physiology*, **132**: 968-978.
- Laemmli UK. 1970.** Cleavage of structural proteins during the assembly of the head of bacteriophage T4. *Nature*, **227**: 680-685.
- Lam HM, Hsieh MH, Coruzzi G. 1998.** Reciprocal regulation of distinct asparagine synthetase genes by light and metabolites in *Arabidopsis thaliana*. *The Plant Journal*, **16**: 345-353.
- Lam HM, Coschigano KT, Oliveira IC, Melo-Oliveira R, Coruzzi GM. 1996.** The molecular-genetics of nitrogen assimilation into amino acids in higher plants. *Annual Review of Plant Biology*, **47**: 569-593.
- Lan MD, Xiong J, You XJ, Weng XC, Zhou X, Yuan BF, Feng YQ. 2018.** Existence of Diverse Modifications in Small-RNA Species Composed of 16–28 Nucleotides. *Chemistry–A European Journal*, **24**: 9949-9956.
- Langfelder P, Horvath S. 2008.** WGCNA: an R package for weighted correlation network analysis. *BMC Bioinformatics*, **9**: 559.
- Lanquar V, Loqué D, Hörmann F, Yuan L, Bohner A, Engelsberger WR, Lalonde S, Schulze WX, von Wirén N, Frommer WB. 2009.** Feedback inhibition of ammonium uptake by a phospho-dependent allosteric mechanism in *Arabidopsis*. *The Plant Cell*, **21**: 3610-3622.

References

- Lesbirel S, Wilson SA. 2019.** The m6A-methylase complex and mRNA export. *Biochimica et Biophysica Acta (BBA)-Gene Regulatory Mechanisms*, **1862**: 319-328.
- Lesbirel S, Viphakone N, Parker M, Parker J, Heath C, Sudbery I, Wilson SA. 2018.** The m⁶A-methylase complex recruits TREX and regulates mRNA export. *Scientific Reports*, **8**: 1-12.
- Le Quéré C, Andrew RM, Friedlingstein P, Sitch S, Pongratz J, Manning AC, et al. 2017.** Global carbon budget 2017. *Earth System Science Data Discussions*: 1-79.
- Lewis DR, Negi S, Sukumar P, Muday GK. 2011.** Ethylene inhibits lateral root development, increases IAA transport and expression of PIN3 and PIN7 auxin efflux carriers. *Development*, **138**: 3485-3495.
- Li B, Li G, Kronzucker HJ, Baluška F, Shi W. 2014.** Ammonium stress in *Arabidopsis*: signaling, genetic loci, and physiological targets. *Trends in Plant Science*, **19**: 107-114.
- Li B, Li Q, Su Y, Chen HAO, Xiong L, Mi G, Kronzucker HJ, Shi W. 2011.** Shoot-supplied ammonium targets the root auxin influx carrier AUX1 and inhibits lateral root emergence in *Arabidopsis*. *Plant, Cell & Environment*, **34**: 933-946.
- Li CF, Zhu Y, Yu Y, Zhao QY, Wang SJ, Wang XC, Yao MZ, Luo D, Li X, et al. 2015.** Global transcriptome and gene regulation network for secondary metabolite biosynthesis of tea plant (*Camellia sinensis*). *BMC genomics*, **16**(1), 560.
- Li G, Coleman GD. 2019.** Nitrogen storage and cycling in trees. *In Advances in Botanical Research*. Academic Press: 127-155.
- Li G, Li B, Dong G, Feng X, Kronzucker HJ, Shi W. 2013.** Ammonium-induced shoot ethylene production is associated with the inhibition of lateral root formation in *Arabidopsis*. *Journal of Experimental Botany*, **64**: 1413-1425.
- Li H. 2018.** Minimap2: pairwise alignment for nucleotide sequences. *Bioinformatics* **34**: 3094–3100.
- Li H, Hu B, Chu C. 2017.** Nitrogen use efficiency in crops: Lessons from *Arabidopsis* and rice. *Journal Experimental Botany*, **68**: 2477–2488.
- Li H, Han JL, Chang YH, Lin J, Yang QS. 2016.** Gene characterization and transcription analysis of two new ammonium transporters in pear rootstock (*Pyrus betulaefolia*). *Journal of Plant Research*, **129**: 737-748.
- Li H, Hu B, Wang W, Zhang Z, Liang Y, Gao X, Li P, Liu Y, Zhang L, Chu C. 2016.** Identification of microRNAs in rice root in response to nitrate and ammonium. *Journal of Genetics and Genomics*, **43**: 651-661.
- Li H, Durbin R. 2009.** Fast and accurate short read alignment with Burrows-Wheeler Transform. *Bioinformatics* **25**: 1754-1760.
- Li K, Cai J, Zhang M, Zhang X, Xiong X, Meng H, Xu X, Huang Z, Peng J, Fan J, et al. 2020.** Landscape and regulation of m6A and m6Am methylome across human and mouse tissues. *Molecular Cell*, **77**: 426-440.

- Li N, de Silva J. 2018.** Theanine: its occurrence and metabolism in tea. *Annual Plant Reviews online*:171-206.
- Li S. 2014.** Redox modulation matters: emerging functions for glutaredoxins in plant development and stress responses. *Plants*, **3**: 559-582.
- Li W, Xiang F, Zhong M, Zhou L, Liu H, Li S, Wang X. 2017.** Transcriptome and metabolite analysis identifies nitrogen utilization genes in tea plant (*Camellia sinensis*). *Scientific Reports*, **7**: 1-12.
- Li X, Ma S, Yi C. 2016.** Pseudouridine: the fifth RNA nucleotide with renewed interests. *Current Opinion in Chemical Biology*, **33**: 108-116.
- Li Y, Wang X, Li C, Hu S, Yu J, Song S. 2014.** Transcriptome-wide N6-methyladenosine profiling of rice callus and leaf reveals the presence of tissue-specific competitors involved in selective mRNA modification. *RNA Biology*, **11**: 1180-1188.
- Lian H, Wang QH, Zhu CB, Ma J, Jin WL. 2018.** Deciphering the epitranscriptome in cancer. *Trends in cancer*, **4**: 207-221.
- Liang G, He H, Yu D. 2012.** Identification of nitrogen starvation-responsive microRNAs in *Arabidopsis thaliana*. *PloS One*, **7**.
- Liao Z, Chen M, Guo L, Gong Y, Tang F, Sun X, Tang K. 2004.** Rapid isolation of high-quality total RNA from taxus and ginkgo. *Preparative Biochemistry & Biotechnology* **34**: 209-214.
- Lichtenthaler HK, Buschmann C. 2001.** Chlorophylls and carotenoids: Measurement and characterization by UV-VIS spectroscopy. *Current Protocols in Food Analytical Chemistry*, **1**: F4-3.
- Liebthal M, Maynard D, Dietz KJ. 2018.** Peroxiredoxins and redox signaling in plants. *Antioxidants & Redox Signaling*, **28**: 609-624.
- Lima JE, Kojima S, Takahashi H, von Wirén N. 2010.** Ammonium triggers lateral root branching in *Arabidopsis* in an AMMONIUM TRANSPORTER1;3-dependent manner. *Plant Cell*, **22**: 3621– 3633.
- Lin Y, Cao Z, Mo Y. 2009.** Functional role of Asp160 and the deprotonation mechanism of ammonium in the *Escherichia coli* ammonia channel protein AmtB. *The Journal of Physical Chemistry*, **113**: 4922-4929.
- Linder B, Grozhik AV, Olarerin-George AO, Meydan C, Mason CE, Jaffrey SR. 2015.** Single-nucleotide-resolution mapping of m6A and m6Am throughout the transcriptome. *Nature Methods*, **12**: 767.
- Liu J, Wang H, Chua NH. 2015.** Long noncoding RNA transcriptome of plants. *Plant Biotechnology Journal*, **13**: 319-328.
- Liu L, Zhang S, Lian C. 2015.** De novo transcriptome sequencing analysis of cDNA library and large-scale unigene assembly in Japanese Red Pine (*Pinus densiflora*). *International Journal of Molecular Sciences*, **16**: 29047-29059.

References

- Liu N, Pan T. 2016.** Probing N 6-methyladenosine (m⁶A) RNA modification in total RNA with SCARLET. *Post-Transcriptional Gene Regulation. Humana Press*, New York, NY: 285-292.
- Liu N, Parisien M, Dai Q, Zheng G, He C, Pan T. 2013.** Probing N⁶-methyladenosine RNA modification status at single nucleotide resolution in mRNA and long noncoding RNA. *RNA*, **19**: 1848-1856.
- Liu SR, Zhou JJ, Hu CG, Wei CL, Zhang JZ. 2017.** MicroRNA-mediated gene silencing in plant defense and viral counter-defense. *Frontiers in Microbiology*, **8**: 1801.
- Liu XY, Koba K, Makabe A, Liu CQ. 2014.** Nitrate dynamics in natural plants: insights based on the concentration and natural isotope abundances of tissue nitrate. *Frontiers in Plant Science*, **5**, 355.
- Liu Y, von Wirén N. 2017.** Ammonium as a signal for physiological and morphological responses in plants. *Journal of Experimental Botany*, **68**: 2581-2592.
- Liu Y, Lai N, Gao K, Chen F, Yuan L, Mi G. 2013.** Ammonium inhibits primary root growth by reducing the length of meristem and elongation zone and decreasing elemental expansion rate in the root apex in *Arabidopsis thaliana*. *PLoS ONE*, **8**: e61031.
- Llebrés MT, Pascual MB, DebilleS, Trontin JF, Harvengt L, Avila C, Cánovas FM. 2018.** The role of arginine metabolic pathway during embryogenesis and germination in maritime pine (*Pinus pinaster* Ait.). *Tree Physiology*, **38**: 471-484.
- Lobit P, López-Pérez L, Cárdenas-Navarro R, Castellanos-Morales VC, Ruiz-Corro R. 2007.** Effect of ammonium/nitrate ratio on growth and development of avocado plants under hydroponic conditions. *Canadian Journal of Plant Science*, **87**: 99-103.
- Loqué D, Mora SI, Andrade SL, Pantoja O, Frommer WB. 2009.** Pore mutations in ammonium transporter AMT1 with increased electrogenic ammonium transport activity. *Journal of Biological Chemistry*, **284**: 24988–24995.
- Loqué D, Lalonde S, Looger LL, von Wirén N, Frommer WB. 2007.** A cytosolic trans-activation domain essential for ammonium uptake. *Nature*, **446**:195-198.
- Loqué D, Yuan L, Kojima S, Gojon A, Wirth J, Gazzarrini S, Ishiyama K, Takahashi H, von Wirén N. 2006.** Additive contribution of AMT1; 1 and AMT1; 3 to high-affinity ammonium uptake across the plasma membrane of nitrogen-deficient *Arabidopsis* roots. *The Plant Journal*, **48**: 522-534.
- Loqué D, Ludewig U, Yuan L, von Wirén N. 2005.** Tonoplast intrinsic proteins AtTIP2; 1 and AtTIP2; 3 facilitate NH₃ transport into the vacuole. *Plant Physiology*, **137**: 671-680.
- Losso A, Bär A, Dämon B, Dullin C, Ganthaler A, Petruzzellis F, Savi T, Tromba G, Nardini A, et al. 2019.** Insights from in vivo micro-CT analysis: testing the hydraulic vulnerability segmentation in *Acer pseudoplatanus* and *Fagus sylvatica* seedlings. *New Phytologist*, **221**: 1831-1842.

- Louloupi A, Ntini E, Conrad T, Ørom UAV. 2018.** Transient N-6-methyladenosine transcriptome sequencing reveals a regulatory role of m6A in splicing efficiency. *Cell Reports*, **23**: 3429-3437.
- Lorenz DA, Sathe S, Einstein JM, Yeo GW. 2020.** Direct RNA sequencing enables m6A detection in endogenous transcript isoforms at base-specific resolution. *RNA*, **26**: 19-28.
- Luo GZ, MacQueen A, Zheng G, Duan H, Dore LC, Lu Z, Liu J, Chen K, Jia G, Bergelson J, et al. 2014.** Unique features of the m6A methylome in *Arabidopsis thaliana*. *Nature Communications*, **5**: 1-8.
- Luo JH, Wang Y, Wang M, Zhang LY, Peng HR, Zhou YY, Jia G, He, Y. 2020.** Natural variation in RNA m6A methylation and its relationship with translational status. *Plant Physiology*, **182**: 332-344.
- Luo J, Qin J, He F, Li H, Liu T, Polle A, Peng C, Luo ZB. 2013.** Net fluxes of ammonium and nitrate in association with H⁺ fluxes in fine roots of *Populus popularis*. *Planta*, **237**: 919-931.
- Lupo D, Li XD, Durand A, Tomizaki T, Cherif-Zahar B, Matassi G, Merrick M, Winkler FK. 2007.** The 1.3-Å resolution structure of Nitrosomonas europaea Rh50 and mechanistic implications for NH₃ transport by Rhesus family proteins. *Proceedings of the National Academy of Sciences*, **104**: 19303-19308.
- Mackay J, Dean J, Plomion C, Peterson DG, Canovas FM, Pavy N, Ingvarsson PK, Savolainen O, Guevara MA, Fluch S, et al. 2012.** Towards decoding conifer mega-genomes. *Plant Molecular Biology*, **80**:555-569.
- Madeira F, Park YM, Lee J, Buso N, Gur T, Madhusoodanan N. Basutkar P, Tivey ARN, Potter SC, Finn RD et al. 2019.** The EMBL-EBI search and sequence analysis tools APIs in 2019. *Nucleic Acids Research*, **47**: 636-641.
- Magallón S, Hilu KW, Quandt D. 2013.** Land plant evolutionary timeline: gene effects are secondary to fossil constraints in relaxed clock estimation of age and substitution rates. *American Journal of Botany*, **100**: 556-573.
- Mähönen AP, Bishopp A, Higuchi M, Nieminen KM, Kinoshita K, Törmäkangas K, Ikeda Y, Oka A, Kakimoto T, Helariutta Y. 2006.** Cytokinin signaling and its inhibitor AHP6 regulate cell fate during vascular development. *Science*, **311**: 94-98.
- Mao C, He J, Liu L, Deng Q, Yao X, Liu C, Qiao Y, Li P, Ming F. 2020.** OsNAC2 integrates auxin and cytokinin pathways to modulate rice root development. *Plant Biotechnology Journal*, **18**: 429-442.
- Marino D, Ariz I, Lasa B, Santamaría E, Fernández-Irigoyen J, González-Murua C, Aparicio-Tejo PM. 2016.** Quantitative proteomics reveals the importance of nitrogen source to control glucosinolate metabolism in *Arabidopsis thaliana* and *Brassica oleracea*. *Journal of Experimental Botany*, **67**: 3313-3323.
- Marschner P. 2012.** Marschner's Mineral Nutrition of Higher Plants (3rd Edition). *Academic Press*, San Diego, CA, USA.

Martin A, Lee J, Kichey T, Gerentes D, Zivy M, Tatout C, et al. 2006. Two cytosolic glutamine synthetase isoforms of maize are specifically involved in the control of grain production. *The Plant Cell*, **18**: 3252-3274.

Martínez de Alba AE, Moreno AB, Gabriel M, Mallory AC, Christ A, Bounon R, Balzergue S, Aubourg S, Gautheret D, Crespi MD, et al. 2015. In plants, decapping prevents RDR6-dependent production of small interfering RNAs from endogenous mRNAs. *Nucleic Acids Research*, **43**: 2902-2913.

Martínez-Pérez M, Aparicio F, López-Gresa MP, Bellés JM, Sánchez-Navarro JA, Pallás V. 2017. *Arabidopsis* m6A demethylase activity modulates viral infection of a plant virus and the m6A abundance in its genomic RNAs. *Proceedings of the National Academy of Sciences*, **114**: 10755-10760.

Masclaux-Daubresse C, Valadier MH, Carrayol E, Reisdorf-Cren M, Hirel B. 2002. Diurnal changes in the expression of glutamate dehydrogenase and nitrate reductase are involved in the C/N balance of tobacco source leaves. *Plant, Cell & Environment*, **25**: 1451-1462.

McDonald TR, Ward JM. 2016. Evolution of electrogenic ammonium transporters (AMTs). *Frontiers in Plant Science*, **7**: 352.

McDonald TR, Dietrich FS, Lutzoni F. 2012. Multiple horizontal gene transfers of ammonium transporters/ammonia permeases from prokaryotes to eukaryotes: toward a new functional and evolutionary classification. *Molecular Biology and Evolution*, **29**: 51-60.

McDonald SM, Plant JN, Worden AZ. 2010. The mixed lineage nature of nitrogen transport and assimilation in marine eukaryotic phytoplankton: a case study of *Micromonas*. *Molecular Biology and Evolution*, **27**: 2268-2283.

McIntyre AB, Gokhale NS, Cerchietti L, Jaffrey SR, Horner SM, Mason CE. 2019. Limits in the detection of m6A changes using MeRIP/m6A-seq. *Scientific Reports*, **10**: 1-15.

Men S, Boutté Y, Ikeda Y, Li X, Palme K, Stierhof YD, Hartmann MA, Moritz T, Grebe M. 2008. Sterol-dependent endocytosis mediates post-cytokinetic acquisition of PIN2 auxin efflux carrier polarity. *Nature Cell Biology*, **10**: 237-244.

Menz J, Li Z, Schulze WX, Ludewig U. 2016. Early nitrogen-deprivation responses in *Arabidopsis* roots reveal distinct differences on transcriptome and (phospho-) proteome levels between nitrate and ammonium nutrition. *The Plant Journal*, **88**, 717-734.

Meng J, Lu Z, Liu H, Zhang L, Zhang S, Chen Y, Rao MK, Huang, Y. 2014. A protocol for RNA methylation differential analysis with MeRIP-Seq data and exomePeak R/Bioconductor package. *Methods*, **69**: 274-281.

Merchante C, Brumos J, Yun J, Hu Q, Spencer KR, Enríquez P, Binder BM, Heber S, Stepanova AN, Alonso JM. 2015. Gene-specific translation regulation mediated by the hormone-signaling molecule EIN2. *Cell*, **163**: 684-697.

- Merkurjev D, Hong WT, Iida K, Oomoto I, Goldie BJ, Yamaguti H, Kawaguchi S, Hirano T, Martin KC, et al. 2018.** Synaptic N 6-methyladenosine (m6A) epitranscriptome reveals functional partitioning of localized transcripts. *Nature Neuroscience*, **21**: 1004-1014.
- Meyer KD. 2019.** DART-seq: an antibody-free method for global m6A detection. *Nature Methods*, **16**: 1275-1280.
- Meyer KD, Patil DP, Zhou J, Zinoviev A, Skabkin MA, Elemento O, Pestova TV, Qian SB, Jaffrey SR. 2015.** 5' UTR m6A promotes cap-independent translation. *Cell*, **163**: 999-1010.
- Meyer KD., Saletore Y, Zumbo P, Elemento O, Mason CE, Jaffrey SR. 2012.** Comprehensive analysis of mRNA methylation reveals enrichment in 3' UTRs and near stop codons. *Cell*, **149**: 1635-1646.
- Michlewski G, Caceres JF. 2019.** Post-transcriptional control of miRNA biogenesis. *RNA*, **25**, 1–16.
- Michniewicz M, Brewer PB, Friml J. 2007.** Polar auxin transport and asymmetric auxin distribution. *The Arabidopsis Book/American Society of Plant Biologists*, **5**.
- Mielecki D, Zugaj DŁ, Muszewska A, Piwowarski J, Chojnacka A, Mielecki M, Nieminuszczy J, Grynberg M, Grzesiuk E. 2012.** Novel AlkB dioxygenases—alternative models for *in silico* and *in vivo* studies. *PLoS One*, **7**.
- Mifflin BJ, Habash DZ. 2002.** The role of glutamine synthetase and glutamate dehydrogenase in nitrogen assimilation and possibilities for improvement in the nitrogen utilization of crops. *Journal of Experimental Botany*, **53**: 979-987.
- Miller AJ, Cramer MD. 2005.** Root nitrogen acquisition and assimilation. *In Root physiology: From gene to function. Springer, Dordrecht*: 1-36.
- Mithran M, Paparelli E, Novi G, Perata P, Loreti E. 2014.** Analysis of the role of the pyruvate decarboxylase gene family in *Arabidopsis thaliana* under low-oxygen conditions. *Plant Biology*, **16**: 28-34.
- Mitra M, Agarwal P, Kundu A, Banerjee V, Roy S. 2019.** Investigation of the effect of UV-B light on Arabidopsis MYB4 (*AtMYB4*) transcription factor stability and detection of a putative MYB4-binding motif in the promoter proximal region of *AtMYB4*. *PloS One*, **14**: e0220123.
- Mittler R. 2002.** Oxidative stress, antioxidants and stress tolerance. *Trends in Plant Science*, **7**:405-410.
- Miyashima S, Roszak P, Sevilem I, Toyokura K, Blob B, Heo, JO, Mellor N, Rinta-Rahko HH, Otero S, et al. 2019.** Mobile PEAR transcription factors integrate positional cues to prime cambial growth. *Nature*, **565**: 490-494.
- Miyashima S, Koi S, Hashimoto T, Nakajima K. 2011.** Non-cell-autonomous microRNA165 acts in a dose-dependent manner to regulate multiple differentiation status in the *Arabidopsis* root. *Development*, **138**:2303-2313.
- Molina-Rueda JJ, Pascual MB, Pissarra J, Gallardo F. 2015.** A putative role for γ -aminobutyric acid (GABA) in vascular development in pine seedlings. *Planta*, **241**: 257-267.

Molinie B, Wang J, Lim KS, Hillebrand R, Lu ZX, Van Wittenberghe N, Howard BD, Daneshvar K, Mullen AC, Dedon P, et al. 2016. m6A-LAIC-seq reveals the census and complexity of the m6A epitranscriptome. *Nature Methods*, **13**: 692.

Moreau D, Bardgett RD, Finlay RD, Jones DL, Philippot L. 2019. A plant perspective on nitrogen cycling in the rhizosphere. *Functional Ecology*, **33**: 540-552.

Moreno-Risueno MA, Martínez M, Vicente-Carbajosa J, Carbonero P. 2007. The family of DOF transcription factors: from green unicellular algae to vascular plants. *Molecular Genetics and Genomics* **277**: 379-390.

Morita MT, Sakaguchi K, Kiyose SI, Taira K, Kato T, Nakamura M, Tasaka M. 2006. A C2H2-type zinc finger protein, SGR5, is involved in early events of gravitropism in *Arabidopsis* inflorescence stems. *The Plant Journal*, **47**: 619-628.

Murik O, Chandran SA, Nevo-Dinur K, Sultan LD, Best C, Stein Y, Hazan C, Ostersetzer-Biran O. 2019. The topologies of N6-Adenosine methylation (m6A) in land plant mitochondria and their putative effects on organellar gene-expression. *The Plant Journal*, **101**: 1269-1286.

Mustroph A, Sonnewald U, Biemelt S. 2007. Characterisation of the ATP-dependent phosphofructokinase gene family from *Arabidopsis thaliana*. *FEBS Letters*, **581**: 2401-2410.

Nagarajan A, Janostiak R, Wajapeyee N. 2019. Dot blot analysis for measuring global N6-methyladenosine modification of RNA. Epitranscriptomics. Humana Press, New York, NY: 263-271.

Nakajima K, Sena G, Nawy T, Benfey, PN. 2001. Intercellular movement of the putative transcription factor SHR in root patterning. *Nature* **413**: 307-311.

Näsholm T, Ekblad A, Nordin A, Giesler R, Höglberg M, Höglberg P. 1998. Boreal forest plants take up organic nitrogen. *Nature*, **392**: 914-916.

NCBI Resource Coordinators. 2016. Database resources of the National Center for Biotechnology Information. *Nucleic Acids Research* **44**: 7-19.

Neale DB, McGuire PE, Wheeler NC, Stevens KA, Crepeau MW, Cardeno C, Zimin AV, Puiu D, et al. 2017. The Douglas-fir genome sequence reveals specialization of the photosynthetic apparatus in *Pinaceae*. *G3: Genes, Genomes, Genetics*, **7**: 3157-3167.

Neale DB, Wegrzyn JL, Stevens KA, Zimin AV, Puiu D, Crepeau MW, Cardeno C, Koriabine M, Holtz-Morris AE, Liechty JD. 2014. Decoding the massive genome of loblolly pine using haploid DNA and novel assembly strategies. *Genome Biology*, **15**: R59.

Negi S, Sukumar P, Liu X, Cohen JD, Muday GK. 2010. Genetic dissection of the role of ethylene in regulating auxin-dependent lateral and adventitious root formation in tomato. *The Plant Journal*, **61**(1), 3-15.

- Negi S, Ivanchenko MG, Muday GK. 2008.** Ethylene regulates lateral root formation and auxin transport in *Arabidopsis thaliana*. *The Plant Journal*, **55**: 175-187.
- Neuhäuser B, Dynowski M, Ludewig U. 2014.** Switching substrate specificity of AMT/MEP/Rh proteins. *Channels*, **8**: 496-502.
- Neuhäuser B, Dynowski M, Ludewig U. 2009.** Channel-like NH₃ flux by ammonium transporter AtAMT2. *FEBS Letters*, **583**: 2833-2838.
- Nguyen G, Rothstein S, Spangenberg G, Kant S. 2015.** Role of microRNAs involved in plant response to nitrogen and phosphorous limiting conditions. *Frontiers in Plant Science*, **6**:629.
- Nguyen T, Li J, Lu CCJ, Mamrosh JL, Lu G, Cathers BE, Deshaies RJ. 2017.** p97/VCP promotes degradation of CRBN substrate glutamine synthetase and neosubstrates. *Proceedings of the National Academy of Sciences*, **114**: 3565-3571.
- Nguyen T, Lee JE, Sweredoski MJ, Yang SJ, Jeon SJ, Harrison JS, et al 2016.** Glutamine triggers acetylation-dependent degradation of glutamine synthetase via the thalidomide receptor cereblon. *Molecular Cell*, **61**: 809-820.
- Nichols JL. 1979.** ‘Cap’ structures in maize poly (A)-containing RNA. *Biochimica et Biophysica Acta (BBA)-Nucleic Acids and Protein Synthesis*, **563**: 490-495.
- Nizampatnam NR, Schreier SJ, Damodaran S, Adhikari S, Subramanian S. 2015.** micro RNA 160 dictates stage-specific auxin and cytokinin sensitivities and directs soybean nodule development. *The Plant Journal*, **84**: 140-153.
- Norton JM, Ouyang Y. 2019.** Controls and adaptive management of nitrification in agricultural soils. *Frontiers in Microbiology*, **10**, 1931.
- Nühse TS, Stensballe A, Jensen ON, Peck SC. 2004.** Phosphoproteomics of the *Arabidopsis* plasma membrane and a new phosphorylation site database. *The Plant Cell*, **16**: 2394-2405.
- Nystedt B, Street NR, Wetterbom A, Zuccolo A, Lin Y-C, Scofield DG, Vezzi F, Delhomme N, Giacomello S, Alexeyenko A. 2013.** The Norway spruce genome sequence and conifer genome evolution. *Nature*, **497**: 579–584.
- Ochando I, Jover-Gil S, Ripoll JJ, Candela H, Vera A, Ponce MR, Martínez-Laborda A, Micol JL. 2006.** Mutations in the microRNA complementarity site of the INCURVATA4 gene perturb meristem function and adaxialize lateral organs in *Arabidopsis*. *Plant Physiology*, **141**: 607-619.
- O’Leary B, Plaxton WC. 2020.** Multifaceted functions of post-translational enzyme modifications in the control of plant glycolysis. *Current Opinion in Plant Biology*, **55**: 28-37.
- Osborne EB, Thunell RC, Gruber N, Feely RA, Benitez-Nelson CR. 2020.** Decadal variability in twentieth-century ocean acidification in the California Current Ecosystem. *Nature Geoscience*, **13**: 43-49.
- Ortigosa F, Valderrama-Martín JM, Urbano-Gámez JA, García-Martín ML, Ávila C, Cánovas FM, Cañas RA. 2020.** Inorganic nitrogen form determines nutrient allocation and metabolic responses in maritime pine seedlings.

References

Ortigosa F, Valderrama-Martín JM, Ávila C, Cánovas FM and Cañas RA. 2019. Understanding plant nitrogen nutrition through a laboratory experiment. *Biochemistry and Molecular Biology Education*, **47**: 450-458.

Pandey SP, Somssich IE. 2009. The role of WRKY transcription factors in plant immunity. *Plant Physiology*, **150**: 1648-1655.

Park BS, Yao T, Seo JS, Wong ECC, Mitsuda N, Huang CH, Chua NH. 2018. *Arabidopsis* NITROGEN LIMITATION ADAPTATION regulates ORE1 homeostasis during senescence induced by nitrogen deficiency. *Nature Plants*, **4**: 898-903.

Parker MT, Knop K, Sherwood AV, Schurch NJ, Mackinnon K, Gould PD, Hall AJW, Barton GJ, Simpson GG. (2020). Nanopore direct RNA sequencing maps the complexity of *Arabidopsis* mRNA processing and m6A modification. *eLife*, **9**.

Patel S, Goyal A. 2017. Chitin and chitinase: Role in pathogenicity, allergenicity and health. *International Journal of Biological Macromolecules*, **97**: 331-338.

Patil DP, Chen CK, Pickering BF, Chow A, Jackson C, Guttman M, Jaffrey SR. 2016. m6A RNA methylation promotes XIST-mediated transcriptional repression. *Nature*, **537**:369–373.

Patterson K, Cakmak T, Cooper A, Lager IDA, Rasmusson AG, Escobar MA. 2010. Distinct signalling pathways and transcriptome response signatures differentiate ammonium-and nitrate-supplied plants. *Plant, Cell & Environment*, **33**: 1486-1501.

Paul S, Datta SK, Datta K. 2015. miRNA regulation of nutrient homeostasis in plants. *Frontiers in Plant Science*, **6**, 232.

Pearson JN, Finnemann J, Schjoerring JK. 2002. Regulation of the high-affinity ammonium transporter (BnAMT1; 2) in the leaves of *Brassica napus* by nitrogen status. *Plant Molecular Biology*, **49**: 483-490.

Peer E, Moshitch-Moshkovitz S, Rechavi G, Dominissini D. 2019. The epitranscriptome in translation regulation. *Cold Spring Harbor Perspectives in Biology*, **11**: a032623.

Peer WA, Murphy AS. 2007. Flavonoids and auxin transport: modulators or regulators?. *Trends in Plant Science*, **12**: 556-563.

Peer E, Rechavi G, Dominissini D. 2017. Epitranscriptomics: regulation of mRNA metabolism through modifications. *Current opinion in chemical biology*, **41**: 93-98.

Pellicer J, Leitch IJ. 2019. The Plant DNA C-values database (release 7.1): an updated online repository of plant genome size data for comparative studies. *New Phytologist*, **226**: 301-305.

- Peng M, Hannam C, Gu H, Bi YM, Rothstein SJ. 2007.** A mutation in NLA, which encodes a RING-type ubiquitin ligase, disrupts the adaptability of *Arabidopsis* to nitrogen limitation. *The Plant Journal*, **50**: 320-337.
- Picon C, Guehl JM, Ferhi A. 1996.** Leaf gas exchange and carbon isotope composition responses to drought in a drought-avoiding (*Pinus pinaster*) and a drought-tolerant (*Quercus petraea*) species under present and elevated atmospheric CO₂ concentrations. *Plant, Cell & Environment*, **19**: 182-190.
- Pien S, Fleury D, Mylne JS, Crevillen P, Inzé D, Avramova Z, Dean C, Grossniklaus U. 2008.** ARABIDOPSIS TRITHORAX1 dynamically regulates FLOWERING LOCUS C activation via histone 3 lysine 4 trimethylation. *The Plant Cell*, **20**: 580-588.
- Pieterse CM., van Wees SC, van Pelt JA, Knoester M, Laan R, Gerrits H, Weisbeek PJ, van Loon LC. 1998.** A novel signaling pathway controlling induced systemic resistance in *Arabidopsis*. *Plant Cell* **10**: 1571–1580.
- Pike CS, Cohen WS, Monroe JD. 2002.** Nitrate reductase: A model system for the investigation of enzyme induction in eukaryotes. *Biochemistry and Molecular Biology Education*, **30**: 111-116.
- Pingali PL. 2012.** Green revolution: impacts, limits, and the path ahead. *Proceedings of the National Academy of Sciences*, **109**: 12302-12308.
- Pontier D, Picart C, El Baidouri M, Roudier F, Xu T, Lahmy S, Llauro C, Azevedo J, Laudie M, Attina A, et al. 2019.** The m6A pathway protects the transcriptome integrity by restricting RNA chimera formation in plants. *Life Science Alliance*, **2**.
- Poovaliah CR, Phalen C, Sniffen GT, Coleman HD. 2019.** Growth and Transcriptional Changes in Poplar Under Different Nitrogen Sources. *Plant Molecular Biology Reporter*, **37**: 291-302.
- Prigge MJ, Otsuga D, Alonso JM, Ecker JR, Drews GN, Clark, SE. 2005.** Class III homeodomain-leucine zipper gene family members have overlapping, antagonistic, and distinct roles in *Arabidopsis* development. *The Plant Cell*, **17**:61-76.
- Prinsi B, Espen L. 2018.** Time-Course of Metabolic and Proteomic Responses to Different Nitrate/Ammonium Availabilities in Roots and Leaves of Maize. *International Journal of Molecular Sciences*, **19**: 2202.
- Provencher SW. 1993.** Estimation of metabolite concentrations from localized in vivo proton NMR spectra. *Magnetic Resonance in Medicine*, **30**: 672-679.
- Purdy SJ, Bussell JD, Nelson DC, Villadsen D, Smith SM. 2011.** A nuclear-localized protein, KOLD SENSITIV-1, affects the expression of cold-responsive genes during prolonged chilling in *Arabidopsis*. *Journal of Plant Physiology*, **168**: 263-269.
- Raherison ES, Giguère I, Caron S, Lamara M, MacKay J. 2015.** Modular organization of the white spruce (*Picea glauca*) transcriptome reveals functional organization and evolutionary signatures. *New Phytologist*, **207**: 172-187.

References

- Ravazzolo L, Trevisan S, Forestan C, Varotto S, Sut S, Dall'Acqua S, Malagoli M, Quaggiotti S. (2020).** Nitrate and ammonium affect the overall maize response to nitrogen availability by triggering specific and common transcriptional signatures in roots. *International Journal of Molecular Sciences*, **21**: 686.
- Rawat SR, Silim SN, Kronzucker HJ, Siddiqi MY, Glass AD. 1999.** *AtAMT1* gene expression and NH₄⁺ uptake in roots of *Arabidopsis thaliana*: evidence for regulation by root glutamine levels. *The Plant Journal*, **19**: 143-152.
- Reichel M, Köster T, Staiger D. 2019.** Marking RNA: m6A writers, readers, and functions in Arabidopsis. *Journal of Molecular Cell Biology*, **11**: 899-910.
- Rennenberg H, Wildhagen H, Ehlting B. 2010.** Nitrogen nutrition of poplar trees. *Plant Biology*, **12**: 275-291.
- Rennenberg H, Dannenmann M, Gessler A, Kreuzwieser J, Simon J, Papen H. 2009.** Nitrogen balance in forest soils: nutritional limitation of plants under climate change stresses. *Plant Biology*, **11**: 4-23.
- Ristova D, Carré C, Pervent M, Medici A, Kim GJ, Scalia D, Ruffel S, Birdbaum KD, Lacombe B, Busch W, et al. 2016.** Combinatorial interaction network of transcriptomic and phenotypic responses to nitrogen and hormones in the *Arabidopsis thaliana* root. *Science Signaling*, **9** :rs13-rs13.
- Ritz C, Spiess AN. 2008.** qpcR: an R package for sigmoidal model selection in quantitative real-time polymerase chain reaction analysis. *Bioinformatics*, **24**: 1549-1551.
- Robertson GP, Vitousek PM. 2009.** Nitrogen in agriculture: balancing the cost of an essential resource. *Annual Review of Environment and Resources*, **34**: 97-125.
- Rothwell GW, Mapes G, Stockey RA, Hilton J. 2012.** The seed cone *Eathiestrobus* gen. nov.: fossil evidence for a Jurassic origin of *Pinaceae*. *American Journal of Botany*, **99**: 708-720.
- Robinson MD, McCarthy DJ, Smyth GK. 2010.** edgeR: a Bioconductor package for differential expression analysis of digital gene expression data. *Bioinformatics* **26**: 139-140.
- Romero-Rodríguez MC, Pascual J, Valledor L, Jorrín-Novo JV. 2014.** Improving the quality of protein identification in non-model species. Characterization of *Quercus ilex* seed and *Pinus radiata* needle proteomes by using SEQUEST and custom databases. *Journal of Proteomics*, **105**: 85-91.
- Roodbarkelari F, Groot EP. 2017.** Regulatory function of homeodomain-leucine zipper (HD-ZIP) family proteins during embryogenesis. *New Phytologist*, **213**: 95-104.
- Roubik DW. (Ed.). 1995** Pollination of cultivated plants in the tropics. *Food & Agriculture Organization*, **118**.
- Ruan J, Gerendás J, Härdter R, Sattelmacher B. 2007.** Effect of root zone pH and form and concentration of nitrogen on accumulation of quality-related

components in green tea. *Journal of the Science of Food and Agriculture*, **87**: 1505-1516.

Ruan L, Wei K, Wang L, Cheng H, Zhang F, Wu L, Bai P, Zhang C. 2016. Characteristics of NH_4^+ and NO_3^- fluxes in tea (*Camellia sinensis*) roots measured by scanning ion-selective electrode technique. *Scientific Reports*, **6**: 1-8.

Rushton PJ, Somssich IEM, Ringler P, Shen QJ. 2010. WRKY transcription factors. *Trends in Plant Science*, **15**: 247-258.

Růžicka K, Zhang M, Campilho A, Bodi Z, Kashif M, Saleh M, Eeckhout D, El-Showk S, Li H, Zhong S, et al. 2017. Identification of factors required for m6A mRNA methylation in *Arabidopsis* reveals a role for the conserved E3 ubiquitin ligase HAKAI. *New Phytologist*, **215**: 157-172.

Sablowski R. 2011. Plant stem cell niches: from signalling to execution. *Current Opinion in Plant Biology*, **14**: 4-9.

Saeidi S, Boroujeni NA, Ahmadi H, Hassanshahian M. 2015. Antibacterial activity of some plant extracts against extended-spectrum beta-lactamase producing *Escherichia coli* isolates. *Jundishapur Journal of Microbiology*, **8**: e15434.

Saitou N, Nei M. 1987. The neighbor-joining method: A new method for reconstructing phylogenetic trees. *Molecular Biology and Evolution* **4**: 406-425.

Sakamoto A, Murata AN. 1998. Metabolic engineering of rice leading to biosynthesis of glycinebetaine and tolerance to salt and cold. *Plant Molecular Biology*, **38**: 1011-1019.

Saleh A, Alvarez-Venegas R, Yilmaz M, Le O, Hou G, Sadler M, Al-Abdallat A, Xia Y et al. 2008. The highly similar *Arabidopsis* homologs of trithorax *ATX1* and *ATX2* encode proteins with divergent biochemical functions. *The Plant Cell*, **20**: 568-579.

Salehin M, Bagchi R, Estelle M. 2015. SCFTIR1/AFB-based auxin perception: mechanism and role in plant growth and development. *The Plant Cell*, **27**: 9-19.

Sasakawa H, Yamamoto Y. 1978. Comparison of the uptake of nitrate and ammonium by rice seedlings: influences of light, temperature, oxygen concentration, exogenous sucrose, and metabolic inhibitors. *Plant Physiology*, **62**: 665-669.

Schimel JP, Bennett J. 2004. Nitrogen mineralization: challenges of a changing paradigm. *Ecology*, **85**: 591-602.

Schwarz R, Dayhoff M. 1979. Matrices for detecting distant relationships. In Dayhoff M., editor, *Atlas of protein sequences*:353-58. *National Biomedical Research Foundation*.

Scutenaire J, Deragon JM, Jean V, Benhamed M, Raynaud C, Favory JJ, Merret R, Bousquet-Antonelli, C. 2018. The YTH domain protein ECT2 is an m6A reader required for normal trichome branching in *Arabidopsis*. *The Plant Cell*, **30**: 986-1005.

Sena G, Jung JW, Benfey PN. 2004. A broad competence to respond to SHORT ROOT revealed by tissue-specific ectopic expression. *Development*, **131**: 2817–2826.

Seoane-Zonjic P, Cañas RA, Bautista R, Gómez-Maldonado J, Arrillaga I, Fernández-Pozo N, Claros MG, Cánovas FM, Ávila C. 2016. Establishing gene models from the *Pinus pinaster* genome using gene capture and BAC sequencing. *BMC genomics*, **17**: 148.

Seoane CLV, Gallego Fernández J, Vidal Pascual C. 2007. Manual of restoration of coastal dunes. *Edited by the Ministry of the Environment of Spain. General Direction of Coasts*. ISBN-13: 978-84-8320-409-2.

Sessa G, Carabelli M, Possenti M, Morelli G, Ruberti I. 2018. Multiple links between HD-Zip proteins and hormone networks. *International Journal of Molecular Sciences*, **19**: 4047.

Shahzad R, Harlina PW, Ayaad M, Ewas M, Nishawy E, Fahad S, Subthain H, Amar MH. 2018. Dynamic roles of microRNAs in nutrient acquisition and plant adaptation under nutrient stress: a review. *Plant Omics*, **11**: 58-79.

Shafiq S, Berr A, Shen WH. 2014. Combinatorial functions of diverse histone methylations in *Arabidopsis thaliana* flowering time regulation. *New Phytologist*, **201**: 312-322.

Sharma S, Lafontaine DL. 2015. ‘View from a bridge’: A new perspective on eukaryotic rRNA base modification. *Trends in Biochemical Sciences*, **40**: 560-575.

Shen L, Liang Z, Wong CE, Yu, H. 2019. Messenger RNA modifications in plants. *Trends in Plant Science*, **24**: 328-341.

Shen L, Liang Z, Yu H. 2017. Dot blot analysis of N6-methyladenosine RNA modification levels. *Bio-Protocols*, **7**(1), 10-21769.

Shen L, Liang Z, Gu X, Chen Y, Teo ZW, Hou X, Cai WM, Dedon PC, Liu L, Yu H. 2016. N6-Methyladenosine RNA modification regulates shoot stem cell fate in *Arabidopsis*. *Developmental Cell*, **38**: 186–200.

Shen Y, Liu Y, Liu L, Liang C, Li QQ. 2008. Unique features of nuclear mRNA poly (A) signals and alternative polyadenylation in *Chlamydomonas reinhardtii*. *Genetics*, **179**: 167-176.

Sheteiwiy MS, Shao H, Qi W, Hamoud YA, Shaghaleh H, Khan NU, Yang R, Tang B. 2019. GABA-alleviated oxidative injury induced by salinity, osmotic stress and their combination by regulating cellular and molecular signals in rice. *International Journal of Molecular Sciences*, **20**: 5709.

Shi Y, Wang H, Wang J, Liu X, Lin F, Lu J. 2018. N6-methyladenosine RNA methylation is involved in virulence of the rice blast fungus *Pyricularia oryzae* (syn. *Magnaporthe oryzae*). *FEMS Microbiology Letters*, **366**: 286.

Shtratnikova VY, Kudryakova NV, Kudoyarova GR, Korobova AV, Akhiyarova GR, Danilova MN, Kustetsov VV, Kulaeva ON. 2015. Effects of nitrate and ammonium on growth of *Arabidopsis thaliana* plants transformed with the ARR5::GUS construct and a role for cytokinins in suppression of disturbances

induced by the presence of ammonium. *Russian Journal of Plant Physiology*, **62**: 741-752.

Silvente S, Reddy PM, Khandual S, Blanco L, Alvarado-Affantranger X, Sanchez F, Lara-Flores M. 2008. Evidence for sugar signalling in the regulation of asparagine synthetase gene expressed in *Phaseolus vulgaris* roots and nodules. *Journal of Experimental Botany*, **59**: 1279-1294.

Silverstein KA, Moskal Jr, WA, Wu HC, Underwood BA, Graham MA, Town CD, VandenBosch KA. 2007. Small cysteine-rich peptides resembling antimicrobial peptides have been under-predicted in plants. *The Plant Journal*, **51**: 262-280.

Sinu PA, Kent SM, Chandrashekar K. 2012. Forest resource use and perception of farmers on conservation of a usufruct forest (Soppinabetta) of Western Ghats, India. *Land Use Policy*, **29**: 702-709.

Sloan KE, Warda AS, Sharma S, Entian KD, Lafontaine DL, Bohnsack MT. 2017. Tuning the ribosome: The influence of rRNA modification on eukaryotic ribosome biogenesis and function. *RNA Biology*, **14**:1138-1152.

Sonoda Y, Ikeda A, Saiki S, von Wirén N, Yamaya T, Yamaguchi J. 2003. Distinct expression and function of three ammonium transporter genes (OsAMT1; 1–1; 3) in rice. *Plant and Cell Physiology*, **44**: 726-734.

Sohar K, Altman J, Lehečková E, Doležal J. 2017. Growth–climate relationships of Himalayan conifers along elevational and latitudinal gradients. *International Journal of Climatology*, **37**: 2593-2605.

Spoel SH, Mou Z, Tada Y, Spivey NW, Genschik P, Dong X. 2009. Proteasome-mediated turnover of the transcription coactivator NPR1 plays dual roles in regulating plant immunity. *Cell*, **137**: 860–872.

Stevens KA, Wegrzyn JL, Zimin A, Puiu D, Crepeau M, Cardeno C, Paul R, Gonzalez-Ibeas D, Koriabine M, Holtz-Morris AE, et al. 2016. Sequence of the sugar pine megagenome. *Genetics*, **204**: 1613-1626.

Steynen QJ, Schultz EA. 2003. The FORKED genes are essential for distal vein meeting in *Arabidopsis*. *Development*, **130**: 4695-4708.

Stoiber MH, Quick J, Egan R, Lee JE, Celniker SE, Neely R, Loman N, Pennacchio LA, Brown J. 2016. De novo identification of DNA modifications enabled by genome-guided nanopore signal processing. *BioRxiv*.

Storey JD, Taylor JE, Siegmund D. 2004. Strong control, conservative point estimation and simultaneous conservative consistency of false discovery rates: a unified approach. *Journal of the Royal Statistical Society: Series B*, **66**: 187-205.

Stotz HU, Thomson J, Wang Y. 2009. Plant defensins: defense, development and application. *Plant Signaling & Behavior*, **4**: 1010-1012.

Straub T, Ludewig U, Neuhäuser B. 2017. The kinase CIPK23 inhibits ammonium transport in *Arabidopsis thaliana*. *The Plant Cell*, **29**: 409-422.

References

- Suárez MF, Avila C, Gallardo F, Cantón FR, García-Gutiérrez A, Claros MG, Cánovas FM. 2002.** Molecular and enzymatic analysis of ammonium assimilation in woody plants. *Journal of Experimental Botany*, **53**: 891-904.
- Su Y, Yang S, Hao D, Jin M, Li Y, Liu Z, Huang Y, Chen, T. 2020.** Internal ammonium excess induces ROS-mediated reaction and causes carbon scarcity in rice. *BMC Plant Biology*.
- Sulis DB, Wang JP. 2020.** Regulation of lignin biosynthesis by post-translational protein modifications. *Frontiers in Plant Science*, **11**.
- Sun L, Di DW, Li G, Kronzucker HJ, Wu X, Shi W. 2020a.** Endogenous ABA alleviates rice ammonium toxicity by reducing ROS and free ammonium via regulation of the SAPK9–bZIP20 pathway. *Journal of Experimental Botany*, **71**: 4562–4577.
- Sun L, Di DW, Li G, Li Y, Kronzucker HJ, Shi W. 2020b.** Transcriptome analysis of rice (*Oryza sativa* L.) in response to ammonium resupply reveals the involvement of phytohormone signaling and the transcription factor OsJAZ9 in reprogramming of nitrogen uptake and metabolism. *Journal of Plant Physiology*, 153137.
- Sun L, Di D, Li G, Kronzucker HJ, Shi W. 2017.** Spatio-temporal dynamics in global rice gene expression (*Oryza sativa* L.) in response to high ammonium stress. *Journal of Plant Physiology*, **212**:94-104.
- Sun SW, Lin YC, Weng YM, Chen MJ. 2006.** Efficiency improvements on ninhydrin method for amino acid quantification. *Journal of Food Composition and Analysis*, **19**: 112-117.
- Suzuki A, Knaff DB. 2005.** Glutamate synthase: structural, mechanistic and regulatory properties, and role in the amino acid metabolism. *Photosynthesis Research*, **83**: 191-217.
- Taiz L, Zeiger E, Møller IM, Murphy A. 2015.** Plant physiology and development.
- Takei K, Ueda N, Aoki K, Kuromori T, Hirayama T, Shinozaki K, Yamaya T, Sakakibara H. 2004.** AtIPT3 is a key determinant of nitrate-dependent cytokinin biosynthesis in *Arabidopsis*. *Plant and Cell Physiology*, **45**: 1053-1062.
- Tang W, He X, Qian L, Wang F, Zhang Z, Sun C, Lin L, Guan C. 2019.** Comparative transcriptome analysis in oilseed rape (*Brassica napus*) reveals distinct gene expression details between nitrate and ammonium nutrition. *Genes*, **10**: 391.
- Tanimoto M, Tremblay R, Colasanti, J. 2008.** Altered gravitropic response, amyloplast sedimentation and circumnutation in the *Arabidopsis* shoot gravitropism 5 mutant are associated with reduced starch levels. *Plant Molecular Biology*, **67**: 57-69.
- Taoka M, Nobe Y, Yamaki Y, Sato K, Ishikawa H, Izumikawa K, Yamauchi Y, Hirota K, et al. 2018.** Landscape of the complete RNA chemical modifications in the human 80S ribosome. *Nucleic Acids Research*, **46**: 9289-9298.

- Taylor AF, Alexander IAN. 2005.** The ectomycorrhizal symbiosis: life in the real world. *Mycologist*, **19**: 102-112.
- Teles YC, Souza MSR, Souza MDFVD. 2018.** Sulphated flavonoids: biosynthesis, structures, and biological activities. *Molecules*, **23**: 480.
- Tercé-Laforgue T, Bedu M, Dargel-Grafin C, Dubois F, Gibon Y, Restivo FM, Hirel B. 2013.** Resolving the role of plant glutamate dehydrogenase: II. Physiological characterization of plants overexpressing the two enzyme subunits individually or simultaneously. *Plant and Cell Physiology*, **54**: 1635-1647.
- Tian Tian, Yue Liu, Hengyu Yan, Qi You, Xin Yi, Zhou Du, Wenying Xu, Zhen Su. 2017.** agriGO v2.0: a GO analysis toolkit for the agricultural community. *Nucleic Acids Research* **45**: 122-129.
- Tischner R. 2000.** Nitrate uptake and reduction in higher and lower plants. *Plant Cell & Environment*, **23**: 1005–1024.
- Theler D, Dominguez C, Blatter M, Boudet, J., Allain FHT. 2014.** Solution structure of the YTH domain in complex with N6-methyladenosine RNA: a reader of methylated RNA. *Nucleic Acids Research*, **42**: 13911-13919.
- Thomsen HC, Eriksson D, Møller IS, Schjoerring JK. 2014.** Cytosolic glutamine synthetase: a target for improvement of crop nitrogen use efficiency?. *Trends in Plant Science*, **19**: 656-663.
- Thüring K, Schmid K, Keller P, Helm M. 2017.** LC-MS analysis of methylated RNA. *RNA Methylation. Humana Press*, New York, NY: 3-18.
- Towbin H, Staehelin T, Gordon J. 1979.** Electrophoretic transfer of proteins from polyacrylamide gels to nitrocellulose sheets: procedure and some applications. *Proceedings of the National Academy of Sciences*, **76**: 4350-4354.
- Tuerto F, Liebers R, Musch T, Schaefer M, Hofmann S, Kellner S, Frye M, Helm M, Stoecklin G, Lyko F. 2012.** RNA cytosine methylation by Dnmt2 and NSun2 promotes tRNA stability and protein synthesis. *Nature Structural & Molecular Biology*, **19**: 900.
- Turano FJ, Dashner R, Upadhyaya A, Caldwell C R. 1996.** Purification of mitochondrial glutamate dehydrogenase from dark-grown soybean seedlings. *Plant Physiology*, **112**: 1357-1364.
- Turchi L, Carabelli M, Ruzza V, Possenti M, Sassi M, Peñalosa A, Sessa G, Salvi S, Forte V, Morelli G, et al. 2013.** *Arabidopsis* HD-Zip II transcription factors control apical embryo development and meristem function. *Development*, **140**: 2118-2129.
- UNFCCC, C. 2015.** Paris agreement. FCCCC/CP/2015/L. 9/Rev. 1.
- Ubeda-Tomás S, Federici F, Casimiro I, Beemster GT, Bhalerao R, Swarup R, Doerner P, Haseloff J, Bennett, MJ. 2009.** Gibberellin signaling in the endodermis controls *Arabidopsis* root meristem size. *Current Biology*, **19**: 1194-1199.

References

- Van Son H, My NTD, Khuong NV. 2014.** Some methods to increase job opportunities for currently new graduates from practical requirements towards global education. *Asian Journal of Education and e-Learning*, **2**.
- Vandivier LE, Gregory BD. 2018.** New insights into the plant epitranscriptome. *Journal of Experimental Botany*, **69**: 4659-4665.
- Vanhala P, Repo A, Liski J. 2013.** Forest bioenergy at the cost of carbon sequestration?. *Current Opinion in Environmental Sustainability*, **5**: 41-46.
- Verspagen JM. 2020.** Acidification slows algal movement. *Nature Climate Change*, 1-2.
- Vespa L, Vachon G, Berger F, Perazza D, Faure JD, Herzog M. 2004.** The immunophilin-interacting protein AtFIP37 from *Arabidopsis* is essential for plant development and is involved in trichome endoreduplication. *Plant Physiology*, **134**:1283–1292.
- Vega-Mas I, Cukier C, Coletto I, González-Murua C, Wang X, Li J, Guo J, Qiao Q, Guo X and Ma Y. 2020.** The WRKY transcription factor PIWRKY65 enhances the resistance of *Paeonia lactiflora* (herbaceous peony) to *Alternaria tenuissima*. *Horticulture Research*, **7**: 1-12.
- Vidal EA, Araus V, Lu C, Parry G, Green PJ, Coruzzi GM, Gutiérrez RA. 2010.** Nitrate-responsive miR393/AFB3 regulatory module controls root system architecture in *Arabidopsis thaliana*. *Proceedings of the National Academy of Sciences*, **107**: 4477-4482.
- Viñas RA, Caudullo G, Oliveira S, de Rigo D. 2016.** *Pinus pinaster* in Europe: distribution, habitat, usage and threats. *European Atlas of Forest Tree Species*; Publications Office of the European Union: Luxembourg.
- Vitsios DM, Kentepozidou E, Quintais L, Benito-Gutiérrez E, van Dongen S, Davis MP, Enright AJ. 2017.** MirNovo: genome-free prediction of microRNAs from small RNA sequencing data and single-cells using decision forests. *Nucleic Acids Research* **45**: e177.
- Vitousek PM, Gosz JR, Grier CC, Melillo JM, Reiners WA. 1982.** A comparative analysis of potential nitrification and nitrate mobility in forest ecosystems. *Ecological Monographs*, **52**: 155-177.
- Vizcaino JA, Cote RG, Csordas A, Dianes JA, Fabregat A, Foster JM, Griss J, Alpi E, Birim M, Contell J, et al. 2013.** The Proteomics Identifications (PRIDE) database and associated tools: status in 2013. *Nucleic Acids Research*, **41**: 1063-1069.
- Voogt P, Poorter H. 1996.** The effects of nutrient fertilization on growth, biomass allocation, and anatomy of maize plants. *Journal of Biological Education*, **30**: 67-72.
- von Wittgenstein NJ, Le CH, Hawkins BJ, Ehlting J. 2014.** Evolutionary classification of ammonium, nitrate, and peptide transporters in land plants. *BMC Evolutionary Biology*, **14**: 11.

- Walters DR, Bingham IJ. 2007.** Influence of nutrition on disease development caused by fungal pathogens: implications for plant disease control. *Annals of Applied Biology*, **151**: 307-324.
- Wan Y, Tang K, Zhang D, Xie S, Zhu X, Wang Z, Lang Z. 2015.** Transcriptome-wide high-throughput deep m⁶A-seq reveals unique differential m⁶A methylation patterns between three organs in *Arabidopsis thaliana*. *Genome Biology*, **16**: 272.
- Wang H, Ng TB. 2000.** Ginkbilobin, a novel antifungal protein from *Ginkgo biloba* seeds with sequence similarity to embryo-abundant protein. *Biochemical and Biophysical Research Communications*, **279**: 407-411.
- Wang J, Lan P, Gao H, Zheng L, Li W, Schmidt W. 2013.** Expression changes of ribosomal proteins in phosphate- and iron-deficient *Arabidopsis* roots predict stress-specific alterations in ribosome composition. *BMC Genomics*, **14**:783.
- Wang JW, Wang LJ, Mao YB, Cai WJ, Xue HW, Chen XY. 2005.** Control of root cap formation by microRNA-targeted auxin response factors in *Arabidopsis*. *The Plant Cell*, **17**: 2204-2216.
- Wang L, Ruan YL. 2013.** Regulation of cell division and expansion by sugar and auxin signaling. *Frontiers in Plant Science*, **4**: 163.
- Wang X, Zhao BS, Roundtree IA, Lu Z, Han D, Ma H, Weng X, Chen K, Shi H, He C. 2015.** N⁶-methyladenosine modulates messenger RNA translation efficiency. *Cell*, **161**: 1388-1399.
- Wang X, Li Z, Kong B, Song C, Cong J, Hou J, Wang S. 2017.** Reduced m⁶A mRNA methylation is correlated with the progression of human cervical cancer. *Oncotarget*, **8**: 98918.
- Wang XQ, Ran JH. 2014.** Evolution and biogeography of gymnosperms. *Molecular Phylogenetics and Evolution*, **75**, 24-40.
- Wang Y, Li Y, Toth JI, Petroski MD, Zhang Z, Zhao JC. 2014.** N⁶-methyladenosine modification destabilizes developmental regulators in embryonic stem cells. *Nature Cell Biology*, **16**: 191-198.
- Wang Z, Tang K, Zhang D, Wan Y, Wen Y, Lu Q, Wang L. 2017.** High-throughput m⁶A-seq reveals RNA m⁶A methylation patterns in the chloroplast and mitochondria transcriptomes of *Arabidopsis thaliana*. *PloS One*, **12**.
- Warda AS, Kretschmer J, Hackert P, Lenz C, Urlaub H, Höbartner C, Sloan KE, Bohnsack MT. 2017.** Human METTL16 is a N⁶-methyladenosine (m⁶A) methyltransferase that targets pre-mRNAs and various non-coding RNAs. *EMBO Reports*. **18**: 2004–2014.
- Warren CR, Adams MA. 2002.** Possible causes of slow growth of nitrate-supplied *Pinus pinaster*. *Canadian Journal of Forest Research*, **32**: 569-580.
- Warren RL, Keeling CI, Yuen MMS, Raymond A, Taylor GA, Vandervalk BP, Mohamadi H, Paulino D, Chiu R, et al. 2015.** Improved white spruce (*Picea glauca*) genome assemblies and annotation of large gene families of conifer terpenoid and phenolic defense metabolism. *The Plant Journal*, **83**: 189-212.

References

- Warren CR, Adams MA. 2002.** Possible causes of slow growth of nitrate-supplied *Pinus pinaster*. *Canadian Journal of Forest Research*, **32**: 569-580.
- Wegrzyn JL, Liechty JD, Stevens KA, Wu L-S, Loopstra CA, Vasquez-Gross HA, Dougherty WM, Lin BY, Zieve JJ, Martínez-García PJ. 2014.** Unique features of the loblolly pine (*Pinus taeda* L.) megagenome revealed through sequence annotation. *Genetics*, **196**: 891–909.
- Wei LH, Song P, Wang Y, Lu Z, Tang Q, Yu Q, Xiao Y, Zhang X, Duan HC, Jia G. 2018.** The m6A reader ECT2 controls trichome morphology by affecting mRNA stability in *Arabidopsis*. *The Plant Cell*, **30**: 968-985.
- Werner T, Motyka V, Laucou V, Smets R, Van Onckelen H, Schmülling T. 2003.** Cytokinin-deficient transgenic *Arabidopsis* plants show multiple developmental alterations indicating opposite functions of cytokinins in the regulation of shoot and root meristem activity. *The Plant Cell*, **15**: 2532-2550.
- Wieringa N, Janssen FJ, Van Driel JH. 2011.** Biology teachers designing context-based lessons for their classroom practice—the importance of rules-of-thumb. *International Journal of Science Education*, **33**: 2437-2462.
- Wendeborn S. 2020.** The chemistry, biology, and modulation of ammonium nitrification in soil. *Angewandte Chemie International Edition*, **59**: 2182-2202.
- Weng YL, Wang X, An R, Cassin J, Vissers C, Liu Y, Xu T, Wang X, Zheng-Hao-Wong S, Joseph J, et al. 2018.** Epitranscriptomic m6A regulation of axon regeneration in the adult mammalian nervous system. *Neuron*, **97**: 313-325.
- Willemsen V, Bauch M, Bennett T, Campilho A, Wolkenfelt H, Xu J, Haseloff J, Scheres B. 2008.** The NAC domain transcription factors FEZ and SOMBRERO control the orientation of cell division plane in *Arabidopsis* root stem cells. *Developmental Cell*. **15**: 913-922.
- Winkler FK. 2006.** Amt/MEP/Rh proteins conduct ammonia. *Pflügers Archiv*, **451**: 701-707.
- Wood CC, Porée F, Dreyer I, Koehler GJ, Udvardi MK. 2006.** Mechanisms of ammonium transport, accumulation, and retention in oocytes and yeast cells expressing *Arabidopsis* AtAMT1; 1. *FEBS Letters*, **580**: 3931-3936.
- Wu Y, Yang W, Wei J, Yoon H, An G. 2017.** Transcription factor OsDOF18 controls ammonium uptake by inducing ammonium transporters in rice roots. *Molecules and Cells*, **40**: 178.
- Wu X, Liu T, Zhang Y, Duan F, Neuhäuser B, Ludewig U, Schulze WX, Yuan L. 2019.** Ammonium and nitrate regulate NH₄⁺ uptake activity of *Arabidopsis* ammonium transporter AtAMT1; 3 via phosphorylation at multiple C-terminal sites. *Journal of Experimental Botany*, **70**: 4919-4930.
- Xiao W, Adhikari S, Dahal U, Chen YS, Hao YJ, Sun BF, Sun HY, Li A, Ping XL, Lai WY, et al. 2016.** Nuclear m6A reader YTHDC1 regulates mRNA splicing. *Molecular Cell*, **61**: 507-519.
- Xiao Y, Wang Y, Tang Q, Wei L, Zhang X, Jia G. 2018.** An Elongation-and Ligation-Based qPCR Amplification Method for the Radiolabeling-Free Detection

of Locus-Specific N6-Methyladenosine Modification. *Angewandte Chemie International Edition*, **57**: 15995-16000.

Xiaoxue Y, Yajun S, Panpan L, ImShik L. 2016. Evolutionary analysis of AMT (Ammonium Transporters) family in *Arabidopsis thaliana* and *Oryza sativa*. *Molecular Soil Biology*, **7**.

Xiong X, Yi C, Peng J. 2017. Epitranscriptomics: toward a better understanding of RNA modifications. *Genomics, Proteomics & Bioinformatics*, **15**: 147.

Xu C, Wang X, Liu K, Roundtree IA, Tempel W, Li Y, Lu Z, He C, Min J. 2014. Structural basis for selective binding of m6A RNA by the YTHDC1 YTH domain. *Nature Chemical Biology*, **10**: 927-929.

Xu G, Fan X, Miller AJ. 2012. Plant nitrogen assimilation and use efficiency. *Annual Review of Plant Biology*, **63**: 153-182.

Xuan YH, Priatama RA, Huang J, Je BI, Liu JM, Park SJ, Piao HL, Son DY, Lee JJ, Park SH, et al. 2013. Indeterminate domain 10 regulates ammonium-mediated gene expression in rice roots. *New Phytologist*, **197**: 791-804.

Xun Z, Guo X, Li Y, Wen X, Wang C, Wang Y. 2020. Quantitative proteomics analysis of tomato growth inhibition by ammonium nitrogen. *Plant Physiology and Biochemistry*, **154**: 129-141.

Xu Z, Zhong S, Li X, Li W, Rothstein SJ, Zhang, S, Bi Y, Xie C. 2011. Genome-wide identification of microRNAs in response to low nitrate availability in maize leaves and roots. *PloS One*, **6**: e28009.

Yamauchi Y, Fukaki H, Fujisawa H, Tasaka, M. 1997. Mutations in the *SGR4*, *SGR5* and *SGR6* loci of *Arabidopsis thaliana* alter the shoot gravitropism. *Plant and Cell Physiology*, **38**: 530-535.

Yan X, Qiao H, Zhang X, Guo C, Wang M, Wang Y, Wang X. 2017. Analysis of the grape (*Vitis vinifera* L.) thaumatin-like protein (TLP) gene family and demonstration that TLP29 contributes to disease resistance. *Scientific Reports*, **7**: 1-14.

Yang H, Xu Y, Zhu W, Chen K, Jiang H. 2007. Detailed mechanism for AmtB conducting $\text{NH}_4^+/\text{NH}_3$: molecular dynamics simulations. *Biophysical Journal*, **92**: 877-885.

Yang L, Perrera V, Saploura E, Apelt F, Bahin M, Kramdi A, Olas J, Mueller-Roeber B, Sokolowska E, Zhang W, et al. 2019. m5C methylation guides systemic transport of messenger RNA over graft junctions in plants. *Current Biology*, **29**: 2465-2476.

Yang SY, Hao DL, Song ZZ, Yang GZ, Wang L, Su YH. 2015. RNA-Seq analysis of differentially expressed genes in rice under varied nitrogen supplies. *Gene*, **555** : 305-317.

Yang Y, Wang F, Wan Q, Ruan J. 2018. Transcriptome analysis using RNA-Seq revealed the effects of nitrogen form on major secondary metabolite biosynthesis in tea (*Camellia sinensis*) plants. *Acta Physiologiae Plantarum*, **40**: 127.

References

- Yao K, Wu YY. 2016.** Phosphofructokinase and glucose-6-phosphate dehydrogenase in response to drought and bicarbonate stress at transcriptional and functional levels in mulberry. *Russian Journal of Plant Physiology*, **63**: 235-242.
- Yin R, Han K, Heller W, Albert A, Dobrev PI, Zažímalová E, Schäffner AR. 2014.** Kaempferol 3-O-rhamnoside-7-O-rhamnoside is an endogenous flavonol inhibitor of polar auxin transport in Arabidopsis shoots. *New Phytologist*, **201**: 466-475.
- Youssef C, Bizet F, Bastien R, Legland D, Bogeat-Triboulot MB, Hummel I. 2018.** Quantitative dissection of variations in root growth rate: a matter of cell proliferation or of cell expansion?, *Journal of Experimental Botany*, **69**: 5157–5168.
- Yu D, Chen C, Chen Z. 2001.** Evidence for an important role of WRKY DNA binding proteins in the regulation of NPR1 gene expression. *The Plant Cell*, **13**: 1527-1540.
- Yu J, Chen M, Huang H, Zhu J, Song H, Zhu J, Park J, Ji SJ. 2018.** Dynamic m6A modification regulates local translation of mRNA in axons. *Nucleic Acids Research*, **46**, 1412–1423.
- Yuan BF. 2017.** Liquid Chromatography-Mass Spectrometry for Analysis of RNA Adenosine Methylation. *RNA Methylation. Humana Press*, New York, NY: 33-42.
- Yuan L, Gu R, Xuan Y, Smith-Valle E, Loqué D, Frommer WB, von Wirén N. 2013.** Allosteric regulation of transport activity by heterotrimerization of *Arabidopsis* ammonium transporter complexes in vivo. *The Plant Cell*, **25**: 974-984.
- Yuan L, Graff L, Loqué D, Kojima S, Tsuchiya YN, Takahashi H, von Wirén N. 2009.** AtAMT1; 4, a pollen-specific high-affinity ammonium transporter of the plasma membrane in *Arabidopsis*. *Plant and Cell Physiology*, **50**: 13-25.
- Yuan L, Loqué D, Kojima S, Rauch S, Ishiyama K, Inoue E, Takahashi E, von Wirén N. 2007** The organization of high-affinity ammonium uptake in *Arabidopsis* roots depends on the spatial arrangement and biochemical properties of AMT1-type transporters. *The Plant Cell*, **19**: 2636–2652.
- Yue H, Nie X, Yan Z, Weining S. 2019.** N6-methyladenosine regulatory machinery in plants: composition, function and evolution. *Plant Biotechnology Journal*, **17**: 1194-1208.
- Zaccara S, Ries RJ, Jaffrey SR. 2019.** Reading, writing and erasing mRNA methylation. *Nature Reviews Molecular Cell Biology*, **20**: 608–624.
- Zeng Y, Wang S, Gao S, Soares F, Ahmed M, Guo H, Wang M, Hua JT, Guan J, Moran MF, et al. 2018.** Refined RIP-seq protocol for epitranscriptome analysis with low input materials. *PLoS Biology*, **16**.
- Zhang B, Wang Q. 2015.** MicroRNA-based biotechnology for plant improvement. *Journal of Cellular Physiology*, **230**: 1-15.

- Zhang Y, McKechnie J, Cormier D, Lyng R, Mabee W, Ogino A, Maclean HL. 2010.** Life cycle emissions and cost of producing electricity from coal, natural gas, and wood pellets in Ontario, Canada. *Environmental Science & Technology*, **44** : 538-544.
- Zhang Z, Theler D, Kaminska KH, Hiller M, de la Grange P, Pudimat R, Rafalska I, Heinrich B, Bujnicki JM, Allain FHT, et al. 2010.** The YTH domain is a novel RNA binding domain. *Journal of Biological Chemistry*, **285**: 14701-14710.
- Zhao L, Zhang H, Kohnen M, Prasad K, Gu L, Reddy AS. 2019.** Analysis of transcriptome and epitranscriptome in plants using PacBio Iso-Seq and Nanopore-based direct RNA sequencing. *Frontiers in Genetics*, **10**: 253.
- Zhao M, Ding H, Zhu JK, Zhang F, Li WX. 2011.** Involvement of miR169 in the nitrogen-starvation responses in *Arabidopsis*. *New Phytologist*, **190**: 906-915.
- Zhao Y, Xu Z, Mo Q, Zou C, Li W, Xu Y, Xie C. 2013.** Combined small RNA and degradome sequencing reveals novel miRNAs and their targets in response to low nitrate availability in maize. *Annals of Botany*, **112**: 633-642.
- Zhao X, Yang Y, Sun BF, Shi Y, Yang X, Xiao W, Hao YJ, Xiao-Li P, Chen YS, Wang WJ, et al. 2014.** FTO-dependent demethylation of N6-methyladenosine regulates mRNA splicing and is required for adipogenesis. *Cell Research*, **24**: 1403-1419.
- Zheng G, Dahl JA, Niu Y, Fedorcsak P, Huang CM, Li CJ, Vågbo CB, Shi Y, Wang WL, Song SH, et al 2013.** ALKBH5 is a mammalian RNA demethylase that impacts RNA metabolism and mouse fertility. *Molecular Cell*, **49**: 18–29.
- Zheng L, Kostrewa D, Bernèche S, Winkler FK, Li XD. 2004.** The mechanism of ammonia transport based on the crystal structure of AmtB of *Escherichia coli*. *Proceedings of the National Academy of Sciences*, **101**: 17090-17095.
- Zhong S, Li H, Bodi Z, Button J, Vespa L, Herzog M, Fray RG. 2008.** MTA is an *Arabidopsis* messenger RNA adenosine methylase and interacts with a homolog of a sex-specific splicing factor. *The Plant Cell*, **20**: 1278-1288.
- Zhou L, Tian S, Qin G .2019.** RNA methylomes reveal the m6A- mediated regulation of DNA demethylase gene SIDML2 in tomato fruit ripening. *Genome Biology*, **20**:156.
- Zhou W, Wei L, Xu J, Zhai Q, Jiang, H, Chen R, Chen Q, Sun J, Chu J Zhu Let al. 2010.** *Arabidopsis* tyrosylprotein sulfotransferase acts in the auxin/PLETHORA pathway in regulating postembryonic maintenance of the root stem cell niche. *The Plant Cell*, **22**: 3692-3709.
- Zhou Y, Bai L, Song CP. 2015.** Ammonium homeostasis and signaling in plant cells. *Science Bulletin*, **60**: 741-747.
- Zhu T, Roundtree IA, Wang P, Wang X, Wang L, Sun C, Tian Y, Li J, He C, Xu Y. 2014.** Crystal structure of the YTH domain of YTHDF2 reveals mechanism for recognition of N6-methyladenosine. *Cell Research*, **24**: 1493-1496.

References

Zimin AV, Stevens KA, Crepeau MW, Puiu D, Wegrzyn JL, Yorke JA, Salzberg SL. 2017. An improved assembly of the loblolly pine mega-genome using long-read single-molecule sequencing. *GigaScience*, **6**: giw016.

Zimin AV, Stevens KA, Crepeau MW, Holtz-Morris A, Koriabine M, Marçais G, Puiu D, Roberts M, Wegrzyn JL, et al. 2014. Sequencing and assembly of the 22-Gb loblolly pine genome. *Genetics*, **196**: 875-890.

Zou N, Li B, Chen H, Su Y, Kronzucker HJ, Xiong L, Baluška F, Shi W. 2013. GSA-1/ARG1 protects root gravitropism in *Arabidopsis* under ammonium stress. *New Phytologist*, **200**: 97–111.

Zou N, Li B, Dong G, Kronzucker HJ, Shi W. 2012. Ammonium induced loss of root gravitropism is related to auxin distribution and TRH1 function and is uncoupled from the inhibition of root elongation in *Arabidopsis*. *Journal of Experimental Botany* **63**:3777–3788.

